Sara Risseeuw

Bruch's membrane calcification in pseudoxanthoma elasticum

Visualizing the visual consequences

Sara Risseeuw

Bruch's membrane calcification in pseudoxanthoma elasticum Visualizing the visual consequences

The research in this thesis was financially supported by the Dr. F.P. Fischer Stichting, Rotterdamse Stichting Blindenbelangen, Stichting Vrienden UMC Utrecht and Stichting PXE-Fonds.

Publication of this thesis was kindly supported by Stichting Blindenhulp, Landelijke Stichting voor Blinden en Slechtzienden, Rotterdamse Stichting Blindenbelangen, ChipSoft, Tramedico, Ursapharm, Horus Pharma, Thea Pharma, Bayer and Low Vision Totaal.

Cover design, illustration & design lay-out: Esther Beekman (www.estherontwerpt.nl)
Printed by: GVO drukkers B.V., Ede

ISBN: 978-94-6332-697-1

Bruch's membrane calcification in pseudoxanthoma elasticum

Visualizing the visual consequences

Verkalking van het membraan van Bruch in pseudoxanthoma elasticum

Inzichten in de oogheelkundige manifestaties en gevolgen

(met een samenvatting in het Nederlands)

PROEFSCHRIFT

ter verkrijging van de graad van doctor aan de
Universiteit Utrecht
op gezag van de
rector magnificus, prof.dr. H.R.B.M. Kummeling,
ingevolge het besluit van het college voor promoties
in het openbaar te verdedigen op

donderdag 26 november 2020 des ochtends te 11.00 uur

door

Sara Risseeuw

geboren op 15 juni 1991
te Doorn

Promotor:
Prof. dr. S.M. Imhof

Copromotoren:
Dr. J. Ossewaarde-van Norel
Dr. R. van Leeuwen

Beoordelingscommissie:
Prof. dr. ir. M.J.C. Eijkemans
Dr. P. Charbel Issa
Prof. dr. M.M. van Genderen
Prof. dr. R.O. Schlingemann
Prof. dr. J.R. Vingerling

Contents

List of abbreviations used in this thesis

Retinal structures

BM	Bruch's membrane
EZ	Ellipsoid zone
GCL	Ganglion cell layer
INL	Inner nuclear layer
IPL	Inner plexiform layer
IS	Inner photoreceptor segments
OPL	Outer plexiform layer
ONL	Outer nuclear layer
OS	Outer photoreceptor segment
RNFL	Retinal nerve fibre layer
RPE	Retinal pigment epithelium

Other abbreviations used in this thesis

ABCC6	ATP binding cassette subfamily 6
ABI	Ankle-brachial index
AMD	Age related macular degeneration
ATP	Adenosine triphosphate
AUC	Area under the curve
BCVA	Best-corrected visual acuity
BMI	Body mass index
CI	Confidence interval
CNV	Choroidal neovascularization
CS	Caesarian section
ERG	Electroretinogram
ETDRS	Early Treatment of Diabetic Retinopathy
FAF	Fundus autofluorescence
GACI	Generalized arterial calcification of infancy
ICC	Intraclass correlation coefficient
ICG-A	Indocyanine green angiography
IICA	Intracranial internal carotid artery
IMT	Intima media thickness
IOP	Intraocular pressure
IQR	Interquartile range
LoA	Limits of agreement

LogMAR	Logarithm of the minimum angle of resolution
MA	Macular atrophy
MCA	Medial cerebral artery
MRI	Magnetic resonance imaging
NIR	Near-infrared reflectance
ODD	Optic disc diameter
OR	Odds ratio
P_i	Inorganic phosphate
PI	Pulsatility index
PP_i	Inorganic pyrophosphate
PXE	Pseudoxanthoma elasticum
RCT	Randomized controlled trial
ROC	Reciever operating characteristic
RR	Relative risk
SD	Standard deviation
SD-OCT	(Spectral domain) optical coherence tomography
TEMP	Treatment of ectopic mineralization in pseudoxanthoma elasticum
VD	Vaginal delivery
VEGF	Vascular endothelial growth factor
WHO	World Health organization


Chapter 1

Introduction

A major part of all persons with pseudoxanthoma elasticum (PXE) suffers from visual impairment.[1] The vision deteriorates relatively early in life, around the age of 50 years.[2] Sight-threatening complications, such as choroidal neovascularization (CNV) and macular atrophy are caused by pathologic calcification of Bruch's membrane (BM), a thin layer just underneath the retina.[3]

Visual impairment and the fearing for it have a major impact on the quality of life of persons with PXE.[4] Up to now, it is not possible to predict visual loss or influence the course of the disease, besides halting CNV with anti-vascular endothelial growth factor (VEGF) inhibitors.

Bruch's membrane: small, but significant

BM is named after the German anatomist Karl Wilhelm Ludwig Bruch and is an acellular membrane between the choroid and the retinal pigment epithelium (RPE) (Figure 1.1). BM is very thin, its thickness ranges from 2 – 5 µm in healthy eyes (for comparison, a healthy retina has a mean foveal thickness of 270 µm).[5,6] It consists of five layers and from the RPE to the choroid, these are: 1) the RPE basement membrane, 2) the inner collagenous layer, 3) the elastin layer, 4) the outer collagenous layer and 5) the basement membrane of the choriocapillaris.[7]

The basement membranes (the 1st and 5th layer) are the thinnest of the five layers and mainly consist of collagens, laminin, and heparan sulphate. The two collagenous layers are also similar and consist, as the name implies, of collagens that are organized in a grid-like structure. The elastin layer consists of multiple layers of elastin fibres that form a perforated sheet, but it also contains a type of collagen. The elastin layer is thinner and more porous in the macula when compared to the peripheral retina.[8]

BM sits between the choroid and the RPE and facilitates passive diffusion between those layers (Figure 1.1). The choroidal blood flow delivers oxygen, nutrients and vitamins, amongst others, to the RPE.[9]

The RPE has multiple important functions which are essential for maintaining the outer retina. Amongst others, it composes the blood-retinal barrier with the help of tight junctions between the RPE cells, it metabolizes the light-sensitive pigments of the photoreceptors in the visual cycle, it absorbs the scattered light in the globe

and it phagocytoses the sheds of the photoreceptor outer segments.[10] Also, the RPE produces factors such as the vascular endothelial growth factor (VEGF), which are essential for maintaining the choriocapillaris.[11] Last, the RPE secretes metabolic waste such as carbon dioxide and oxidized lipids to the choroid. [9]

The passive diffusion of oxygen and nutrients, and metabolic waste products and growth factors is modulated by the hydrostatic pressure on both sides of BM and the concentration of the molecules, but also depends on the structure of BM.[12] Besides facilitating passive diffusion, BM also functions as a support layer for RPE cell adhesion and restricting the movement of cells between the retina and choroid.[9]

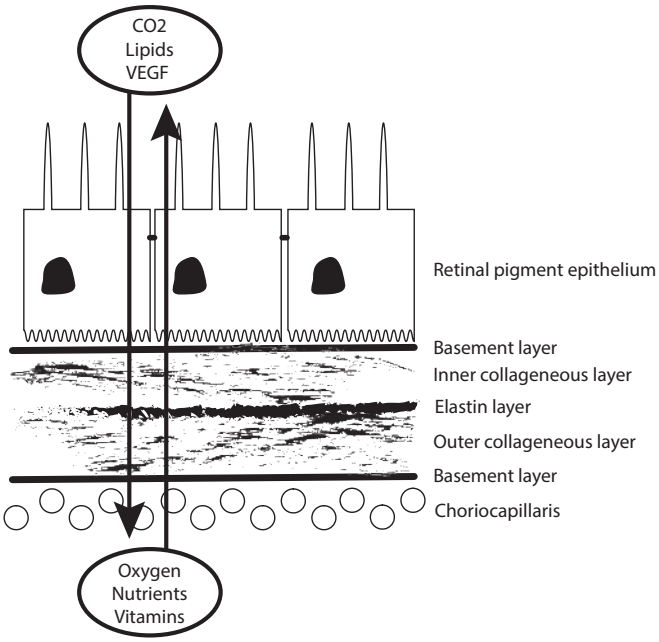

Figure 1.1 The position of Bruch's membrane (BM) between the retinal pigment epithelium (RPE) and the choriocapillaris and an illustration of its five layers. A healthy BM is permeable and facilitates the diffusion of substances between the RPE and the choriocapillaris. The RPE gets rid of waste products (e.g. CO_2 and lipids) and produces factors (e.g. VEGF) necessary for maintaining the choriocapillaris and choroid. The choriocapillaris delivers oxygen, nutrients and vitamins from the blood which are essential for the vitality of the RPE and outer retina. This is a schematic illustration to illustrate BM and the displayed thicknesses are not proportional.

The structure and properties of BM change with increasing age, which is a physiological phenomenon. The collagen fibres cross-link and become denser, thereby increasing the thickness of the collagen layer.[7,9] Together with an accumulation of lipids and waste products, this causes the BM to almost double in thickness throughout life.[6,7,13–15] With increasing age, the elastin layer loses its elasticity and it also appears to thicken, which is more pronounced in the peripheral retina when compared to the macula.[13,16,17] Not only the elasticity has local differences; in the macula lipids accumulate more and faster.[18]

Furthermore, ageing plays a role in BM mineralization, with deposition of calcium, iron and zinc.[9] Calcium is mainly deposited in the elastic layer, and calcification of the elastin layer is common with ageing; a study with 182 donor eyes older than 33 years found calcification of the elastic layer in 59% of the maculae, and the prevalence increased with age.[14] Together, these structural age-related changes have an impact on the permeability of BM. With increasing age, the capacity of BM to exchange molecules between the RPE and the choriocapillaris is reduced.[19–22] Again, this effect of ageing appears to be more pronounced in the macular area.[19,22]

Pathological changes in Bruch's membrane

Changes in the structure or properties of BM often result in changes in structure or function of the adjacent tissue (the outer retina or choroid). BM likely plays a role in the pathogenesis of the multifactorial disease age-related macular degeneration (AMD), which is the leading cause of visual impairment in Europe.[23,24] Age itself is the most important risk factor for AMD and due to the ageing population, the prevalence of AMD is expected to increase in the next decades.[25] The early stage of AMD is asymptomatic but AMD eventually may progress to atrophic ("dry") or neovascular ("wet") AMD, causing a loss of vision.

Different changes in the ageing of BM may attribute to the development of AMD. The elastin layer is thinner in the macular area compared to the peripheral area, which may make the macula more prone to disease.[8] The decreasing permeability, which is more pronounced in the macula, may lead to accumulation of RPE-secreted lipids and proteins between the RPE basal membrane and the inner collagenous layer of BM, forming a 'lipid wall'.[9,26] A build-up of these lipids can be seen as basal linear deposits or soft drusen, and might subsequently further decrease the BM permeability causing a vicious cycle of decreased BM permeability.[27,28] A thickened and less permeable BM impedes oxygen and nutrient exchange, and clinically this translates that soft drusen are an important clinical predictor for the progression to late AMD.[29]

Furthermore, calcification of the elastin layer of BM reduces the elasticity, making the membrane more prone to focal breaks and allowing the ingrowth of vessels from the choroid, causing CNV.[30] If the decreased permeability also impacts the diffusion of oxygen, this leads to hypoxia in the macula and VEGF expression by the RPE, which subsequently may accelerate the growth of CNV.[31] CNV in neovascular AMD can be treated with VEGF inhibitors, but for atrophic AMD there is no treatment yet.

Besides AMD, changes in BM also play a role in Sorsby fundus dystrophy. Sorsby fundus dystrophy is a disease caused by mutations in the tissue inhibitor of metalloproteinase 3 (*TIMP3*) gene, leading to an increased expression of the TIMP3 protein from the RPE. The overexpression in Sorsby fundus dystrophy leads to an accumulation of TIMP3 in BM, thereby thickening BM and impairing its functions.[32] Similar to AMD, patients with Sorsby fundus dystrophy suffer from visual loss due to CNV and atrophy, however relatively early in life.[33,34]

Pseudoxanthoma elasticum

Another disease that specifically affects BM is pseudoxanthoma elasticum (PXE). PXE is a rare autosomal recessive disorder (OMIM #264800) in which a double mutation in the *ABCC6* gene leads to a calcification of elastic fibres in the skin, vasculature and eyes.[35–37] The estimated prevalence of PXE is at least 1 per 56.000, meaning that in the Netherlands there are at least 300 PXE patients.[38]

The classical clinical presentation of PXE consists of a triad consisting of skin involvement, eye involvement and arterial calcification.[39] PXE used to be called "Grönblad-Strandberg syndrome", after the Swedish ophthalmologist Ester Grönblad who, together with dermatologist James Strandberg recognized the association between the typical skin and ocular phenotypes in 1929.[40,41] In 1963, the classical triad was confirmed by Goodman et al, with an extensive description of 12 patients.[42]

Pathogenesis

PXE is caused by mutations in the *ABCC6* gene, encoding an ATP efflux transporter (ATP binding cassette subfamily C member 6 - *ABBC6*), which is mainly expressed in the liver.[35,36,43] The ATP that is released by the liver is the main source of circulating inorganic pyrophosphate (PP_i), which is a strong inhibitor of ectopic calcification by inhibiting the growth of hydroxyapatite crystals.[44] Mutations in the *ABCC6* gene lead to insufficient levels of ATP expressed by the liver, thereby leading to low levels of PP_i

in PXE patients.[43,44] Since PP_i is a strong inhibitor of ectopic calcification, the low levels of PP_i very likely cause the ectopic calcification in PXE patients (as illustrated in Figure 1.2).

A lack of PP_i leads to ectopic mineralization in other monogenetic diseases as well. Mutations in the *ENPP1* gene also lead to suppressed PP_i, since this gene encodes a protein that generates PP_i by using ATP.[45] *ENPP1* mutations are associated with generalized arterial calcification of infancy (GACI, OMIM #208000), a rare disease that is often lethal to infants due to extensive calcification of large arteries.[45,46]

Interestingly, the clinical manifestations of PXE and GACI largely overlap, emphasizing the key role of PP_i in the pathophysiological pathway of soft tissue calcification.[47] Mutations in the *NT5E* gene encoding *CD73* also lead to decreased PP_i levels, by accelerating the breakdown of PP_i to inorganic phosphate (Pi).[48] While PP_i is an anti-mineralization factor, P_i is a pro-mineralization factor, and the high P_i levels in patients with *CD73* mutations lead to arterial calcifications, mainly in older patients.[49]

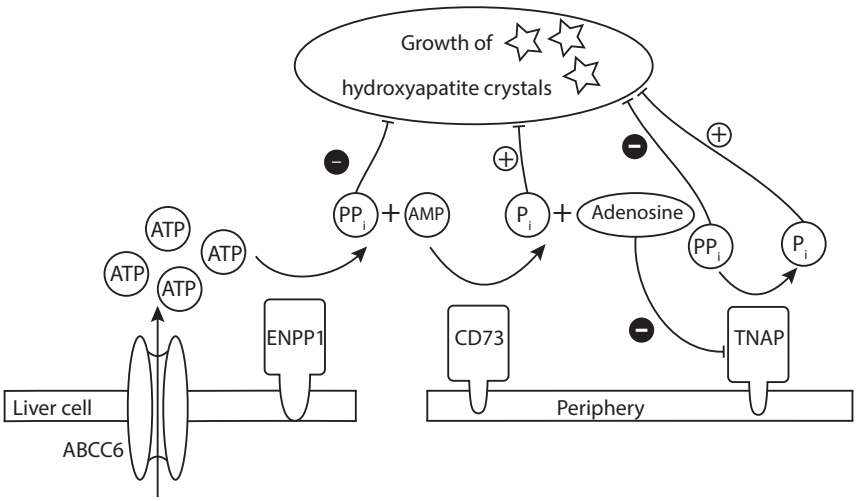

Figure 1.2 Model of the pathway leading to ectopic calcification in various diseases associated with inorganic pyrophosphate (PP_i). Mutations in the *ABCC6* gene or ENPP1 gene lead to low levels of PP_i. *CD73* or *TNAP* deficiencies also lead to ectopic calcification. This figure is based on the work of Jansen et al. Arterioscler Thromb Vasc Biol 2014;34:1985-1989 and Uitto et al. J Invest Dermatol 2016;136:550-556.

Clinical aspects

The skin involvement of PXE is often the patient's first notion of the disease, around the second or third decade.[50] The ectopic calcification in PXE leads to calcification and fragmentation of elastic fibres in the skin. Clinically, this results in xanthoma-like yellowish papules or plaques (hence the name) in the skinfolds. These are mainly seen in the neck, elbows and armpits, and often symmetrically distributed.[39] Besides cosmetic preferences, the skin lesions rarely cause any clinical complaints.

In the vasculature, the elastic fibres of the medial layer of the medium and small-sized arteries are affected.[51] Arterial calcification is predominantly present in the intracranial internal carotid artery, and the arm and leg arteries.[52] This calcification leads to arterial thickening and subsequent stiffening in PXE patients, thereby increasing the risk of peripheral arterial disease which is prevalent in almost half of all PXE patients.[51,53,54] Also, the intracranial arteries are predilection locations for arterial calcification and thus PXE patients have a higher risk of developing cerebrovascular complications.[55]

Bruch's membrane calcification in PXE

The largest burden for PXE patients are the clinical consequences of BM calcification in the eye.[4] In PXE donor eyes, BM is abnormally calcified and thickened, already at a young age. In a donor eye of a 17-year old PXE patient, the BM of the posterior pole was already three times thicker as compared to an age-matched control; 7.4 μm in PXE, versus 2.5 μm in the control.[56]

Early histopathological findings in donor eyes report patchy areas of basophilia in BM, especially at the posterior pole, which indicate calcium deposits.[57–59] The presence of calcium in BM was proven by Klien in 1947, and she also found that BM was often fragmented in the calcified areas, similar to the findings in skin lesions.[60] However, she investigated eyes with angioid streaks but without a definite PXE diagnosis. Later it was found that the calcium deposits consisted of calcium phosphates including hydroxyapatite.[61] A more recent study revealed that not only the elastic fibres in BM were calcified, but fibres in the connective tissue surrounding BM as well.[62] Furthermore, this study mentioned damaged collagen fibres in the BM and surrounding connective tissues.[62] Unfortunately, due to its rarity, PXE donor eyes are scarce and further histopathological data and its correlation with imaging have yet to be investigated.

To study the histopathology of PXE without the need for human tissue, Gorgels et al. developed an *ABCC6*$^{-/-}$ mouse as an animal model.[63] Besides BM calcification, they found abnormal fibres branching and running crisscross through both the elastin layer and the collagenous zones in the mice' eyes, and they found that these calcified fibres contained collagen.[63,64] Also, older mice had more severe calcification than younger mice which supports that PXE is a progressive disease.[64]

Based on these observations and the recent discovery of low PP_i levels in PXE, it could be plausible that *ABCC6* mutations in PXE do not specifically lead to calcification of elastic fibres. However, they might rather predispose a tendency to calcification of elastic or collagen fibres, and that tissue properties and species differences determine whether elastin or collagen will be predominantly calcified.[62,64]

Peau d'orange and angioid streaks

Clinically, BM calcification leads to peau d'orange, which is a mottled and speckled pattern in the fundus (Figure 1.3). Peau d'orange is hypothesized to be the visible transition zone of the calcified BM and the less affected BM in the retinal periphery.[65] It is typically seen at the posterior pole in childhood and is thought to spread centrifugally during life.[65,66] The presence of peau d'orange, and thus BM calcification, precedes the formation of angioid streaks in the brittle calcified BM.[67,68]

Angioid streaks are defects in BM and can be seen as irregular jagged break lines.[69] Typically, they originate from the optic disc, surround it concentrically, and radiate outwards to the periphery, but do not cross the transition zone of calcified BM.[65] It is assumed that angioid streaks develop as a consequence of mechanical stress exerted on the eye.[70,71]

The exerted stress could be eye movements where the extraocular muscles put traction on the eye close to the optic nerve or pressure on the globe. This causes the brittle BM to break, similar to a cracked egg-shell, and to form angioid streaks.[68] This pathogenesis of angioid streaks implies that angioid streaks are not pathognomic for PXE, but could be prevalent in other diseases with BM alterations as well. Indeed, angioid streaks are found in several other ocular or systemic diseases, amongst which Paget disease, hemoglobinopathies (sickle cell anaemia, thalassemia), trauma and other miscellaneous diseases.[50,72] However, the majority of angioid streaks is associated with PXE.[73,74]

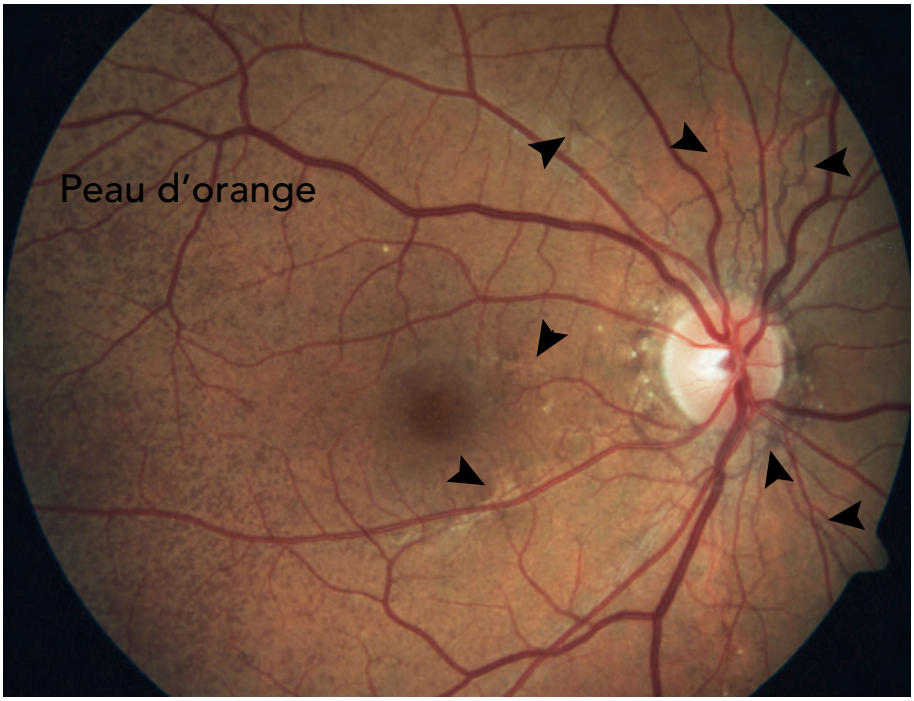

Figure 1.3 The fundus of a 24-year-old PXE patient. Note the speckled aspect temporal from the macula, this is the so-called peau d'orange. Angioid steaks are visible around the optic disk and inferior from the macula and indicated with black arrowheads.

Choroidal neovascularization

BM calcification with angioid streaks lead to CNV, the ingrowth of fibrovascular tissue from the choroid, in up to 86% of PXE patients.[75] The pathogenesis likely resembles an accelerated version of the pathogenesis of CNV in late AMD. The thickening and calcification of BM in PXE reduce its permeability, causing relative hypoxia in the outer retina. This leads to increased VEGF secretion by the RPE which accumulates because the permeability of BM is reduced. Local BM defects, the angioid streaks, will enable CNV to arise due to the high VEGF levels expressed by the RPE.[31]

In PXE patients, both the occult type 1 and the classic type 2 CNV are present. Type 1 CNV is a growth of fibrovascular tissue beneath the RPE, through the angioid streaks. Sometimes, this develops into the classic type 2 CNV in which the fibrovascular tissue grows between the RPE and the photoreceptor layer.[76] Besides classic and occult CNV,

polypoidal choroidal vasculopathy has also been described in PXE patients.[76,77] In PXE patients, classic CNV is the most common and unfortunately this type has the worst visual prognosis.[76] If active, CNV can lead to visual loss due to exudation and subretinal haemorrhage, which is toxic for the photoreceptors. In a later stage, scarring occurs, which further impedes the visual function.

Often, PXE patients develop CNV before the age of 50 years.[72] One study found that the first CNV occurred at a mean age of 44 years.[2] Because angioid streaks are frequent in the posterior pole, CNV has a large impact on the visual function of patients with PXE already at a young age.

Atrophy

Besides CNV, macular atrophy also attributes to visual loss in PXE patients.[78,79] Macular atrophy resembles geographic atrophy in AMD. Macular atrophy presents as a loss of the photoreceptors, RPE and choriocapillaris in the posterior pole. It can be seen as a sharply demarcated area of hypopigmentation in the fundus.[80]

In contrast to CNV, the pathophysiology of this RPE atrophy remains poorly understood. It is assumed that the loss of photoreceptors follows the dysfunction of the RPE in PXE.[81] Possibly, this RPE and outer retina atrophy then leads to closure of the choriocapillaris,[81] but other studies indicate that changes in the choriocapillaris precede RPE atrophy and photoreceptor loss.[82]

Despite extensive studies that investigate dry AMD, the exact mechanism and sequence of atrophic changes have not been not fully clarified yet, which illustrates the complex relationship of the choriocapillaris, BM and the outer retina. However, it has become clear that age-related changes in BM, such as lipid accumulation, impede the permeability of BM and thereby play an important role in dry AMD and geographic atrophy. [23,80,83]

In PXE, it is likely that the pathological calcification of BM affects the permeability of BM and thereby leads to the presence of atrophy in 20% of the eyes of PXE patients.[78] Often, atrophy occurs at the borders of CNV, which might have a different pathophysiological mechanism than macular atrophy. However, in 7-32% of the eyes, the atrophy is independent of the presence of CNV.[78,84]

The mean growth rate of all atrophy in PXE is 1.7 – 2.2 mm^2 per year but atrophy in eyes without CNV progress up to 3.3 mm^2 per year.[78,84] Compared to geographic atrophy in dry AMD, with a mean growth rate of 1.2 – 2.8 mm^2 per year, macular atrophy in PXE progresses faster.[80] More importantly, macular atrophy in PXE presents earlier in life, often already in the sixth decade compared to a peak prevalence in persons over 75 years with AMD.[85] The earlier presentation and faster progression may be explained by the earlier onset and severity of BM pathology in PXE when compared to AMD. Again, these findings illustrate the important role of BM in the vitality of the outer retina. Thus, although macular atrophy is less prevalent than CNV, it should be considered as an important cause of vision loss.

Visual outcome

The occurrence of CNV and macular atrophy attributes to visual loss in PXE patients. Though definitions of visual impairment differ, visual impairment is common in PXE patients. One study in 71 PXE patients (mean age of 47 years), found that 39% of the patients had a best-corrected visual acuity (BCVA) of the better eye lower than 0.50 in decimals.[1] Another study in 40 patients (mean age of 43 years) found that 17% of the patients had a BCVA lower than 0.40 in decimals in both eyes.[2] In a third study with 53 patients (mean age of 43 years), 19% of the patients had a bilateral BCVA lower than 0.10 in decimals.[86] In all these studies, visual loss and impairment was associated with higher age, with an onset of visual loss around the fifth decade.[2,86] However, little is known on the age-specific visual acuity of PXE patients, which would be valuable information for the counselling of patients.

In PXE patients, visual impairment has a major impact on the quality of life, more than the presence of cardiovascular disease.[4] More so, younger PXE patients without visual impairment report a lower quality of life than PXE patients that are visually impaired, which may be explained by the foresight of visual loss.[4] Since young PXE patients are often aware of the visual loss of their relatives with PXE, this affects their emotional well-being and decisions in life planning.

However, there is a large variation regarding the ophthalmological phenotype, also in patients with similar age, or between family members with the same mutation.[87] Several studies have attempted to establish genotype-phenotype associations but did not result in clinically relevant findings regarding the visual prognosis.[88,89] Up to now, only the presence of angioid streaks in the foveal area might predict the occurrence of CNV that often causes central vision loss. Other risk factors to predict CNV and macular atrophy have yet to be discovered.

Besides the visual acuity that often deteriorates in life, other aspects of visual functioning are also important for the visual outcome, such as the visual field and the electrophysiological function of the retina. Unfortunately, data is limited regarding visual outcome other than the visual acuity. It was suggested that PXE patients may have generalized retinal dysfunction, although the electrophysiological evidence is not concluding.[90–92] Furthermore, recently it was found that PXE patients have an impaired dark adaptation.[93] These findings suggest that BM calcification also may affect the vitality of the photoreceptors.

Treatment for PXE

In PXE patients, the complications such as peripheral arterial disease, CNV, and macular atrophy are the results of ectopic calcification. Up to now, no treatment exists that can prevent the ectopic calcification. The only widely used treatment to halt visual deterioration due to CNV is treatment with VEGF inhibitors, similar to patients with wet AMD.

VEGF inhibition

Treatment with VEGF inhibitors is administered as intra-ocular injections with bevacizumab, ranibizumab or aflibercept.[94–96] Ranibizumab and bevacizumab are monoclonal antibodies that bind to the VEGF protein and prevent it from binding to the receptor, thereby inhibiting angiogenesis.[97] Aflibercept has a receptor fragment resembling the VEGF receptor and thereby serves as a trap for the VEGF proteins and placental growth factor.[97,98]

In patients with PXE, anti-VEGF treatment has shown beneficial outcomes regarding visual acuity and CNV activity. Multiple studies reported an improved visual acuity and decreased signs of CNV activity, with different regimes of administering the VEGF inhibitors.[99] In the Netherlands, VEGF inhibition for PXE patients is administered at fixed intervals, starting with a cycle of three injections every four weeks, and depending on the CNV activity, the interval can then be extended (the so-called treat-and-extend regime).

VEGF inhibitors were first introduced as a potential treatment of neovascular disease in 2006.[100] Therefore, a lot of PXE patients did not have the opportunity to benefit from this treatment, which has likely attributed to the high prevalence of visual impairment

in PXE patients. Before 2006, other therapies were used to treat CNV such as laser photocoagulation and photodynamic therapy.[99] However, the outcome of these therapies was inferior to VEGF inhibition in PXE patients.[99]

In a pooled analysis, in 11 studies (166 patients) photodynamic therapy resulted in a deteriorated BCVA with a mean change of 0.41 LogMAR (95% CI 0.25 – 57), compared to an improved BCVA (mean change -0.18 LogMAR, 95% CI -0.32 - -0.03) in 14 studies (167 patients) on VEGF inhibitors ($P < 0.0001$).[99] The results of treatment with VEGF inhibitors are best in the early stages of CNV and in later stages, macular atrophy often interferes with the visual outcome and impedes the assessment of CNV activity.[101] Furthermore, CNV in angioid streaks recur more often than in AMD. Therefore, PXE patients need prolonged treatment and more intensive monitoring compared to AMD patients.[102,103]

Unfortunately, there may be a drawback for treatment with VEGF inhibitors. In patients with late AMD, treatment with VEGF inhibitors was associated with an increased risk and progression of geographic atrophy.[104,105] Since VEGF from the RPE maintains the choriocapillaris, the suppression of VEGF levels may cause choriocapillaris atrophy which subsequently affects the nutrient flow to the retina. However, the precise effects and mechanism have not been established yet. Also, it is likely that, on an individual level, the benefits of VEGF inhibition outweigh the possible risk of atrophy. Furthermore, BM calcification in PXE patients may interfere with these effects and alter the risk of macular atrophy.

Theoretically, the risk of atrophy is higher in PXE patients, because of the already impaired diffusion of between the RPE and choriocapillaris. However, since macular atrophy might be the natural endpoint of BM calcification, it is plausible that eventually nearly all PXE patients will develop atrophy. This attenuates the clinical implications of the association between VEGF inhibition and the risk of atrophy. Despite the undoubted benefits of VEGF inhibition in PXE, it is essential to find a causal treatment that prevents ectopic calcification and thereby CNV and macular atrophy all together.

Finding a causal treatment

Since the low levels of PP_i in PXE appear to play a major role in the ectopic calcification, supplementation of PP_i would be an obvious treatment option for PXE patients.[43] In *ABCC6*$^{-/-}$ mice, intraperitoneal supplementation of PP_i did indeed prevent ectopic calcification.[106] However, the pharmaceutical properties of PP_i impede the use of PP_i as

a therapeutic supplement in humans up to now; oral supplementation is ineffective so it needs to be administered intravenously.[107]

Bisphosphonates, a common drug type, are synthetic and stable PP_i analogues and may therefore substitute as PP_i supplementation.[107] In GACI patients, treatment with bisphosphonates was associated with improved survival and reduced arterial calcification.[46,108] In *ABCC6*$^{-/-}$ mice, the bisphosphonate etidronate was found to reduce ectopic calcification in mice that were treated before the onset of ectopic calcification.[106,109,110]

Together with the evidence that bisphosphonates reduce arterial wall calcification in human subjects,[111] this led to the design of a randomised double-blind placebo-controlled trial to test the effect of etidronate in PXE patients. In this trial, etidronate was associated with reduced arterial calcification in the femoral arteries and fewer excessive CNV activity that necessitated prompt treatment.[112] The latter finding is remarkable since data on possible effects of bisphosphonates on CNV are conflicting. In two studies, the bisphosphonate alendronate was associated with better visual outcome in patients with CNV due to AMD or myopia.[113,114] In contrast, in a large scale population study, bisphosphonates were associated with a higher risk of CNV.[115] Especially in PXE patients, with high visual morbidity due to CNV, there is a crucial need to learn more about the effects of etidronate on CNV activity and the ophthalmological safety since etidronate will likely be introduced as a treatment in most PXE patients.

More importantly, the effect of etidronate on BM calcification needs to be established. Currently, there is a severe lack of suitable biomarkers that can serve as an endpoint in clinical trials that investigate possible treatment. Gliem et al. recently proposed to use the eccentricity of the leading edge of peau d'orange as a surrogate marker, but this is only possible in relatively young PXE patients. Also, it represents the topographic distribution of BM calcification, rather than the severity of BM calcification.[116,117] Lastly, there is a lack of understanding of the natural progression of BM calcification, which impedes trial design and finding relevant effects of possible treatments on the ophthalmological manifestations of PXE.

Visualizing Bruch's membrane calcification

A clinical endpoint for the severity of BM calcification will most likely be an imaging-based biomarker, since BM calcification in PXE leads to very distinctive features on retinal imaging. A retinal-imaging based biomarker has several advantages; it is often non-invasive, fast and relatively cheap. Furthermore, innovation in imaging technology has led to the development of high-speed and very sensitive cameras with less and less interfering noise. Several imaging modalities that visualize the changes in BM in PXE patients are described below.

Optical coherence tomography

Optical coherence tomography (OCT) imaging is widely used in ophthalmology to visualize structural properties of tissues. OCT imaging of the retina approaches histology, especially since the introduction of the spectral domain (SD) OCT, which has an axial resolution of up to 5 μm in 2006.[118]

The currently used SD-OCT imaging resembles ultrasound imaging, but uses infrared light directed in a laser beam onto the fundus with a confocal scanner. Interferometry is used to set a reference measure for interpreting the back-reflected light, by splitting the infrared laser beam into two paths: one to the fundus and another one to a reference arm.[119] The back-reflected light is combined with the output from the reference arm, which results in two waves of which the interference can be quantified. For each scan point, a reflectivity profile in the depth direction (z-axis) is created, the so-called A-scan (amplitude scan). A-scans are combined into a cross-sectional image, the B-scan (brightness scan) when the beam scans laterally across the fundus.

The use of infrared light has multiple advantages. It is comfortable for the patient and it penetrates deep in the retinal tissue, which allows for good visualization of deeper layer in the depth direction.

OCT imaging delivers two types of information: structural, and reflective properties of the retinal tissue. These properties can be affected by age or the presence of retinal disease.[120] For example, in clinical practice CNV is often easily detected with OCT, as a subretinal structure. Furthermore, since SD-OCT has a high axial resolution and signal-to-noise ratio, it is widely used to quantify retinal layer thicknesses for both clinical and research purposes.[118]

Measurement of reflectivity is less commonly used. First, the inner retinal layers have very low reflective properties and are very dark on OCT imaging without post-processing of the reflectivity values. To enhance to contrast, the reflectivity of nearly all OCT scans is converted to the fourth root which is a processing step that needs to be accounted for. Also, the grey values cannot be measured directly but need to be normalized first. However, reflectivity profiles are used to semi-quantify retinal disease such as AMD, often by visualizing the profiles of the four hyperreflective bands.[121]

On OCT, these bands represent from anterior to posterior: the external limiting membrane, the ellipsoid zone of the photoreceptors, the interdigitation of the cones with the RPE (or the outer segments of the photoreceptors) and the RPE and BM (Figure 1.0B).[122,123] BM cannot be visualized separately from the RPE (yet); the axial resolution of SD-OCT currently is maximum 5 µm, but BM is only 2 – 5 µm thin.[6,118] Despite that, the RPE-BM layer appears more reflective in PXE patients than controls, most due to the BM calcification, as illustrated in Figure 1.4.[3,124,125]

Near-infrared reflectance imaging

In PXE patients, near-infrared reflectance imaging (NIR) is superior in visualizing the pattern of BM calcification. Reflectance imaging, or fundus reflectometry, describes the quantitative assessment of the light that is back-reflected by the fundus.[126] Different

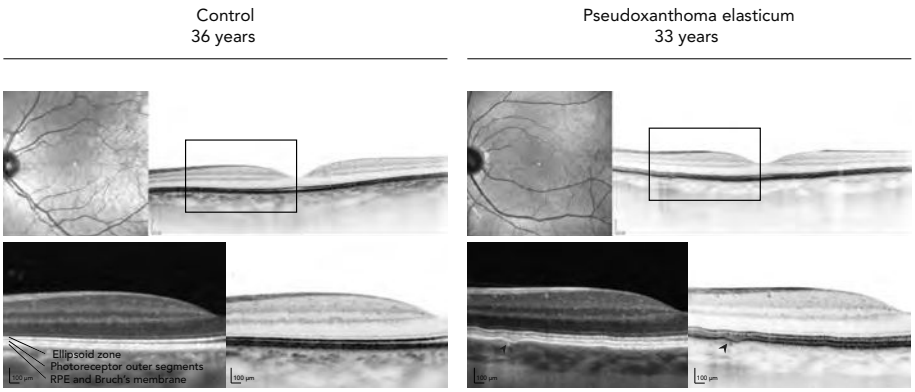

Figure 1.4 OCT-imaging of a 36-year-old control and a 33-year-old patient with pseudoxanthoma elasticum (PXE). The rectangles in the OCT images mark the area that is magnified in the images below. In the magnified images, there are increased reflectivity vales on the level of Bruch's membrane in the patient with PXE. In the PXE patient, the black arrowhead marks an angioid streak; a break in the calcified Bruch's membrane.

wavelengths can be used, but the near-infrared spectrum (above 790 nm) is superior in visualizing deep fundus structures compared to shorter wavelengths.[127] This is mainly due to the lower absorption of the light by melanin in the RPE with increasing wavelengths.[127] This increases the visibility of structures underneath the RPE, such as drusen in dry AMD and BM calcification in PXE.[69,128]

In the UMC Utrecht, NIR imaging is acquired with a monochromatic diode laser source of 820 nm wavelength. With confocal scanning, the laser scans across the fundus in a raster pattern, illuminating and recording the corresponding elements at a very high speed. This minimizes the scattering of light, thereby improving contrast and allowing high-resolution imaging, with a lateral resolution of up to 5 µm per pixel in a 30° image. On NIR imaging, the presumed area of BM calcification is hyperreflective and often has a speckled aspect (Figure 1.5). In older patients, the speckled aspect is often more temporal. Angioid streaks are hyporeflective compared to the (hyperreflective) surrounding.

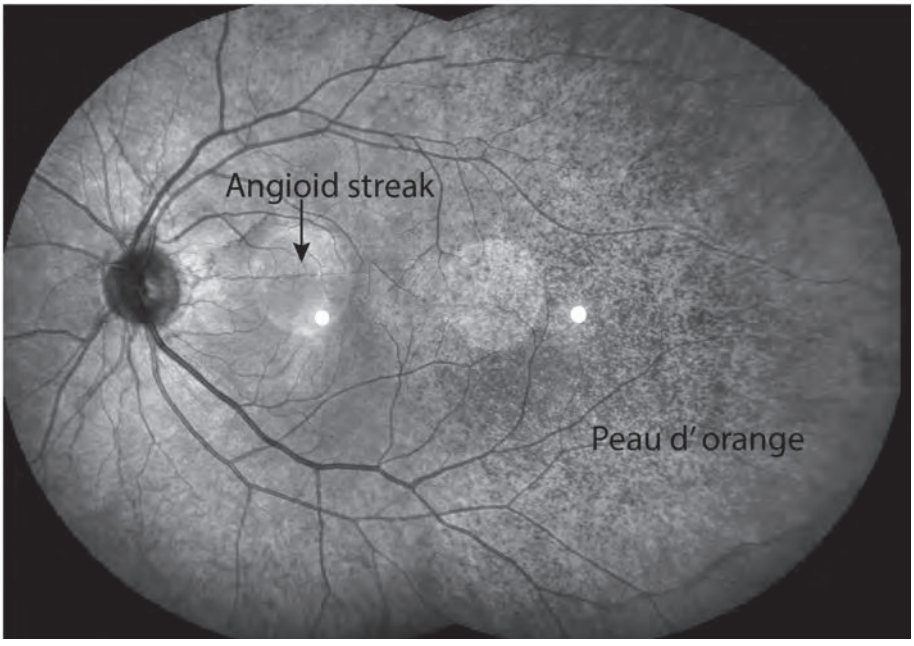

Figure 1.5 Near-infrared reflectance imaging showing the typical speckled pattern of hyperreflectivity and its centrifugal spread in a 31-year-old PXE patient. An angioid streak is indicated which runs through the macula.

Late-phase indocyanine green angiography

Indocyanine green angiography (ICG-A) is a dye-based imaging method of the retinal and choroidal vasculature, which uses intravenously injected ICG. It is commonly used in ophthalmology to detect abnormalities under the RPE. ICG absorbs light with a peak absorption at 805 nm and has a wide fluorescence spectrum with a peak at 835 nm.[129] For ICG-A imaging, a diode laser wavelength of 790 nm for excitation is used with a barrier filter at 830 nm to separate excitation and fluorescence light. Because of the higher wavelengths, abnormal structures underneath the RPE and the choroidal vasculature are better visible which makes ICG-A superior to fluorescein angiography for visualizing deep sub-RPE and choroidal alterations. ICG is a large molecule that binds to plasma proteins, is cleared from the plasma by the liver and stays in the vessels for up to 20 – 30 minutes. After this time, in the so-called late phase, the ICG dye is

Figure 1.6 Late-phase indocyanine green angiography of a 47-year-old PXE patient. There is hypofluorescence throughout the posterior pole. The angioid streaks are clearly visible in this area and are relatively hyperfluorescent.

washed out from the vessels and the fluorescence derives from choroidal staining and ICG uptake by the RPE cells.[130]

In PXE patients, late-phase ICG-A (>30 minutes after the injection of the ICG solution) often reveals a typical pattern resembling peau d'orange: an area of decreased fluorescence with speckled borders in the posterior pole (Figure 1.6).[131,132] The histopathological substrate of these findings has yet to be discovered. It was hypothesized that the decreased fluorescence could be the direct result of blockage of the choroid by BM calcification, but another theory is that the decreased fluorescence is due to a dysfunctional RPE leading to a reduced dye uptake.[65,130]

Fundus autofluorescence

Fundus autofluorescence (FAF) imaging uses the natural autofluorescent properties of the fundus and is superior in visualizing the vitality of the RPE. FAF makes uses of the fluorescent metabolites of vitamin A in lipofuscin granules, which are located in the RPE. These metabolites, so-called bisretinoids, are stored in lipofuscin granules after phagocytosis of the photoreceptor outer segments by the RPE cells. The lipofuscin granules are typically excited with blue light of 488 nm and have a broad emission spectrum, centered around 610 nm.[133,134] A barrier filter of 500 nm is then used to separate the excitation and fluorescence light. A high FAF signal indicates increased lipofuscin, and a strongly attenuated FAF signal indicates RPE cell death (RPE atrophy). Though lipofuscin is naturally present in the RPE, increased levels of lipofuscin are associated with inherited retinal dystrophies and are thought to be toxic.[135,136]

FAF does not directly visualize the calcification process in BM, but PXE patients have typical features that likely represent RPE dysfunction following BM calcification (Figure 1.7). Pattern-dystrophy like changes are visible as focal patterns of increased FAF and are common in PXE.[137,138] Wing-like areas of increased FAF along angioid streaks are called the parastreak phenomenon and are seen in 21% of PXE eyes.[138] A recent study used quantitative FAF and found overall reduced FAF levels indicating reduced lipofuscin levels in PXE patients, possibly due to a slowed visual cycle as a result of BM calcification.[117]

Insights from imaging

Since the wide introduction of these techniques in the first decade of this century, its applications have tremendously increased the insight into the characteristics of BM calcification. Using OCT, angioid streaks on NIR and fundoscopy were detected as

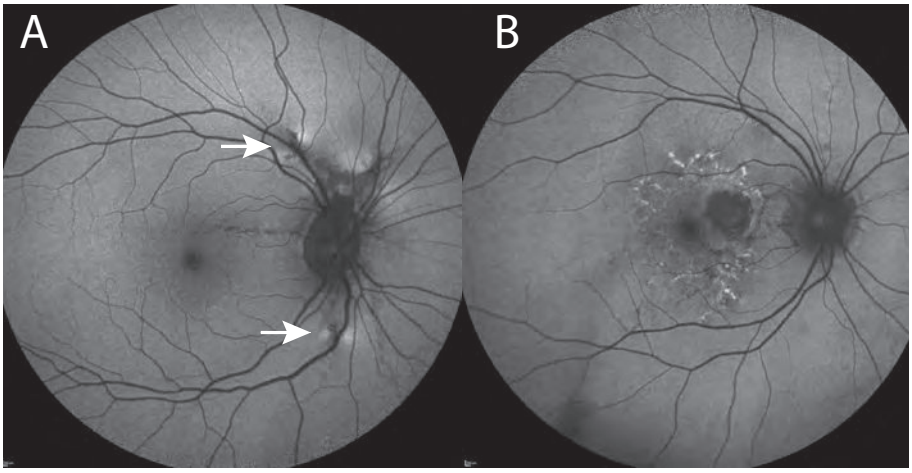

Figure 1.7 Fundus autofluorescence of PXE patients. Increased fluorescence along angioid streaks is indicated with white arrows (**A**). Otherwise, this resembles a fairly normal fundus autofluorescence. Pattern-dystrophy like changes are patterns of focally increased fluorescence (**B**). The dark spot within the area of increased fluorescence is an atrophic area.

interruptions of the RPE-BM layer, demonstrating *in vivo* that the primary alterations are located at the level of BM.[125]

Especially the use of NIR, of which the speckled aspect is very specific for PXE, has aided in better diagnostic options and BM-specific imaging for PXE.[139] A comparison of the speckled pattern on NIR with the speckled decreased fluorescence on late-phase ICG-A showed that the borders of the decreased fluorescence with late-phase ICG-A are located more central than the peau d'orange visible in the fundus and on NIR.[65] These findings led to a hypothetical model proposed by Charbel Issa et al, which describes different areas in the fundus that are separated by speckled transition zones that resemble different stages of BM alterations (Figure 1.8).[65] Due to the centrifugal spread, it is assumed that the BM is more severely affected centrally and close to the optic disc, than in the periphery, but this has not been verified in longitudinal studies yet.

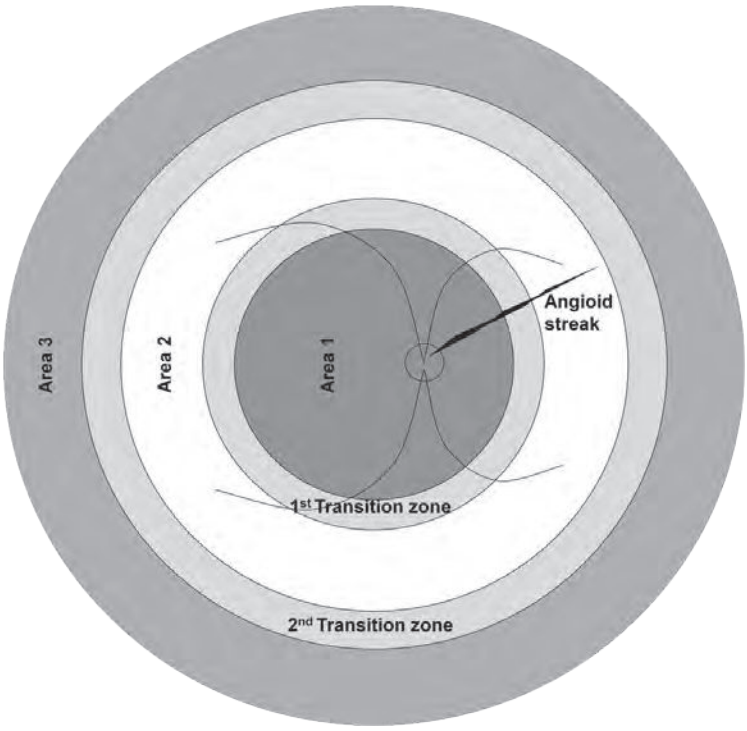

Figure 1.8 A theoretical model of the different areas in the fundus that are separated by speckled transition zones. The areas have different characteristics on multimodal retinal imaging and likely represent different stages of BM alterations. Area 1 represents ICG-A hypofluorescence. Area 2 represents fundus hyperreflectivity on NIR. Area 3 represents a normal fundus reflex. The 2nd transition zone represents peau d'orange. This figure is reprinted from: Charbel Issa et al. Ophthalmology 2010;117:1406-1414.

Aims and outline of this thesis

This thesis investigates the determinants and consequences of BM calcification in PXE patients. Different aspects of PXE make it challenging to gain more insight in this sight-threatening disease and to obtain certain answers to clinically relevant questions: its rarity, its vast heterogeneity, and its high frequency of end-stage macular disease impede the conduct of large scale epidemiological studies with high-quality data. Moreover, biomarkers for BM calcification are lacking.

To gain more insight into BM calcification in PXE patients and its consequences, this thesis focuses on three major aims:

I. To study the manifestations of PXE in the eye by investigating the natural history of BM calcification and describing its clinical consequences.
II. To gain insight into the determinants of the visual prognosis and to investigate whether treatment can modify disease complications.
III. To develop an imaging-based biomarker that will aid both clinical monitoring of disease and may serve as an endpoint in research and upcoming trials.

Part 1. Clinical consequences of BM calcification

The first part of this thesis focuses on a better understanding of the course of the disease and the implications for patients.

In **Chapter 2**, we describe the natural history of BM calcification and investigate its longitudinal characteristics to establish more insight into the course of BM calcification.

In **Chapter 3**, we study the visual burden in PXE by describing the age-specific characteristics of visual acuity, the prevalence of visual impairment in PXE patients and the underlying retinal pathology, and compare this to patients with late AMD.

In **Chapter 4**, we focus on the characteristics of choroidal thinning in PXE patients and determine the underlying cause of this.

For a long time, pregnant PXE patients were advised to undergo assisted delivery or even a caesarean section because of fear that vaginal delivery could be harmful to the eyes, but no supporting evidence existed. In **Chapter 5**, we study the retinal imaging before and after a delivery to investigate the safety of a vaginal delivery.

Part 2. Individualizing the visual prognosis

The second part of this thesis focuses on gaining insight in determinants of visual outcome, to better predict the visual prognosis for an individual.

In **Chapter 6,** we analyse the effect of the severity of the *ABCC6* variants on skin lesions and on arterial and BM calcification to gain insight into possible genotype-phenotype correlations.

In **Chapter 7**, we investigate the effect of the extent of BM calcification on macular degeneration to be able to predict which patients will develop CNV and atrophy, leading to visual impairment.

In **Chapter 8**, we evaluate the effect of etidronate on subclinical CNV activity in PXE patients in a post-hoc analysis of the "Treatment of Ectopic Mineralization in PXE" trial.

Part 3. Towards a quantitative measurement of BM calcification

There is a pressing need for a quantitative biomarker for BM calcification to investigate the effect of possible treatments and for clinical monitoring. In ***Chapter 9***, we aim to develop a method to quantify OCT reflectivity that can distinguish between PXE and controls.

References

1. Ebran J-M, Milea D, Trelohan A, et al. New insights into the visual prognosis of pseudoxanthoma elasticum. *Br J Ophthalmol*. 2014;98(1):142-143.
2. Orssaud C, Roche O, Dufier J-L, Germain DP. Visual Impairment in Pseudoxanthoma Elasticum: A Survey of 40 Patients. *Ophthalmic Genet*. 2015;36(4):327-332.
3. Gliem M, De Zaeytijd J, Finger RP, Holz FG, Leroy BP, Issa PC. An update on the ocular phenotype in patients with pseudoxanthoma elasticum. *Front Genet*. 2013;4(APR):14.
4. Finger RP, Fenwick E, Marella M, et al. The relative impact of vision impairment and cardiovascular disease on quality of life: the example of pseudoxanthoma elasticum. *Health Qual Life Outcomes*. 2011;9:113.
5. Grover S, Murthy RK, Brar VS, Chalam K V. Normative Data for Macular Thickness by High-Definition Spectral-Domain Optical Coherence Tomography (Spectralis). *Am J Ophthalmol*. 2009;148(2):266-271.
6. Ramrattan RS, Van der Schaft TL, Mooy CM, De Bruijn WC, Mulder PGH, De Jong PTVM. Morphometric analysis of Bruch's membrane, the choriocapillaris, and the choroid in aging. *Investig Ophthalmol Vis Sci*. 1994;35(6):2857-2864.
7. Hogan MJ, Alvarado J. Studies on the Human Macula: IV. Aging Changes in Bruch's Membrane. *Arch Ophthalmol*. 1967;77(3):410-420.
8. Chong NHV, Keonin J, Luthert PJ, et al. Decreased thickness and integrity of the macular elastic layer of Bruch's membrane correspond to the distribution of lesions associated with age-related macular degeneration. *Am J Pathol*. 2005;166(1):241-251.
9. Booij JC, Baas DC, Beisekeeva J, Gorgels TGMF, Bergen AAB. The dynamic nature of Bruch's membrane. *Prog Retin Eye Res*. 2010;29(1):1-18.
10. Thumann G, Dou G, Wang Y, Hinton DR. *Cell Biology of the Retinal Pigment Epithelium*. Vol 1. Fifth Edit. Elsevier Inc.; 2012.
11. Saint-Geniez M, Kurihara T, Sekiyama E, Maldonado AE, D'Amore PA. An essential role for RPE-derived soluble VEGF in the maintenance of the choriocapillaris. *Proc Natl Acad Sci U S A*. 2009;106(44):18751-18756.
12. Guymer R, Bird AC. *Age Changes in Bruch's Membrane and Related Structures*. Vol 18.; 1998.
13. Newsome DA, Huh W, Green WR. Bruch's membrane age-related changes vary by region. *Curr Eye Res*. 1987;6(10):1211-1221.
14. van der Schaft TL, Mooy CM, de Bruijn WC, Oron FG, Mulder PGH, de Jong PTVM. Histologic Features of the Early Stages of Age-related Macular Degeneration: A Statistical Analysis. *Ophthalmology*. 1992;99(2):278-286.
15. Sheraidah G, Steinmetz R, Maguire J, Pauleikhoff D, Marshall J, Bird AC. Correlation between Lipids Extracted from Bruch's Membrane and Age. *Ophthalmology*. 1993;100(1):47-51.
16. Chong NHV, Keonin J, Luthert PJ, et al. Decreased thickness and integrity of the macular elastic layer of Bruch's membrane correspond to the distribution of lesions associated with age-related macular degeneration. *Am J Pathol*. 2005;166(1):241-251.
17. Ugarte M, Hussain AA, Marshall J. An experimental study of the elastic properties of the human Bruch's membrane-choroid complex: Relevance to ageing. *Br J Ophthalmol*. 2006;90(5):621-626.
18. Holz FG, Sheraidah G, Pauleikhoff D, Bird AC. Analysis of Lipid Deposits Extracted From Human Macular and Peripheral Bruch's Membrane. *Arch Ophthalmol*. 1994;112(3):402-406.
19. Moore DJ, Hussain AA, Marshall J. Age-related variation in the hydraulic conductivity of Bruch's membrane. *Investig Ophthalmol Vis Sci*. 1995;36(7):1290-1297.
20. Starita C, Hussain AUA, Patmore A, Marshall J. Localization of the site of major resistance to fluid transport in Bruch's membrane. *Investig Ophthalmol Vis Sci*. 1997;38(3):762-767.
21. Moore DJ, Clover GM. The effect of age on the macromolecular permeability of human Bruch's membrane. *Investig Ophthalmol Vis Sci*. 2001;42(12):2970-2975.

22. Hussain AA, Starita C, Hodgetts A, Marshall J. Macromolecular diffusion characteristics of ageing human Bruch's membrane: Implications for age-related macular degeneration (AMD). *Exp Eye Res*. 2010;90(6):703-710.
23. Bhutto I, Lutty G. Understanding age-related macular degeneration (AMD): Relationships between the photoreceptor/retinal pigment epithelium/Bruch's membrane/choriocapillaris complex. *Mol Aspects Med*. 2012;33(4):295-317.
24. Bourne RRA, Jonas JB, Flaxman SR, et al. Prevalence and causes of vision loss in high-income countries and in Eastern and Central Europe: 1990-2010. *Br J Ophthalmol*. 2014;98(5):629-638.
25. Colijn JM, Buitendijk GHS, Prokofyeva E, et al. Prevalence of Age-Related Macular Degeneration in Europe: The Past and the Future. *Ophthalmology*. 2017;124(12):1753-1763.
26. Curcio CA, Johnson M, Rudolf M, Huang JD. The oil spill in ageing Bruch membrane. *Br J Ophthalmol*. 2011;95(12):1638-1645.
27. Fields MA, Del Priore L V., Adelman RA, Rizzolo LJ. Interactions of the choroid, Bruch's membrane, retinal pigment epithelium, and neurosensory retina collaborate to form the outer blood-retinal-barrier. *Prog Retin Eye Res*. Published online 2019.
28. Curcio CA. Soft drusen in age-related macular degeneration: Biology and targeting via the oil spill strategies. *Investig Ophthalmol Vis Sci*. 2018;59(4):AMD160-AMD181.
29. Klein R, Klein BEK, Tomany SC, Meuer SM, Huang G-H. *Ten-Year Incidence and Progression of Age-Related Maculopathy The Beaver Dam Eye Study*. Vol 109.; 2002.
30. Spraul CW, Lang GE, Grossniklaus HE, Lang GK. Histologic and morphometric analysis of the choroid, Bruch's membrane, and retinal pigment epithelium in postmortem eyes with age-related macular degeneration and histologic examination of surgically excised choroidal neovascular membranes. *Surv Ophthalmol*. 1999;44(2 SUPPL. 1):10-32.
31. Schlingemann RO. Role of growth factors and the wound healing response in age-related macular degeneration. *Graefe's Arch Clin Exp Ophthalmol*. 2004;242(1):91-101.
32. Christensen DRG, Brown FE, Cree AJ, Ratnayaka JA, Lotery AJ. Sorsby fundus dystrophy – A review of pathology and disease mechanisms. *Exp Eye Res*. 2017;165:35-46.
33. Gourier H, Chong N. Can Novel Treatment of Age-Related Macular Degeneration Be Developed by Better Understanding of Sorsby's Fundus Dystrophy. *J Clin Med*. 2015;4(5):874-883.
34. Sivaprasad S, Webster AR, Egan CA, Bird AC, Tufail A. Clinical Course and Treatment Outcomes of Sorsby Fundus Dystrophy. Published online 2008.
35. Bergen AAB, Plomp AS, Schuurman EJ, et al. Mutations in ABCC6 cause pseudoxanthoma elasticum. *Nat Genet*. 2000;25(2):228-231.
36. Le Saux O, Urban Z, Tschuch C, et al. Mutations in a gene encoding an ABC transporter cause pseudoxanthoma elasticum. *Nat Genet*. 2000;25(2):223-227.
37. Ringpfeil F, Lebwohl MG, Christiano AM, Uitto J. Pseudoxanthoma elasticum: mutations in the MRP6 gene encoding a transmembrane ATP-binding cassette (ABC) transporter. *Proc Natl Acad Sci U S A*. 2000;97(11):6001-6006.
38. Kranenburg G, Baas AF, de Jong PA, Asselbergs FW, Visseren FLJ, Spiering W. The prevalence of pseudoxanthoma elasticum: Revised estimations based on genotyping in a high vascular risk cohort. *Eur J Med Genet*. 2019;62(2):90-92.
39. Plomp AS, Toonstra J, Bergen AAB, van Dijk MR, de Jong PTVM. Proposal for updating the pseudoxanthoma elasticum classification system and a review of the clinical findings. *Am J Med Genet A*. 2010;152A(4):1049-1058.
40. Grönblad E. Angioid streaks — Pseudoxanthoma elasticum: Vorläufige Mitteilung. *Acta Ophthalmol*. 1929;7(1-4):329-329.
41. Strandberg J. Pseudoxanthoma Elasticum. *Z Haut Geschlechtskr*. 1929;31:689-694.
42. Goodman RM, Smith EW, Paton D, et al. Pseudoxanthoma elasticum: a clinical and histopatholocial study. *Medicine (Baltimore)*. 1963;42:297-334.

43. Jansen RS, Kucukosmanoglu A, de Haas M, et al. ABCC6 prevents ectopic mineralization seen in pseudoxanthoma elasticum by inducing cellular nucleotide release. *Proc Natl Acad Sci U S A*. 2013;110(50):20206-20211.
44.. Jansen RS, Duijst S, Mahakena S, et al. ABCC6-mediated ATP secretion by the liver is the main source of the mineralization inhibitor inorganic pyrophosphate in the systemic circulation-brief report. *Arterioscler Thromb Vasc Biol*. 2014;34(9):1985-1989.
45. Rutsch F, Ruf N, Vaingankar S, et al. Mutations in ENPP1 are associated with "idiopathic" infantile arterial calcification. *Nat Genet*. 2003;34(4):379-381.
46. Rutsch F, Böyer P, Nitschke Y, et al. Hypophosphatemia, hyperphosphaturia, and bisphosphonate treatment are associated with survival beyond infancy in generalized arterial calcification of infancy. *Circ Cardiovasc Genet*. 2008;1(2):133-140.
47. Nitschke Y, Rutsch F. Generalized arterial calcification of infancy and pseudoxanthoma elasticum: two sides of the same coin. *Front Genet*. 2012;3:302.
48. Hilaire CS, Ziegler SG, Markello TC, et al. NT5E mutations and arterial calcifications. *N Engl J Med*. 2011;364(5):432-442.
49. Li Q, Arányi T, Váradi A, Terry SF, Uitto J. Research Progress in Pseudoxanthoma Elasticum and Related Ectopic Mineralization Disorders. *J Invest Dermatol*. 2016;136(3):550-556.
50. Hu X, Plomp AS, van Soest S, Wijnholds J, de Jong PTVM, Bergen AAB. Pseudoxanthoma elasticum: a clinical, histopathological, and molecular update. *Surv Ophthalmol*. 2003;48(4):424-438.
51. Lefthériotis G, Omarjee L, Le Saux O, et al. The vascular phenotype in pseudoxanthoma elasticum and related disorders: Contribution of a genetic disease to the understanding of vascular calcification. *Front Genet*. 2013;4(FEB):1-9.
52. Kranenburg G, de Jong PA, Mali WP, Attrach M, Visseren FLJ, Spiering W. Prevalence and severity of arterial calcifications in pseudoxanthoma elasticum (PXE) compared to hospital controls. Novel insights into the vascular phenotype of PXE. *Atherosclerosis*. 2017;256:7-14.
53. Kranenburg G, Visseren FLJ, de Borst GJ, de Jong PA, Spiering W. Arterial stiffening and thickening in patients with pseudoxanthoma elasticum. *Atherosclerosis*. 2018;270:160-165.
54. Leftheriotis G, Abraham P, Le Corre Y, et al. Relationship between ankle brachial index and arterial remodeling in pseudoxanthoma elasticum. *J Vasc Surg*. 2011;54(5):1390-1394.
55. Kauw F, Kranenburg G, Jaap Kappelle L, et al. Cerebral disease in a nationwide Dutch pseudoxanthoma elasticum cohort with a systematic review of the literature. Published online 2016.
56. Mansour AM, Henkind P. Marked thickening of Bruch's membrane in a 17-year-old patient with angioid streaks [6]. *Eye*. 1998;12(5):898-900.
57. Böck J. Zur Klinik und Anatomie der gefäßähnlichen Streifen im Augenhintergrund. *Z Augenheilk*. 1938;95:1-49.
58. Hagedoorn A. Angioid streaks. *Arch Ophthalmol*. 1939;21:935-965.
59. Verhoeff FH. Histological findings in a case of angioid streaks. *Br J Ophthalmol*. 1948;32(9):531-544.
60. Klien BA. Angioid streaks. A clinical and histophathologic study. *Am J Ophthalmol*. 1947;30(8):955-968.
61. Jensen OA. Bruch's membrane in pseudoxanthoma elasticum. *Albr von Graefes Arch fur Klin und Exp Ophthalmol*. 1977;203(3-4):311-320.
62. Gheduzzi D, Sammarco R, Quaglino D, et al. Extracutaneous ultrastructural alterations in pseudoxanthoma elasticum. *Ultrastruct Pathol*. 2003;27(6):375-384.
63. Gorgels TGMF, Hu X, Scheffer GL, et al. Disruption of Abcc6 in the mouse: novel insight in the pathogenesis of pseudoxanthoma elasticum. *Hum Mol Genet*. 2005;14(13):1763-1773.
64. Gorgels TGMF, Teeling P, Meeldijk JD, et al. Abcc6 deficiency in the mouse leads to calcification of collagen fibers in Bruch's membrane. *Exp Eye Res*. 2012;104:59-64.
65. Charbel Issa P, Finger RP, Gotting C, Hendig D, Holz FG, Scholl HPN. Centrifugal fundus abnormalities in pseudoxanthoma elasticum. *Ophthalmology*. 2010;117(7):1406-1414.

66. Naouri M, Boisseau C, Bonicel P, et al. Manifestations of pseudoxanthoma elasticum in childhood. *Br J Dermatol*. 2009;161(3):635-639.
67. Krill AE, Klien BA, Archer DB. Precursors of angioid streaks. *Am J Ophthalmol*. 1973;76(6):875-879.
68. Mansour AM, Ansari NH, Shields JA, Annesley, Jr. WH, Cronin CM, Stock L. Evolution of Angioid Streaks. *Ophthalmologica*. 1993;207(2):57-61.
69. Charbel Issa P, Finger RP, Holz FG, Scholl HPN. Multimodal Imaging Including Spectral Domain OCT and Confocal Near Infrared Reflectance for Characterization of Outer Retinal Pathology in Pseudoxanthoma Elasticum. *Investig Opthalmology Vis Sci*. 2009;50(12):5913.
70. Hagedoorn A. Angioid streaks and traumatic ruptures of Bruch's membrane. *Br J Ophthalmol*. 1975;59(5):267.
71. Jampol LM, Acheson R, Eagle RC, Serjeant G, O'Grady R. Calcification of Bruch's Membrane in Angioid Streaks With Homozygous Sickle Cell Disease. *Arch Ophthalmol*. 1987;105(1):93-98.
72. Finger RP, Charbel Issa P, Ladewig MS, et al. Pseudoxanthoma elasticum: genetics, clinical manifestations and therapeutic approaches. *Surv Ophthalmol*. 2009;54(2):272-285.
73. Scholz RO. Angioid streaks. *Arch Ophthalmol*. 1941;26(4):677-695.
74. Connor JP, Juergens JL, Perry HO, Hollenhorst RW, Edwards JE. Pseudoxanthoma elasticum and angioid streaks. A review of 106 cases. *Am J Med*. 1961;30(4):537-543.
75. Georgalas I, Papaconstantinou D, Koutsandrea C, et al. Angioid streaks, clinical course, complications, and current therapeutic management. *Ther Clin Risk Manag*. 2009;5(1):81-89.
76. Nakagawa S, Yamashiro K, Tsujikawa A, et al. The time course changes of choroidal neovascularization in angioid streaks. *Retina*. 2013;33(4):825-833.
77. Baillif-Gostoli S, Quaranta-El Maftouhi M, Mauget-Faysse M. Polypoidal choroidal vasculopathy in a patient with angioid streaks secondary to pseudoxanthoma elasticum. *Graefes Arch Clin Exp Ophthalmol*. 2010;248(12):1845-1848.
78. Gliem M, Muller PL, Birtel J, Hendig D, Holz FG, Charbel Issa P. Frequency, Phenotypic Characteristics and Progression of Atrophy Associated With a Diseased Bruch's Membrane in Pseudoxanthoma Elasticum. *Invest Ophthalmol Vis Sci*. 2016;57(7):3323-3330.
79. Tsui I, Fuchs BS, Chou CL, Chang S, Tsang SH. Non-vascular vision loss in pseudoxanthoma elasticum. *Doc Ophthalmol*. 2008;117(1):65-67.
80. Holz FG, Strauss EC, Schmitz-Valckenberg S, Van Lookeren Campagne M. Geographic atrophy: Clinical features and potential therapeutic approaches. *Ophthalmology*. 2014;121(5):1079-1091.
81. Bird AC, Phillips RL, Hageman GS. Geographic atrophy: a histopathological assessment. *JAMA Ophthalmol*. 2014;132(3):338-345.
82. Mullins RF, Johnson MN, Faidley EA, Skeie JM, Huang J. Choriocapillaris vascular dropout related to density of drusen in human eyes with early age-related macular degeneration. *Investig Ophthalmol Vis Sci*. 2011;52(3):1606-1612.
83. Handa JT, Bowes Rickman C, Dick AD, et al. A systems biology approach towards understanding and treating non-neovascular age-related macular degeneration. *Nat Commun*. 2019;10(1):3347.
84. Schoenberger SD, Agarwal A. Geographic chorioretinal atrophy in pseudoxanthoma elasticum. *Am J Ophthalmol*. 2013;156(4):715-723.
85. Klein R, Peto T, Bird A, Vannewkirk MR. The epidemiology of age-related macular degeneration. *Am J Ophthalmol*. 2004;137(3):486-495.
86. Hocaoglu M, Karacorlu M, Sayman Muslubas I, Arf S, Ozdemir H, Uysal O. Visual impairment in pseudoxanthoma elasticum: A survey of 53 patients from Turkey. *Eur J Ophthalmol*. 2016;26(5):449-453.
87. Plomp AS, Bergen AAB, Florijn RJ, et al. Pseudoxanthoma elasticum: Wide phenotypic variation in homozygotes and no signs in heterozygotes for the c.3775delT mutation in ABCC6. *Genet Med*. 2009;11(12):852-858.

88. Legrand A, Cornez L, Samkari W, et al. Mutation spectrum in the ABCC6 gene and genotype–phenotype correlations in a French cohort with pseudoxanthoma elasticum. *Genet Med*. 2017;19(8):909-917.
89. Pfendner EG, Vanakker OM, Terry SF, et al. Mutation detection in the ABCC6 gene and genotype phenotype analysis in a large international case series affected by pseudoxanthoma elasticum. *J Med Genet*. 2007;44(10):621-628.
90. Audo I, Vanakker OM, Smith A, et al. Pseudoxanthoma elasticum with generalized retinal dysfunction, a common finding? *Invest Ophthalmol Vis Sci*. 2007;48(9):4250-4256.
91. François J, Rouck A. Electrophysiological Studies in Groenblad-strandberg Syndrome. In: *Doc. Ophthalmol. Proc. Ser.* ; 1980:19-25.
92. Holz FG, Jubb C, Fitzke FW, Bird AC, Pope FM. Dark adaptation and scotopic perimetry over "peau d'orange" in pseudoxanthoma elasticum. *Br J Ophthalmol*. 1994;78(1):79-80.
93. Hess K, Gliem M, Birtel J, et al. Impaired Dark Adaptation Associated With a Diseased Bruch Membrane in Pseudoxanthoma Elasticum. *Retina*. 2019;Publish Ah:1.
94. Finger RP, Charbel Issa P, Ladewig M, Holz FG, Scholl HPN. Intravitreal bevacizumab for choroidal neovascularisation associated with pseudoxanthoma elasticum. *Br J Ophthalmol*. 2008;92(4):483-487.
95. Mimoun G, Tilleul J, Leys A, Coscas G, Soubrane G, Souied EH. Intravitreal ranibizumab for choroidal neovascularization in angioid streaks. *Am J Ophthalmol*. 2010;150(5):692-700.e1.
96. Gliem M, Birtel J, Herrmann P, et al. Aflibercept for choroidal neovascularizations secondary to pseudoxanthoma elasticum: a prospective study. *Graefe's Arch Clin Exp Ophthalmol*. 2020;258(2):311-318.
97. Avery RL, Castellarin AA, Steinle NC, et al. Systemic pharmacokinetics following intravitreal injections of ranibizumab, bevacizumab or aflibercept in patients with neovascular amd. *Br J Ophthalmol*. 2014;98(12):1636-1641.
98. Holash J, Davis S, Papadopoulos N, et al. VEGF-Trap: A VEGF blocker with potent antitumor effects. *Proc Natl Acad Sci U S A*. 2002;99(17):11393-11398.
99. Gliem M, Finger RP, Fimmers R, Brinkmann CK, Holz FG, Charbel Issa P. Treatment of choroidal neovascularization due to angioid streaks. A Comprehensive Review. *Retina*. 2013;33(7):1300-1314.
100. Rosenfeld PJ, Brown DM, Heier JS, et al. Ranibizumab for Neovascular Age-Related Macular Degeneration. *N Engl J Med*. 2006;355(14):1419-1431.
101. Finger RP, Charbel Issa P, Schmitz-Valckenberg S, Holz FG, Scholl HN. Long-term effectiveness of intravitreal bevacizumab for choroidal neovascularization secondary to angioid streaks in pseudoxanthoma elasticum. *Retina*. 2011;31(7):1268-1278.
102. Sawa M, Gomi F, Tsujikawa M, Sakaguchi H, Tano Y. Long-term Results of Intravitreal Bevacizumab Injection for Choroidal Neovascularization Secondary to Angioid Streaks. *Am J Ophthalmol*. 2009;148(4):584-590.e2.
103. Chatziralli I, Saitakis G, Dimitriou E, et al. Angioid Streaks: A comprehensive review from pathophysiology to treatment. *Retina*. 2019;39(1):1-11.
104. Grunwald JE, Daniel E, Huang J, et al. Risk of geographic atrophy in the comparison of age-related macular degeneration treatments trials. *Ophthalmology*. 2014;121(1):150-161.
105. Young M, Chui L, Fallah N, et al. Exacerbation of choroidal and retinal pigment epithelial atrophy after anti-vascular endothelial growth factor treatment in neovascular age-related macular degeneration. *Retina*. 2014;34(7):1308-1315.
106. Pomozi V, Brampton C, van de Wetering K, et al. Pyrophosphate Supplementation Prevents Chronic and Acute Calcification in ABCC6-Deficient Mice. *Am J Pathol*. 2017;187(6):1258-1272.
107. Orriss IR, Arnett TR, Russell RGG. Pyrophosphate: A key inhibitor of mineralisation. *Curr Opin Pharmacol*. 2016;28:57-68.

108. Edouard T, Chabot G, Miro J, et al. Efficacy and safety of 2-year etidronate treatment in a child with generalized arterial calcification of infancy. *Eur J Pediatr*. 2011;170(12):1585-1590.
109. Li Q, Sundberg JP, Levine MA, Terry SF, Uitto J. The effects of bisphosphonates on ectopic soft tissue mineralization caused by mutations in the ABCC6 gene. *Cell Cycle*. 2015;14(7):1082-1089.
110. Li Q, Kingman J, Sundberg JP, Levine MA, Uitto J. Etidronate prevents, but does not reverse, ectopic mineralization in a mouse model of pseudoxanthoma elasticum (Abcc6-/-). *Oncotarget*. 2018;9(56):30721-30730.
111. Kranenburg G, Bartstra JW, Weijmans M, et al. Bisphosphonates for cardiovascular risk reduction: A systematic review and meta-analysis. *Atherosclerosis*. 2016;252:106-115.
112. Kranenburg G, de Jong PA, Bartstra JW, et al. Etidronate for Prevention of Ectopic Mineralization in Patients With Pseudoxanthoma Elasticum. *J Am Coll Cardiol*. 2018;71(10):1117-1126.
113. Honda S, Nagai T, Kondo N, et al. Therapeutic effect of oral bisphosphonates on choroidal neovascularization in the human eye. *J Ophthalmol*. 2010;2010.
114. Miki A, Honda S, Nagai T, Tsukahara Y, Negi A. Effects of oral bisphosphonates on myopic choroidal neovascularisation over 2 years of follow-up: comparison with anti-VEGF therapy and photodynamic therapy. A pilot study. *Br J Ophthalmol*. 2013;97(6):770-774.
115. Mammo Z, Guo M, Maberley D, Matsubara J, Etminan M. Oral Bisphosphonates and Risk of Wet Age-Related Macular Degeneration. *Am J Ophthalmol*. 2016;168:62-67.
116. Gliem M, Hendig D, Finger RP, Holz FG, Charbel Issa P. Reticular pseudodrusen associated with a diseased bruch membrane in pseudoxanthoma elasticum. *JAMA Ophthalmol*. 2015;133(5):581-588.
117. Gliem M, Müller PL, Birtel J, et al. Quantitative fundus autofluorescence in pseudoxanthoma elasticum. *Investig Ophthalmol Vis Sci*. 2017;58(14):6159-6165.
118. Nassif NA, Cense B, Park BH, et al. In vivo high-resolution video-rate spectral-domain optical coherence tomography of the human retina and optic nerve. *Opt Express*. 2004;12(3):367.
119. Aumann S, Donner S, Fischer J, Müller F. Optical Coherence Tomography (OCT): Principle and Technical Realization. In: *High Resolution Imaging in Microscopy and Ophthalmology*. Springer International Publishing; 2019:59-85.
120. Chen X, Hou P, Jin C, et al. Quantitative analysis of retinal layer optical intensities on three-dimensional optical coherence tomography. *Invest Ophthalmol Vis Sci*. 2013;54(10):6846-6851.
121. Wu Z, Ayton LN, Guymer RH, Luu CD. Relationship Between the Second Reflective Band on Optical Coherence Tomography and Multifocal Electroretinography in Age-Related Macular Degeneration. *Investig Opthalmology Vis Sci*. 2013;54(4):2800.
122. Spaide RF, Curcio CA. Anatomical correlates to the bands seen in the outer retina by optical coherence tomography: literature review and model. *Retina*. 2011;31(8):1609-1619.
123. Staurenghi G, Sadda S, Chakravarthy U, Spaide RF. Proposed Lexicon for Anatomic Landmarks in Normal Posterior Segment Spectral-Domain Optical Coherence Tomography: The IN•OCT Consensus. *Ophthalmology*. 2014;121(8):1572-1578.
124. Spaide RF. Peau d'orange and angioid streaks: manifestations of Bruch membrane pathology. *Retina*. 2015;35(3):392-397.
125. Charbel Issa P, Finger RP, Holz FG, Scholl HPN. Multimodal imaging including spectral domain OCT and confocal near infrared reflectance for characterization of outer retinal pathology in pseudoxanthoma elasticum. *Invest Ophthalmol Vis Sci*. 2009;50(12):5913-5918.
126. Berendschot TTJM, Delint PJ, Van Norren D. *Fundus Reflectance-Historical and Present Ideas*. Vol 22.; 2003.
127. Elsner AE, Burns SA, Weiter JJ, Delori FC. Infrared imaging of sub-retinal structures in the human ocular fundus. *Vision Res*. 1996;36(1):191-205.
128. Theelen T, Berendschot TTJM, Hoyng CB, Boon CJF, Klevering BJ. Near-infrared reflectance imaging of neovascular age-related macular degeneration. *Graefe's Arch Clin Exp Ophthalmol*. 2009;247(12):1625-1633.

129. Cherrick GR, Stein SW, Leevy CM, Davidson CS. Indocyanine green: observations on its physical properties, plasma decay, and hepatic extraction. *J Clin Invest*. 1960;39:592-600.
130. Chang AA, Zhu M, Billson F. The Interaction of Indocyanine Green with Human Retinal Pigment Epithelium. *Investig Opthalmology Vis Sci*. 2005;46(4):1463.
131. Blanco Rivera MC, Gómez Ulla De Irazazábal F, Ferrer Jaureguizar J, Abelenda Pose D. Indocyanine green angiography in angioid streaks. *Acta Ophthalmol Scand*. 2001;75:261-265.
132. Lafaut BA, Leys AM, Scassellati-Sforzolini B, Priem H, De Laey JJ. Comparison of fluorescein and indocyanine green angiography in angioid streaks. *Graefes Arch Clin Exp Ophthalmol*. 1998;236(5):346-353.
133. Delori FC, Dorey CK, Staurenghi G, Arend O, Goger DG, Weiter JJ. In vivo fluorescence of the ocular fundus exhibits retinal pigment epithelium lipofuscin characteristics. *Investig Ophthalmol Vis Sci*. 1995;36(3):718-729.
134. Sparrow JR, Wu Y, Nagasaki T, Yoon KD, Yamamoto K, Zhou J. Fundus autofluorescence and the bisretinoids of retina. *Photochem Photobiol Sci*. 2010;9(11):1480-1489.
135. Sparrow JR, Nakanishi K, Parish CA. The lipofuscin fluorophore A2E mediates blue light-induced damage to retinal pigmented epithelial cells. *Investig Ophthalmol Vis Sci*. 2000;41(7):1981-1989.
136. Von Rückmann A, Fitzke FW, Bird AC. In vivo fundus auto fluorescence in macular dystrophies. *Arch Ophthalmol*. 1997;115(5):609-615.
137. Agarwal A, Patel P, Adkins T, Gass JDM. Spectrum of pattern dystrophy in pseudoxanthoma elasticum. *Arch Ophthalmol (Chicago, Ill 1960)*. 2005;123(7):923-928.
138. Finger RP, Charbel Issa P, Ladewig M, Gotting C, Holz FG, Scholl HPN. Fundus autofluorescence in Pseudoxanthoma elasticum. *Retina*. 2009;29(10):1496-1505.
139. De Zaeytijd J, Vanakker OM, Coucke PJ, De Paepe A, De Laey J-J, Leroy BP. Added value of infrared, red-free and autofluorescence fundus imaging in pseudoxanthoma elasticum. *Br J Ophthalmol*. 2010;94(4):479-486.

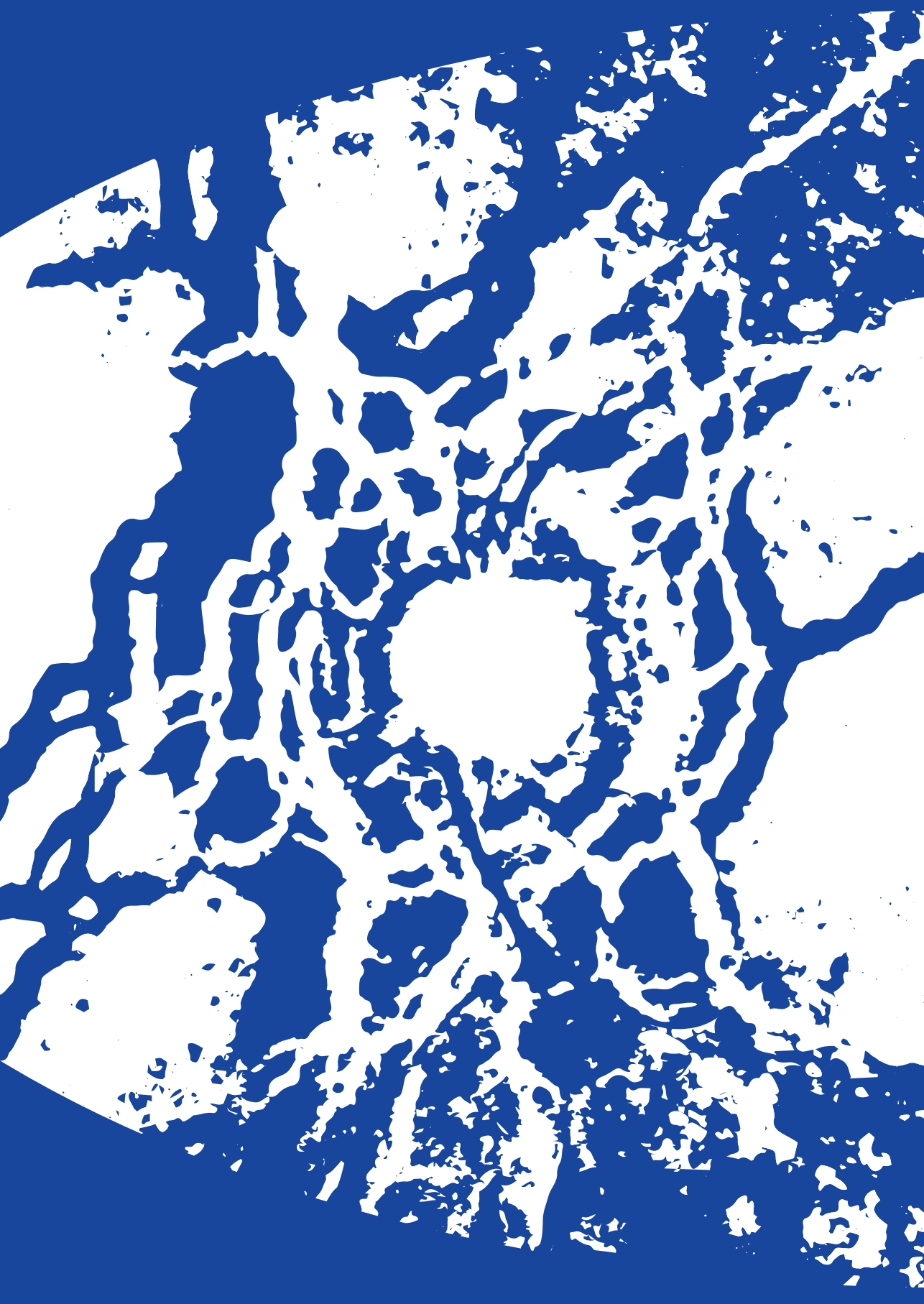


PART ONE


Chapter 2

The natural history of Bruch's membrane calcification in pseudoxanthoma elasticum

Sara Risseeuw
Redmer van Leeuwen
Saskia M. Imhof
Wilko Spiering
Jeannette Ossewaarde – van Norel

Submitted

Abstract

Objective

To describe the natural history of Bruch's membrane calcification in patients with pseudoxanthoma elasticum (PXE).

Design

Cross-sectional and longitudinal cohort study.

Subjects

All 242 eyes of 121 PXE patients younger than 50 years, of which 78 patients had follow-up imaging after more than one year.

Methods

All patients underwent multimodal imaging, including color fundus photography, near-infrared reflectance imaging (NIR) and indocyanine green angiography (ICG-A). We determined the distance from the optic disc to the central and temporal border of peau d'orange on NIR, expressed in horizontal optic disc diameter (ODD). The length of the longest angioid streak was classified into five zones. If available, late-phase ICG-A was graded for a hypofluorescent area.

Main outcome measures

Age-specific changes of peau d'orange, angioid streaks, and ICG-A hypofluorescence as surrogate markers for the extent of BM calcification.

Results

In cross-sectional analysis, longer angioid streaks were associated with increasing age (*P* for trend <0.001).The temporal border of peau d'orange had a weak association with increasing age (ß 0.02, 95% CI 0.00 – 0.04), while the central border had a strong association (ß 0.12, 95% CI 0.09 – 0.15). Longitudinal analysis revealed a median shift of the central border to the periphery of 0.08 ODD per year (IQR 0.00 – 0.17, $P < 0.001$). This shift was more pronounced in patients younger than 20 years (0.12 ODD per year (IQR 0.08 – 0.28) than in patients older than 40 years (0.07 ODD per year (IQR -0.05 – 0.15). The temporal border did not shift during follow-up ($P = 0.69$). New or growing angioid streaks were detected in 39 of 156 (25%) eyes. The hypofluorescent area on ICG-A was only visible in the fourth or fifth decade and correlated with longer angioid streaks.

Conclusions

In PXE patients, the speckled BM calcification slowly confluences during life. The location of the temporal border of peau d'orange remains rather constant, whereas the central border shifts to the periphery. This suggests the presence of a predetermined area for BM calcification. A larger ICG-A hypofluorescent area correlates with older age and longer angioid streaks, which implies that it depends on the degree of BM calcification.

Background

PXE is a rare autosomal recessive disorder (OMIM #264800) in which biallelic mutations in the *ABCC6* gene lead to calcification of elastic fibres in the skin, vasculature and Bruch's membrane (BM) of the eyes.[1–3] BM calcification eventually causes macular degeneration and subsequent visual impairment at a relatively young age.[4,5]

The typical manifestations of BM calcification in the fundus are peau d'orange and angioid streaks. Peau d'orange describes the speckled pattern seen with fundoscopy and near-infrared reflectance (NIR) imaging and is believed to be the transition zone between a calcified BM and a normal fundus.[6,7] The presence of peau d'orange precedes the formation of angioid streaks in the brittle calcified BM.[8,9] Angioid streaks are breaks in BM which are visible as irregular jagged lines in the fundus and are probably caused by mechanical stress exerted on the eye.[10] Angioid streaks are not visible yet at birth, and are believed to occur around the second decade of life.[9] In younger patients, peau d'orange is often present in the posterior pole, while later disease stages often present with more peripheral peau d'orange.[11] Furthermore, on late-phase indocyanine green angiography (ICG-A), a typical hypofluorescent area with a speckled border is found in the posterior pole, mimicking peau d'orange, but located more centrally.[6] These findings led to the hypothetical model of a centrifugal spread of BM calcification by Charbel Issa et al.[6]

Little information is available on the natural course of BM calcification. The recent start of therapeutic developments, such as etidronate and dietary pyrophosphate, necessitates knowledge on the natural course of BM calcification.[12,13] Also, more severe BM calcification increases the risk for macular degeneration and thereby has an impact on the visual prognosis.[14]

We aim to investigate the natural history of BM calcification in PXE patients younger than 50 years, before the onset of frequent macular degeneration in the sixth decade which impedes the assessment of early clinical features in the fundus of a PXE patient. We studied the age-specific manifestations of peau d'orange, angioid streaks and ICG-A hypofluorescence, which we used as surrogate markers for BM calcification. Moreover, we studied longitudinal changes of these features over the period of at least one year.

Methods

Design and study population

We performed this retrospective cross-sectional and longitudinal cohort study within the Dutch National Expertise Center for PXE, a multidisciplinary tertiary referral center that is situated at the University Medical Center Utrecht, the Netherlands. We included all patients with a diagnosis of PXE according to the criteria as proposed by Plomp et al.[2] All patients fulfilled at least two of the three following criteria: skin involvement (papules, plaques or a positive skin biopsy), eye involvement (peau d'orange or angioid streaks longer than one disk diameter), and/or genetic confirmation (a double *ABCC6* mutation or a first degree relative with PXE). The institutional ethics committee approved the study protocol (METC 19/257) and additional informed consent was obtained for all patients who agreed to a late-phase ICG-A (METC 18/767).

We included patients younger than 50 years at the time of their first 55° near-infrared reflectance (NIR) imaging of the retina. This resulted in a study population of 121 patients.

Ophthalmological data

The standard ophthalmological examination included a best-corrected-visual acuity (BCVA) measurement and fundoscopy. Retinal imaging consisted of color fundus photography (FF 450 plus, Carl Zeiss Meditec AG, Jena, Germany), spectral-domain optical coherence tomography (SD-OCT), 55° NIR imaging and fundus autofluorescence (FAF) (all three by Spectralis HRA-OCT, Heidelberg Engineering, Heidelberg, Germany). Late-phase ICG-A was either performed on clinical indication, or for research purposes with the patient's approval and written informed consent. If the patient had visited our department more than once, we also investigated the data on the most recent visit.

We classified the BCVA of the better eye according to the severity of visual impairment according to the criteria of the World Health Organization.[15]

Assessment of angioid streaks

We measured the spread of angioid streaks as a proxy for the extent of BM calcification.[6,16] Using 55° NIR imaging, we evaluated the length of the longest angioid streak from the center of the optic disk. This was graded into angioid streaks extending less than 3 mm from the center of the optic disk (zone 1), 3 – 6 mm from the center of the optic

disk (zone 2), 6 – 9 mm from the center of the optic disk (zone 3) and more than 9 mm from the center of the optic disk (zone 4). Some eyes did not have detectable angioid streaks. The grading of angioid streaks was irrespective of their topographical location in the retina and based on both central and mid-peripheral 55° NIR imaging.

Also, we graded the presence of angioid streaks in the macula by manually positioning the ETDRS grid on the foveal dip and grading the presence or absence of angioid streaks in the central 3000 µm diameter on the 30° NIR imaging. Furthermore, we assessed longitudinal changes of angioid streaks. To do so, we compared all available central and mid-peripheral 55° NIR imaging of the first and last visit to determine lengthening of, or new and/or branching angioid streaks. Last, we assessed changes in angioid streaks within the central 3000 µm by comparing the first and last 30° NIR imaging. If necessary, fundus photography was used to verify changes in angioid streaks.

Assessment of peau d'orange

We measured the distance of the central and peripheral borders of peau d'orange on NIR imaging along a virtual axis from the temporal border of the optic disc to the temporal periphery through the fovea (Figure 2.1). For each eye, we assembled the central and the temporal 55° NIR imaging to create an aligned montage (Adobe Photoshop CS6, Adobe Systems Inc, San Jose, CA, USA). The peripheral and central border of peau d'orange were defined as the temporal and central ending of an area with characteristic speckling with hypo- and hyperreflectivity on NIR, respectively. We used color fundus photography and 30° NIR imaging to verify the location of the borders, if necessary.

In some patients, the central border of the peau d'orange coincided with temporal sparing, a phenomenon of an island of relative decreased reflectivity temporal from the macula (Figure 2.2, B3 and C1).[6] Most PXE patients present with temporal sparing and we assume that it is a phenomenon that is independent of the spread of BM calcification. However, the speckled aspect of temporal sparing resembles peau d'orange, which impedes the assessment of peau d'orange if the central border is in that area. Therefore, if the temporal sparing coincided with the presumed central border of peau d'orange, we assessed the total area of peau d'orange within the posterior pole to determine the most accurate position of the central border.

Measurements were made semi-quantitively, by using the horizontal optic disk diameter (ODD) as the measurement unit in ImageJ (ImageJ, https://imagej.nih.gov/ij/). The ODD was chosen to enable longitudinal measurements within one patient and to correct for differences in refraction error and image settings.

We assessed the intra-observer and inter-observer reproducibility of this measurement in a subset of 10 patients (20 eyes). For the temporal border, the intra-observer agreement had a mean difference of -0.13 ODD (95% limits of agreement (LoA) -0.80 – 0.55). The intra-observer reliability was excellent with an intraclass correlation coefficient (ICC) of 0.96 (95% confidence interval (CI) 0.89 – 0.98).[17] The central border had an intra-observer difference of -0.02 (95% LoA -0.51 – 0.46) and also high reliability (ICC 0.99, 95% CI 0.99 – 1).

Inter-observer reproducibility was assessed by three graders (SR, RvL, JOvN) and analyzed in three pairs of measurements. For the temporal border, the mean differences were -0.25, 0.01 and 0.08 ODD and the ICC's were moderate to excellent

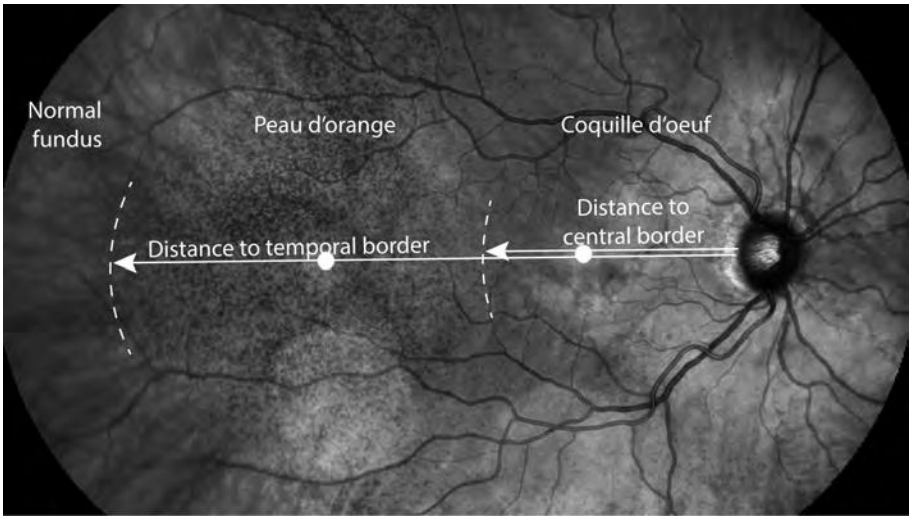

Figure 2.1 Assessment of the borders of peau d'orange in patients with PXE using near infrared reflectance imaging (NIR). The 55° central and temporal NIR images were merged. The temporal and central border of peau d'orange were defined as ending of an area with characteristic speckling with hypo- and hyperreflectivity on NIR along a line through the optic disc and the fovea. The white dots on the papillo-foveal axis are imaging artefacts.

(0.69, 0.87 and 0.83, respectively).[17] For the central border, the mean differences were 0.07, 0.25 and 0.28 ODD and the ICC's were moderate to excellent (0.86, 0.95 and 0.64, respectively).[17]

Ophthalmological phenotype

We graded the presence of (in-)active CNV and macular atrophy in the posterior pole per eye. A CNV was present in case of sub- or intraretinal fluid and/or a neovascular complex on SD-OCT, leakage of CNV and/or staining of scars on fluorescein- or ICG angiography and/or hemorrhage, scarring or hyperpigmentation on color fundus photography. Grading of macular atrophy was based on the loss of the RPE signal on SD-OCT, sharply demarcated areas of hypofluorescence on FAF and hypopigmentation and visible choroidal vessels on color fundus photography in the posterior pole with a minimal size of the atrophic largest lesion of at least half the area of the optic disk.

Presence of pattern dystrophy-like changes was based on focal increased autofluorescence on FAF in the posterior pole resembling pattern dystrophies in an area of at least 1 ODD diameter.[18,19] If available, the late-phase ICG-A was assessed for the presence of a speckled hypofluorescent area superimposed on the physiological hypofluorescence in the macula.[6] Late-phase ICG-A was captured at least 30 minutes after administration of the ICG dye.

Data analyses

Categorical data is presented as numbers (percentages), normally distributed data as mean (± standard deviation) and data with a non-parametric distribution as median (interquartile range (IQR)). Differences between groups were tested with the Pearsons Chi-Square test or the Mann-Whitney U test when appropriate. The one-sample Wilcoxon signed-rank test was used to test for a longitudinal difference of the border of peau d'orange. To test for a trend effect of age on the extent of angioid streaks, logistic or linear regression models were built with age or angioid streaks as a continuous determinant. To investigate longitudinal changes, we excluded patients with a follow-up duration of less than 12 months. To obtain information on the progression of peau d'orange, we calculated the difference of the borders of peau d'orange between the first and last visit. Then, we corrected this for the duration of follow-up to obtain a measure of change per year of follow-up.

Associations between age, peau d'orange, and angioid streaks were investigated with linear regression analysis with the right eye as the outcome. Linear mixed model

analysis was used to test for differences on eye level while correcting for both eyes of a patient and to test for a trend effect of angioid streaks on peau d'orange on eye level. The dependent variable was set as a fixed effect and the individual patient was modelled as a random intercept. A *P*-value <0.05 was considered statistically significant. We used R version 3.6.1 for data analysis. The package 'nlme' (version 3.1 – 140) was used for mixed model analysis.

Results

In total, 121 PXE patients were included. The median age was 37 years (IQR 26 – 46), ranging from 9 to 49 years and 87 of them (72%) were female. Further characteristics of the total group and stratified per decade are presented in Table 2.1. Two patients, both in the fifth decade, were visually impaired due to PXE-related macular degeneration and two patients had an amblyopic eye.

Angioid streaks

Cross-sectional analysis

The length of angioid streaks was associated with age (Table 2.1). The percentage of patients with the longest angioid streaks, increased from 6% in patients aged 0 – 19 years to 52% in patients aged 40 – 49 years. The mean age of the 7 patients without angioid streaks was 12 ± 2 years. For zone 1 (n = 3) the mean age was 31 ± 13 years, for zone 2 (n = 46) 32 ± 11 years, for zone 3 (n = 26) 37 ± 11 years and for zone 4 (n = 39) this was 41 ± 8 years. Angioid streaks in the central 3000 µm of the macula were present in 130 eyes of 76 PXE patients (54% of all eyes). In three eyes of two patients, the presence of macular angioid streaks could not be assessed due to extensive pathology.

Longitudinal analysis

Of all patients, 78 had follow-up imaging with a minimum duration of one year (median duration 41 months, IQR 26 – 53 months). The imaging of these patients was evaluated for changes in length and development growth of new angioid streaks. Of the 156 eyes, 117 (75%) did not show changes in angioid streaks. However, in 27 eyes (17%) of 23 patients (mean age at baseline 30 years, range 15 – 48) we observed lengthening of angioid streaks. In 12 eyes (8%) of 11 patients (mean age at baseline 31 years, range 14 – 48) we observed new (branches of) angioid streaks. In total, changes in angioid streaks were observed in 39 eyes (25%) with a cumulative follow-up of 254 patient years. Examples of patients with changes in angioid streaks are presented in Figure 2.2.

Table 2.1 Patient characteristics

		Overall	0 - 19 years	20 - 29 years	30 - 39 years	40 - 49 years	Nominal *P*	*P* for trend
		N = 121	*N* = 17	*N* = 27	*N* = 23	*N* = 54		
Female		87 (72%)	13 (77%)	23 (85%)	19 (83%)	32 (59%)	0.04	0.03
Phenotype[a]								
BCVA best eye (decimals)		1.12 [1.00 – 1.23]	1.05 [1.00 – 1.20]	1.20 [1.07 – 1.41]	1.20 [1.00 – 1.35]	1.05 [0.95 – 1.20]	0.23	0.16
BCVA worst eye (decimals)		1.05 [0.80 – 1.10]	0.95 [0.83 – 1.00]	1.05 0.95 – 1.20]	1.00 [0.85 – 1.15]	0.89 [0.63 – 1.00]	0.009	0.02
Presence of (in-) active CNV		15 (12%)	0	0	1 (4%)	14 (26%)	0.001	0.02
Macular atrophy		3 (3%)	0	0	0	3 (6%)	0.28	>0.99
Pattern dystrophy like changes		13 (9%)	0	0	0	13 (21%)	0.001	0.99
Angioid streaks[a]								
Extent from optic disc	None	7 (6%)	7 (41%)	0	0	0	<0.001	<0.001
	< 3 mm	3 (3%)	0	2 (7%)	0	1 (2%)		
	3 – 6 mm	46 (38%)	7 (41%)	15 (56%)	11 (48%)	13 (24%)		
	6 – 9 mm	26 (2%)	2 (12%)	6 (22%)	6 (26%)	12 (22%)		
	> 9 mm	39 (32%)	1 (6%)	4 (15%)	6 (26%)	28 (52%)		
In central 3000 µm		66 (55%)	5 (29%)	9 (33%)	14 (61%)	38 (72%)	0.001	<0.001
Peau d'orange[a,b]								
Temporal border (ODD)		8.7 [7.8 - 9.8]	8.5 [7.9 - 9.4]	8.6 [7.8 - 9.2]	8.6 [7.7 - 9.7]	8.7 [8.1 - 10.2]	0.53	0.04
Central border (ODD)		2.6 [1.5 - 4.9]	1.2 [0.9 - 1.5]	1.8 [1.4 - 2.5]	3.7 [1.6 - 4.9]	4.7 [3.0 - 7.1]	<0.001	<0.001

Abbreviations: CNV; choroidal neovascularization, ODD; horizontal optic disc diameter
Data are presented as number (percentage) or as median (interquartile range). Nominal testing for difference is based on chi-square test and Mann-Whitney U test. The *P* for trend was the *P*-value of the estimate of the age category as a continuous determinant in a linear, logistic or ordinal regression analysis, with the corresponding patient characteristic as outcome.
a. Details on phenotype, angioid streaks and peau d'orange are presented for the right eyes.
b. The temporal border in the right eye could be measured in 111 eyes and the central border in 114 eyes.

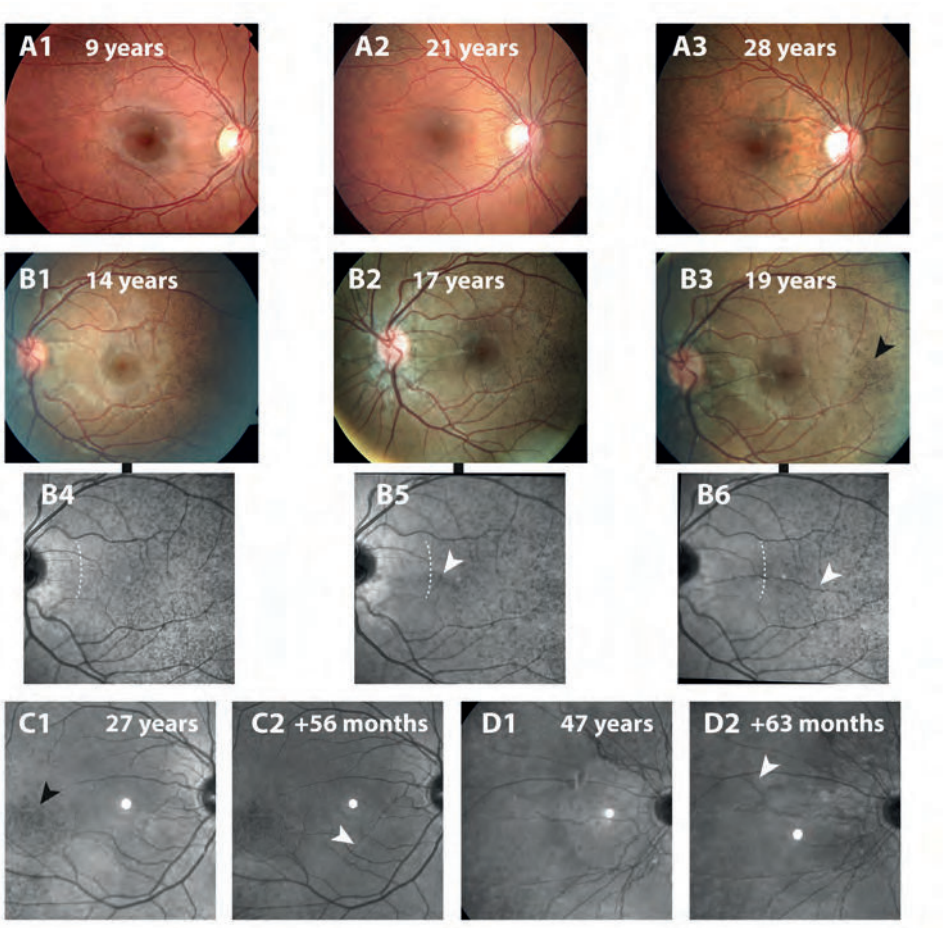

Figure 2.2 Progression of angioid streaks and peau d'orange in patients with pseudoxanthoma elasticum (PXE). The upper row (A1-A3) is the right eye of a female patient at the age of 9 years, 21 years and 28 years. The first fundus photograph (A1) only reveals peau d'orange, which progresses together with appearing (A2) and growing (A3) of angioid streaks. Figures B1-B6 represent fundus photographs (B1-B3) and corresponding 30° near infrared imaging (NIR) (B4-B6) of a female patient at the age of 14 years with follow-up imaging after 37 months (aged 17 years) and 56 months (aged 19 years). The white arrowheads indicate the development of a new angioid streak in the macula (B5), which grows further in less than two years (B6). Progression of the central border of peau d'orange is visible on 30° NIR imaging and indicated with dashed lines (B4-B6). Growth of, or new angioid streaks were assessed with 55° NIR imaging in two patients (C and D). C2 shows lengthening of an angioid streak with a follow-up interval of 56 months after the first visit age at 27 years (C1). In D, the occurrence of new angioid streaks presenting as a new branch nasal of the optic nerve is visible in a patient aged 47 years at baseline (D1) with an interval of 63 months (D2). The black arrowheads (B3, C1) indicate islands of decreased reflectivity in NIR imaging, the so called 'temporal sparing'.

New angioid streaks in the central 3000 µm of the macula developed in 5 eyes of 4 patients. These new streaks developed at the age of 16 (in both eyes), 28, 44, and 48 years. In total, longer or new angioid streaks were observed in 10 eyes (6%) in 254 patient years.

Peau d'orange

Cross-sectional analysis

The temporal border of peau d'orange could be measured in 221 eyes of 116 PXE patients, and the central border in 229 eyes of 117 PXE patients. The location of the temporal border remains rather constant with increasing age, whereas the location of the central border shifts to the temporal periphery with age (Table 2.1). The temporal border ranged from 8.5 ODD in patients aged 0 – 19 years to 8.7 ODD in patients aged 40 – 49 years. There was a small but statistically significant association between temporal border and age (ß 0.02 ODD, 95% CI 0.00 – 0.04, Figure 2.3). The central border ranged from 1.2 ODD in patients aged 0 – 19 years to 4.7 ODD in patients aged 40 – 49 years. The association with age was much stronger for the central border (ß 0.12 ODD, 95% CI 0.09 – 0.15). Longer angioid streaks were associated with both the location of the temporal border (ß 0.38 ODD, 95% CI 0.20 – 0.57, 95% CI, Figure 2.4) and the location of the central border (ß 0.67 ODD, 95% CI 0.45 – 0.89)) of the peau d'orange.

Longitudinal analysis

In the 78 patients (156 eyes) with at least 1 year follow-up, 72 (51%) of the 140 eyes with repeated measurements of the temporal border had a positive shift and 68 eyes (49%) had a negative shift. For the central border, 150 eyes had repeated measurements of which 112 (75%) showed a positive shift and 38 eyes (25%) a negative shift. The repeated measurements per eye are visualized in relation to the patients age in Supplementary Figure S2.1.

The temporal border of peau d'orange did not progress within a patient (median 0.00 ODD per year, IQR -0.12 – 0.12, $P = 0.69$). The central border did progress with a statistically significant median shift to the temporal periphery of 0.08 ODD per year (IQR 0.00 – 0.17, $P < 0.001$). This shift was larger in younger patients: the median progression in patients under 20 years at baseline was 0.12 ODD per year (IQR 0.08 – 0.28), in patients aged 20 – 29 years 0.09 ODD per year (IQR 0.01 – 0.18), in patients aged 30 – 39 years 0.09 ODD per year (IQR -0.01 – 0.14) and in patients aged 40 – 49 years this was 0.07 ODD per year (IQR -0.05 – 0.15). Examples of patients with progression of the central border of peau d'orange are presented in Figure 2.2.

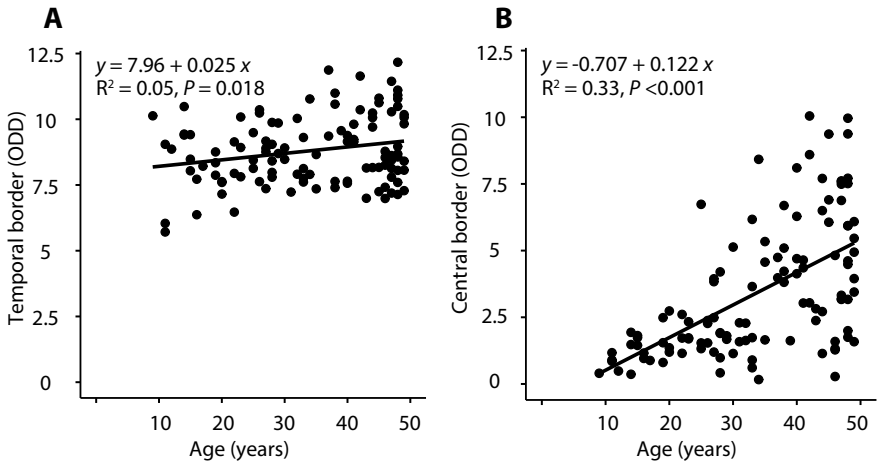

Figure 2.3 Correlation between age and extent of peau d'orange. The scatterplots show the temporal (A) and the central (B) border of the peau d'orange in optic disc diameter (ODD). Data is presented for the right eye only. The temporal border could be measured in 111 eyes and the central border in 114 eyes. In the top left, the regression equation (with age as determinant and distance as dependent variable) is displayed, with below the R2 and the P value for the estimate.

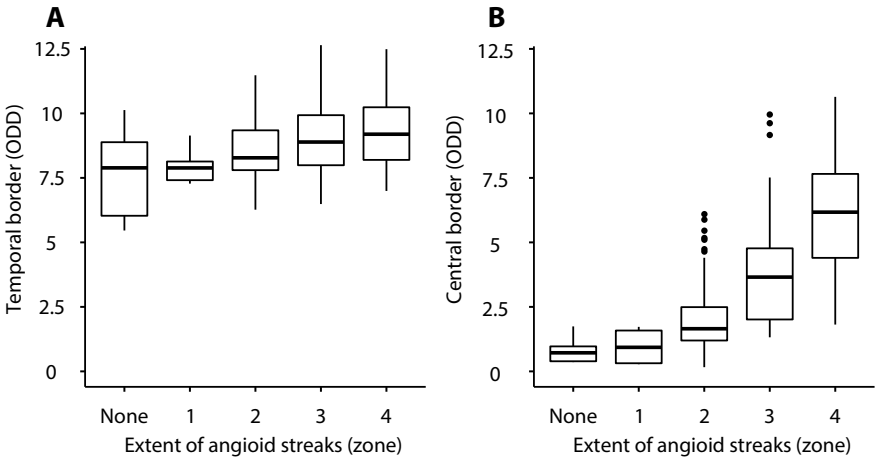

Figure 2.4 Correlation between extent of angioid streaks and extent of peau d'orange . The boxplots show the median and interquartile range of the extent of peau d'orange, expressed as optic disc diameter (ODD), for the temporal border (A) and the central border (B), stratified for the extent of angioid streaks. Data are presented per eye.

The appearance of temporal border differed between young and older patients. In younger patients, e.g. under 20 years, the temporal border appeared sparsely speckled (Supplementary Figure S2.2A). Some older patients with nearly confluent BM calcification had a patchy pattern around the confluent BM calcification (Supplementary Figure S2.2B).

Late-phase indocyanine green angiography

Of 23 PXE patients, late-phase ICG-A was collected. Of those patients, 1 was under 20 years, 3 were aged 20 – 29 years, 4 were aged 30 – 39 years and 15 were older than 40 years. The PXE-specific changes of a hypofluorescent area and a speckled transition zone were symmetrical over both eyes.

Of those 23 patients, 16 patients had a hypofluorescent area or speckles (median age 44 years, IQR 42 - 48). The 7 patients without a hypofluorescent area or speckles were significantly younger (median age 28 years, IQR 23 – 36) (P = 0.002). The youngest patient with hypofluorescent speckles was 31 years and the oldest patient without hypofluorescent speckles was 45 years. Age-specific examples of multimodal imaging including ICG-A are presented in Figure 2.5. Early hypofluorescent changes were visible in the macular area, and showed subtle, but detectable centrifugal progression over time (Figure 2.6). Temporal sparing, defined as an island of normal fluorescence in the hypofluorescent area on ICG-A, appeared to disappear over time by becoming confluently hypofluorescent (Figure 2.6, A and C).

The extent of the hypofluorescent area on ICG-A imaging varied largely between patients of similar age, which appeared to correlate with the length of angioid streaks. The longer the angioid streaks, the larger the ICG-A hypofluorescent area. This is illustrated in Supplementary Figure S2.3.

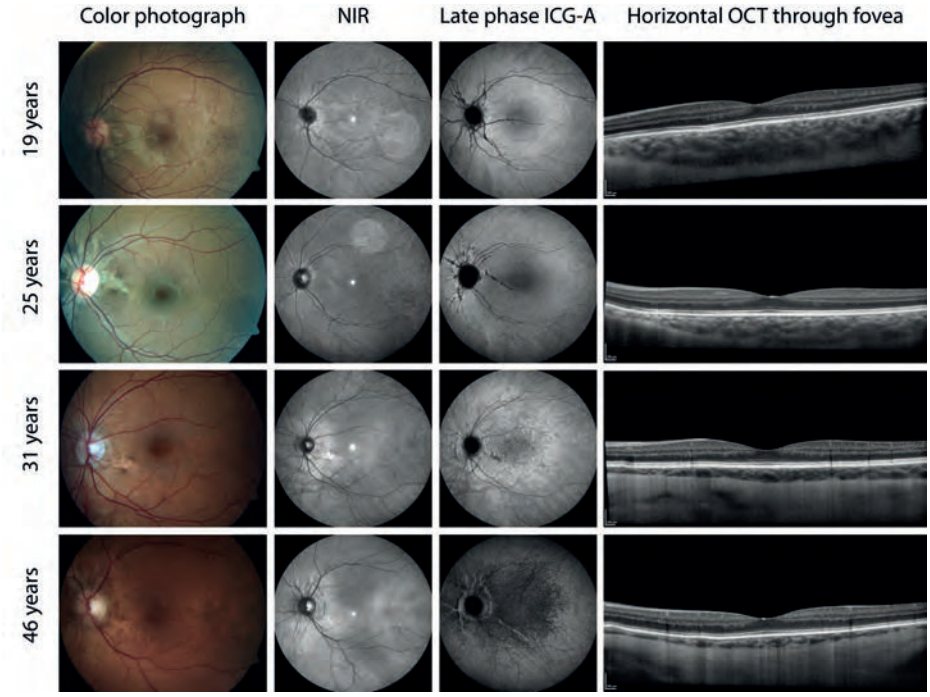

Figure 2.5 Typical multimodal imaging of four PXE patients in different decades, all without CNV or atrophy. The left column shows color fundus photographs, the second column near-infrared reflectance imaging (NIR), the third late-phase indocyanine green angiography (ICG-A), and the fourth column shows a horizontal optical coherence tomography (OCT) through the fovea. In the younger patients, there is no pattern of hypofluorescence on late-phase ICG-A yet. After the age of thirty years, a central area of hypofluorescence appears (third row), which often progresses until the fifth decade (bottom row). This pattern of hypofluorescence on ICG-A does not seem to correlate with findings on color photographs, NIR or OCT.

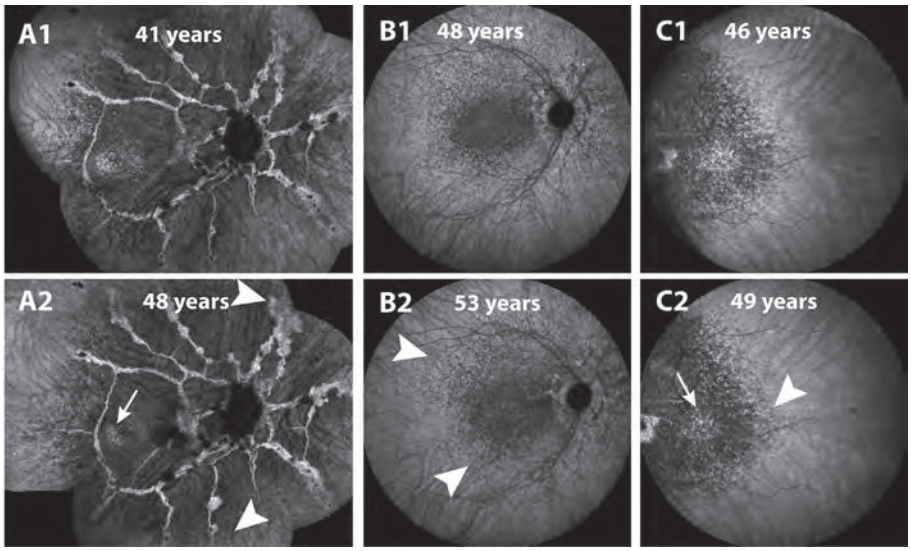

Figure 2.6 Late-phase indocyanine green (ICG) angiographies of three patients with follow-up imaging in the row below. The hypofluorescent speckled central area is characteristic for PXE patients. The mostly subtle changes are indicated by white arrowheads. The white arrows indicate the temporal island which appears to disappear over time by becoming confluently hypofluorescent. A: fundus of a right eye at 41 and 48 years. B: posterior pole of a right eye at 48 and 53 years. C: temporal imaging of a left eye at 46 and 49 years.

Discussion

This study is the first to provide detailed information on the spread of peau d'orange in a large cohort of relatively young PXE patients. The central border likely demarcates confluent BM calcification and progresses in both cross-sectional and longitudinal analyses. The peripheral border demarcates the normal fundus appearance and shows very little progression towards the retinal periphery (Figure 2.3). This suggests that the area of confluent BM calcification enlarges, in contrast to the area of peau d'orange, or the 2nd transition zone[6], which does not spread centrifugally but rather becomes narrower. This is supported by the finding that in some younger patients the peripheral speckled borders are hardly detectable and become more pronounced with increasing age (Supplementary Figure 2.2).

Based on these findings, we hypothesize that there is a predetermined area for BM calcification, that is visible early in life as peau d'orange throughout the posterior pole. With age, the BM calcification progresses and confluences, which leads to an area of confluent BM calcification with a 'coquille d'oeuf' or 'cracked eggshell' aspect in the fundus. The larger this area of confluent BM calcification is, the narrower the zone of peau d'orange will become and the more peripheral it will be visible.

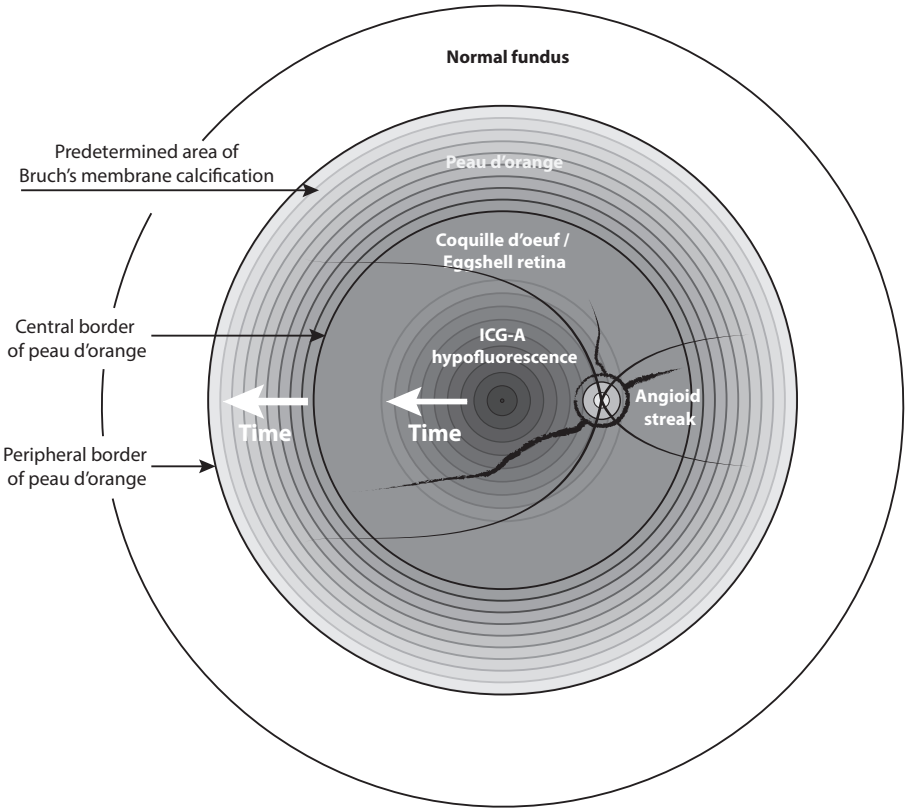

Figure 2.7 Proposed model for the changes in the fundus of a patient with pseudoxanthoma elasticum (PXE) showing the changes that can be seen on different imaging modalities. In the early diseases stage, there already is a predefined area for Bruch's membrane (BM) calcification. This has a speckled aspect: peau d'orange. This area will fill up with more confluent BM calcification during life: coquille d'oeuf. During life, a pattern of ICG-A decreased fluorescence appears, which starts in the macula and spreads centrifugally during life. This model is a modification from the model as proposed by Charbel Issa et al.

Later in life, in the fourth or fifth decade, a hypofluorescent pattern will appear on late-phase ICG-A. This area starts in the macula and then spreads centrifugally. This hypothesis is a modification of the model proposed by Charbel Issa et al in 2010, and a modified schematic figure is presented in Figure 2.7.

The application of the border of peau d'orange as a surrogate marker for the extent of BM calcification in PXE is not a new concept. Two studies measured the central border of peau d'orange and found an association with more reticular pseudodrusen and with reduced quantitative autofluorescence.[20,21] These measurements were performed on 30° macular NIR imaging, but in most eyes with PXE the peau d'orange extends further to the periphery than 30° or 8.6 mm from the temporal border of the optic disc. We adjusted the before mentioned method to a standardized semi-quantitative measurement that is suitable for both central and peripheral measurements.

The strong correlation of the central border of peau d'orange with the extent of angioid streaks confirms our interpretation of the central border as a surrogate marker for the extent of BM calcification. However, this method relies on a subjective assessment of the border. Our intra-grader reproducibility was excellent, but the inter-grader reproducibility showed more variation, partly due to different assessments of the ODD. Therefore, we emphasize that this method allows for cross-sectional and longitudinal comparisons within a cohort, but comparisons of absolute values between cohorts should be interpreted with caution.

We observed that the hypofluorescent area on late-phase ICG-A is larger in older patients if compared with younger patients and that slow progression can be detected over a timespan of several years. Furthermore, the hypofluorescence seems to correlate with the length of the angioid streaks, thus with the degree of BM calcification. Possibly, the ICG-A hypofluorescence in PXE patients is caused by impaired uptake of the ICG dye by the RPE as a result of decreased BM permeability. In a healthy eye, the ICG dye diffuses outside the choroidal vessels and accumulates in the choroidal interstitial tissue and RPE, which attributes to the fluorescence patterns in the late-phase of ICG-A.[22–24] A less permeable BM due to calcification may inhibit the uptake of ICG dye by the RPE cells. This theory is supported by similar ICG-A findings in patients with Sorsby dystrophy, also a disease with BM changes.[25] Also, scattered ICG-A hypofluorescence is associated with higher age in normal subjects and it correlates with soft drusen, which are local deposits of lipids in BM.[26,27] Lastly, the temporal island with reduced NIR reflectivity correlates with an island of ICG-A isofluorescence, which suggests that BM

permeability is relatively normal in an area without BM calcification. If the decreased ICG-A fluorescence would originate at RPE level, increased FAF would be expected as a sign of RPE dysfunction, which we did not observe. We therefore hypothesize that ICG-A hypofluorescence does not represent RPE dysfunction, but rather is a result of a reduced influx of ICG dye into the RPE cell caused by a less permeable BM.

A surprising finding of this study was that the peripheral border of peau d'orange does not seem to be age-dependent, but rather is a static feature of a PXE patient. During life, the area demarcated by the peripheral borders of peau d'orange fills up and the hyperreflective speckles confluence. Although there was a statistically significant association between the peripheral border and age in cross-sectional analysis, the absolute difference between the youngest and oldest age groups was only 0.2 ODD. In longitudinal analysis we did not find a shift to the periphery. Possibly, the sparse speckling at a young age has an impact on the visibility of the border. Therefore, we assume that the peripheral border, thus a 'predetermined area of BM calcification', is a static feature.

The underlying pathology of this predetermined area of BM calcification has yet to be unraveled. Possibly, PXE patients have a predisposition for calcification of a certain type of collagen or elastin fibres in BM, or to a specific topographical area of BM. This is supported by the findings of Gheduzzi et al. and Gorgels et al., that apart from elastin fibres, collagen fibres also are affected, which was more pronounced in *ABCC6* $^{-/-}$ mice than in humans.[28,29] The predetermined area of BM calcification might also have other relevant structural characteristics, such as a thinner and more porous elastic layer.[30,31] Chong et al. found that the elastic layer thickness increases rather abruptly at 14 – 16 mm temporal from the optic disc.[30] This area correlates with the findings of our study: the median temporal border of peau d'orange was 15.4 mm (8.7 ODD, converted with a mean horizontal optic disc diameter of 1.77 mm).[30,32] Furthermore, the two collagenous layers that enfold the elastic layer double in thickness in the peripheral region anterior to the equator, which corresponds with the location of histopathological BM changes in PXE[33–35] Possibly, these topographical differences of the BM layers attribute to a predetermined area for calcification of fibres in BM. However, even though it is plausible that the underlying topographical structure of BM and its properties play a role in the area of BM calcification in PXE, this is still speculative. A histopathological correlation study with imaging is much needed to investigate the molecular and histopathological changes underpinning PXE in the eye.

It is thought that angioid streaks are limited to the 'coquille d'oeuf' area, in which BM changes are confluent and the BM is brittle and prone to break.[6,10,36] Interestingly, we observed that in younger patients, angioid streaks often start in the 'coquille d'oeuf' area, but extend into the area of peau d'orange (Figure 2.2, B3). This finding suggests that the formation of angioid streaks does not only depend on confluent BM calcification.

Furthermore, we demonstrated that both angioid streaks and the central border of peau d'orange slowly progress during life, and younger patients show faster progression than older patients. The reason why peau d'orange in younger patients appears to progress faster is unknown. Maybe, the shift in peau d'orange must be considered relative to the area of coquille d'oeuf, since the confluence of a large concentric area of peau d'orange will take longer than the confluence of a smaller area. Moreover, there is variety between patients in the age-specific extent of BM calcification: some patients progress faster than others (Figure 2.3B). Maybe, faster progression is associated with lower levels of inorganic pyrophosphate, an inhibitor of ectopic calcification implicated in the pathophysiology of PXE.[37]

We observed that PXE patients had more often macular angioid streaks with increasing age (Table 2.1). This was surprising to us since we observed little longitudinal changes of angioid streaks in the central 3000 µm in this study. The increasing prevalence might be explained by the slightly skewed sex distribution: there are more men in the fifth decade than in the earlier decades in our cohort. Possibly, women present earlier and more often with skin changes and mild fundus changes, whereas men more often present later with visual complaints, around the fifth decade. Since these men present with visual complaints, they likely have a higher prevalence of macular pathology due to central angioid streaks. Based on our findings, angioid streaks in the central 3000 µm might progress, but very slowly and the risk of growth during the course of a few years is very small.

Strengths of this study include the relatively large sample of PXE patients under 50 years, the use of follow-up imaging, and the use of different measures based on multimodal imaging.

A limitation of this study is that the longitudinal assessment of peau d'orange was not blinded for patient or for visit (baseline or follow-up). Theoretically this may have led to an observer bias. However, we do believe that our measurements represent

longitudinal progression, because progression of peau d'orange is visible within an individual on longitudinal imaging. Also, the cross-sectional age-specific data show a change at group level which suggests that there must be individual progression.

In summary, we described the natural course of different manifestations of BM calcification in PXE patients at an early disease stage. We hypothesize that there is a predetermined area for BM calcification that will confluence with increasing age. The typical pattern of decreased ICG fluorescence develops in the fourth or fifth decade and appears to depend on the extent of BM calcification. Histopathologic correlation with imaging is needed to explain the histopathologic processes accounting for the areas of peau d'orange, coquille d'oeuf and ICG-A hypofluorescence.

References

1. Bergen AAB, Plomp AS, Schuurman EJ, et al. Mutations in *ABCC6* cause pseudoxanthoma elasticum. *Nat Genet*. 2000;25(2):228-231.
2. Plomp AS, Toonstra J, Bergen AAB, van Dijk MR, de Jong PTVM. Proposal for updating the pseudoxanthoma elasticum classification system and a review of the clinical findings. *Am J Med Genet A*. 2010;152A(4):1049-1058.
3. Le Saux O, Urban Z, Tschuch C, et al. Mutations in a gene encoding an ABC transporter cause pseudoxanthoma elasticum. *Nat Genet*. 2000;25(2):223-227.
4. Finger RP, Charbel Issa P, Ladewig MS, et al. Pseudoxanthoma elasticum: genetics, clinical manifestations and therapeutic approaches. *Surv Ophthalmol*. 2009;54(2):272-285.
5. Risseeuw S, Ossewaarde-van Norel J, Klaver CCW, Colijn JM, Imhof SM, van Leeuwen R. Visual Charbel Issa P, Finger RP, Gotting C, Hendig D, Holz FG, Scholl HPN. Centrifugal fundus abnormalities in pseudoxanthoma elasticum. *Ophthalmology*. 2010;117(7):1406-1414.
7. Charbel Issa P, Finger RP, Holz FG, Scholl HPN. Multimodal Imaging Including Spectral Domain OCT and Confocal Near Infrared Reflectance for Characterization of Outer Retinal Pathology in Pseudoxanthoma Elasticum. *Investig Opthalmology Vis Sci*. 2009;50(12):5913.
8. Krill AE, Klien BA, Archer DB. Precursors of angioid streaks. *Am J Ophthalmol*. 1973;76(6):875-879.
9. Mansour AM, Ansari NH, Shields JA, Annesley, Jr. WH, Cronin CM, Stock L. Evolution of Angioid Streaks. *Ophthalmologica*. 1993;207(2):57-61.
10. Jampol LM, Acheson R, Eagle RC, Serjeant G, O'Grady R. Calcification of Bruch's Membrane in Angioid Streaks With Homozygous Sickle Cell Disease. *Arch Ophthalmol*. 1987;105(1):93-98.
11. Gliem M, De Zaeytijd J, Finger RP, Holz FG, Leroy BP, Issa PC. An update on the ocular phenotype in patients with pseudoxanthoma elasticum. *Front Genet*. 2013;4(APR):14.
12. Kranenburg G, de Jong PA, Bartstra JW, et al. Etidronate for Prevention of Ectopic Mineralization in Patients With Pseudoxanthoma Elasticum. *J Am Coll Cardiol*. 2018;71(10):1117-1126.
13. Pomozi V, Julian CB, Zoll J, et al. Dietary Pyrophosphate Modulates Calcification in a Mouse Model of Pseudoxanthoma Elasticum: Implication for Treatment of Patients. *J Invest Dermatol*. 2019;139(5):1082-1088.
14. Risseeuw S, Ossewaarde-van Norel J, van Buchem C, Spiering W, Imhof SM, van Leeuwen R. The extent of angioid streaks correlates with macular degeneration in pseudoxanthoma elasticum. *Am J Ophthalmol*. Published online 2020.
15. World Health Organization. ICD-10 Definition.
16. Risseeuw S, Norel JO Van, Buchem C Van, Imhof SM, Leeuwen R Van. The extent of angioid streaks correlates with macular degeneration in pseudoxanthoma elasticum. *Am J Ophthalmol*. Published online 2020.
17. Koo TK, Li MY. A Guideline of Selecting and Reporting Intraclass Correlation Coefficients for Reliability Research. *J Chiropr Med*. 2016;15(2):155-163.
18. Agarwal A, Patel P, Adkins T, Gass JDM. Spectrum of pattern dystrophy in pseudoxanthoma elasticum. *Arch Ophthalmol (Chicago, Ill 1960)*. 2005;123(7):923-928.
19. Finger RP, Charbel Issa P, Ladewig M, Gotting C, Holz FG, Scholl HPN. Fundus autofluorescence in Pseudoxanthoma elasticum. *Retina*. 2009;29(10):1496-1505.
20. Gliem M, Hendig D, Finger RP, Holz FG, Charbel Issa P. Reticular pseudodrusen associated with a diseased bruch membrane in pseudoxanthoma elasticum. *JAMA Ophthalmol*. 2015;133(5):581-588.
21. Gliem M, Müller PL, Birtel J, et al. Quantitative fundus autofluorescence in pseudoxanthoma elasticum. *Investig Ophthalmol Vis Sci*. 2017;58(14):6159-6165.

22. Chang AA, Morse LS, Handa JT, et al. Histologic localization of indocyanine green dye in aging primate and human ocular tissues with clinical angiographic correlation. *Ophthalmology*. 1998;105(6):1060-1068.
23. Chang AA, Zhu M, Billson F. The Interaction of Indocyanine Green with Human Retinal Pigment Epithelium. *Investig Opthalmology Vis Sci*. 2005;46(4):1463.
24. Tam J, Liu J, Dubra A, Fariss R. In vivo imaging of the human retinal pigment epithelial mosaic using adaptive optics enhanced indocyanine green ophthalmoscopy. *Investig Ophthalmol Vis Sci*. 2016;57(10):4376-4384.
25. Gliem M, Müller PL, Mangold E, et al. Sorsby fundus dystrophy: Novel mutations, novel phenotypic characteristics, and treatment outcomes. *Investig Ophthalmol Vis Sci*. 2015;56(4):2664-2676.
26. Chen L, Zhang X, Liu B, Mi L, Wen F. Age-related scattered hypofluorescent spots on late-phase indocyanine green angiography: the multimodal imaging and relevant factors. *Clin Exp Ophthalmol*. 2018;46(8):908-915.
27. Chen L, Zhang X, Li M, Gan Y, Wen F. Drusen and age-related scattered hypofluorescent spots on late-phase indocyanine green angiography, a candidate correlate of lipid accumulation. *Investig Ophthalmol Vis Sci*. 2018;59(12):5237-5245.
28. Gheduzzi D, Sammarco R, Quaglino D, et al. Extracutaneous ultrastructural alterations in pseudoxanthoma elasticum. *Ultrastruct Pathol*. 2003;27(6):375-384.
29. Gorgels TGMF, Teeling P, Meeldijk JD, et al. *Abcc6* deficiency in the mouse leads to calcification of collagen fibers in Bruch's membrane. *Exp Eye Res*. 2012;104:59-64.
30. Chong NHV, Keonin J, Luthert PJ, et al. Decreased thickness and integrity of the macular elastic layer of Bruch's membrane correspond to the distribution of lesions associated with age-related macular degeneration. *Am J Pathol*. 2005;166(1):241-251.
31. Hogan MJ, Alvarado J. Studies on the Human Macula: IV. Aging Changes in Bruch's Membrane. *Arch Ophthalmol*. 1967;77(3):410-420.
32. Quigley HA, Brown AE, Morrison JD, Drance SM. The Size and Shape of the Optic Disc in Normal Human Eyes. *Arch Ophthalmol*. 1990;108(1):51.
33. Newsome DA, Huh W, Green WR. Bruch's membrane age-related changes vary by region. *Curr Eye Res*. 1987;6(10):1211-1221.
34. Klien BA. Angioid streaks. A clinical and histophathologic study. *Am J Ophthalmol*. 1947;30(8):955-968.
35. Verhoeff FH. Histological findings in a case of angioid streaks. *Br J Ophthalmol*. 1948;32(9):531-544.
36. Spaide RF. Peau d'orange and angioid streaks: manifestations of Bruch membrane pathology. *Retina*. 2015;35(3):392-397.
37. Jansen RS, Kucukosmanoglu A, de Haas M, et al. *ABCC6* prevents ectopic mineralization seen in pseudoxanthoma elasticum by inducing cellular nucleotide release. *Proc Natl Acad Sci U S A*. 2013;110(50):20206-20211.

Supplementary figures

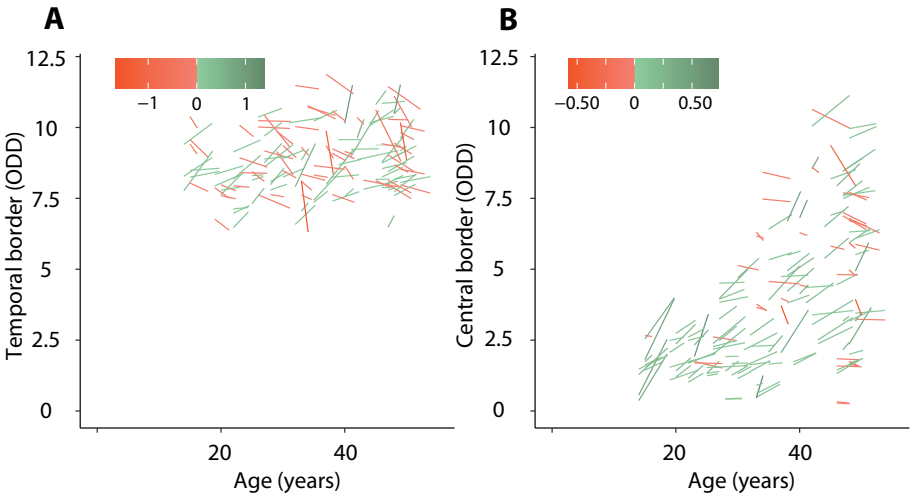

Supplementary Figure S2.1 Repeated measures of the temporal and central border of peau d'orange for patients with a minimum follow-up of 12 months. Each line represents one patient. The x-axis represents the age of the patient and the y-axis represents the eccentricity of the peau d'orange in optic disc diameter (ODD) per eye. The color of the lines represent the magnitude of the change (between baseline and follow-up) in ODD per year.

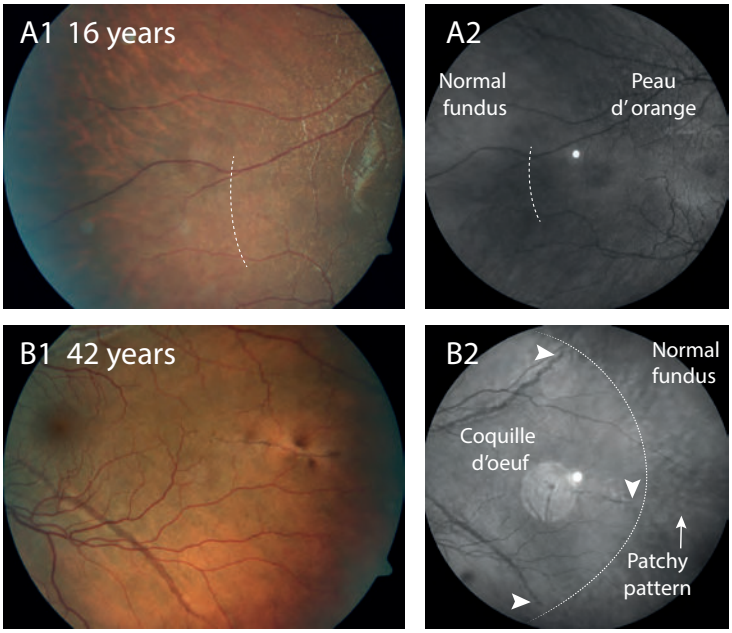

Supplementary Figure S2.2 Characteristics of the temporal border of peau d'orange of two patients. One patient is in an early stage of the disease stage (**A**) and one patient in a late stage of the disease (**B**). The patient in an early stage does not have angioid streaks yet and the temporal peau d'orange shows a sparsely speckled pattern which is best visible on color fundus photography and the border is indicated with a dashed line (**A1-A2**). In contrast, in the late stage, in which BM calcification appears confluent and angioid streaks extend to the periphery, there is no typical peau d'orange visible. The angioid streaks extend to the far periphery in the coquille d'oeuf (white arrowheads) and peripheral from the coquille d'oeuf a patchy pattern is visible (**B2**). The dotted line indicates the approximate border between the coquille d'oeuf and the limited peau d'orange.

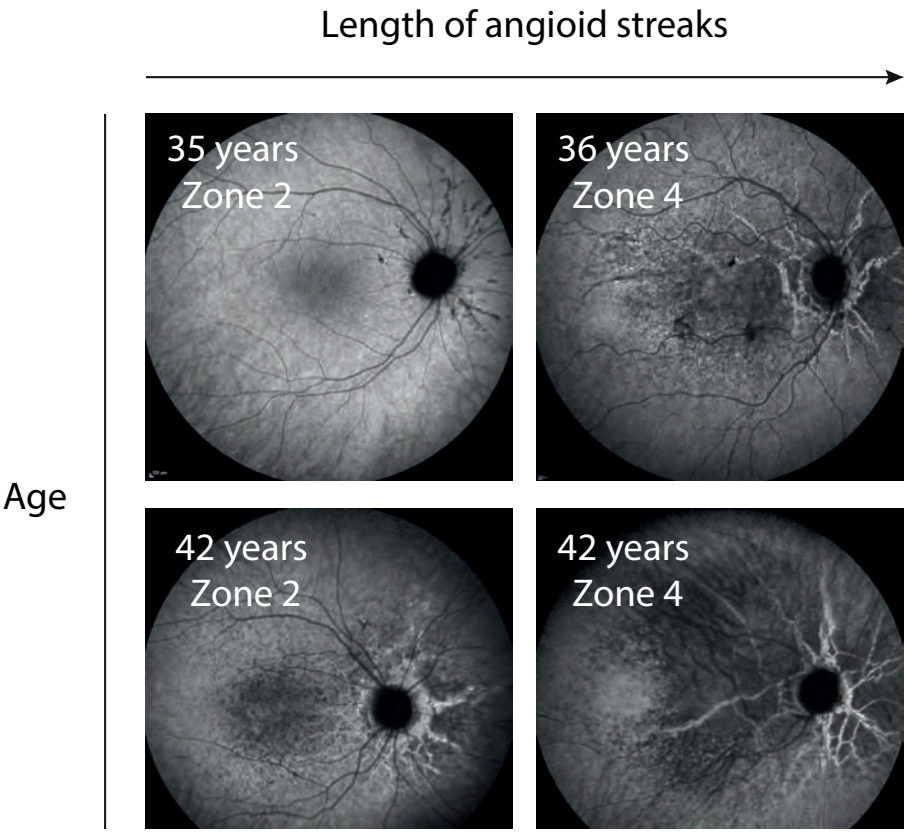

Supplementary Figure S2.3
Characteristics of late-phase indocyanine green (ICG) hypofluerescence in four different pseudoxanthoma elasticum patients with comparable ages but different length of angioid streaks. In zone 2, the longest angioid streak extends 3 – 6 mm from the center of the optic disc, while in zone 4 the longest angioid streaks extends > 9 mm from the center of the optic disc. Longer angioid streaks appear to correlate with more extensive ICG hypofluorescence.


Chapter 3

Visual acuity in pseudoxanthoma elasticum

Sara Risseeuw
Jeannette Ossewaarde-van Norel
Caroline C. W. Klaver
Johanna M. Colijn
Saskia M. Imhof
Redmer van Leeuwen

Retina. 2019;39:1580-1587

Abstract

Purpose

To assess the age-specific proportion of visual impairment in patients with pseudoxanthoma elasticum (PXE) and to compare this with foveal pathology and similar data of late age-related macular degeneration (AMD) patients.

Methods

Cross-sectional data of 195 patients with PXE were reviewed, including best-corrected visual acuity and imaging. WHO criteria were used to categorize bilateral visual impairment. These results were compared to similar data of 131 patients with late AMD from the Rotterdam Study.

Results

Overall, 50 PXE patients (26.0%) were visually impaired, including 21 (11%) with legal blindness. Visual functioning declined with increasing age. In patients over 50 years, 37% was visually impaired and 15% legally blind. Foveal choroidal neovascularization (CNV) was found in 84% of eyes with a BCVA lower than 20/70 (0.30), and macular atrophy (MA) in the fovea in 16%. In late AMD patients, 40% was visually impaired and 13% legally blind. Visual impairment started about 20 years later as compared to PXE patients.

Conclusion

Visual impairment and blindness are frequent in PXE, particularly in patients over 50 years. Whilst CNV is associated with the majority of vision loss, MA is also common. The proportion of visual impairment in PXE is comparable with late AMD, but manifests earlier in life.

Introduction

Pseudoxanthoma elasticum (PXE) is a rare autosomal recessive disorder.[1] Bi-allelic mutations in the *ABCC6* gene causes ectopic mineralization of elastic fibers in the skin, vasculature and Bruch's membrane (BM) in the retina.[2–4] The latter leads to breaks, seen as angioid streaks and peau d'orange, both part of the typical phenotype of PXE.[5]

Angioid streaks allow for choroidal neovascularization (CNV) to develop in up to 86% of PXE patients,[6] often with a first episode before the age of fifty.[7–9] Because angioid streaks are most prevalent in the posterior pole,[5] CNV will have a significant impact on visual function due to subretinal hemorrhage, exudation and fibrovascular scarring.

Up to now, CNV is the only ocular complication of PXE that can be treated. Intravitreal treatment with inhibitors of vascular endothelial growth factor (VEGF) might reduce visual impairment due to CNV in PXE in the long term.[9–11] However, macular atrophy (MA), with a presentation that is similar to geographic atrophy in late age-related macular degeneration (AMD), also attributes to visual loss in PXE,[12,13] affecting up to 32% of all patients.[13–15]

Young PXE patients are aware of the visual impairment of family members and the prospect of vision loss reduces their emotional well-being.[16] Detailed information on visual prognosis of PXE patients is important for counseling. Moreover, the specific pathology underlying visual loss is relevant for clinical practice and should direct future research.

Extensive data on PXE patients are collected in the Dutch National Expertise Center for PXE. The aim of the present study is to describe the visual acuity of 195 patients with PXE, to determine the age-specific proportion of patients with visual impairment and to compare that with patients with late AMD. In addition, the relative contributions of CNV and MA to the visual loss are established.

Methods

Recruitment of patients

This cross-sectional, retrospective study was conducted at University Medical Center Utrecht, where the Dutch National Expertise Center for PXE is situated. This study is in adherence to the Declaration of Helsinki and its further amendments.

All patients visiting the National Expertise Center underwent an extensive physical and ophthalmological examination. Patients with at least two major diagnostic criteria (characteristic fundus pathology, typical skin lesions and/or genetic confirmation) were considered to have a definitive diagnosis of PXE and were included in this study.[17] Patients with a probable or possible diagnosis of PXE were excluded. All patients visiting the National Expertise Center between July 2013 and April 2017 were included, using the most recent findings in case of multiple consultations. 76 patients participated in the randomized, placebo-controlled, double blinded 'Treatment of Ectopic Mineralization in patients with PXE' (TEMP) trial (Dutch Trial Register, number NTR5180*)*, investigating the effect of etidronate on vascular and retinal calcifications. We report the clinical data measured at baseline visit of those patients.

Measurements on patients, reporting data

All PXE patients underwent a routine ophthalmologic examination, including best-corrected visual acuity (BCVA) and indirect ophthalmoscopy. Imaging included central and peripheral spectral domain optical coherence tomography (SD-OCT) imaging, fundus autofluorescence imaging, near-infrared reflectance imaging (all Spectralis HRA-OCT, Heidelberg Engineering, Heidelberg, Germany) and color fundus photography (FF 450 plus, Carl Zeiss Meditec AG, Jena, Germany). Fluorescein angiography (FA) was performed by indication. BCVA of patients participating in the TEMP-trial was measured using Early Treatment Diabetic Retinopathy Study (ETDRS) charts, otherwise Snellen charts were used.[18]

Data on demographics and the use of intravitreal VEGF inhibitors were collected from medical charts. The BCVA of the best eye was graded according to the definitions of visual impairment and blindness from the World Health Organization: worse than 20/70 (0.30) but equal to or better than 20/200 (0.10) was graded as moderate visual impairment, a BCVA worse than 20/200 (0.10) but equal to or better than 20/400 (0.05) was graded as severe visual impairment and a BCVA worse than 20/400 (0.05) was graded as blindness.[19] At least two individuals (SR, AO, or RvL) assessed the available

imaging on the likely cause of visual loss and graded foveal pathology as CNV, MA or mixed with either CNV or MA being predominant (Figure 3.1). The foveal area was defined as the central macular area with a diameter of 1000 µm. In case both CNV and MA were observed in the foveal area, consensus was found whether CNV or MA had the most impact on visual acuity in the concerning eye. The presence of angioid streaks was not considered as a cause of visual loss and was categorized as 'no foveal pathology causing visual loss'.

The presence of (in)active CNV was based on the following features: sub- or intraretinal fluid, signs of neovascular or fibrotic tissue on SD-OCT imaging; leakage of neovascular tissue or staining of fibrovascular scars on FA (if available); and fibrotic tissue, hyperpigmentation or hemorrhage on fundus photography. The presence of MA was based on: loss of the retinal pigment epithelium layer on SD-OCT; sharply demarcated areas of hypofluorescence on FAF and hyperreflectivity on NIR; and areas of hypopigmentation and visible choroidal vessels on fundus photography and window defects on FA if available. Both an atrophic zone surrounding an inactive CNV and peripapillar atrophy were considered unrelated to the macular atrophy and not categorized as such.

To compare these results to a disease with similar phenotype and treatment, we used data on visual functioning of patients with prevalent late AMD from the Rotterdam Study. The Rotterdam Study is a large population-based study, consisting of three cohorts, on diseases of the elderly in persons of 45 years and older.[20,21] Visual acuity was assessed after optimal refractive correction with a the Lighthouse Distance Visual Acuity Test, a modified version of the ETDRS chart and fundus color photographs were graded according to the Rotterdam Classification.[18,22] All patients with late AMD had at least one eye with geographic atrophy and/or CNV.

Statistical analysis

BCVA was converted to the logarithm of the minimum angle of resolution (LogMAR) for statistical purposes. Statistical analysis was performed using SPSS Statistics version 22 (IBM Corp., Armonk, NY, USA). Values are presented as numbers with percentage (%), mean with standard deviation (± SD) or as median with interquartile range (IQR), depending on the distribution of the values. Differences between groups were tested with chi-square test or one-way ANOVA. A p-value of < 0.05 was considered statistically significant.

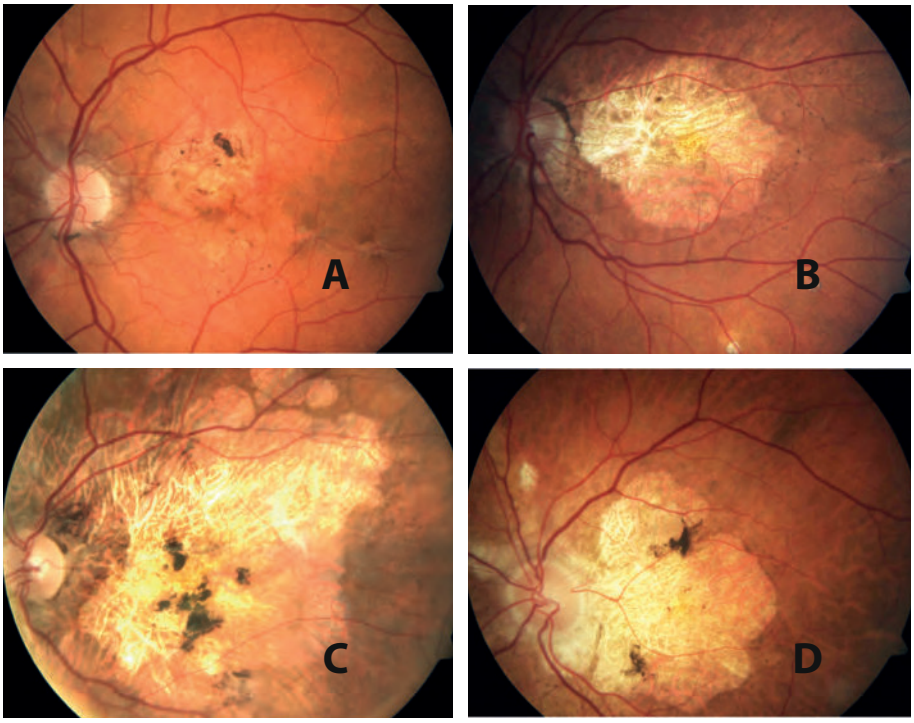

Figure 3.1 Color fundus photographs illustrating the classification of foveal pathology correlated with visual loss in pseudoxanthoma elasticum. Foveal pathology is defined as the likely cause of visual loss. A; foveal choroidal neovascularization. B; macular atrophy in the fovea. C; mixed macular pathology with foveal choroidal neovascularization. D; mixed macular pathology with foveal macular atrophy.

Results

Patient characteristics

In total, 195 PXE patients were included. Three patients were excluded from further analysis of visual function because the BCVA measurements were unreliable. Therefore, data on visual functioning have been analyzed in 192 PXE patients.

The mean age was 53.2 years (±14.7) and 35.6% was male. Historical data regarding VEGF-inhibitors were known of 191 patients, of which 36 patients (18.8%) had received at least one injection with VEGF-inhibitors in one eye and 49 patients (25.7%) in both eyes.

Visual acuity and visual impairment

The median BCVA was 20/22 (0.91) in the best eye and 20/40 (0.50) in the worst eye. Further, the median BCVA of the worst eye was 20/40 (0.50) after the age of 50 and of the best eye after the age of 60 years (Figure 3.2).

Of all patients, 8.3% was moderately visually impaired, 6.8% was severely visually impaired and 10.9% was legally blind (all bilateral). Age-specific proportion of patients with visual impairment is presented in Figure 3.3. Of all patients under 50 years, one patient was legally blind and one was moderately visually impaired. However, of all patients over 50 years, 36.9% had any form of visual impairment, and legal blindness was found in 15.4%. The proportion of patients increased with age: in the sixth decade 21.1% of all patients was visually impaired. This percentage increased in the seventh decade to 43.6% and rose to 85.7% in the eighth decade. Also, the percentage of legal blindness increased from 3.4% in patients in their fifth decade to 42.9% in patients in their eighth decade.

Foveal pathology

A total of 381 eyes of 191 patients were available for imaging analysis. Twenty-three eyes had a BCVA worse than 20/70 (0.30) but equal to or better than 20/200 (0.10), 25 eyes had a BCVA less than 20/200 (0.10) but equal to or better than 20/400 (0.05), and 83 eyes had a BCVA worse than 20/400 (0.05). Correlations between BCVA and foveal pathology are presented in Table 3.1.

Foveal pathology was observed in 190 (49.9%) eyes. A total of 131 eyes had a BCVA lower than 20/70 (0.30), which was caused by CNV in 110 eyes (84.0%) and by MA in

21 eyes (16.0%). The mean BCVA of eyes without CNV or MA (20/20, logMAR 0.00 ± 0.11) was significantly better than the BCVA of eyes with foveal CNV (20/214, logMAR 1.03 ± 0.71, $p < 0.0001$) and eyes with MA in the fovea (20/200, logMAR 1.00 ± 0.58, $p < 0.0001$). Age was significantly higher in eyes with foveal CNV (61.1 ± 9.0 years) or MA (59.3 ± 7.7 years) than in eyes without CNV or MA (40.8 ± 14.1, $p < 0.0001$). There was no statistically significant age difference between eyes with foveal CNV and MA.

Of all 190 eyes with observed foveal pathology, 63 eyes (33.1%) had CNV without MA, 14 (7.4%) had MA without CNV, and 113 eyes (59.5%) had signs of both CNV and MA. In 98 of those 113 eyes (86.7%), CNV was the predominant foveal feature.

Visual function and macular pathology in late AMD

We analyzed data of 131 patients with prevalent late AMD from the Rotterdam Study. All patients were older than 50 years and 48 patients (36.6%) were male. In total, 52 patients (39.7%) had any form of visual impairment, of which 17 (13.0%) were legally blind. The age-specific proportion of patients with visual impairment in patients with

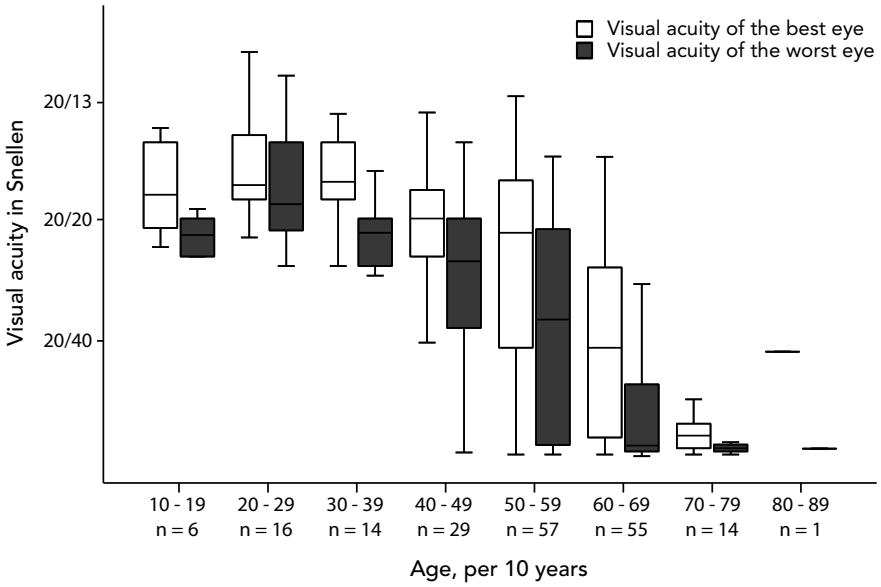

Figure 3.2 Best-corrected visual acuity of best and worst eye of 192 patients with pseudoxanhoma elasticum, stratified per 10 years of age.

late AMD is presented in Figure 3.3. The proportion of patients with visual impairment increased with age from 10.0% in the seventh decade to 60% in patients over 90 years. In the total group of 131 patients, macular pathology consisted of geographic atrophy only in 53 patients (40.5%), CNV only in 45 patients (34.4%) and a mixed phenotype (both geographic atrophy and CNV in one or both eyes) in 33 patients (25.2%). The proportion of patients with visual impairment was 30.2% in patients with dry AMD, 26.7% in patients with wet AMD and 72.7% in patients with a mixed phenotype.

Visual impairment started about 20 years earlier in PXE patients when compared to late AMD patients (Figure 3.3). Severe visual impairment and blindness in PXE patients started at the age of 40-49 years, while in late AMD patients this started at 60-69 years. Moreover, in PXE patients aged 60–69 years, any form of visual impairment was seen in 45%, while a similar proportion in late AMD patients was found at the age of 80-89 years.

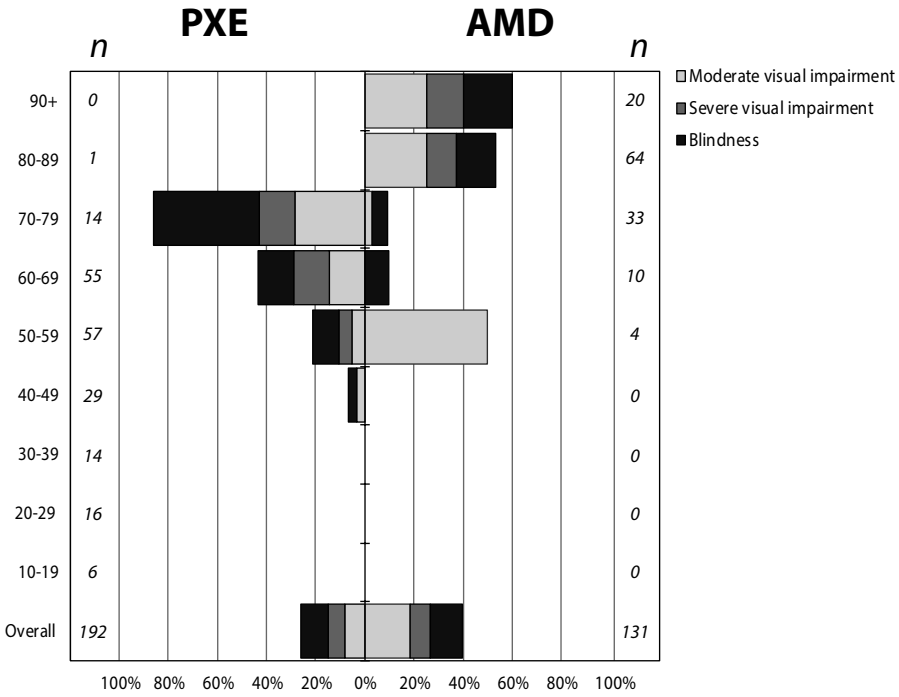

Figure 3.3 Percentage of visual impairment in patients with pseudoxanthoma elasticum (PXE) and late age-related macular degeneration (AMD), in the total study group as well as stratified per 10 years of age.

Table 3.1 Correlation between best-corrected visual acuity (BCVA) and retinal abnormality in 381 eyes with PXE

	Total of eyes[a]	Foveal abnormality			Macular abnormality[b]		
		None	CNV	MA	CNV	MA	Mixed
	N=381	N=191 (%)	N=161 (%)	N=29 (%)	N=63 (%)	N=14 (%)	N=113 (%)
BCVA ≥ 20/70 (0.30)	250	191 (76.4)	51 (20.4)	8 (3.2)	32 (12.8)	5 (2.0)	22 (8.8)
20/200 (0.10) ≤ BCVA < 20/70 (0.30)	23	0	20 (87.0)	3 (13.0)	7 (30.4)	0	16 (69.6)
20/400 (0.05) ≤ BCVA < 20/200 (0.10)	25	0	19 (76.9)	6 (24.0)	7 (28.0)	2 (8.0)	16 (64.0)
BCVA <20/400 (0.05)	83	0	71 (85.5)	12 (14.5)	17 (20.5)	7. (8.4)	59 (71.1)

Best-corrected visual acuity is categorized according to the World Health Organisation criteria of visual impairment. The fovea is defined as the area around the foveola with a diameter of 1000 µm. Foveal pathology is defined as the likely cause of visual loss. BCVA; best corrected visual acuity, reported in decimals, N; number of eyes.

a. A total of 382 eyes had eligible VA measurements. Imaging of one eye was inconclusive and thus not included in this table.

b. Abnormality observed in the total macular area, not necessarily in the fovea or causing visual loss.

Discussion

The aim of this study was to investigate the impact of PXE on visual functioning. We observed that 37% of all patients over 50 years are visually impaired and that visual deterioration of the first eye already starts after the age of 40 years.

These results are in line with three previous studies on visual impairment in PXE. One study on 71 PXE patients found that 39.4% had a bilateral BCVA lower than 20/40 (0.50), all older than 39 years.[23] In another population of 40 PXE patients, a BCVA ≤ 20/50 (0.40) was found in 17%.[24] A cohort of 53 patients with PXE showed a mean BCVA of 20/160 (0.13), and 19% had a bilateral BCVA ≤ 20/200 (0.10) in both eyes.[25] In all these studies, age was correlated with visual loss, but no age-specific data on visual impairment were provided. Our study is the first to report an age-stratified description of visual functioning in PXE patients, which is relevant for the patients prognosis and counselling. However, a detailed description of visual prognosis in PXE patients is challenging since there may be a selection bias. If the study cohort consists solely of PXE patients who visited an eye medical center, there will be a selection of patients with visual complaints, causing an overestimation of visual impairment. However, in our cohort, PXE patients were referred based on PXE diagnosis, irrespective of visual symptoms, therefore decreasing the likelihood of selection bias.

We found the proportion of patients with visual impairment and legal blindness to increase with age. Of patients over 50 years, 37% has any form of visual impairment and 15% has legal blindness. However, visual function of the worst eye already declines at a younger age. The incidence of CNV rises with age up to 86% of all PXE patients, but is common in patients under 50.[6] One study found the first CNV to occur at a mean age of 44.3 years,[24] which is compatible with our results regarding visual acuity in the worst eye. Visual loss, but also the prospect of losing vision, has a huge impact on the quality of life and emotional well-being of PXE patients.[16] Altogether, PXE causes an important visual burden in patients in their working age.

We wanted to identify the foveal pathology that caused visual loss. A prior or active CNV was the cause in the vast majority (84%), but in 16% of eyes with a BCVA < 20/70 (0.30), MA in the fovea was the underlying cause of vision loss. These findings are comparable with prior studies. A large study in 276 eyes of 139 PXE patients found both MA and CNV to increase with age and found MA in 32% of the eyes with PXE, and in 7% even without signs of CNV.[13] Another study in 41 eyes of patients found MA

without signs of CNV in 20% of the eyes, and of the six eyes with MA that were eligible for VA analysis, three (50%) ended with a VA lower than 20/70 (0.30).[15] Although we specifically studied foveal pathology in order to correlate this to VA, our results are in line with the before mentioned: MA in the foveal area was found in 7.6% of all eyes, and another 25.7% had MA in combination with foveal CNV.

Visual impairment due to MA in PXE is a relatively poorly described phenomenon, in contrast to CNV. However, new insights in the prevalence and progression of MA have been reported recently.[12–15,26–28] It is suggested that age-related changes in BM such as calcification and thickening impede survival of retinal pigment epithelium (RPE) cells[29] and attribute to the development of geographic atrophy in AMD.[30] This might also explain the incidence of MA in PXE, since PXE affects the retina at the level of BM. Also, the role of inactive pyrophosphate, an inhibitor of ectopic mineralization that is lowered in patients with PXE[31], has yet to be discovered. Although less frequent than in late AMD, MA is still the cause of 16% of visual loss in PXE patients and cannot be prevented by anti-VEGF treatment. Therefore, a treatment inhibiting the ongoing calcification of BM is required to prevent MA in PXE.

We compared visual impairment in PXE and late AMD because of the overlap in clinical characteristics and treatment. Patients with late AMD were selected from a population study based on diagnosis of end-stage disease, which usually comes with visual loss. In contrast, PXE patients were selected based on clinical criteria. Therefore, it is not possible to compare the absolute risks of visual impairment based on these data. However, we can compare the age-specific proportion of visual impairment and blindness in patients with PXE and late AMD. This proportion is similar in PXE patients older than 50 years and late AMD patients (37% vs 40% visual impairment and 15% vs 13% blindness in PXE and late AMD, respectively). But, the onset of visual impairment is about 20 years earlier in patients with PXE than in patients with late AMD. Thus, compared to late AMD, visual burden in PXE patients is much higher, because it occurs earlier in life.

We recorded the use of anti-VEGF injections to evaluate the need of treatment, and found that 44.5% of all PXE patients had ever received one or more anti-VEGF injections. Anti-VEGF as a therapy to treat CNV was introduced in 2006.[32] We may assume that a considerable proportion of the PXE patients in our cohort already suffered from CNV before anti-VEGF therapy was available. Treatment with anti-VEGF has been proven beneficial in PXE,[11,28,32–35] and may reduce visual impairment in PXE. A point of concern

is the possible effect of anti-VEGF injections on progression of retinal and choroidal atrophy.[33,36,37] Anti-VEGF therapy will suppress RPE-produced VEGF, which may be essential for maintaining the choriocapillaris. A longitudinal design is required to study the impact of anti-VEGF treatment on visual functioning in PXE patients.

This is the largest cohort of PXE patients so far, enabling us to provide age-specific data on visual functioning. Other strengths of this study include standard BCVA measurements and ophthalmological imaging performed at the same date in a single center. Also, our study is the first to define the underlying pathology of visual impairment using different imaging modalities. Several limitations need to be addressed as well. The cross-sectional design of this study is able to show prevalence of visual impairment, while a longitudinal design is required to study the incidence and natural course of visual impairment in PXE. Furthermore, older PXE patients with CNV will not have benefited from anti-VEGF therapy before its introduction in 2006. This cohort effect may have a negative impact on visual acuity in older age-groups.

In conclusion, visual impairment and blindness are frequent amongst PXE patients, in the largest cohort published so far. Of all PXE patients over 50 years, 37% is visually impaired and 15% is legally blind (WHO criteria). CNV attributed the most (84%) to visual deterioration in eyes with a BCVA< 20/70 (0.30), while MA is the cause of visual loss in 16% of the eyes. Compared to late AMD, visual impairment in PXE starts about 20 years earlier.

References

1. Uitto J, Váradi A, Bercovitch L, Terry PF, Terry SF. Pseudoxanthoma elasticum: Progress in research toward treatment: Summary of the 2012 PXE international research meeting. *J Invest Dermatol*. 2013;133(6):1444-1449.
2. Le Saux O, Urban Z, Tschuch C, et al. Mutations in a gene encoding an ABC transporter cause pseudoxanthoma elasticum. *Nat Genet*. 2000;25(2):223-227.
3. Bergen AAB, Plomp AS, Schuurman EJ, et al. Mutations in *ABCC6* cause pseudoxanthoma elasticum. *Nat Genet*. 2000;25(2):228-231.
4. Ringpfeil F, Lebwohl MG, Christiano AM, Uitto J. Pseudoxanthoma elasticum: mutations in the MRP6 gene encoding a transmembrane ATP-binding cassette (ABC) transporter. *Proc Natl Acad Sci U S A*. 2000;97(11):6001-6006.
5. Gliem M, De Zaeytijd J, Finger RP, Holz FG, Leroy BP, Issa PC. An update on the ocular phenotype in patients with pseudoxanthoma elasticum. *Front Genet*. 2013;4(APR):14.
6. Georgalas I, Papaconstantinou D, Koutsandrea C, et al. Angioid streaks, clinical course, complications, and current therapeutic management. *Ther Clin Risk Manag*. 2009;5(1):81-89.
7. Finger RP, Charbel Issa P, Ladewig MS, et al. Pseudoxanthoma elasticum: genetics, clinical manifestations and therapeutic approaches. *Surv Ophthalmol*. 2009;54(2):272-285.
8. Nakagawa S, Yamashiro K, Tsujikawa A, et al. The time course changes of choroidal neovascularization in angioid streaks. *Retina*. 2013;33(4):825-833.
9. Finger RP, Charbel Issa P, Hendig D, Scholl HPN, Holz FG. Monthly ranibizumab for choroidal neovascularizations secondary to angioid streaks in pseudoxanthoma elasticum: a one-year prospective study. *Am J Ophthalmol*. 2011;152(4):695-703.
10. Finger RP, Charbel Issa P, Ladewig M, Holz FG, Scholl HPN. Intravitreal bevacizumab for choroidal neovascularisation associated with pseudoxanthoma elasticum. *Br J Ophthalmol*. 2008;92(4):483-487.
11. Gliem M, Figuer RP, Fimmers R, Brinkmann CK, Holz FG, Charbel P. Treatment of choroidal neovascularization due to angioid streaks. A Comprehensive Review. *Retina*. 2013;33(7):1300-1314.
12. Tsui I, Fuchs BS, Chou CL, Chang S, Tsang SH. Non-vascular vision loss in pseudoxanthoma elasticum. *Doc Ophthalmol*. 2008;117(1):65-67.
13. Gliem M, Muller PL, Birtel J, Hendig D, Holz FG, Charbel Issa P. Frequency, Phenotypic Characteristics and Progression of Atrophy Associated With a Diseased Bruch's Membrane in Pseudoxanthoma Elasticum. *Invest Ophthalmol Vis Sci*. 2016;57(7):3323-3330.
14. Finger RP, Charbel Issa P, Ladewig M, Gotting C, Holz FG, Scholl HPN. Fundus autofluorescence in Pseudoxanthoma elasticum. *Retina*. 2009;29(10):1496-1505.
15. Schoenberger SD, Agarwal A. Geographic chorioretinal atrophy in pseudoxanthoma elasticum. *Am J Ophthalmol*. 2013;156(4):715-723.
16. Finger RP, Fenwick E, Marella M, et al. The relative impact of vision impairment and cardiovascular disease on quality of life: the example of pseudoxanthoma elasticum. *Health Qual Life Outcomes*. 2011;9:113.
17. Plomp AS, Toonstra J, Bergen AAB, van Dijk MR, de Jong PTVM. Proposal for updating the pseudoxanthoma elasticum classification system and a review of the clinical findings. *Am J Med Genet A*. 2010;152A(4):1049-1058.
18. ETDRS Research Group. No Title. In: *Early Treatment of Diabetic Retinopathy Study (ETDRS) Manual of Operations*. National Technical Information Service; 1985:1-74.
19. World Health Organization. ICD-10 Definition.
20. Hofman A, Grobbee DE, de Jong PT, van den Ouweland FA. Determinants of disease and disability in the elderly: the Rotterdam Elderly Study. *Eur J Epidemiol*. 1991;7(4):403-422.
21. Ikram MA, Brusselle GGO, Murad SD, et al. The Rotterdam Study: 2018 update on objectives, design and main results. *Eur J Epidemiol*. 2017;32(9):807-850.

22. Van Leeuwen R, Chakravarthy U, Vingerling JR, et al. Grading of age-related maculopathy for epidemiological studies: Is digital imaging as good as 35-mm film? *Ophthalmology*. 2003;110(8):1540-1544.
23. Ebran J-M, Milea D, Trelohan A, et al. New insights into the visual prognosis of pseudoxanthoma elasticum. *Br J Ophthalmol*. 2014;98(1):142-143.
24. Orssaud C, Roche O, Dufier J-L, Germain DP. Visual Impairment in Pseudoxanthoma Elasticum: A Survey of 40 Patients. *Ophthalmic Genet*. 2015;36(4):327-332.
25. Hocaoglu M, Karacorlu M, Sayman Muslubas I, Arf S, Ozdemir H, Uysal O. Visual impairment in pseudoxanthoma elasticum: A survey of 53 patients from Turkey. *Eur J Ophthalmol*. 2016;26(5):449-453.
26. Sawa M, Ober MD, Freund KB, Spaide RF. Fundus autofluorescence in patients with pseudoxanthoma elasticum. *Ophthalmology*. 2006;113(5):814-20.e2.
27. Audo I, Vanakker OM, Smith A, et al. Pseudoxanthoma Elasticum with Generalized Retinal Dysfunction, a Common Finding? *Investig Opthalmology Vis Sci*. 2007;48(9):4250.
28. Querques G, Bux A V, Prascina F, Noci ND. Intravitreal avastin for choroidal neovascularization associated with stargardt-like retinal abnormalities in pseudoxanthoma elasticum. *Middle East Afr J Ophthalmol*. 2010;17(4):387-389.
29. Gullapalli VK, Sugino IK, Van Patten Y, Shah S, Zarbin MA. Impaired RPE survival on aged submacular human Bruch's membrane. *Exp Eye Res*. 2005;80(2):235-248.
30. Bird AC, Phillips RL, Hageman GS. Geographic atrophy: a histopathological assessment. *JAMA Ophthalmol*. 2014;132(3):338-345.
31. Jansen RS, Duijst S, Mahakena S, et al. *ABCC6*-mediated ATP secretion by the liver is the main source of the mineralization inhibitor inorganic pyrophosphate in the systemic circulation-brief report. *Arterioscler Thromb Vasc Biol*. 2014;34(9):1985-1989.
32. Rosenfeld PJ, Brown DM, Heier JS, et al. Ranibizumab for Neovascular Age-Related Macular Degeneration. *N Engl J Med*. 2006;355(14):1419-1431.
33. Finger RP, Charbel Issa P, Schmitz-Valckenberg S, Holz FG, Scholl HN. Long-term effectiveness of intravitreal bevacizumab for choroidal neovascularization secondary to angioid streaks in pseudoxanthoma elasticum. *Retina*. 2011;31(7):1268-1278.
34. Teixeira A, Moraes N, Farah ME, Bonomo PP. Choroidal neovascularization treated with intravitreal injection of bevacizumab (Avastin) in angioid streaks. *Acta Ophthalmol Scand*. 2006;84(6):835-836.
35. Myung JS, Bhatnagar P, Spaide RF, et al. Long-term outcomes of intravitreal antivascular endothelial growth factor therapy for the management of choroidal neovascularization in pseudoxanthoma elasticum. *Retina*. 2010;30(5):748-755.
36. Young M, Chui L, Fallah N, et al. Exacerbation of choroidal and retinal pigment epithelial atrophy after anti-vascular endothelial growth factor treatment in neovascular age-related macular degeneration. *Retina*. 2014;34(7):1308-1315.
37. Grunwald JE, Daniel E, Huang J, et al. Risk of geographic atrophy in the comparison of age-related macular degeneration treatments trials. *Ophthalmology*. 2014;121(1):150-161.


Chapter 4

Is arterial stiffness in the carotid artery associated with choroidal thinning in patients with pseudoxanthoma elasticum or controls?

Sara Risseeuw
Jonas Bartstra
Jeannette Ossewaarde – van Norel
Lennart J. Geurts
Catherina H.Z. Li
Saskia M. Imhof
Wilko Spiering
Pim A. de Jong
Redmer van Leeuwen

Acta Ophthalmologica. 2020;98:492-299

Abstract

Purpose

Patients with pseudoxanthoma elasticum (PXE) develop calcification of Bruch's membrane and choroidal thinning, as well as calcification of intracranial arteries, leading to arterial stiffness. We investigated whether arterial stiffness is associated with choroidal thinning in PXE patients, besides the presumed effect of BM calcification.

Methods

Cross-sectional study with 75 PXE patients and 40 controls. Macular choroidal thickness was measured using optical coherence tomography scans. Functional magnetic resonance imaging was used to calculate the pulsatility index (PI) of the carotid siphon as a measure of arterial stiffness. Associations between PI and choroidal thickness were investigated using linear mixed effects models adjusted for age and ocular axial length. Furthermore, we investigated choroidal thickness in relation to the presence of retinal pigment epithelium (RPE) atrophy, its topographical distribution and age.

Results

Median age was 58 years (IQR 53–66) in PXE patients and 62 years (IQR 56–67) in controls (p=0.08). PXE patients had a thinner choroid than controls (138 µm versus 248 µm, p<0.01). No association was observed between PI and choroidal thickness in PXE patients (β=-1.6, 95%CI -59.4–54.5) nor in controls (β=-47.6, 95%CI -129.7–31.9). In PXE patients, RPE atrophy was associated with a thinner choroid (p<0.01). Also, the nasal choroid was thinner than the temporal choroid, and choroidal thickness already decreased with age in PXE eyes without RPE atrophy.

Conclusion

There was no independent association between measures of arterial stiffness and choroidal thinning in PXE patients and controls. Probably, changes in Bruch's membrane lead to choroidal thinning in PXE.

Introduction

Pseudoxanthoma elasticum (PXE) is a rare genetic disease leading to ectopic calcification of elastic tissues, including the arteries, skin, and Bruch's membrane in the retina. [1] Clinically, this leads to peripheral arterial disease, pseudoxanthomas on the skin, and macular degeneration with considerable visual morbidity.[2] Calcification in the vasculature is predominantly present in the intracranial internal carotid artery (IICA) and the arm and leg arteries.[3] Calcification in the eyes occurs in Bruch's membrane (BM) and is visible as peau d'orange and angioid streaks, which are breaks in the brittle BM.[4] In angioid streaks, choroidal neovascularizations (CNV) and subsequent scarring may develop. In addition, severe visual loss is caused by macular atrophy and since PXE is a progressive disease, the visual acuity deteriorates with older age.[5,6]

Furthermore, the choroid is significantly thinner in patients with PXE.[7–9] The cause of the choroidal thinning is unclear. The choroid is a vascular tissue that receives most of the ocular blood flow.[10] Integrity of the choroid is essential for retinal functioning by exchanging nutrients and oxygen across the retinal pigment epithelium (RPE), and ultimately choroidal disease can cause degenerative changes in the retina.[10] Gliem et al. found that choroidal thinning in PXE patients seems to follow the centrifugal pattern of BM calcification, suggesting that BM calcification affects choroidal thickness.[7] Probably, BM calcification impedes diffusion of factors secreted by the RPE, such as vascular endothelial growth factor (VEGF), which are essential for maintaining the integrity of the choroid. However, it is plausible that arterial calcification in PXE is associated with choroidal thinning as well, since systemic vascular changes are known to affect the choroidal thickness.[11,12]

In the general population, arterial stiffness increases with age and is associated with end-organ damage in the kidneys and the brain.[13] This might be due to reduced pulse pressure dampening and increased pulsatile load in the microvasculature of these organs.[13] Arterial calcification contributes to arterial stiffness,[14] and the progressive arterial calcification in PXE is therefore thought to cause the increased arterial stiffness seen in these patients.[15] Recently, it was shown that calcification of the IICA is associated with an increased pulsatility index (PI) in the intracranial arteries in PXE patients. The PI is a proxy for carotidal vascular stiffness[16], and contributed to microvascular damage and cognitive decline in PXE patients (Bartstra et al, manuscript in preparation).

The choroidal vasculature is supplied by the ophthalmic artery, which branches from the IICA. Over 80% of its blood flows to the choroid.[11] The choroid can regulate perfusion pressure to some degree, but its autoregulation is assumed to be less effective than the autoregulation of other tissues, such as the retina.[10,17] Therefore, increased vascular stiffness in the IICA might contribute to microvascular damage and thinning of the choroid.

The aim of this study is to determine whether arterial stiffness is associated with choroidal thinning in patients with PXE, besides the presumed effect of BM calcification. Also, we aim to investigate whether a possible relationship between arterial stiffness and choroidal thinning is part of a normal aging process in controls. In addition, we investigated choroidal thickness in relation to age, the presence of RPE degeneration, and the presumed spread of BM calcification.

Methods

Participants

This cross-sectional study (METC number 16-622) was conducted in adherence to the tenets of the Declaration of Helsinki. PXE patients and controls were recruited from the Dutch National Expertise Center for PXE in the University Medical Center in Utrecht, the Netherlands.

Diagnosis of PXE was confirmed when a patient fulfilled at least two of the major diagnostic criteria:[1] skin involvement (yellowish papules/plaques), eye involvement (peau d'orange, angioid streaks) or genetic confirmation (biallelic *ABCC6* gene mutations, first-degree PXE relative). An aged-matched control group was recruited from genetically non-related family members or friends of PXE patients, who did not meet the PXE criteria. Participants were included when they underwent the optional ophthalmologic examination. Participants were excluded if they met any of the following criteria: under 18 years old; unable or unwilling to sign informed consent; severe renal impairment (eGFR<30ml/min/1.73m^2); pacemaker or implantable cardiac defibrillator; metallic foreign body in the eye or claustrophobia; an ocular axial length <20.5 mm or >26.5 mm.

All participants underwent an ophthalmological examination including dilated fundus and slit-lamp examination, automatic refractometry, spectral domain optical

coherence tomography (SD-OCT) imaging, and ultrasound biometry. Best corrected visual acuity (BCVA) was measured using the Early Treatment Diabetic Retinopathy Study (ETDRS) charts. The phenotype in the posterior pole was assessed according to previously reported criteria and categorized into four groups to assess the severity of macular degeneration: no RPE atrophy or CNV, choroidal neovascular (CNV) lesions, RPE atrophy or mixed.[5] Age, sex, body mass index (BMI), blood pressure, smoking history and details on other vascular measurements were obtained from medical files if available. Other vascular measurements included intima media thickness (IMT), ankle brachial index (ABI), and the severity and volume of IICA calcification. The majority of participants (71.3%) underwent brain magnetic resonance imaging (MRI).

Measurement of choroidal thickness

Enhanced depth imaging SD-OCT was obtained after pupil dilatation (Heidelberg Engineering, Heidelberg, Germany). The 20° x 5° OCT volumes consisted of seven horizontal and seven vertical B-scans through the macular area which were averaged 25 times. All scans were assessed in the Heidelberg Eye Explorer software (Heidelberg Engineering, Heidelberg, Germany) by manually measuring the choroidal thickness, defined as the distance between the outer border of the hyperreflective RPE/BM band and the inner surface of the sclera (Figure 4.1). An ETDRS grid (with diameters of 1, 3 and 6 mm) was centered on the foveal dip. Measurements were made subfoveal and at 500 µm and 1500 µm distance parafoveal in the horizontal and vertical scans, resulting in a total of 9 measurement points: nasal, temporal, superior and inferior to the foveal centre. We averaged these measurements to obtain a mean choroidal thickness per eye, which was used in further analysis unless mentioned otherwise. The 20° scans often did not reach 3000 µm eccentricity, since one degree of visual angle equals 288 µm on the retina. Therefore, we did not include measurements at 3000 µm in the measurement protocol. In some cases, the foveal centre could not be identified visually on OCT scans alone as a result of retinal or BM changes and fixation affected by macular pathology. Colour fundus photographs and the average optic disc to fovea distance of 4.7 mm were then used to identify the most plausible foveal dip.[18,19] Measurements were performed by two researchers (CL and SR) and all measurements were visually verified by one grader (SR).

Choroidal thickness measurements are known to be highly reproducible in eyes without pathology.[20] However, these data have not been reported yet for PXE eyes, therefore we assessed the agreement and reliability of choroidal thickness measurements in PXE eyes. Two researchers (CL and SR) measured the subfoveal choroidal thickness in a

random subset of 20 PXE eyes. The mean difference was 12 µm (95% CI 3 – 21 µm) and 95% limits of agreement were -25µm (95% CI -41 – -10 µm) and 50 µm (95% CI 34 – 66 µm) for the lower and upper limit, respectively. The intraclass correlation coefficient was 0.98 (95% CI 0.91 – 0.99) based on an average measures, absolute-agreement two-way model.[21]

MRI acquisition and processing

Time-resolved 2D phase contrast (2Dpc) scanning was performed on a 3 Tesla MRI (Ingenia CX, Philips, the Netherlands). The 2Dpc acquisitions were planned at the IICA segment C4, C6 and at the origin of the middle cerebral artery (MCA).[22] An in-house developed Matlab script (Mathworks Inc., Natick, Massachusetts) was used to quantify the blood flow in these locations. The PI was derived from the blood flow time curves and was calculated using the following formula:

$$PI = \frac{V_{max} - V_{min}}{V_{mean}}$$

with V_{max} being the peak systolic flow, V_{min} the lowest diastolic flow, and V_{mean} the mean blood flow during one cardiac cycle. The mean of the PI in C4 and MCA was used for further analysis. The PI at segment C6 was hard to measure due to imaging artefacts and therefore not included in the averaged PI for further analysis.

For further insight into the vascular status of PXE patients and its potential effect on choroidal thickness, measurements of carotid intima media thickness (IMT) using ultrasound, the ankle-brachial index (ABI) and siphon calcification on CT scan (both the absolute mass and a severity classification) were collected. These parameters were not available from controls. Further details on these measurements can be found in the supplementary methods.

Data analysis

BCVA was converted to the logarithm of the minimum angle of resolution (logMAR) for statistical purposes. Continuous variables are presented as mean ± standard deviation (SD) or as median (interquartile range (IQR)), depending on their distribution. Categorical variables are presented as numbers (%). To test differences between PXE patients and controls, we used the Chi-square test for categorical variables, the two-sample t-test for normal distributions and the Mann-Whitney U test for non-normal distributions. ANOVA test was used to test differences between the severity of macular degeneration. A *p*-value of <0.05 was considered statistically significant.

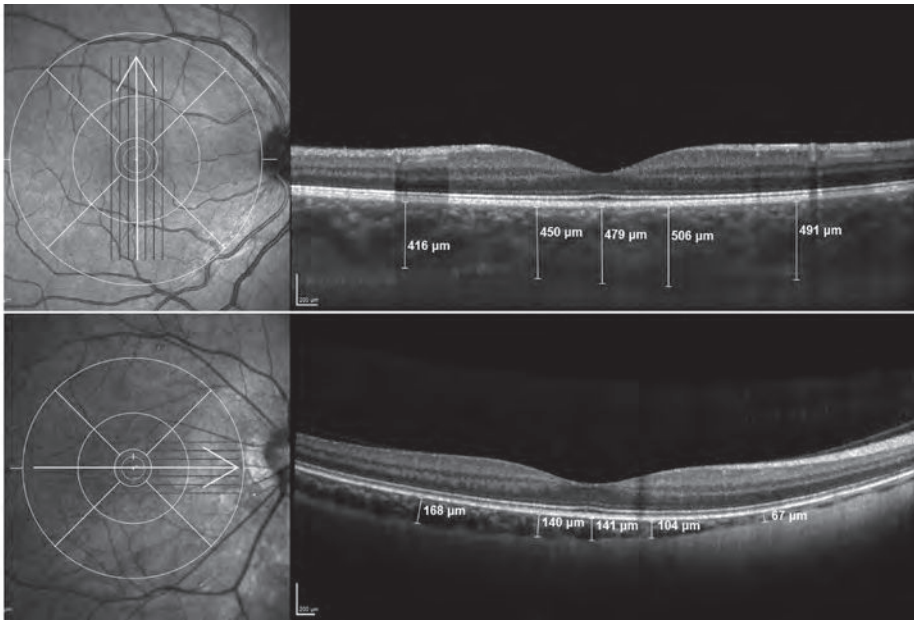

Figure 4.1 Choroidal thickness measurements in Heidelberg Eye Explorer. Choroidal thickness was defined as the outer border of the hyperreflective retinal pigment epithelium and Bruch's membrane to the inner surface of the sclera. An ETDRS grid (1, 3, 6mm) was placed over the foveal dip. Measurements were made subfoveal and at 0.5 and 1.5 mm distance from the fovea in the horizontal and vertical scans. This resulted in 9 measurement points. Above: OCT scan of 27-year old control. Bottom: scan of 28-year old PXE patient.

Missing values on baseline characteristics were considered 'missing at random' and imputed using multiple imputation for further association analyses.[23] The highest proportion of missing values was 17%, therefore we used m=20 imputed and combined datasets for further multivariable analyses.

We used a linear mixed effects model to analyze the association between PI and choroidal thickness, since this allows for the use of correlated data of two eyes of a participant. In this model, we modeled the individual patient as a random effect to investigate the unilateral effect of the PI on choroidal thickness.[24] Crude models and models adjusted for age and axial length were constructed, since age is a possible confounder and axial length is known to affect choroidal thickness.[25] Based on previous

research, other confounders might include cardiovascular risk factors (blood pressure, BMI, smoking).[25–27] We identified possible confounders based using both rationale and a simulation of the optimal cut-off percentage for the 'change in estimate'.[28]

We repeated the analysis in subgroups of PXE patients to investigate the effect of RPE integrity on choroidal thinning. Therefore, we stratified for eyes without the presence of RPE atrophy or CNV and eyes with RPE atrophy.

BM calcification follows a centrifugal spread, which means that BM calcification is more severe in the nasal area than the temporal area.[29] Therefore, we plotted the topographical distribution of choroidal thickness to investigate the relationship between choroidal thinning and the presumed spread of BM calcification. To study the effect of age on choroidal thickness, we performed a linear regression with age as the determinant and choroidal thickness as the outcome.
R version 3.4.1 was used for statistical analysis. Add-on packages 'mice' (version 3.4.0) and 'lme4' (version 1.1 – 20) were used for multiple imputation and mixed model regression, respectively.

Results

In total, 75 PXE patients and 40 controls were included. Patient characteristics are presented in Table 4.1. Median age was 58 years (range 53 - 66) in PXE patients and 62 years (range 53 - 67) in controls. Cardiovascular risk factors such as BMI and mean arterial pressure were similar in the two groups, but the use of cholesterol lowering medication was higher in PXE patients. Visual acuity was worse in PXE patients as compared to controls. Mean choroidal thickness was lower in PXE patients than controls, 138 µm versus 248 µm ($p < 0.01$), respectively.

Choroidal thickness and pulsatility index

No significant differences in PI were found between PXE patients and controls. We analyzed the association between mean PI and mean choroidal thickness using a mixed model for PXE patients and controls separately. In the crude models, mean PI was not significantly associated with choroidal thickness in both PXE and controls (details on the models can be found in Table 4.2). The associations diminished when corrected for age and axial length in both PXE patients (β = -1.6 µm, 95% CI -59.4 – 54.5, $p = 0.96$) and controls (β = -47.6 µm, 95% CI -129.7 – 31.9, $p = 0.26$).

Table 4.1 Patient characteristics of controls and pseudoxanthoma elasticum (PXE) patients

			Controls		PXE patients	p-value
		Number[a]	n=40	Number[a]	n=75	
Patient data	Age in years		62 [56 – 67]		58 [53 – 66]	0.08
	Gender (female)		18 (45%)		39 (52%)	0.60
	BMI	*n = 34*	26.35 [23.62 – 27.95]		25.6 [23.2 – 27.7]	0.48
	Mean arterial pressure		93 [852 – 100]		96 [90 – 105]	0.08
	Smoking status: never	*n = 20*	10 (50%)		38 (51%)	>0.99
	Use of antihypertensive drugs	*n = 39*	10 (26%)		23 (31%)	0.73
	Use of anti-diabetic drugs		0		3 (4%)	0.52
	Use of cholesterol lowering drugs		8 (20%)		43 (57%)	<0.01
Carotid stiffness[b]	Pulsatility index C4 (proximal)	*n = 34*	1.02 [0.92 – 1.21]	*n = 48*	1.11 [1.00 – 1.25]	0.20
	Pulsatility index MCA (distal)	*n = 34*	0.90 [0.80 – 1.03]	*n = 48*	1.00 [0.87 – 1.14]	0.11
	Mean pulsatility index	*n = 34*	0.97 [0.86 – 1.10]	*n = 48*	1.05 [0.95 – 1.20]	0.10
Eye data[b]	Visual acuity (logMar)	*n = 37*	0.00 [-0.08 – 0.06]	*n = 74*	0.70 [0.06 – 1.13]	<0.01
	Axial length (*mm*)	*n = 37*	24.1 (SD 1.1)	*n = 64*	24.1 (SD 0.9)	0.77
	Spherical refractive error (D)	*n = 38*	-0.12 [-2.44 – 1.47]	*n = 73*	-0.38 [-1.50 – 0.38]	0.27
	Mean choroidal thickness (*μm*)	*n = 39*	248 [214 – 295]	*n = 74*	138 [88 – 179]	<0.01

Abbreviations: BMI; body mass index, MCA; medial cerebral artery, logMAR; logarithm of the minimum angle of resolution, D; diopters
Values are presented as number (%), mean (standard deviation) or median [interquartile range].
P-values were based on Chi-square test for categorical variables, the two-sample t-test for normal distributions and the Mann-Whitney U test for non-normal distributions.
a. In case of missing data, the number patients with available data is presented.
b. Pulsatility index and eye data were measured on both the left and right side. The presented data are the averaged data of the left and right side. For exact locations in the carotid artery, see supplementary figure 1.

Table 4.2 Crude and adjusted associations of pulsatility index as a proxy for carotidal vascular stiffness and mean choroidal thickness

		Crude				Adjusted for age and axial length			
		Estimate	95% CI		p-value	Estimate	95% CI		p-value
PXE	Mean pulsatility index	-53.2	-118.6	6.6	0.06	-1.6	-59.4	54.4	0.96
	Age in years					-4.8	-6.5	-3.0	<0.01
	Axial length in mm					3.4	-11.4	18.3	0.65
Controls	Mean pulsatility index	-68.6	-147.3	8.4	0.08	-47.6	-129.7	31.9	0.26
	Age in years					-0.8	-3.9	2.3	0.64
	Axial length in mm					-20.7	-37.7	-3.6	0.02

Abbreviations: CI; confidence interval, PXE; Pseudoxanthoma Elasticum
All models are mixed model linear regression models. Herein, determinants are modeled as fixed effects and different measurements per person (right or left side) are modeled as random effects.

In patients with PXE, age was the most important determinant of choroidal thinning (β = -4.8 µm, 95% CI -6.5 – -3.0, $p < 0.01$), whereas in the control group this was axial length (β = -20.7 µm, 95% CI -37.7 – -3.6, $p = 0.02$). Other possible confounding variables, such as BMI and mean arterial pressure were not associated with choroidal thickness (data not shown) and did not improve the models.

Association between choroidal thickness and RPE atrophy

Of all PXE eyes, 34 (22.8%) had no RPE atrophy or CNV, 39 (26.2%) had CNV, 11 (7.4%) had RPE atrophy and 65 (43.6%) had a combination of CNV and RPE atrophy. RPE atrophy and CNV were associated with choroidal thinning: eyes without CNV and RPE atrophy had a mean choroidal thickness of 206 (SD 65 µm, compared to 163 (SD 68) µm in eyes with CNV or scarring, and 103 (SD 63) µm in eyes with RPE atrophy with or without CNV (p <0.01). Further details are presented in Table 4.3.

In the stratified analysis, a possible crude effect of PI on choroidal thickness was largest in eyes without RPE atrophy or CNV (β -137.9 µm, 95% CI -276.4 – -0.5, $p = 0.05$). However, the adjusted analyses again showed no statistically significant association between mean PI and mean choroidal thickness in both categories.

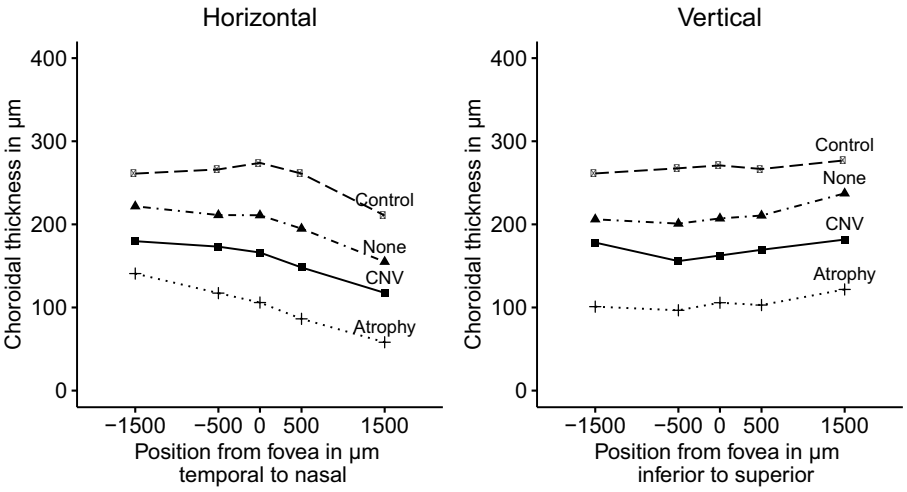

Figure 4.2 Topographical distribution of choroidal thickness in pseudoxanthoma elasticum (PXE) patients and controls. The graphs show the choroidal thickness at each measurement position on horizontal and vertical optical coherence tomography scans. PXE eyes were categorized into three groups based on the ocular phenotype: no RPE atrophy or CNV (none), CNV without RPE atrophy, and RPE atrophy with or without CNV.

Table 4.3 The association of vascular stiffness with choroidal thickness, stratified for integrity of the retinal pigment epithelium

					Model details							
					Crude				Adjusted			
RPE integrity	Mean age	Mean choroidal thickness	Mean PI	Determinants	Estimate	95% CI		p-value	Estimate	95% CI		p-value
No RPE atrophy or CNV	49.1 (SD 7.5)	206 (SD 65)	0.91 (SD 0.17)	Mean PI	-137.9	-276.4	-0.5	0.05	-82.8	-234.1	60.4	0.29
n = 34 eyes				Axial length (mm)					24.9	0.1	48.3	0.03
				Age (years)					-3.2	-6.6	0.2	0.08
RPE atrophy with or without CNV[a]	62.6 (SD 10.4)	103 (SD 63)	1.19 (SD 0.22)	Mean PI	34.5	-28.2	92.0	0.25	34.6	-28.0	92.0	0.26
				Axial length (mm)					-4.8	-30.6	20.7	0.72
n = 76 eyes				Age (years)					-4.7	-9.8	0.4	0.09

Abbreviations: CI; confidence interval, PI; pulsatilitiy index, CNV; choroidal neovascularization, RPE; retinal pigment epithelium
All models are mixed model linear regression models with determinants as fixed effects and different measurements per person (right or left side) as random effects.
a. Atrophy is defined as macular atrophy with loss of RPE alone, or in combination with CNV.

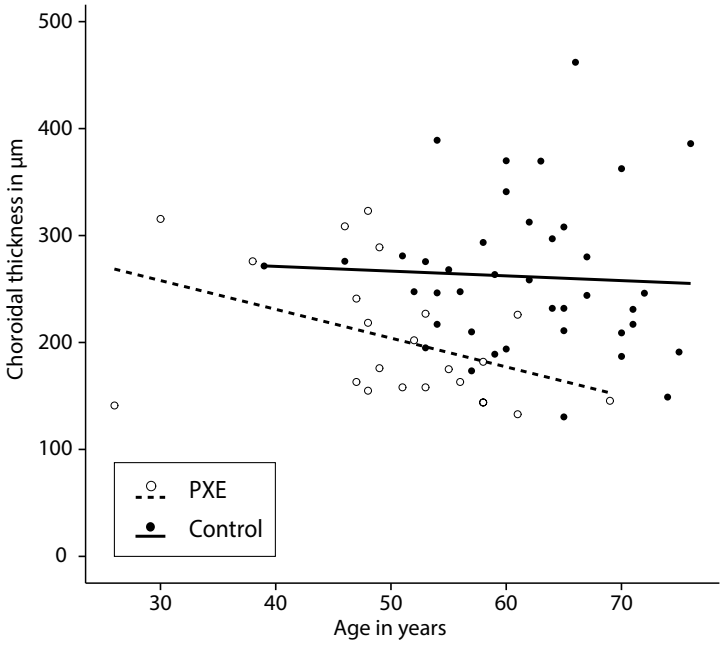

Figure 4.3 Mean choroidal thickness plotted against age for both controls and PXE patients. For controls, both eyes were averaged. For PXE patients, only eyes without RPE atrophy or CNV were included and averaged in case both eyes had no RPE atrophy or CNV.

Distribution of choroidal thickness

In both controls and PXE subgroups, the most nasal measurement on the horizontal scan was thinner than the other four measurements (Figure 4.2). Also, in PXE patients without macular degeneration, the choroid was thinner than in the control group on all positions.

The effect of age on mean choroidal thickness is plotted in Figure 4.3. In this graph, only controls and PXE patients without RPE atrophy or CNV are shown. In linear regression analysis, age was negatively associated with choroidal thickness in PXE patients (β = -2.7 µm, 95% CI -5.3 – -0.1, p = 0.05), but not in controls (β = -0.4 µm, CI -3.3 – 2.4, p = 0.76).

Other vascular parameters in patients with PXE

For the other vascular parameters, data were only available in PXE patients. The median IMT was 0.70 mm (IQR 0.63 – 0.82) and median ABI in rest was 0.97 (IQR 0.73 – 1.04). Most PXE patients had calcification in the IICA: 15 (20.3%) had no calcification, 17 (23.0%) had mild calcification, 15 (20.3%) had moderate calcification and 27 (36.5%) had severe calcification. The median IICA calcification mass score was 16.6 (IQR 7.7 – 50.9). Only IMT showed a negative association with mean choroidal thickness in the crude models (Table 4.4). However, when adjusted for age and axial length, these effects disappeared. Ankle-brachial index and siphon calcification were not associated with choroidal thickness.

Table 4.4 Correlations between vascular status measurements and mean choroidal thickness in PXE patients

	Crude				Adjusted for age and axial length			
	Estimate	95% CI		p-value	Estimate	95% CI		p-value
Intima media thickness	-199.9	-308.6	-91.1	0.00	-44.3	-156.8	68.2	0.45
Age in years					-4.3	-5.9	-2.6	<0.01
Axial length in mm					-7.0	-19.4	5.7	0.26
Ankle-brachial index	51.9	-30.0	133.8	0.22	-10.2	-78.5	58.2	0.77
Age in years					-4.7	-6.1	-3.2	<0.01
Axial length in mm					-6.6	-18.9	6.2	0.29
Siphon score								
1 vs 0	1.1	-50.6	52.7	0.97	17.4	-24.1	58.6	0.43
2 vs 0	-5.4	-57.8	47.0	0.84	8.5	-33.4	50.3	0.70
3 vs 0	-10.7	-57.7	36.2	0.66	16.5	-21.7	54.6	0.41
Age in years					-4.7	-6.1	-3.3	<0.01
Axial length in mm					-7.3	-19.4	5.7	0.25
Siphon calcification mass	-0.2	-0.5	0.1	0.12	-0.1	-0.4	0.1	0.25
Age in years					-4.6	-6.2	-3.1	<0.01
Axial length in mm					4.3	-10.3	19.0	0.56

Abbreviations: CI; confidence interval, PXE; Pseudoxanthoma Elasticum
All models are mixed model linear regression models. Herein, determinants are modeled as fixed effects and different measurements per person (right or left side) are modeled as random effects.

Discussion

In this study, we found no association of choroidal thinning in PXE patients with arterial stiffening, hence, the diseased Bruch's membrane remains the most likely explanation. This is supported by the strong association between choroidal thickness and the severity of macular degeneration. In addition, another important determinant of choroidal thinning in PXE eyes without RPE atrophy or CNV is age, whereas age is no important determinant of choroidal thinning in controls. This implicates that BM calcification progresses with age in PXE patients, which then progressively impairs the vitality of tissues adjacent to the BM. In this study, we could not demonstrate a relationship between increased arterial stiffness in the IICA and choroidal thickness in patients with PXE. Furthermore, we found no association with choroidal thickness and other vascular parameters in PXE patients. Also, in controls we found no association between the IICA PI and choroidal thickness.

Increased pulsatility is associated with increased microvascular damage in high flow, low impedance organs such as the kidneys and brain.[30] This effect is demonstrated in brain tissue where different indicators of carotid stiffness are associated with impaired cognitive functioning[31,32] brain atrophy and white matter lesions[32] and subcortical infarctions.[33] In the latter study, the pulsatile parameter had the highest predictive value, implicating that an increased pulse pressure is responsible for microvascular damage.[33]

Interestingly, the effect of an increased pulse pressure on the choroid, also a high flow organ, has not been investigated extensively. Therefore, the association between vascular disease and the choroidal vasculature is less ambiguous. In a study of 43 healthy, young controls, there was no correlation between carotid PI and choroidal thickness. [34] However, in the same study there was a positive correlation between end-diastolic blood flow and choroidal thinning. Although these analyses were not corrected for age, they might suggest that changes in hemodynamics could affect choroidal thickness. Diseases that cause a reduced ocular blood flow, e.g. carotid artery stenosis, might also affect choroidal thickness. Three studies investigated this association and findings were inconsistent. One study found a negative correlation between the extent of stenosis and choroidal thickness[35], whereas another study found a positive correlation.[36] In another study, the choroid was thinner in patients with carotid artery stenosis, but there was no correlation with the extent of stenosis.[37] These findings, together with our results, suggest that there are no reasons to assume that

the relationship between IICA hemodynamics and choroidal thinning is an important pathophysiological process.

Our findings support the alternative hypothesis that choroidal thinning in PXE is caused by BM calcification, and subsequently by a diseased RPE. This is supported by the observed distribution of choroidal thinning in PXE patients, following the centrifugal spread of calcification from the optic nerve to the periphery.[29] Two previous studies in PXE patients found that the nasal choroid was thinner than the temporal choroid, and this was already detectable in eyes without macular degeneration.[7,9] One of these studies also investigated the choroidal vasculature using en-face OCT imaging and found that the vascular density was reduced in PXE patients when compared to controls.[7] Furthermore, in line with our findings, these studies found a correlation between the severity of macular degeneration in PXE and choroidal thickness, and demonstrated that choroidal thickness is already reduced in relatively young patients without CNV or atrophy.[7,9]

Our findings provide relevant insights into the relationship between the choroid and the RPE. The choroid supplies the retina with oxygen and nutrients, and relies on autoregulation, which is the ability of the tissue to regulate the perfusion pressure, to achieve an adequate blood flow.[10] The RPE disposes its waste products via the choroid and also secretes products (such as VEGF) that regulate the choroid. These physiological processes may be affected by changes in BM, which is located between the choroid and the RPE.[10] It is likely that BM calcification in PXE impedes the diffusion of RPE products to the choroid. This might impair autoregulation of the choroid and subsequently cause structural changes, such as thinning, of the choroid. This may compromise the supply of oxygen and nutrients to the RPE, which could ultimately contribute to an atrophic RPE and thereby even less production of factors that support the choroid. However, this possible pathophysiological process is speculative. Changes in BM are part of normal aging and are also associated with other diseases, such as age-related macular degeneration.[38] To further explore and quantify the effect of BM calcification on choroidal thinning, a biomarker for the severity of BM calcification is warranted. Unfortunately, such an endpoint is still lacking.

Strengths of this study include the large number of PXE patients in combination with the detailed and extensive vascular and ophthalmological measurements. To our knowledge, this is the first cohort investigating the association between vascular stiffness parameters and ocular pathology in patients with PXE.

Some limitations need to be addressed as well. There was no significant difference in PI between PXE patients and controls. Unpublished data of our study group did show a higher PI in PXE patients when compared to controls in a slightly larger study population (Bartstra et al, manuscript in preparation). Hence, the difference in sample size might explain why the difference in PI between PXE patients and controls did not reach statistical significance.

Furthermore, we used a combination of the most proximal and the most distal measurements of the IICA (segments C4 and MCA) to obtain the mean vascular stiffness, since the middle measurement (segment C6) had many missing data due to imaging artefacts. However, this location is the most interesting for the purpose of this study, since it is closest to the branching ophthalmic artery and thereby to the choroid.

Choroidal thickness is known to vary within individuals as a result of age, axial length, circadian rhythm, and fluid intake.[39] We corrected for age and axial length, since these appear to have the largest influence on choroidal thickness.[25] However, no data on the time of choroidal measurement and fluid intake were available.

In summary, PXE patients have a thinner choroid than controls. No independent association between vascular stiffness and mean choroidal thickness could be demonstrated in both PXE patients and controls, suggesting that the observed choroidal thinning in PXE patients is likely to be the result of BM calcification.

References

1. Plomp AS, Toonstra J, Bergen AAB, van Dijk MR, de Jong PTVM. Proposal for updating the pseudoxanthoma elasticum classification system and a review of the clinical findings. *Am J Med Genet A*. 2010;152A(4):1049-1058.
2. Finger RP, Charbel Issa P, Ladewig MS, et al. Pseudoxanthoma elasticum: genetics, clinical manifestations and therapeutic approaches. *Surv Ophthalmol*. 2009;54(2):272-285.
3. Kranenburg G, de Jong PA, Mali WP, Attrach M, Visseren FLJ, Spiering W. Prevalence and severity of arterial calcifications in pseudoxanthoma elasticum (PXE) compared to hospital controls. Novel insights into the vascular phenotype of PXE. *Atherosclerosis*. 2017;256:7-14.
4. Gliem M, De Zaeytijd J, Finger RP, Holz FG, Leroy BP, Issa PC. An update on the ocular phenotype in patients with pseudoxanthoma elasticum. *Front Genet*. 2013;4(APR):14.
5. Risseeuw S, Ossewaarde-van Norel J, Klaver CCW, Colijn JM, Imhof SM, van Leeuwen R. Visual Acuity in Pseudoxanthoma Elasticum. *Retina*. 2019;39(8):1580-1587.
6. Gliem M, Muller PL, Birtel J, Hendig D, Holz FG, Charbel Issa P. Frequency, Phenotypic Characteristics and Progression of Atrophy Associated With a Diseased Bruch's Membrane in Pseudoxanthoma Elasticum. *Invest Ophthalmol Vis Sci*. 2016;57(7):3323-3330.
7. Gliem M, Fimmers R, Muller PL, et al. Choroidal changes associated with Bruch membrane pathology in pseudoxanthoma elasticum. *Am J Ophthalmol*. 2014;158(3):644.
8. Dolz-Marco R, Andreu-Fenoll M, Hernández-Martínez P, Pinazo-Durán MD, Gallego-Pinazo R. Automated macular choroidal thickness measurement by swept-source optical coherence tomography in pseudoxanthoma elasticum. *Int J Retin Vitr*. 2016;2:15.
9. Ellabban AA, Tsujikawa A, Matsumoto A, et al. Macular choroidal thickness and volume in eyes with angioid streaks measured by swept source optical coherence tomography. *Am J Ophthalmol*. 2012;153(6):1133-1143.
10. Nickla DL, Wallman J. The multifunctional choroid. *Prog Retin Eye Res*. 2010;29(2):144-168.
11. Bhutto I, Lutty G. Understanding age-related macular degeneration (AMD): Relationships between the photoreceptor/retinal pigment epithelium/Bruch's membrane/choriocapillaris complex. *Mol Aspects Med*. 2012;33(4):295-317.
12. Ahmad M, Kaszubski PA, Cobbs L, Reynolds H, Smith RT. Choroidal thickness in patients with coronary artery disease. Paul F, ed. *PLoS One*. 2017;12(6):e0175691.
13. Mitchell GF. Aortic stiffness, pressure and flow pulsatility, and target organ damage. *J Appl Physiol*. 2018;125(6):1871-1880.
14. Tsao CW, Pencina KM, Massaro JM, et al. Cross-sectional relations of arterial stiffness, pressure pulsatility, wave reflection, and arterial calcification. *Arterioscler Thromb Vasc Biol*. 2014;34(11):2495-2500.
15. Kranenburg G, Visseren FLJ, de Borst GJ, de Jong PA, Spiering W. Arterial stiffening and thickening in patients with pseudoxanthoma elasticum. *Atherosclerosis*. 2018;270:160-165.
16. de Riva N, Budohoski KP, Smielewski P, et al. Transcranial Doppler Pulsatility Index: What it is and What it Isn't. *Neurocrit Care*. 2012;17(1):58-66.
17. Kur J, Newman EA, Chan-Ling T. Cellular and physiological mechanisms underlying blood flow regulation in the retina and choroid in health and disease. *Prog Retin Eye Res*. 2012;31(5):377-406.
18. Jonas RA, Wang YX, Yang H, et al. Optic Disc-Fovea Distance, Axial Length and Parapapillary Zones. The Beijing Eye Study 2011. *PLoS One*. 2015;10(9):e0138701.
19. van de Put MAJ, Nayebi F, Croonen D, et al. Design and validation of a method to determine the position of the fovea by using the nerve-head to fovea distance of the fellow eye. *PLoS One*. 2013;8(5):e62518.
20. Malamas A, Dervenis N, Kilintzis V, Chranioti A, Topouzis F. Inter- and intraobserver repeatability and reproducibility of choroidal thickness measurements using two different methods. *Int Ophthalmol*. 2019;39(5):1061-1069.

21. Koo TK, Li MY. A Guideline of Selecting and Reporting Intraclass Correlation Coefficients for Reliability Research. *J Chiropr Med*. 2016;15(2):155-163.
22. Bouthillier A, van Loveren HR, Keller JT. Segments of the Internal Carotid Artery: A New Classification. *Neurosurgery*. 1996;38(3):425-433.
23. Donders ART, van der Heijden GJMG, Stijnen T, Moons KGM. Review: A gentle introduction to imputation of missing values. *J Clin Epidemiol*. 2006;59(10):1087-1091.
24. Ying G-S, Maguire MG, Glynn R, Rosner B. Tutorial on Biostatistics: Statistical Analysis for Correlated Binary Eye Data. *Ophthalmic Epidemiol*. 2018;25(1):1-12.
25. Wei W Bin, Xu L, Jonas JB, et al. Subfoveal choroidal thickness: the Beijing Eye Study. *Ophthalmology*. 2013;120(1):175-180.
26. Lau KK, Pego P, Mazzucco S, et al. Age and sex-specific associations of carotid pulsatility with small vessel disease burden in transient ischemic attack and ischemic stroke. *Int J Stroke*. 2018;13(8):832-839.
27. Gattoussi S, Cougnard-Grégoire A, Korobelnik JF, et al. Choroidal thickness, vascular factors, and age-related macular degeneration: the ALIENOR study. *Retina*. 2019;39(1):34-43.
28. Lee PH. Is a cutoff of 10% appropriate for the change-in-estimate criterion of confounder identification? *J Epidemiol*. 2014;24(2):161-167.
29. Charbel Issa P, Finger RP, Gotting C, Hendig D, Holz FG, Scholl HPN. Centrifugal fundus abnormalities in pseudoxanthoma elasticum. *Ophthalmology*. 2010;117(7):1406-1414.
30. O'Rourke MF, Safar ME. Relationship Between Aortic Stiffening and Microvascular Disease in Brain and Kidney. *Hypertension*. 2005;46(1):200-204.
31. Geijselaers SLC, Sep SJS, Schram MT, et al. Carotid stiffness is associated with impairment of cognitive performance in individuals with and without type 2 diabetes. The Maastricht Study. *Atherosclerosis*. 2016;253:186-193.
32. Jochemsen HM, Muller M, Bots ML, et al. Arterial stiffness and progression of structural brain changes: The SMART-MR study. *Neurology*. 2015;84(5):448-455.
33. Mitchell GF, Van Buchem MA, Sigurdsson S, et al. Arterial stiffness, pressure and flow pulsatility and brain structure and function: The Age, Gene/Environment Susceptibility-Reykjavik Study. *Brain*. 2011;134(11):3398-3407.
34. Agladioglu K, Pekel G, Citisli V, Yagci R. Choroidal thickness and retinal vascular caliber correlations with internal carotid artery Doppler variables. *J Clin Ultrasound*. 2015;43(9):567-572.
35. Wang H, Wang YL, Li HY. Subfoveal choroidal thickness and volume in severe internal carotid artery stenosis patients. *Int J Ophthalmol*. 2017;10(12):1870-1876.
36. Akçay BİS, Kardeş E, Maçin S, et al. Evaluation of Subfoveal Choroidal Thickness in Internal Carotid Artery Stenosis. *J Ophthalmol*. 2016;2016:1-6.
37. Sayin N, Kara N, Uzun F, Akturk IF. A Quantitative Evaluation of the Posterior Segment of the Eye Using Spectral-Domain Optical Coherence Tomography in Carotid Artery Stenosis: a Pilot Study. *Ophthalmic Surgery, Lasers Imaging Retin*. 2015;46(2):180-185.
38. Booij JC, Baas DC, Beisekeeva J, Gorgels TGMF, Bergen AAB. The dynamic nature of Bruch's membrane. *Prog Retin Eye Res*. 2010;29(1):1-18.
39. Usui S, Ikuno Y, Akiba M, et al. Circadian Changes in Subfoveal Choroidal Thickness and the Relationship with Circulatory Factors in Healthy Subjects. *Investig Opthalmology Vis Sci*. 2012;53(4):2300.

Supplementary methods

All measurements were performed by experienced professionals in the vascular laboratory of the department of vascular medicine of UMC Utrecht.

Measurement of carotid IMT

The carotid IMT, which reflects the arterial wall burden,[1] was measured using ultrasound (Esaote, Florence, Italy) in the left and right carotid artery in the transversal, the posterolateral and the anterolateral direction. The average of these three measurements from both sides was taken for acquisition of one final IMT value.

Measurement of ankle-brachial index (ABI)

Ankle-brachial index (ABI) Patients were rested in a supine position and the systolic blood pressure was measured in the left and right brachial arteries, the tibial posterior arteries and in the dorsal pedal arteries. The lowest value of the left and right side ABI was used.

Measurement of CT scan calcifications

A semi-quantitative scoring system with four categories (no calcification, mild calcification, moderate calcification and severe calcification) was used as a measure of the severity of arterial calcification in the carotid siphon. It was graded as 'no calcification' in the case of absence of calcification, 'mild calcification' in case of 1-3 small calcifications, 'moderate calcification' in case of 3-5 small calcifications and 'severe calcification' in case of more than 5 small calcifications or at least one large calcification on the CT slides of the artery. The inter-observer agreement of the scoring system was 'good' for the carotid siphon, with a weighed Cohen's kappa value of 0.70.[2] The inter-observer agreement was based upon the systematic scoring of 25 random scans by two board certified radiologists. The scoring of the full number of CT scans was performed by one of the two radiologists in random order blinded for clinical data. Calcification scoring was carried out using low-dose (<3 mSv) full-body CT scan without contrast, performed on CT scanner Brilliance 64 (Philips, Cleveland, Ohio).

In addition, calcification mass was quantified on CT scans from the treatment of ectopic mineralization in pseudoxanthoma elasticum (TEMP)-trial (Siemens Biograph 40, Siemens Healthcare, Erlangen, Germany).[3] In short, calcification mass was quantified with an in house developed software tool (iX Viewer). Calcifications were defined as hyperdense arterial wall lesions with a density above 130 Hounsfield (HU) units.

Calcification mass scores were computed as the product of the volume of the lesion in ml and the mean attenuation in HU of the lesion.[4]

1. Kranenburg G, Visseren FLJ, de Borst GJ, de Jong PA, Spiering W. Arterial stiffening and thickening in patients with pseudoxanthoma elasticum. *Atherosclerosis*. 2018;270:160-165.
2. Kranenburg G, de Jong PA, Mali WP, Attrach M, Visseren FLJ, Spiering W. Prevalence and severity of arterial calcifications in pseudoxanthoma elasticum (PXE) compared to hospital controls. Novel insights into the vascular phenotype of PXE. *Atherosclerosis*. 2017;256:7-14.
3. Kranenburg G, de Jong PA, Bartstra JW, et al. Etidronate for Prevention of Ectopic Mineralization in Patients With Pseudoxanthoma Elasticum. *J Am Coll Cardiol*. 2018;71(10):1117-1126.
4. Hoffmann U, Kwait DC, Handwerker J, Chan R, Lamuraglia G, Brady TJ. Vascular Calcification in ex Vivo Carotid Specimens: Precision and Accuracy of Measurements with Multi–Detector Row CT. *Radiology*. 2003;229(2):375-381.


Chapter 5

Is vaginal delivery harmful to patients with pseudoxanthoma elasticum?

Sara Risseeuw
Hilin Yildirim
Wilko Spiering
Saskia M. Imhof
Redmer van Leeuwen
Jeannette Ossewaarde – van Norel

Retinal Cases & Brief Reports. 2020, online ahead of print.
doi: 10.1097/ICB.0000000000000997

Abstract

Purpose

To investigate the effect of a vaginal delivery (VD) on retinal pathology in patients with pseudoxanthoma elasticum (PXE).

Methods and patients

Retrospective case-series. All 14 consecutive women with PXE who visited the ophthalmology department during pregnancy and after delivery between 2010 and 2018 were included. Pre- and postpartum imaging consisted of color imaging, near infrared imaging and OCT, and was assessed on occurrence of (sub)retinal hemorrhages and change in angioid streaks.

Results

14 patients (15 deliveries) were included, of whom 11 patients (79%) had a VD and 3 patients (21%) a secondary caesarian section (CS). Data of three patients with VD (four deliveries) could not be assessed for (sub)retinal hemorrhage within ten weeks postpartum. The median age at delivery was 31 years (IQR 29 – 37). One patient with VD (9%) had a choroidal neovascularization and was treated with anti-VEGF injections prior to assisted delivery. All patients had angioid streaks in the central 5500 µm of the posterior pole of both eyes. After delivery, no patient in the VD or CS group presented with progression of angioid streaks or (sub)retinal hemorrhage.

Conclusions and relevance

Pushing during the expulsion phase of VD seems safe in PXE patients without active choroidal neovascularization and the presence of angioid streaks alone should not be an indication for elective CS.

Background

In patients with pseudoxanthoma elasticum (PXE), biallellic mutations in the *ABCC6* gene lead to ectopic mineralization in the skin, vasculature and Bruch's membrane (BM) underneath the retina.[1] Calcification of BM presents in fundo as peau d'orange and angioid streaks, which are breaks in the brittle BM.[2] Eventually, choroidal neovascularization (CNV) and macular atrophy cause deterioration of visual acuity at a relatively young age.[2–4]

There is uncertainty about the risk of vaginal delivery (VD) on ocular complications in patients with PXE.[5] The Valsalva maneuver during VD increases the retinal venous pressure[6], which may lead to preretinal hemorrhages due to spontaneous rupture of retinal capillaries.[7] It is plausible that a CNV is more prone to rupture due to the fragile vasculature.[8] Furthermore, the effect of both pregnancy and the Valsalva maneuver during VD on progression of angioid streaks is unclear.[5,9,10] The clinical impression is that women have a more severe phenotype than men, which might be explained by hormonal influences on disease progression and possibly hormonal changes during pregnancy play a role as well. In clinical practice, some ophthalmologists advice no pushing or even elective caesarian section (CS) to prevent ocular complications, but there are hardly any data available supporting such advice.[5,9]

The aim of this study is to investigate the effect of VD on the occurrence of (sub)retinal hemorrhages and on the progression of angioid streaks in patients with PXE.

Methods

We conducted an observational case series at the Dutch National Expertise Center for PXE of the University Medical Center Utrecht. This study is in adherence to the Declaration of Helsinki and its further amendments. The Institutional Ethics Board approved the study protocol (number 18/076). We retrospectively investigated data of all consecutive female patients with PXE who had delivery from 2010 until 2018 and had ophthalmological imaging pre- and postpartum. PXE was diagnosed according to the criteria proposed by Plomp et al. and only patients with a definitive diagnosis were included.[11]

Ophthalmological imaging consisted of color fundus photography (FF 450 plus; Carl Zeiss Meditec AG, Jena, Germany), 55-degree near-infrared reflectance imaging (NIR), and optical coherence tomography (OCT) (both Spectralis HRA-OCT; Heidelberg Engineering, Heidelberg, Germany). Assessment of imaging before and after delivery was performed by three experienced graders (SR, RL and JO). Presence of CNV, location and progression of angioid streaks, and the presence of subretinal or retinal hemorrhages were scored. Presence of CNV was assessed using OCT and color fundus photography. Angioid streaks were evaluated using NIR and color fundus photography for location in the central 5500 µm and central 1000 µm diameter of the posterior pole, and for any progression in length, width or appearance of new streaks. Presence of hemorrhages was assessed at a maximum of ten weeks after delivery using both central and peripheral color fundus photographs and OCT. Information on visual acuity was extracted from the medical charts, if available.

Results

In total, 14 PXE patients (15 deliveries) with eligible imaging were included. The individual patient data is presented in Table 5.1. Eleven patients (79%) had VD (n = 12), and three patients (21%) underwent secondary CS for medical emergencies (in two patients due to fetal distress during the partus, in one patient due to severe preeclampsia).

The median age of the women at delivery was 31 years (IQR 29 – 37). One patient had unilateral CNV, for which she received an anti-VEGF injection two weeks before delivery. This patient had a vacuum extraction on ocular indication. All patients had angioid streaks in the central 5500 µm diameter of the posterior pole in both eyes. Furthermore, nine (64%) patients had angioid streaks in the central 1000 µm diameter in at least one eye, and six patients (43%) in both eyes.

No retinal hemorrhages were found in the eight patients who had postpartum imaging within ten weeks after delivery. Also, no patient showed any changes in length, width or number of angioid streaks after delivery. Pre- and postpartum fundus imaging of three patients is presented in Figure 5.1. Furthermore, no patient reported vision loss.

Table 5.1 Demographic and ocular characteristics of patients

		Location of angoid streaks[a]				Time between imaging and delivery (weeks)		
Patient	Age (years)	Right eye	Left eye	CNV	Delivery	Before	After	Reason of intervention
1	37	< 5500 µm	< 5500 µm	No	Vaginal	8	9	
2	29	< 5500 µm	< 5500 µm	No	Vaginal – vacuum	5	8	Prolonged labor
3	40	< 1000 µm	< 5500 µm	No	Vaginal	25	7	
4	31	< 1000 µm	< 1000 µm	No	Vaginal	4	5	
5	38	< 1000 µm	< 5500 µm	Left eye, treated	Vaginal - vacuum	19	3	CNV bleeding risk
6	26	< 5500 µm	< 5500 µm	No	Vaginal	5	16	
7 [b]	29 ; 31	< 1000 µm	< 1000 µm	No	Vaginal (both)	80 ; 181	133 ; 32	
8	36	< 1000 µm	< 1000 µm	No	Vaginal	87	40	
9	31	< 1000 µm	< 1000 µm	No	Caesarian section	3	25	Fetal distress
10	34	< 1000 µm	< 1000 µm	No	Caesarian section	5	72	Fetal distress
11	43	< 1000 µm	< 5500 µm	No	Caesarian section	21	54	Severe pre-eclampsia
12	29	< 5500 µm	< 5500 µm	No	Vaginal	5	2	
13	29	< 1000 µm	< 1000 µm	No	Vaginal	10	7	
14	27	< 5500 µm	< 5500 µm	No	Vaginal	18	5	

Data are presented per delivery, separated with a semicolon when necessary

a. Presence of angioid streaks in the central 5500 µm diameter or central 1000 µm of the posterior pole

b. Of patient 7, two deliveries were assessed.

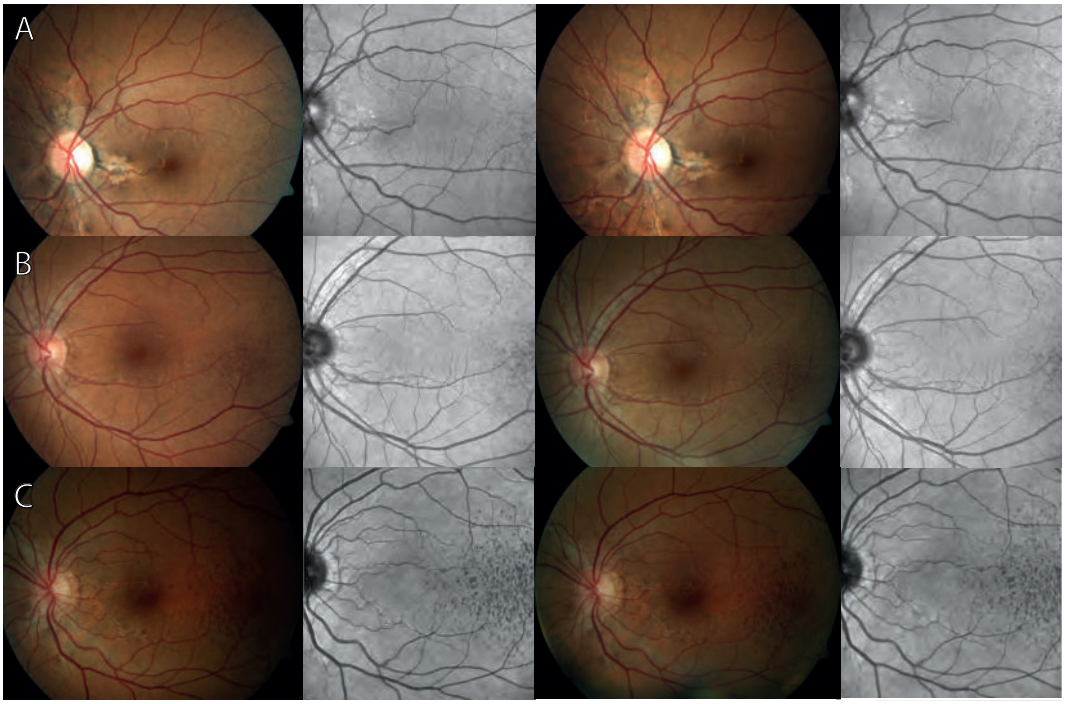

Figure 5.1 Pre- and postpartum fundus photography and near infrared imaging of three patients with PXE. A: Left eye of 31-year-old woman with angioid streaks in the central 1000 µm diameter of the posterior pole, 4 weeks before (left) and 5 weeks after (right) vaginal delivery (patient 4). B: Left eye of a 29-year-old woman with angioid streaks in the central 5500 µm diameter of the posterior pole, 5 weeks before (left) and 2 weeks after (right) vaginal delivery (patient 12). C: Left eye of a 29-year-old woman with angioid streaks in the central 1000 µm diameter of the posterior pole, 10 weeks before (left) and 7 weeks after (right) vaginal delivery (patient 13). In all three patients, peau d'orange is visible as a speckled pattern on both fundus photography and near infrared imaging temporal of the macular area.

Discussion

This is the first study to systematically assess the retinal consequences of VD in women with PXE. The effect of pushing on patients with CNV still remains unknown. There is probably no deteriorating effect of VD on ocular outcome.[9] In a questionnaire held under 407 women with PXE, subretinal hemorrhage was reported in <1% of all pregnancies.[10] Only one case report that investigated ocular outcome after VD was published, which did not show retinal changes ten weeks postpartum.[12] This is in line with our findings.

During the Valsalva maneuver in the expulsion phase, the intrathoracic pressure increases and reduces venous return to the heart. This leads to a decrease in blood pressure and an increase in central venous pressure (CVP). Increased CVP causes an increase in intraocular pressure (IOP), due to choroidal swelling and impeded drainage of aqueous humor.[6] An increase in IOP might alter the scleral curvature[13] and theoretically lead to progression or new angioid streaks by exerting mechanical stress on BM. However, changes of pre-existing AS were not observed in our series, implicating that VD is safe regarding the short-term progression of angioid streaks.

It is plausible that the increased CVD during VD has consequences for eyes with CNVs, since these are more prone to rupture due to the fragile vasculature.[8] In literature, elective CS for pregnant women with active CNV is recommended to minimize the risk of bleeding.[5,9,10] Also, in daily practice subretinal hemorrhage from CNV after Valsalva maneuver is occasionally seen. In our series there was only one eye with CNV treated with anti-VEGF injections, therefore we cannot draw conclusions whether a CS or a vacuum assisted delivery is required for pregnant patients with CNV. The use of medical intervention or prophylactic anti-VEGF treatment before the expected delivery data to reduce the risk of bleeding in patients with CNV should be considered per patient.

Similar to angioid streaks in PXE, patients with high myopia may develop breaks in BM (lacquer cracks) and subsequently CNV.[14] In a study of 50 myopic patients, VD did not cause retinal deterioration shortly after delivery.[15] Despite the high prevalence of myopia, there is a lack of data on the effect of VD on the bleeding risk of myopic CNV.

Some limitations of the present study need to be addressed. The sample size is small due to the low prevalence of PXE patients and difficulty of obtaining retinal imaging shortly after delivery. We used an arbitrary timeframe of ten weeks after delivery.

However, very small hemorrhages that resolve within ten weeks might have been missed. Standardized assessment of the imaging by three graders did not detect any progression of angioid streaks. A quantitative method is required to detect possible pixel-sized differences in angioid streaks, but such a method does not exist yet. Furthermore, detailed information on the VD was not available in all patients. Since we did not find an effect on ocular outcome, it is unlikely that the duration of the second stage of delivery and the birth weight are of relevance.

In conclusion, VD is not associated with (sub)retinal hemorrhage or progression of angioid streaks in women with PXE without a CNV. While all pregnant PXE patients should be checked for active CNV, pushing during VD seems safe in PXE patients without CNV. The presence of angioid streaks alone should not be an indication for medical interventions during delivery.

References

1. Bergen AAB, Plomp AS, Schuurman EJ, et al. Mutations in *ABCC6* cause pseudoxanthoma elasticum. *Nat Genet*. 2000;25(2):228-231.
2. Gliem M, Zaeytijd J De, Finger RP, Holz FG, Leroy BP, Charbel Issa P. An update on the ocular phenotype in patients with pseudoxanthoma elasticum. *Front Genet*. 2013;4:14.
3. Risseeuw S, Ossewaarde-van Norel J, Klaver CCW, Colijn JM, Imhof SM, van Leeuwen R. Visual acuity in pseudoxanthoma elasticum. *Retina*. April 2018:1.
4. Gliem M, Muller PL, Birtel J, Hendig D, Holz FG, Charbel Issa P. Frequency, Phenotypic Characteristics and Progression of Atrophy Associated With a Diseased Bruch's Membrane in Pseudoxanthoma Elasticum. *Invest Ophthalmol Vis Sci*. 2016;57(7):3323-3330.
5. Farhi D, Descamps V, Picard C, Mahieu-Caputo D, Doan S, Crickx B. Is pseudoxanthoma elasticum with severe angioid streaks an indication for Caesarean section? *J Eur Acad Dermatol Venereol*. 2006;20(10):1361-1362.
6. Jünemann AGM, Sterk N, Rejdak R. Einfluss des Geburtsmodus auf vorbestehende Augenerkrankungen. *Der Ophthalmol*. 2012;109(3):229-234.
7. Li N, Zhu Z, Yi G, Li S, Han X. Valsalva Retinopathy in Twin-Pregnancy: A Case Report and Literature Review. *Am J Case Rep*. 2018;19:5-9.
8. Errera M-H, Kohly RP, da Cruz L. Pregnancy-associated retinal diseases and their management. *Surv Ophthalmol*. 2013;58(2):127-42.
9. Camacho M, Rengel C, López-Herrero E, Carrillo JL, Eslava AJ, Valdivielso P. Approach to the management of pregnancy in patients with pseudoxanthoma elasticum: a review. *J Obstet Gynaecol (Lahore)*. 2016;36(8):1061-1066.
10. Bercovitch L, Leroux T, Terry S, Weinstock MA. Pregnancy and obstetrical outcomes in pseudoxanthoma elasticum. *Br J Dermatol*. 2004;151(5):1011-1018.
11. Plomp AS, Toonstra J, Bergen AAB, van Dijk MR, de Jong PTVM. Proposal for updating the pseudoxanthoma elasticum classification system and a review of the clinical findings. *Am J Med Genet A*. 2010;152A(4):1049-1058.
12. Xiromeritis P, Valembois B. Pseudoxanthoma elasticum and pregnancy. *Arch Gynecol Obstet*. 2006;273(4):253-254.
13. Asejczyk-Widlicka M, Pierscionek BK. The elasticity and rigidity of the outer coats of the eye. *Br J Ophthalmol*. 2008;92(10):1415-8.
14. Kim YM, Yoon JU, Koh HJ. The analysis of lacquer crack in the assessment of myopic choroidal neovascularization. *Eye (Lond)*. 2011;25(7):937-46.
15. Neri A, Grausbord R, Kremer I, Ovadia J, Treister G. The management of labor in high myopic patients. *Eur J Obstet Gynecol Reprod Biol*. 1985;19(5):277-279.

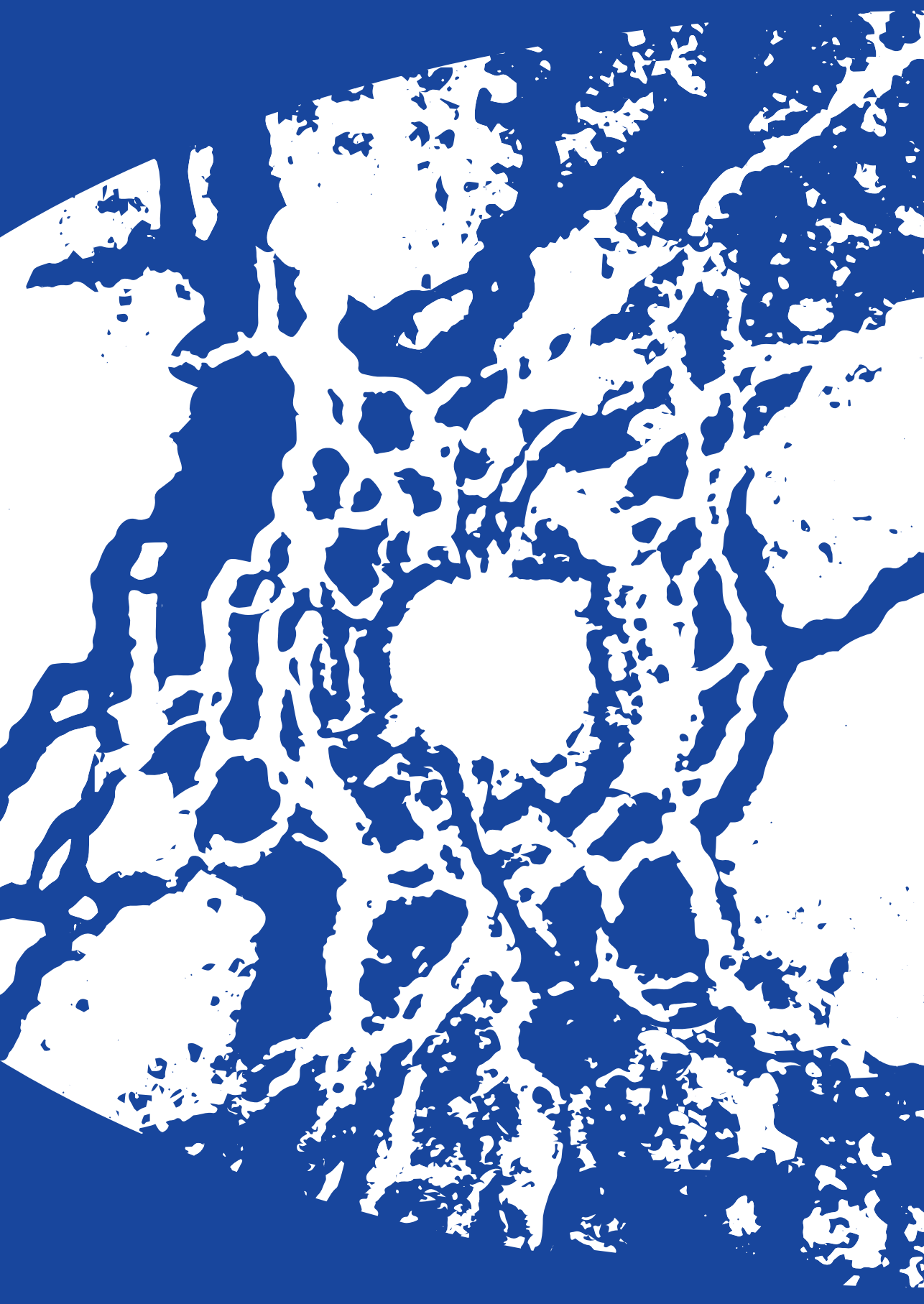


PART TWO

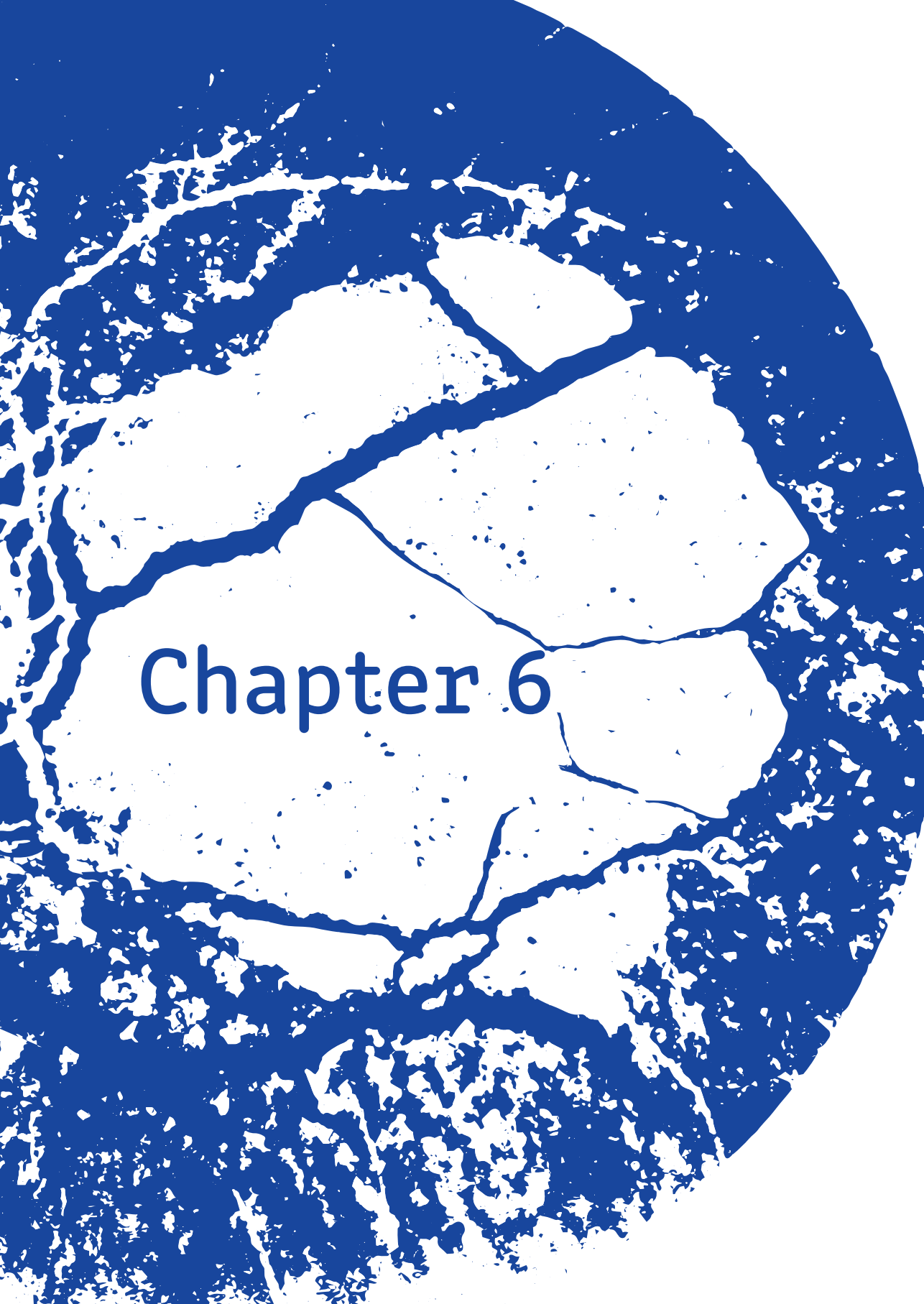
Chapter 6

Genotype-phenotype correlation in pseudoxanthoma elasticum

Jonas W. Bartstra*
Sara Risseeuw*
Pim A. de Jong
Bram van Os
Lianne Kalsbeek
Chris Mol
Annette F. Baas
Olivier Vanakker
Jeroen Hendrikse
Willem P.Th.M. Mali
Saskia M. Imhof
Jeannette Ossewaarde-van Norel
Redmer van Leeuwen**
Wilko Spiering**
Authors with * and ** contributed equally

Manuscript in preparation

Abstract

Introduction

The autosomal recessive disorder pseudoxanthoma elasticum (PXE) is caused by pathogenic variants in the *ABCC6* gene. PXE is characterized by fragmentation and calcification of the elastic fibers of the skin, peripheral arteries and Bruch's membrane in the eyes, leading to pseudoxanthoma's, peripheral arterial disease and angioid streaks. Due to a variable phenotype and rarity of the disease, currently no clear genotype-phenotype correlation has been established. To gain better insight into the pathogenesis of PXE, we investigated the association the *ABCC* genotypes and measures of ectopic calcification in different affected tissues.

Methods

PXE patients underwent a standardized examination, including *ABCC6* sequencing. Genetic variants were classified as truncating or non-truncating and patients were grouped as having two truncating, mixed or two non-truncating variants. Arterial calcification mass was quantified on low dose, whole body CT scans and peripheral arterial disease was assessed with the ankle brachial index. The presence of pseudoxanthoma's in the skin was systematically scored at eight locations of the body. The length of retinal angioid streaks, presence of choroidal neovascularization, severity of macular atrophy and best-corrected visual acuity were used for Bruch's membrane calcification. Regression models were built to test the association between genotype and phenotypes adjusted for age and sex.

Results

Of 287 clinically confirmed PXE patients, 154 patients (53%, median age 51 years) had two truncating variants, 91 (32%, median age 53 years) had a mixed genotype, 18 (6%, median age 47 years) had two non-truncating variants. When adjusted for age and sex, patients with a mixed genotype had lower peripheral and total arterial calcification mass scores (β: -0.36, 95% CI: -0.64; -0.18 and β: -0.29, 95%CI: -0.47; -0.10, respectively), shorter angioid streaks (proportional odds ratio (OR): 0.60, 95% CI 0.46; 0.99) and less often CNV (OR: 0.37 95%CI: 0.18; 0.76) than patients with two truncating variants. No association with skin pseudoxanthomas was found.

Conclusion

PXE patients with a mixed genotype have less severe arterial and ophthalmological phenotypes than patients with two truncating variants of the *ABCC6* gene. Further research into the role of environmental risk factors and genetic modifiers might provide further insights into the unexplained phenotypic variability.

Introduction

Pseudoxanthoma elasticum (PXE) is a rare autosomal recessive disorder characterized by the fragmentation and calcification of the elastic fibers of the skin, the peripheral arteries and the Bruch's membrane in the eyes.[1] In the skin, this results in pseudoxanthomas and severe skin loosening due to reduced elasticity.[1] In the vasculature, this results in peripheral arterial disease (PAD) but gastrointestinal bleeding and microvascular brain damage have also been reported.[1–3] Calcification of Bruch's membrane in the retina results in peau d'orange and angioid streaks. The latter are fractures of Bruch's membrane, which allow for the ingrowth of choroidal neovascularization (CNV) with subsequent exudation and a risk of retinal hemorrhage and scarring.[4] Together with macular atrophy, this attributes to a high risk of visual impairment in PXE.[5]

PXE is caused by pathogenic variants in the *ABCC6* gene, although overlapping phenotypes due to variants in the *ENPP1* and *GGCX* genes have been reported.[6] *ABCC6* encodes the multidrug resistant protein 6 (MRP6) transporter and is mainly expressed in the liver and the kidneys.[7] The precise function of *ABCC6* and its substrate is not yet fully understood. There is still debate whether low-grade inflammation[8], primary elastin degradation or the primary deficiency in calcification inhibitors underlie the systemic calcification PXE.[7] It has been shown that PXE results in low systemic levels of inorganic pyrophosphate (PP_i). PP_i is an important inhibitor of calcification and the low levels seen in PXE might be an important link in the increased multi-organ calcification.[7,9]

The phenotype of PXE highly varies between patients and even within families with the same causative variants.[10] Several studies investigated the association between the different genotypes and the clinical phenotypes in order to better predict the course of disease for individual patients. These studies are complicated by the high number of *ABCC6* variants. Most of the more than 300 variants that cause PXE are unique for different families.[11,12] In addition, due to the rarity of the disease, most studies are hindered by low patient numbers to reach adequate statistical power. One study showed that patients with two loss-of-function variants have an increased risk on severe claudication and retinal hemorrhage or scarring, compared with patients with one or two non-truncating variants.[12] However, most studies could not find a genotype-phenotype correlation.[13,14] Most studies used (a modified version of) the Phenodex classification, which is a composite score of clinical signs in organs affected by PXE. Since ectopic calcification underpins these clinical outcomes, measures of ectopic calcification may be a better endpoint for genotype-phenotype studies.

To gain better insight into the etiology of PXE and the role of calcification in different organs, we studied genotypes, calcification measures and clinical phenotypes in the skin, arteries and the eyes in a large cohort of PXE patients. Furthermore, the associations between genotypes and these different phenotypes in PXE were investigated.

Methods

Participants

PXE patients were recruited from the Dutch National Expertise Center for PXE in the University Medical Center Utrecht, the Netherlands. Based on an estimated prevalence of 1:25.000 to 1:50.000, we assume that 40-90% of the PXE patients in the Netherlands have been seen in our hospital. All patients had a clinical diagnosis of PXE based on the criteria of Plomp et al.[1] In short, patients had to have two of the following three criteria: skin involvement (pseudoxanthomas), eye involvement (peau d'orange and/or angioid streaks) or genetic confirmation (biallelic variants in the *ABCC6* gene or a first degree relative with PXE).

PXE patients in our center under a standardized clinical workup which involves genotyping and vascular, dermatological and ophthalmological phenotyping. Phenotyping included vascular function tests, a whole-body CT scan to measure arterial calcification, photography of the affected skin areas and ophthalmological examination including retinal imaging to visualize peau d'orange, angioid streaks, CNV and macular atrophy. For this study, clinical data (genetics, CT scans, ankle-brachial index after treadmill tests, skin photography, ophthalmological examination and imaging) was used. This cross-sectional study was approved by the medical ethical review board of the University Medical Center Utrecht (METC 15/446 and 18/767). Participants gave written informed consent for the use of their medical files for research purposes.

Genotyping

Genomic DNA was isolated from whole blood. Specific primers were used to avoid the amplification of *ABCC6* pseudogenes ψ1 and ψ2. All *ABCC6* exons and the flanking intron sequences were analyzed as part of genetic screening for regular clinical care. Sangers sequencing was performed to identify single nucleotide polymorphisms, small deletions, and insertions. Multiplex ligation-dependent probe amplification

(MLPA) was used to screen for larger deletions in the *ABCC6* gene (MLPA kit P092B). The pathogenicity of all *ABCC6* variants was estimated based on the Sherlock criteria and classified as benign, likely benign, variant of unknown significance (VUS), likely pathogenic, or pathogenic.[15]

Pathogenic variants were classified in three groups: (1) truncating variants (nonsense, out-of-frame insertions or deletions, splice site variants that result in a frameshift, and deletions of the whole *ABCC6* gene), (2) non-truncating variants with presumably some residual conservation of the protein function (missense variants, in-frame insertions or deletions and splice site variants that result in the lack of an in frame exon) and (3) splice-site variants in which the effect of the variant is not clear. Next, we created three groups of patients: (1) two truncating variants, (2) mixed genotype of one truncating and one non-truncating variant, and (3) two non-truncating variants.

Arterial phenotypes

Arterial calcification

Arterial calcification mass was measured on unenhanced low dose (<3 mSv for a 70 kg adult), whole body CT multi-detector row CT scanners (Siemens or Philips, mAs dependent on body weight, 100 or 120 kVp, slice thickness <1 mm which were resampled to 5 mm slices with 4 mm increment) in the carotid siphon, common carotid artery, coronary arteries, thoracic and abdominal aorta, iliac arteries and the femoral and crural arteries. The peripheral artery score was calculated as the sum of the calcification mass scores in the femoral and crural arteries. The total arterial calcification score was calculated as the sum of the mass scores in all different measured arterial beds. Arterial calcification was defined as hyperdense arterial wall lesions with a density above 130 Hounsfield Units (HU). Calcification mass scores were computed as the product of the volume of the lesion in ml and the mean attenuation in HU.

Ankle-brachial index

The ankle-brachial index (ABI) after treadmill test was used to measure peripheral arterial disease. To calculate the ABI, the systolic blood pressure was measured in the left and right brachial arteries, the tibial posterior arteries and in the dorsal pedal arteries. During the treadmill test, patients were encouraged to walk on a treadmill with a 10% slope and a speed of 3.5 km/h for 6 minutes. Patients who stopped prematurely due to pain (claudication) were encouraged to continue walking as soon as possible. During recovery, the ABI was measured during 10 min in a supine position. The lowest value of these ABI measurements was used as the post-treadmill test ABI.

ABI measurements were performed by experienced technicians. Peripheral arterial disease (PAD) was defined as an ABI below 0.90.

Skin phenotype

The presence of pseudoxanthomas was systematically scored in the neck (posterior, lateral, anterior), lower lip, axillas, elbows, umbilicus, and groins. The total number of locations was used as a measure of the extent of the skin involvement.

Ophthalmological phenotypes

All patients underwent routine ophthalmological examination, including best-corrected visual acuity (BCVA) and indirect ophthalmoscopy. Imaging included macular spectral domain optical coherence tomography (SD-OCT), fundus autofluorescence (FAF), near-infrared reflectance imaging (NIR) (al ISpecralis HRA-OCT, Heidelberg Engineering, Heidelberg, Germany) and color fundus photography (FF 450 plus, Carl Zeiss Meditec AG, Jena, Germany). For this study, we used the first ophthalmological data.

Length of angioid streaks

Since angioid streaks are assumed to develop in an already calcified area of BM, the length of angioid streaks on 55° NIR imaging was used as a proxy for the extent of Bruch's membrane calcification. The length of the longest angioid streak from the center of the optic disc to the retinal periphery was measured and graded into four zones: zone 1 (<3 mm from the center of the optic disc), zone 2 (3-6 mm), zone 3 (6-9 mm) and zone 4 (>9 mm). We used five 55° NIR images of the posterior pole and the midperiphery for the grading and when in doubt, we used color fundus photography for comparison. In eyes with extensive macular pathology, grading of angioid streaks was not possible and these were graded as 'not assessable' and excluded from the analysis.

Macular phenotype

The presence of CNV and the severity of macular atrophy were scored in both eyes by three experienced graders (SR, RvL, JOvN). The presence of (in)active CNV was based on assessment of SD-OCT, fundus photography and fluorescein- or indocyanine green angiography, if available. The presence of macular atrophy was based on FAF, SD-OCT, color fundus photography and NIR. The largest area of macular atrophy was graded as 'no atrophy', 'mild atrophy' (<twice the area of the optic disc) or 'severe atrophy' (>twice the area of the optic disc) based on the size of the largest atrophic area. Outer

retinal atrophy surrounding an (in)active CNV was considered to be independent of macular atrophy and not classified as such. Before 2018, both Snellen charts and Early Treatment of Diabetic Retinopathy Study (ETDRS) charts were used for measuring BCVA.[16] From 2018 on, only ETDRS charts were used. BCVA was converted to the logarithm of the minimum angle of resolution (logMAR).

Statistical analysis

Patient characteristics are presented as mean ± standard deviation for normal distributions, median [interquartile range (IQR)] for non-parametric distributions and number (%) for categorical variables. *ABCC6* variants that were classified as benign or likely benign were excluded from the analysis. For the ophthalmological phenotypes, data of the right eye was used for descriptive and regression analyses. If the imaging from the right eye was not assessable, the left eye was used.

Regression models were built with the genotypes as the determinant and the calcification and clinical phenotypes as the outcome for all clinically proven PXE patients. Log10 transformation was performed on the calcification mass scores. Linear regression models were built for continuous outcomes (calcification mass scores, ABI, BCVA), logistic regression models were used for binary outcomes (presence of CNV), ordinal logistic regression models were built for ordinal outcomes (extent of angioid streaks, severity of macular atrophy) and Poisson regression models were built for count data (number of locations of pseudoxanthomas). All models were adjusted for age and sex. The models including arterial calcification mass were additionally adjusted for scanner vendor and differences in settings, since this affects calcification mass scores.[17] As a sensitivity analysis, additional models excluding patients with a VUS were built. The length of angioid streaks mainly varies in patients younger than 50 years and appears static in patients older than 50 years.[18] Therefore, we performed a subgroup analysis in patients younger than 50 years for the association of genotype with the length of angioid streaks. Additional models were built excluding patients with two non-truncating variants since this group had very low patient numbers. A P-value <0.05 was regarded statistically significant. All analyses were performed in R studio version 1.1.456. The additional package 'ordinal' (version 2019.12-10) was used to build ordinal logistic regression models.

Results

Participants

In total, 289 PXE patients were included. Genotyping was performed in 280 patients (97%), 272 patients (94%) had a CT scan, 283 patients (98%) had ABI measurements, in 278 patients (96%) the pseudoxanthomas were scored and 287 patients (99%) had retinal imaging. In total, 154 patients (53%) had two truncating variants, 91 (32%) had a mixed genotype, 18 (6%) had two non-truncating variants, 3 (1%) had one or two alternative splice variants in which the effect of the variant was not clear, in 6 patients (2%) only one pathogenic variant was found and in 2 patients (1%) no pathogenic variants were found.

Patient characteristics

The median age at genetic analysis was 51 [IQR, 41-60] years in patients with two truncating variants, 53 [IQR, 40 -60] years (P = 0.78 vs two truncating variants) in patients with a mixed genotype, and 47 [IQR, 44-54] years (P = 0.41) in patients with two non-truncating variants. PXE patients with two truncating variants had more often peripheral arterial calcification (88% vs. 76%, P = 0.01) than patients with a mixed genotype.

Although not statistically significant, patients with two truncating variants seemed to have a higher peripheral arterial calcification mass score (612 [IQR, 52-2142] vs. 229 [IQR, 2-1642]], P = 0.07), a lower ABI (0.90 [IQR, 0.59-1.03] vs. 0.98 [IQR, 0.69-1.06], P = 0.06) and more often CNV (95 (63%) vs. 46 (51%), P = 0.07). The prevalence and number of locations of pseudoxanthomas did not differ between the groups of patients (Table 6.1). Figure 6.1 visualizes the phenotypes stratified for by genotypes. Since PXE is a slowly progressive disease, we also looked at the association between phenotypes and genotype per decade (Figure 6.2).

The two subgroup analyses showed that patients with two truncating variants have longer angioid streaks than patients with a mixed genotype (P = 0.02 and P = 0.05 for excluded VUS and patients younger than 50 years, respectively) (Supplemental Table S6.1, Supplemental Figure S6.1). Patient characteristics for patients with a possible splice variant in which the effect is not clear and patients with only one or no variants are presented in Supplemental table S6.2.

Table 6.1 Patient characteristics of all clinically confirmed PXE patients

	Two truncating variants[1]	Mixed genotype[2]	Two non-truncating variants[3]	*P* [1 vs. 2]	*P* [1 vs. 3]
Total, n	**154**	**91**	**18**		
Age	51 [41-60]	53 [40 -60]	47 [44-54]	0.78	0.41
Male sex	53 (34)	35 (39)	5 (28)	0.52	0.57
Vascular, n	**145**	**87**	**18**		
Peripheral arterial calcification					
Prevalence	128 (88)	66 (76)	14 (78)	0.01	0.21
Mass score	612 [52-2142]	229 [2-1642]	196 [4-552]	0.07	0.06
Total body arterial calcification					
Prevalence	140 (97)	81 (93)	18 (100)	0.23	0.42
Mass score	2053 [210-5909]	1076 [46-4006]	280 [53-2836]	0.14	0.17
Ankle brachial index	0.90 [0.59-1.03]	0.98 [0.69-1.06]	0.89 [0.69-1.06]	0.06	0.74
Peripheral arterial disease	75 (50)	37 (41)	9 (50)	0.17	0.80
Pseudoxanthomas, n	**150**	**87**	**18**		
Prevalence	133 (89)	78 (90)	17 (94)	0.45	0.17
Number of locations	4 [2-5]	3 [2-5]	3 [2-5]	0.78	0.67
Ophthalmology, n	**152**	**91**	**18**		
Extent of angioid streaks					
Missing	6	5	1		
<3 mm	2 (1)	1 (1)	0 (0)	0.10	0.45
3-6 mm	28 (19)	29 (34)	6 (35)		
6-9 mm	48 (33)	22 (26)	4 (24)		
>9 mm	68 (47)	34 (40)	7 (41)		
CNV, presence	95 (63)	46 (51)	8 (44)	0.07	0.24
Atrophy					
Mild	18 (12)	13 (14)	2 (11)	0.87	0.22
Severe	21 (14)	12 (13)	0 (0)		
Visual acuity, logMAR	0.10 [0.00-0.80]	0.08 [-0.02-0.48]	0.03 [-0.07-0.37]	0.43	0.20

Data is presented as median [IQR] or n (%). Data was analysed with the Mann-Whitney U test or the $\chi 2$ test when appropriate.
CNV = Choroidal neovascularization, LogMAR = Logarithm of the minimum angle of resolution, Peripheral arterial disease was defined as an ankle brachial index <0.90.
Data are presented for the right eye, unless imaging could not be assessed, then the left eye was used. The extent of the angioid streaks was measured as the extent of the longest angioid streak from the center of the optic disk on 55° near infrared reflectance (NIR) imaging. One patient did not have 55° NIR imaging, and in 11 patients, severe scarring or atrophy impaired reliable grading.

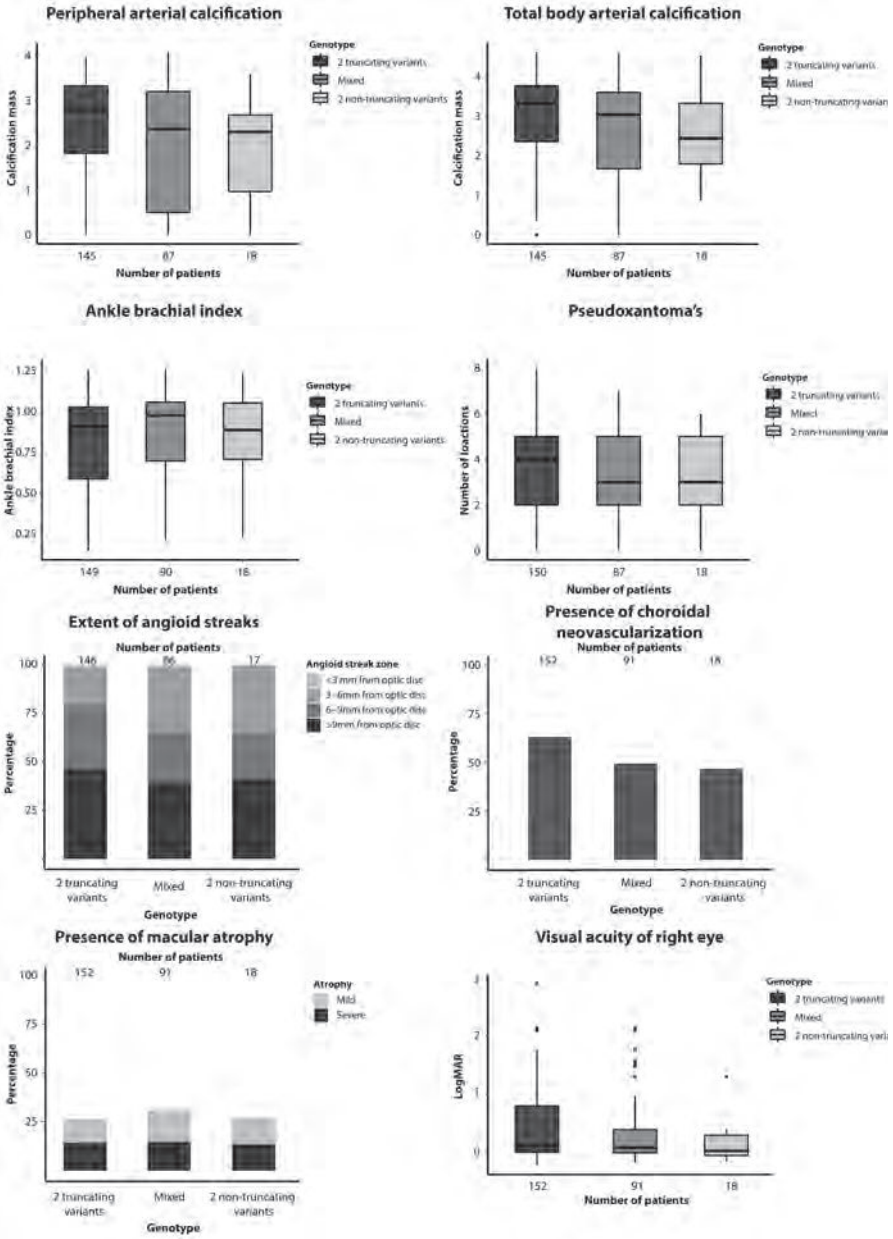

Figure 6.1 Correlation between genotypes and different vascular, skin and ophthalmological phenotypes in all clinically confirmed PXE patients. Patients with two truncating variants have higher arterial calcification mass, lower ankle brachial index, longer angioid streaks and more choroidal neovascularization than patients with a mixed genotype.

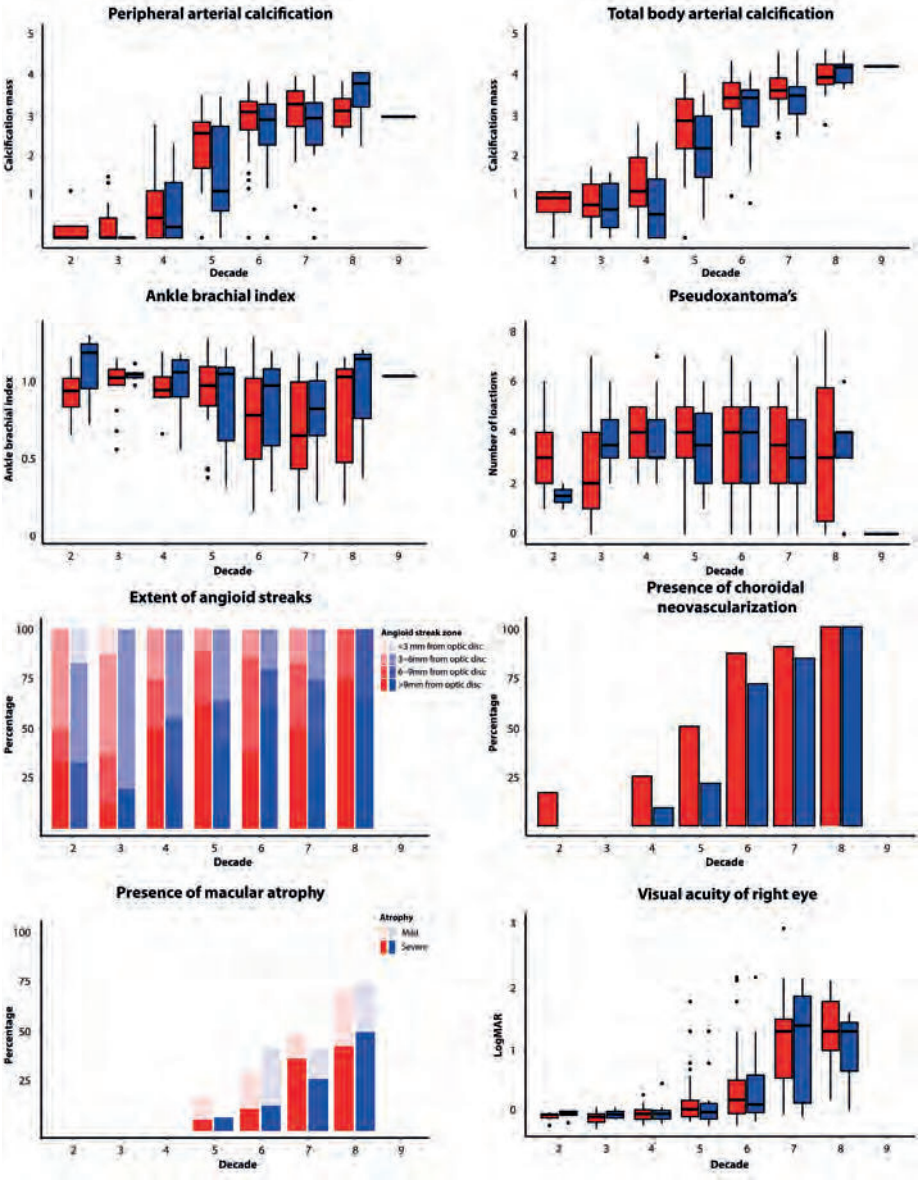

Figure 6.2 PXE is a slowly progressive disease. Except for the number of locations with pseudoxanthomas on the skin, the severity of all phenotypes increases with age in both patients with two truncating variants (red) and patients with a mixed genotype (blue). Data on patients with two non-truncating variants was not shown, since patients numbers were too low to show per decade. For eye data, details of the right eye are shown.

Table 6.2 Genotype-phenotype correlation in pseudoxanthoma elasticum

	All clinically confirmed PXE patients	Patients with variant of unknown significance excluded
Phenotypes	β /OR/RR [95%CI]	β /OR/RR [95%CI]
Vascular		
Peripheral calcification, mass score, β[1]	-0.25 [-0.43; -0.08]	-0.17 [-0.38; 0.02]
Total body calcification, mass score, β[1]	-0.13 [-0.27; 0.01]	-0.09 [-0.25; 0.06]
Ankle brachial index, β[1]	0.03 [-0.02; 0.08]	0.00 [-0.06; 0.06]
Skin		
Pseudoxanthomas, number of locations, RR[2]	0.97 [0.87; 1.08]	1.04 [0.92; 1.17]
Ophthalmology		
Angioid streaks, extending zones, pOR[3]	0.72 [0.49; 1.06]	0.87 [0.55; 1.37]
Angioid streaks, extending zones, pOR[3], younger patients	0.55 [0.31; 0.97]	0.60 [0.30; 1.18]
CNV, presence, OR[4]	0.53 [0.31; 0.89]	0.71 [0.39; 1.26]
Atrophy, severity, pOR[3]	0.80 [0.47; 1.33]	0.99 [0.55; 1.77]
Visual acuity, β[1]	-0.00 [-0.20; 0.03]	-0.02 [-0.15; 0.11]

Independent variable: two truncating variants, mixed genotype, two non-truncating variants. Two truncating variants was used as the reference. All models were adjusted for age and sex. Regression models were built with genotype as the determinant and the different phenotypes as the outcome.
[1] = linear regression model (β), [2] = Poisson regression model (rate ratio (RR)), [3] = ordinal regression model (proportional odds ratio (pOR)), [4] = logistic regression model (OR).

Genotype-phenotype association

When adjusted for age and sex, there was a statistically significant association between the genotypes (two truncating variants, mixed genotype, two non-truncating variants) and peripheral arterial calcification mass scores (β: -0.25, 95%CI [-0.43; -0.08]), length of angioid streaks in patients younger than 50 years (proportional OR 0.55, 95% [0.31; 0.97]) and the presence of CNV (OR: 0.53, 95% CI [0.31; 0.89]). However, these associations attenuated after exclusion of patients with a VUS (Table 6.2).

Table 6.3 Genotype-phenotype correlation in pseudoxanthoma elasticum with two truncating variants and a mixed genotype

	All clinically confirmed PXE patients	Patients with variant of unknown significance excluded
Phenotypes	β /OR/RR [95%CI]	β /OR/RR [95%CI]
Vascular		
Peripheral calcification, mass score, β[1]	-0.36 [-0.64; -0.18]	-0.35 [-0.59; -0.09]
Total body calcification, mass score, β[1]	-0.29 [-0.47; -0.10]	-0.23 [-0.44; -0.02]
Ankle brachial index, β[1]	0.05 [-0.02; 0.12]	0.03 [-0.05; 0.10]
Skin		
Pseudoxanthomas, number of locations, RR[2]	1.00 [0.86; 1.15]	1.11 [0.95- 1.31]
Ophthalmology		
Angioid streaks, extending zones, pOR[3]	0.60 [0.46; 0.99]	0.63 [0.35; 1.14]
Angioid streaks, extending zones, pOR[3], younger patients	0.36 [0.15; 0.83]	0.34 [0.13; 0.83]
CNV, presence, OR[4]	0.37 [0.18 ; 0.76]	0.49 [0.22; 1.10]
Atrophy, severity, pOR[3]	0.96 [0.50; 1.83]	1.23 [0.59; 2.52]
Visual acuity, β[1]	-0.08 [-0.23; 0.07]	0.05 [-0.12; 0.22]

Two truncating variants was used as the reference. All models were adjusted for age and sex. Regression models were built with genotype as the determinant and the different phenotypes as the outcome.

[1] = linear regression model (β), [2] = Poisson regression model (rate ratio (RR)), [3] = ordinal regression model (proportional odds ratio (pOR)), [4] = logistic regression model (OR).

Because of the low number of patients with two non-truncating variants (n=18), this group was excluded for a subgroup analysis. In this analysis, patients with a mixed genotype had lower peripheral and total arterial calcification mass scores (β: -0.36, 95%CI: -0.64; -0.18 and β: -0.29, 95%CI: -0.47; -0.10, respectively), shorter angioid streaks (proportional OR: 0.60 [0.46; 0.99]) and a lower prevalence of CNV (OR: 0.37 95%CI: 0.18; 0.76) than patients with two truncating variants. After exclusion of patients with a VUS, these results remained statistically significant for the peripheral and total arterial calcification mass scores and the angioid streaks in younger patients (Table 6.3).

Discussion

In this study, we show that PXE patients with a mixed genotype have less severe arterial calcification, shorter angioid streaks and a lower prevalence of CNV compared to patients with two truncating variants in the *ABCC6* gene. Although these findings emphasize the role of *ABCC6* in ectopic calcification in PXE, we could not confirm an association between the genotype and skin involvement, peripheral arterial disease, macular atrophy or visual acuity.

Our findings are in line with a previous study in which patients with two loss-of-function variants had an increased risk of severe claudication and vascular surgery, and retinal hemorrhage as measured with the Phenodex classification.[12] Most genotype-phenotype correlation studies in PXE, however, did not find a correlation between genotype and dermatological, arterial or ophthalmological phenotype.[10,13,14,19–21] Besides the large heterogeneity in clinical phenotypes, these studies are typically hindered by lower patient numbers (15-100 patients) due to the rarity of the disease.[10,19–21] Even though we included a fairly sized cohort, we still had borderline statistical power and larger studies might be warranted. Most studies have looked into the correlation between the genotype and clinical outcomes based on the Phenodex classification.[13] This classification includes clinical outcomes in all affected organs in PXE, but does not include measures of ectopic calcification. Since calcification in the vasculature and Bruch's membrane underlies and probably precedes the clinical consequences of PXE, measures of calcification in these organs might provide a better intermediate measure for genotype-phenotype correlation studies.

Approximately 50% of PXE patients in our cohort had PAD which is in line with a previous study.[3] Although the prevalence of PAD was slightly higher in PXE patients with two truncating variants, compared to patients with a mixed genotype, this difference was not statistically significant. Previous studies showed that the presence and extent of femoral artery calcification correlates with peripheral arterial disease in PXE.[22] The clear association between genotype and arterial calcification mass in our study suggests that patients with more a severe genotype might suffer from more severe PAD. Larger studies into the correlation between arterial calcification mass and peripheral arterial disease in PXE are awaited.

Especially in PXE patients younger than 50 years, two truncating variants increased the risk of longer angioid streaks compared with a mixed genotype. Eventually, CNV will develop in nearly all PXE patients[18,23] but patients with two truncating variants tend to develop CNV earlier (Figure 6.2). Since longer streaks were recently shown to increase the risk for CNV and macular atrophy, the increased length of angioid streaks at a younger age might underlie the association between the genotype and CNV that we found.

Since Bruch's membrane calcification impedes the diffusion of oxygen and nutrients to the outer retina and has an effect on the vitality of the outer retina at a young age, macular atrophy could be considered as the natural endpoint of Bruch's membrane calcification. Macular atrophy might thus serve as a better clinical endpoint to study Bruch's membrane calcification in PXE.[24] In this study, however, we did not find an increased risk of macular atrophy for more severe genotypes. Probably, environmental risk factors, such as smoking, or genetic modifiers, such as variants of the VEGFA gene are involved in the variability in the ophthalmological phenotype as well.[21,25]

Currently, over 300 different variants in the *ABCC6* gene have been described. The most common variants in our cohort were the truncating p.Arg1141* variant, the p.Trp1259Glyfs*14 and p.Lys1394fs frameshift variants and the exon 23-29 deletion, which corresponds with previous publications on *ABCC6* variants in PXE.[10,12,13] However, 57 of the 92 individual variants in our cohort were missense variants. Since most of these variants are unique for different families, 28 of these 57 missense variants were classified as a VUS.[15] Since all PXE patients had a confirmed clinical diagnosis, we included patients with a VUS in our primary analysis. Subgroup analysis excluding those patients with a VUS yielded similar point estimates but resulted in wider confidence intervals and loss of statistical power. Since different missense variants result in proteins with differing residual transporter function or proteins that are retained intracellular, such variants might still result in a non-functional protein.[11] Additional functional analysis of missense variants in the *ABCC6* gene could provide further insight into the unexplained phenotypic variability.

The precise function of *ABCC6* is still not clear, but it has been shown that PXE patients have lower systemic levels of PPi.[7,9,26] PP_i is an important inhibitor of calcification and the low levels seen in PXE likely play a role in the high calcification propensity in PXE. PP_i might therefore be an important biomarker for the severity or predict the progression of PXE. Intraperitoneal PP_i supplementation halted calcification in mice

and oral PP_iincreased plasma PP_i levels in healthy volunteers.[9,27] However, currently no data on the association between genotypes and plasma PP_i levels, or the association between plasma PP_i and calcification and clinical consequences are available.

A strength of this study is the large amount of multidisciplinary data we collected in a relatively large number of PXE patients.

Several limitations of this study have to be addressed. Due to the small number of patients with two non-truncating variants, no conclusions can be drawn for this group. However, since the phenotypes in this group were comparable to the phenotypes in the group with a mixed genotype, we expect that these patients have a milder phenotype than patients with two truncating variants. The quantification of pseudoxanthomas based on the number of affected locations, is a very rough estimate of the skin involvement in PXE. Currently, new in vivo methods to quantify elastin degradation, using two-photon microscopy, or calcification of the skin using sodium fluoride PET/CT (NaF-PET/CT) are being developed.[28] Future research could study the genotype-phenotype correlation based on these more sophisticated methods.

Since we used data from regular clinical care, there is some heterogeneity in the CT scanner used (Siemens or Philips) and the settings of the scanner (100 or 120 kVp). These differences might have had an effect on the arterial calcification mass scores.[17,29] However, since we adjusted for CT vendor and settings in our regression models, we think it did not affect the findings of this study.

The categorical classification of the length of angioid streaks leads to loss of information when compared to a continuous measure. Other approaches, including quantification of BM reflectivity on macular OCT-scans and measurement of the border of peau d'orange on 30° NIR imaging are under development. However, these measurements are only possible in the early stage of disease when there is no macular degeneration yet.[30,31] The length of angioid streaks is the first measure that allows semi-quantitative measurements in nearly all PXE patients, including those with end-stage disease.

In 8 clinically confirmed PXE patients, only one or no *ABCC6* variants were found. Since MLPA currently only covers 23 of the 31 coding exons of the *ABCC6* gene, it might be that large deletions in the other eight exons were missed.[32] Since we excluded these patients from our genotype-phenotype analysis, this did not affect our results. Last, we did not perform segregation analyses in all patients. We therefore cannot prove that

the pathogenic variants we found in heterozygous patients were indeed on different alleles.

In conclusion, we show that PXE patients with a mixed genotype have less severe arterial and ophthalmological phenotypes than PXE patients with two truncating variants in the *ABCC6* gene. However, other measures of ectopic calcification and its consequences were not associated with genotype. Further research into the role of PP_i, environmental risk factors or modifier genes might provide further insights into the unexplained phenotypic variability and further improve risk classification in PXE.

References

1. Plomp AS, Toonstra J, Bergen AAB, van Dijk MR, de Jong PTVM. Proposal for updating the pseudoxanthoma elasticum classification system and a review of the clinical findings. Am J Med Genet A. 2010;152A(4):1049-1058.
2. Pavlovic AM, Zidverc-Trajkovic J, Milovic MM, et al. Cerebral small vessel disease in pseudoxanthoma elasticum: three cases. *Can J Neurol Sci*. 2005;32(1):115-118.
3. Leftheriotis G, Abraham P, Le Corre Y, et al. Relationship between ankle brachial index and arterial remodeling in pseudoxanthoma elasticum. *J Vasc Surg*. 2011;54(5):1390-1394.
4. Spraul CW, Lang GE, Grossniklaus HE, Lang GK. Histologic and morphometric analysis of the choroid, Bruch's membrane, and retinal pigment epithelium in postmortem eyes with age-related macular degeneration and histologic examination of surgically excised choroidal neovascular membranes. *Surv Ophthalmol*. 1999;44(2 SUPPL. 1):10-32.
5. Risseeuw S, Ossewaarde-van Norel J, Klaver CCW, Colijn JM, Imhof SM, van Leeuwen R. Visual Acuity in Pseudoxanthoma Elasticum. *Retina*. 2019;39(8):1580-1587.
6. Nitschke Y, Baujat G, Botschen U, et al. Generalized arterial calcification of infancy and pseudoxanthoma elasticum can be caused by mutations in either ENPP1 or *ABCC6*. *Am J Hum Genet*. 2012;90(1):25-39.
7. Jansen RS, Duijst S, Mahakena S, et al. *ABCC6*-mediated ATP secretion by the liver is the main source of the mineralization inhibitor inorganic pyrophosphate in the systemic circulation-brief report. *Arterioscler Thromb Vasc Biol*. 2014;34(9):1985-1989.
8. Mention P-J, Lacoeuille F, Leftheriotis G, Martin L, Omarjee L. 18F-Flurodeoxyglucose and 18F-Sodium Fluoride Positron Emission Tomography/Computed Tomography Imaging of Arterial and Cutaneous Alterations in Pseudoxanthoma Elasticum. *Circ Cardiovasc Imaging*. 2018;11(1):1-5.
9. Dedinszki D, Szeri F, Kozák E, et al. Oral administration of pyrophosphate inhibits connective tissue calcification. *EMBO Mol Med*. 2017;9(11):1463-1470.
10. Plomp AS, Bergen AAB, Florijn RJ, et al. Pseudoxanthoma elasticum: Wide phenotypic variation in homozygotes and no signs in heterozygotes for the c.3775delT mutation in *ABCC6*. *Genet Med*. 2009;11(12):852-858.
11. Pomozi V, Brampton C, Fulop K, et al. Analysis of pseudoxanthoma elasticum-causing missense mutants of *ABCC6* in vivo; pharmacological correction of the mislocalized proteins. *J Invest Dermatol*. 2014;134(4):946-953.
12. Legrand A, Cornez L, Samkari W, et al. Mutation spectrum in the *ABCC6* gene and genotype–phenotype correlations in a French cohort with pseudoxanthoma elasticum. *Genet Med*. 2017;19(8):909-917.
13. Pfendner EG, Vanakker OM, Terry SF, et al. Mutation detection in the *ABCC6* gene and genotype-phenotype analysis in a large international case series affected by pseudoxanthoma elasticum. *J Med Genet*. 2007;44(10):621-628.
14. Iwanaga A, Okubo Y, Yozaki M, et al. Analysis of clinical symptoms and *ABCC6* mutations in 76 Japanese patients with pseudoxanthoma elasticum. *J Dermatol*. Published online February 2017.
15. Nykamp K, Anderson M, Powers M, et al. Sherloc: A comprehensive refinement of the ACMG-AMP variant classification criteria. *Genet Med*. 2017;19(10):1105-1117.
16. ETDRS Research Group. No Title. In: *Early Treatment of Diabetic Retinopathy Study (ETDRS) Manual of Operations*. National Technical Information Service; 1985:1-74.
17. Willemink MJ, Vliegenthart R, Takx RAP, et al. Coronary artery calcification scoring with state-of-the-art ct scanners from different vendors has substantial effect on risk classification. *Radiology*. 2014;273(3):695-702.

18. Risseeuw S, Ossewaarde-van Norel J, van Buchem C, Spiering W, Imhof SM, van Leeuwen R. The extent of angioid streaks correlates with macular degeneration in pseudoxanthoma elasticum. *Am J Ophthalmol*. Published online 2020.
19. Schulz V, Hendig D, Szliska C, Gotting C, Kleesiek K. Novel mutations in the *ABCC6* gene of German patients with pseudoxanthoma elasticum. *Hum Biol*. 2005;77(3):367-384.
20. Chassaing N, Martin L, Mazereeuw J, et al. Novel *ABCC6* mutations in pseudoxanthoma elasticum. *J Invest Dermatol*. 2004;122(3):608-613.
21. De Vilder EYG, Hosen MJ, Martin L, et al. VEGFA variants as prognostic markers for the retinopathy in Pseudoxanthoma elasticum. *Clin Genet*. Published online April 8, 2020.
22. Leftheriotis G, Kauffenstein G, Hamel JF, et al. The contribution of arterial calcification to peripheral arterial disease in pseudoxanthoma elasticum. *PLoS One*. 2014;9(5):e96003.
23. Georgalas I, Papaconstantinou D, Koutsandrea C, et al. Angioid streaks, clinical course, complications, and current therapeutic management. *Ther Clin Risk Manag*. 2009;5(1):81-89.
24. Gliem M, Muller PL, Birtel J, Hendig D, Holz FG, Charbel Issa P. Frequency, Phenotypic Characteristics and Progression of Atrophy Associated With a Diseased Bruch's Membrane in Pseudoxanthoma Elasticum. *Invest Ophthalmol Vis Sci*. 2016;57(7):3323-3330.
25. Zarbock R, Hendig D, Szliska C, Kleesiek K, Gotting C. Vascular endothelial growth factor gene polymorphisms as prognostic markers for ocular manifestations in pseudoxanthoma elasticum. *Hum Mol Genet*. 2009;18(17):3344-3351.
26. Sánchez-Tévar AM, García-Fernández M, Murcia-Casas B, et al. Plasma inorganic pyrophosphate and alkaline phosphatase in patients with pseudoxanthoma elasticum. *Ann Transl Med*. 2019;7(24):798.
27. Pomozi V, Julian CB, Zoll J, et al. Dietary Pyrophosphate Modulates Calcification in a Mouse Model of Pseudoxanthoma Elasticum: Implication for Treatment of Patients. *J Invest Dermatol*. 2019;139(5):1082-1088.
28. Gutierrez-Cardo A, Lillo E, Murcia-Casas B, et al. Skin and Arterial Wall Deposits of 18F-NaF and Severity of Disease in Patients with Pseudoxanthoma Elasticum. *J Clin Med*. 2020;9(5):1393.
29. Gräni C, Vontobel J, Benz DC, et al. Ultra-low-dose coronary artery calcium scoring using novel scoring thresholds for low tube voltage protocols—a pilot study. *Eur Heart J Cardiovasc Imaging*. 2018;19(12):1362-1371.
30. Gliem M, Müller PL, Birtel J, et al. Quantitative Fundus Autofluorescence in Pseudoxanthoma Elasticum. *Investig Opthalmology Vis Sci*. 2017;58(14):6159.
31. Risseeuw S, Bennink E, Poirot MG, et al. A reflectivity measure to quantify Bruch's membrane calcification in patients with pseudoxanthoma elasticum using optical coherence tomography. *Transl Vis Sci Technol*. Published online 2020.
32. Legrand A, Benistan K, Mazzella JM, et al. Clinical utility gene card: For pseudoxanthoma elasticum. *Eur J Hum Genet*. 2018;26(6):919-924.

Supplementary data

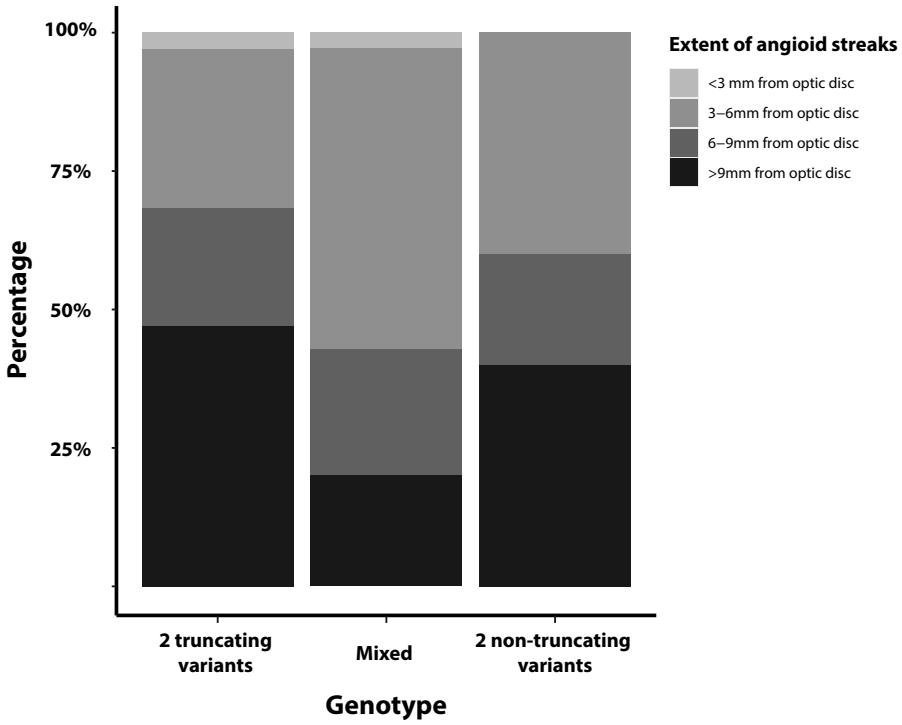

Figure S6.1 Length of angioid streaks per genotype group in younger PXE patients younger than 50 years. Patients with a mixed genotype (n=34) have significantly shorter angioid streaks compared to patients with two truncating variants (n=64) (P = 0.05). No difference was found between patients with two truncating and patients with two non-truncating variants (n=10).

Supplementary Table S6.1 Patient characteristics in patients with a variant of unknown significance excluded

	Two truncating variants[1]	Mixed genotype[2]	Two non-truncating variants[3]	P [1 vs. 2]	P [1 vs. 3]
Total, n	**151**	**66**	**12**		
Age	51 [40-60]	51 [37-60]	49 [45-54]	0.67	0.70
Male sex	53 (35)	27 (41)	4 (33)	0.41	0.90
Vascular, n	**142**	**62**	**12**		
Peripheral arterial calcification					
Prevalence	125 (88)	48 (77)	11 (92)	0.05	0.71
Mass score	608 [40-2140]	274 [2-1548]	232 [132-607]	0.14	0.29
Total body arterial calcification					
Prevalence	137 (97)	57 (92)	12 (100)	0.17	0.51
Mass score	1944 [216-5698]	1014 [38-4273]	520 [147-2108]	0.24	0.32
Ankle brachial index	0.89 [0.59-1.03]	0.98 [0.57 -1.07]	0.80 [0.67-0.92]	0.15	0.29
Peripheral arterial disease	74 (51)	28 (42)	8 (67)	0.27	0.29
Pseudoxanthomas, n	**147**	**64**	**12**		
Prevalence	130 (88)	59 (92)	12 (100)	0.41	0.21
Number of locations	4 [2-5]	4 [2-5]	3 [2-5]	0.38	0.90
Ophthalmology, n	**149**	**66**	**12**		
Spread of angioid streaks, OD					
Missing	6	4	1		
<3 mm	2 (1)	1 (2)	0 (0)	0.02	0.42
3-6 mm	28 (20)	24 (39)	3 (27)		
6-9 mm	46 (32)	10 (16)	1 (9)		
>9 mm	67 (47)	27 (44)	7 (64)		
CNV, prevalence	93 (62)	34 (51)	7 (58)	0.13	0.78
Atrophy, OD					
Mild	18 (12)	9 (14)	2 (17)	0.83	0.36
Severe	21 (14)	11 (17)	0 (0)		
Visual acuity, logMAR, OD	0.10 [-0.01-0.80]	0.09 [-0.02-0.85]	0.04 [-0.08-0.39]	0.91	0.40

Data is presented as median [IQR] or n (%). Data was analysed with the Mann-Whitney U test or the $\chi 2$ test when appropriate.
CNV = Choroidal neovascularization, LogMAR = Logarithm of the minimum angle of resolution, peripheral arterial disease was defined as an ankle brachial index<0.90.
Data are presented for the right eye, unless imaging could not be assessed, then the left eye was used. The extent of the angioid streaks was measured as the extent of the longest angioid streak from the center of the optic disk on 55° near infrared reflectance (NIR) imaging. One patient did not have 55° NIR imaging, and in 10 patients, severe scarring or atrophy impaired reliable grading.

Supplementary table S6.2 Patient characteristics in patients with possible splice site variants and patients where only one or no variants were found

	Possible splice site variant	One pathogenic variant	No pathogenic variants
Total, n	**3**	**6**	**2**
Age	51	58 [54-65]	45
Male sex	2 (67)	2 (33)	1 (50)
Vascular, n			
Peripheral arterial calcification			
Prevalence	2 (100)	5 (83)	1 (50)
Mass score	3511	943 [47-2540]	1291
Total body arterial calcification			
Prevalence	2 (100)	6 (100)	1 (50)
Mass score	5860	2338 [765-8637]	1488
Ankle brachial index	0.82	0.98 [0.65-1.18]	1.12
Peripheral arterial disease	2 (67)	2 (40)	0 (0)
Pseudoxanthomas, n	**2**	**6**	**2**
Prevalence	2 (100)	6 (100)	2 (100)
Number of locations	4	2 [2-4]	3
Ophthalmology, n	**3**	**6**	**2**
Spread of angioid streaks, OD			
<3 mm	0 (0)	0 (0)	1 (50)
3-6 mm	1 (33)	1 (25)	1 (50)
6-9 mm	1 (33)	2 (50)	0 (0)
>9 mm	1 (33)	1 (25)	0 (0)
CNV, prevalence	1 (33)	5 (83)	1 (50)
Atrophy, OD			
Mild	0 (0)	0 (0)	0 (0)
Severe	0 (0)	1 (17)	0 (0)
Visual acuity, logMAR, OD	-0.10	0.26 [0-1.51]	-0.12

CNV = Choroidal neovascularization, LogMAR = Logarithm of the minimum angle of resolution, peripheral arterial disease was defined as an ankle brachial index<0.90.


Chapter 7

The extent of angioid streaks correlates with macular degeneration in pseudoxanthoma elasticum

Sara Risseeuw
Jeannette Ossewaarde – van Norel
Colette van Buchem
Wilko Spiering
Saskia M Imhof
Redmer van Leeuwen

American Journal of Ophthalmology. 2020;220:82-99.

Abstract

Purpose

To investigate whether the extent of Bruch's membrane (BM) calcification is associated with choroidal neovascularization (CNV) and macular atrophy in patients with pseudoxanthoma elasticum (PXE) by using the extent of angioid streaks as a surrogate marker for the degree of BM calcification.

Design

Retrospective cross-sectional study.

Methods

We investigated 301 PXE patients (median age 52 years, range 9–79) in a tertiary referral center. For both eyes, we graded the extent of angioid streaks, i.e. their distance from the optic disk, into five groups. Imaging was systematically assessed for signs of CNV and macular atrophy. Associations between extent of angioid streaks and CNV or macular atrophy were investigated using regression analysis.

Results

CNV was present in 148 patients (49%) and retinal atrophy in 71 patients (24%). The extent of angioid streaks was associated with older age (P for trend = 1.92×10^{-15}) and a higher prevalence of CNV and/or macular atrophy (P for trend = 4.22×10^{-10} and P for trend = 5.17×10^{-6}, respectively). In addition, the extent of angioid streaks was associated with the presence of CNV when adjusted for age and sex (odds ratio (OR) 1.9, 95% CI 1.3 - 2.9) and with more severe macular atrophy (proportional OR 2.3, 95% CI 1.5 - 3.6).

Conclusions

In PXE patients, longer angioid streaks are associated with an increased risk of CNV and macular atrophy, even after adjustment for age. These findings are relevant when counseling PXE patients on their visual prognosis.

Background

Pseudoxanthoma elasticum is a rare disorder in which biallelic mutations of the *ABCC6* gene lead to calcification of elastic fibres in the skin, vasculature and eyes.[1] Clinically, calcification of Bruch's membrane (BM) leads to peau d'orange, which is hypothesized to be the visible transition zone of calcified BM.[2,3] Peau d'orange is typically seen at the posterior pole in childhood, is thought to spread centrifugally during life, and precedes the formation of angioid streaks in the brittle calcified BM.[3,4] Angioid streaks are defects in BM and present as irregular jagged breaklines.[5] They originate from the optic disc, surround it concentrically, and radiate outwards to the periphery, but do not cross the transition zone of calcified BM.[3] Angioid streaks allow for the ingrowth of fibrovascular tissue, causing choroidal neovascularizations (CNV) with the subsequent risk of hemorrhage, exudation and scarring. Furthermore, PXE patients often suffer from macular atrophy, similar to geographic atrophy in age-related macular degeneration.[6] Both CNV and macular atrophy contribute to a high prevalence of visual impairment in PXE patients.[7]

PXE is a slowly progressive disease and the prevalence of CNV and macular atrophy increases with increasing age.[6,7] However, even in patients with similar age and genotype the severity of macular degeneration is highly variable.[7–9] To predict the visual prognosis in PXE, it is necessary to gain insight in the determinants of CNV and macular atrophy. Gliem et al proposed that BM calcification is a risk factor for atrophy of the outer retina and retinal pigment epithelium (RPE), which can be considered as a natural endpoint in PXE.[6] Angioid streaks predispose to the occurrence of CNV and therefore the location of the angioid streaks (foveal or extrafoveal) is highly relevant for visual function. Moreover, the extent of angioid streaks is limited to the area of BM calcification, and thus depends on the degree of BM calcification.

We hypothesize that patients with a larger extent of BM calcification have a higher risk of developing macular degeneration and thereby a worse visual prognosis. The aim of this study is to investigate whether the extent of angioid streaks, as a proxy for the degree of BM calcification, is associated with the occurrence of CNV and macular atrophy in PXE patients.

Methods

Study design and population

This monocenter cross-sectional study was performed at the University Medical Center Utrecht in the Netherlands, which houses the Dutch National Expertise Center for PXE. The study adhered to the tenets of the declaration of Helsinki and the Institutional Ethics Committee approved the study protocol (METC 19/257). All patients had a confirmed diagnosis of PXE, according to the criteria as proposed by Plomp et al.[10] PXE was diagnosed if at least two major diagnostic criteria were present (skin involvement, eye involvement and genetic confirmation of *ABCC6* mutations).[10] All PXE patients with an ophthalmologic examination were included in this study, resulting in 301 patients. Genetic data was available in 296 patients: 281 patients had at least two *ABCC6* mutations, 11 had one mutation and in 4 patients no mutations in the *ABCC6* gene were found.

Ophthalmologic measurements

We investigated the data acquired on the first visit of the patients at the ophthalmology department. All patients underwent routine ophthalmologic examination, including best-corrected visual acuity (BCVA). Imaging included color fundus photography (FF 450 plus, Carl Zeiss Meditec AG, Jena, Germany), spectral domain optical coherence tomography (SD-OCT), near-infrared reflectance imaging (NIR) and fundus autofluorescence (FAF) (all Spectralis HRA-OCT, Heidelberg Engineering, Heidelberg, Germany). Fluorescein angiography and/or indocyanine green angiography was performed on indication. BCVA was used to classify the presence and severity of visual impairment, based on the visual acuity of the better eye, according to the World Health Organization.[11] Before 2018, both Snellen charts and Early Treatment of Diabetic Retinopathy Study (ETDRS) charts were used.[12] From 2018 on, only ETDRS charts were used. The BCVA was converted to the logarithm of the minimum angle of resolution (logMAR).

Per eye, the available imaging was graded on the presence or absence of CNV and macular atrophy in the posterior pole by three individuals (SR, RvL, JOvN). The presence of CNV was based on sub- or intraretinal fluid and/or neovascular or fibrotic tissue on SD-OCT, leakage of neovascular tissue and/or staining of fibrovascular scars on fluorescein- or indocyanine green angiography, and hemorrhage, subretinal fibrosis or hyperpigmentation on fundus photography. The presence of macular atrophy was based on the focal loss of the RPE layer on SD-OCT, sharply demarcated areas of

hypofluorescence on FAF and hyperreflectivity on NIR, hypopigmentation and visible choroidal vessels on fundus photography, or window defects on FA. If macular atrophy was present, it was classified into 'mild atrophy' or 'severe atrophy', based on the size of the atrophic area. If the atrophic area was smaller than the equivalent of twice the area of optic disk, it was graded as 'mild atrophy', and if it was larger than the equivalent of twice the area of the optic disk, it was graded as 'severe atrophy'. In case of multiple atrophic areas, we graded the largest atrophic area. An atrophic zone < 0.5 diameter of the optic disk surrounding an (in)active CNV, and peripapillary atrophy were considered unrelated to macular atrophy and therefore not classified as macular atrophy. If an atrophic area surrounding to an (in-)active CNV was larger than 0.5 diameter of the optic disk, only the area >0.5 diameter of the optic disk surrounding the CNV was graded, and the atrophic area directly adjacent to the CNV was excluded from grading.

Furthermore, the presence of pattern dystrophy like changes was graded on FAF imaging. In 285 patients, FAF imaging was obtained at the same time as the imaging for the grading of the ophthalmological phenotype. The FAF imaging was assessed for the presence of increased autofluorescence in the posterior pole resembling pattern dystrophy. Eyes with extensive scarring of FAF imaging of inadequate image quality for a reliable assessment were classified as 'not assessable'.

Angioid streaks were evaluated and graded using five 55° NIR images of the posterior pole and mid-periphery. In case of doubt, color fundus photography was also used. Since angioid streaks originate at the optic disk and spread towards the periphery, we constructed a grading system based on the distance from the center of the optic disc to the longest angioid streak. We defined five zones, based on the extent of the longest angioid streak: zone 1 corresponds with angioid streaks within a 3 mm radius, zone 2 corresponds with angioid streaks extending up to 6 mm, zone 3 corresponds with angioid streaks extending up to 9 mm, and zone 4 corresponds with angioid streaks that are longer than 9 mm (Figure 7.1). Eyes of young patients with peau d'orange but without detectable angioid streaks were classified as 'zone 0'. Eyes with extensive macular pathology in which grading of angioid streaks was not possible were classified as 'not assessable'.

Of all 301 patients, four patients did not have 55°NIR imaging, in seven patients no angioid streaks were visible and in nine patients the image quality or severe scarring impaired reliable grading. Thus, grading could be performed in 297 patients, resulting in 288 patients of which at least one eye could be assessed.

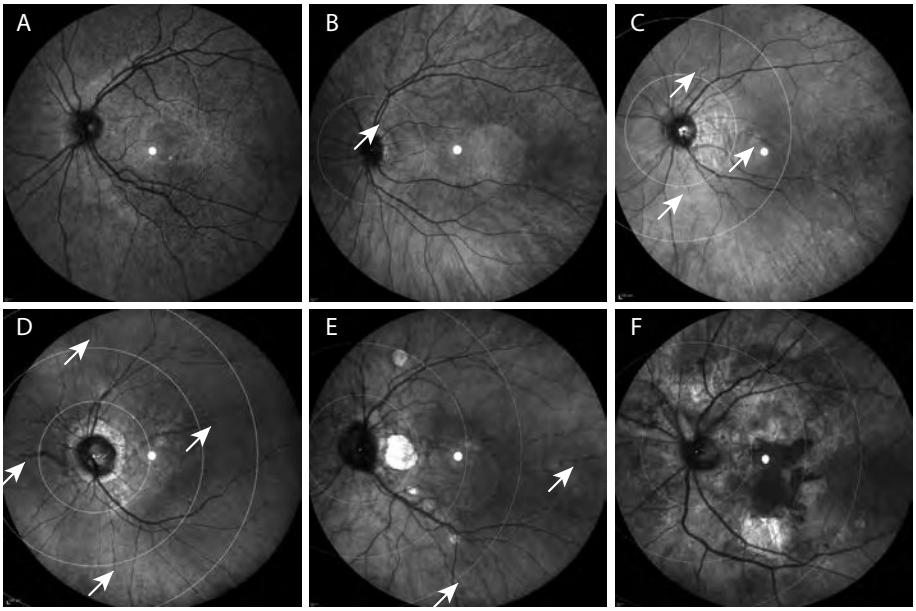

Figure 7.1 Grading of angioid streaks performed with Heidelberg Eye Explorer, based on five 55° near infrared reflectance images of the posterial pole and the midperiphery. The white circles represent circles with a 3 mm, a 6 mm and a 9 mm radius and are centered on the optic nerve. The white arrows indicate angioid streaks. Angioid streaks were classified into five zones. If there were no detectable angioid streaks, the eye was classified as zone 0 (**A**). Zone 1 corresponds with angioid streaks within 3 mm of the optic disc center (**B**), zone 2 corresponds with angioid streaks extending up to 3 to 6 mm from the optic disc center (**C**), zone 3 corresponds with angioid streaks extending up to 6 to 9 mm from the optic disc center (**D**) and zone 4 with angioid streaks that extend further than 9 mm from the optic disc center (**E**). In eyes with extensive macular pathology, grading of angioid streaks was not possible and graded as 'not assessable' (F).

To investigate the inter-observer agreement of the angioid streaks grading system, we compared the scoring of 25 random patients (50 eyes) by two experienced ophthalmology graders (CvB and SR). Inter-observer agreement of the angioid streaks grading system was quantified by the weighted kappa, which was 0.84 (P <0.001). This can be interpreted as a strong agreement.[13]

Data analyses

The correlation between the extent of angioid streaks between the right and left eye was assessed with the Goodman-Kruskal gamma, which is a measure of association between categorical variables.[14] For descriptive analysis at patient level, the extent of angioid streaks in the right eye was used. If the imaging of the right eye was not assessable, imaging of the left eye was used. Eyes graded as 'not assessable' were excluded from association and regression analyses.

Continuous variables are presented as mean ± standard deviation (SD), or as median with interquartile range (IQR), depending on the distribution. Categorical variables are presented as numbers (%). The association between the extent of angioid streaks and other variables was analyzed using linear, logistic or ordinal regression analysis, when appropriate. The extent of angioid streaks was entered as a continuous variable to test for trend. A *P*-value of <0.05 was considered statistically significant.

We used regression analysis to investigate the association between the extent of angioid streaks and the presence of CNV and the severity of macular atrophy. To test the association with the presence of CNV, we used logistic regression analysis. To test the association with the severity of atrophy, we used ordinal regression analysis. The models are presented as crude models and age- and sex adjusted models. The extent of angioid streaks was modelled as a continuous determinant. In all analyses the right eye was used first, and the left eye was used as confirmation.

R version 3.4.1 was used for data analysis. Additional packages 'mess' (version 2019.4-25) and 'ordinal' (version 0.5.6) were used to measure Goodman-Kruskal gamma and ordinal regression, respectively.

Results

In total, 301 PXE patients were included. The patient characteristics are presented in Table 7.1 for both the total group and for subgroups of extent of angioid streaks. The median age was 52 years (range 9 - 79, IQR 41 – 60) and the majority was female (63%). The length of the angioid streaks increased with age (Figure 7.2A). Also, the prevalence of CNV and the severity of atrophy increased with age. (Figure 7.2B).

PXE patients with longer angioid streaks were older and more often male, had worse BCVA, more often CNV, more severe macular atrophy and had more often pattern dystrophy like changes (Table 7.1). Details on inter-eye correlation of the extent of angioid streaks can be found in Table 7.2. According to the Goodman-Kruskal gamma test, there was a positive correlation between the extent of angioid streaks of both eyes ($\gamma = 0.97$, 95% confidence interval (CI) 0.95; 0.99), which can be considered as a very strong correlation.[15]

Table 7.1 Patient characteristics

		Total		Zone 1 < 3 mm	Zone 2 3 – 6 mm	Zone 3 6 – 9 mm	Zone 4 > 9 mm	*P*	*P* for trend
	Number	*301*		*3*	*78*	*81*	*119*		
Age		52 (41; 60)		25 (24; 34)	45 (28; 57)	54 (48; 60)	52 (47; 61)	8.36×10^{-9}	1.92×10^{-15}
Sex	Female	189 (63%)		2 (67%)	61 (78%)	49 (61%)	64 (54%)	0.01	2.17×10^{-3}
Opththalmological manifestations									
Visual acuity[c]		0.08 (-0.02; 0.70)	-0.02 (-0.04; 0.01)	-0.08 (-0.12; -0.08)	0.01 (-0.08; 0.10)	0.08 (0.00; 0.40)	0.20 (0.00; 1.26)	6.97×10^{-6}	2.56×10^{-7}
Visual impairment		86 (29%)	0	0	7 (9%)	19 (24%)	48 (40%)	1.01×10^{-5}	6.69×10^{-7}
Signs of(in) active CNV		148 (49%)	0	0	14 (18%)	47 (58%)	75 (63%)	2.00×10^{-10}	4.22×10^{-10}
Severity of atrophy	None	229 (76%)	7 (100%)	3 (100%)	72 (92%)	64 (80%)	79 (66%)	9.68×10^{-4}	5.17×10^{-6}
	Mild	35 (12%)	0	0	6 (8%)	10 (12%)	17 (14%)		
	Severe	36 (12%)	0	0	0	7 (9%)	23 (19%)		
Pattern dystrophy like changes[d]		116 (44%)	0	0	15 (19%)	37 (50%)	62 (63%)	1.41×10^{-8}	2.34×10^{-9}

Abbreviations: CNV; choroidal neovascularization

Data are presented as number (%) or median (interquartile range). All eye-specific details are shown for the right eye, unless this imaging could not be assessed,then the left eye was used.

a. Stratified details for the extent of angioid streaks are presented for 288 PXE patients. Four patients did not have 55° infrared imaging, and in nine patients the quality of the imaging or severe scarring or atrophy impaired reliable grading.

b. The extent of the angioid streaks was measured as the extent of the longest angioid streak from the center of the optic disk on 55° near infrared imaging.

c. Visual acuity is the best corrected visual acuity presented as the logarithm of the minimum angle of resolution

d. Pattern dystrophy like changes were assessed in 285 patients with available fundus autofluorescence imaging. In total, 28 right eyes and 28 left eyes had severe scarring of low image quality and were excluded. This resulted in data from 264 patients that are presented in this table.

Table 7.2 Inter-eye correlation of the extent of angioid streaks

		Zone of right eye					
		0	1	2	3	4	NA
Zone of left eye		*n = 7*	*n = 3*	*n = 90*	*n = 73*	*n = 112*	*n = 12*
0	*n = 7*	7	0	0	0	0	0
1	*n = 3*	0	1	2	0	0	0
2	*n = 78*	0	2	71	4	1	0
3	*n = 78*	0	0	16	52	10	0
4	*n = 115*	0	0	1	14	97	3
NA	*n = 16*	0	0	0	3	4	9

The extent of angioid streaks was measured in 297 PXE patients, since four patients did not have 55° infrared imaging. If no angioid streaks were detected, the eye was classified as zone 0. Zone 1 corresponds with angioid streaks within 3 mm from the optic disc center, zone 2 corresponds with angioid streaks extending up to 3 to 6 mm from the optic disc center, zone 3 corresponds with angioid streaks extending up to 6 to 9 mm from the optic disc center and zone 4 with angioid streaks that extend further than 9 mm from the optic disc center. In eyes with extensive scarring and atrophy, grading of angioid streaks was not possible and graded as 'not assessable' (NA).

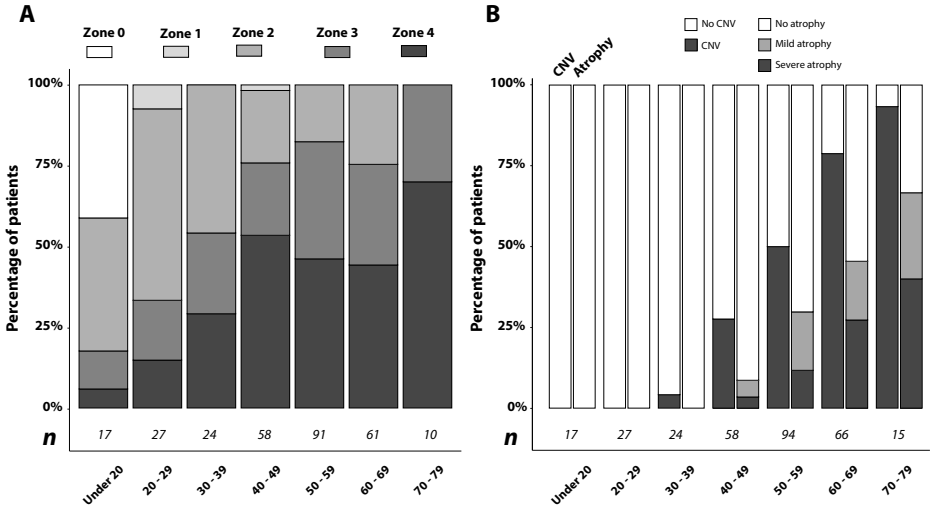

Figure 7.2 The extent of angioid streaks (**A**) and presence of choroidal neovascularization and macular atrophy (**B**) in the right eye, presented for age in years. The numbers on the bottom represent the number of patients within each group. The zones (**A**) represent the extent of the longest angioid streak. Zone 0 corresponds with no angioid streaks, zone 1 with angioid streaks extending up to 3 mm, zone 2 with angioid streaks extending between 3 – 6 mm, zone 3 with angioid streaks extending between 6 – 9 mm and zone 4 with angioid streaks extending further than 9 mm from the optic disc center.

Table 7.3 Association between the extent of angioid streaks and macular degeneration

		Crude model Estimate [95% CI]	Age adjusted Estimate [95% CI]	Age and sex adjusted Estimate [95% CI]
Signs of (in) active CNV[a]	Right eye	2.2 [1.7; 3.0]	2.0 [1.4; 3.0]	1.9 [1.3; 2.9]
	Left eye	2.4 [1.8; 3.2]	2.0 [1.4; 2.9]	1.9 [1.4; 2.8]
Severity of atrophy[b]	Right eye	2.5 [1.7; 3.8]	2.3 [1.5; 3.7]	2.3 [1.5; 3.6]
	Left eye	2.3 [1.7; 3.4]	2.0 [1.4; 3.0]	2.0 [1.4; 3.0]
Pattern dystrophy like changes[a]	Right eye[c]	2.6 [1.9 – 3.7]	2.9 [1.9 – 4.7]	2.9 [1.9 – 4.7]
	Left eye[c]	2.4 [1.8 – 3.4]	2.4 [1.6 – 3.8]	2.4 [1.6 – 3.7]

Abbreviations: CI; confidence interval, CNV; choroidal neovascularization.
If the extent of angioid streaks was graded as not assessable, the eye was excluded from analysis. For right eye analysis, 281 were included. For left eye analysis, 285 eyes were included in analysis.
a. Models represent logistic regression models with the zone of angioid streaks as a continuous determinant. The estimate represents the odds ratio.
b. Models represent ordinal regression models with the zone of angioid streaks as continuous determinant. The estimate represents the proportional odds ratio.
c. If the eye had severe scarring of the fundus autofluorescence was of low quality, the eye was excluded from analyses. For both the right and the left eye, 252 eyes were included in the analyses.

In crude analysis, CNV occurred more often in eyes with longer angioid streaks (odds ratio (OR) 2.2, 95% CI 1.7; 3.0)(Table 3). This effect persisted when adjusted for age and sex (OR 1.9 95% CI 1.3; 2.9). In this multivariable analysis, age was an important determinant of CNV (OR 1.1, 95% CI 1.1; 1.2). Interestingly, men had an increased risk of CNV in this multivariable analysis (OR 2.0, 95% CI 1.1; 3.7). Confirmation in the left eye yielded similar results for all analyses (Table 7.3).

Longer angioid streaks were also associated with more severe macular atrophy, even when adjusted for age and sex (proportional OR 2.3, 95% CI 1.5; 3.6, Table 7.3). Thus, there is a 2.3-times increased odds of having more severe atrophy if the extent of angioid streaks increases with one zone. In multivariable analysis, adjusted for age and sex, only age was an important determinant (proportional OR 1.1, 95% CI 1.1; 1.2), and male sex was not (proportional OR 1.4, 95% CI 0.7; 2.6). Again, confirmation in the left eye yielded similar results.

Furthermore, pattern like dystrophy changes on FAF imaging presented more often in eye with longer angioid streaks (crude OR 2.6, 95% CI 1.9; 3.7, Table 7.3). This effect remained after adjusting for age and sex (OR 2.9, 95% CI 1.9 – 4.7). In this multivariable analysis age was associated with the presence of pattern like dystrophy changes on FAF (OR 1.2, 95% CI 1.1; 1.2) but male sex was not (OR 1.0, 95% CI 0.5; 2.0).

Discussion

In this study, we developed a measure for the extent of angioid streaks as a surrogate marker for the degree of BM calcification that can be used in nearly all PXE patients. The length of angioid streaks is symmetrical between both eyes, and angioid streaks appear to extend further with increasing age. Longer angioid streaks are associated with a higher risk of CNV and macular atrophy, also when adjusted for age and sex.

We hypothesize that the extent of angioid streaks increases with age and represents the natural course of calcification in PXE patients. It is known that peau d'orange precedes angioid streaks, which fits with our data. The youngest patients did not have angioid streaks yet. We also found that aging, and thus a longer disease duration, is associated with longer angioid streaks. Even though our data is cross-sectional, we assume that angioid streaks are not a static phenomenon and that there is a slow growth of angioid streaks towards the retinal periphery during life. Mansour et al. already described growth of angioid streaks in two patients, but is unknown whether these patients had PXE.[16] Hypothetically, the growth of angioid streaks with increasing age depends on two factors. First, it is assumed that a calcified BM may develop angioid streaks.[3] Second, it is assumed that mechanical stress, like eye movements or pressure on the globe, causes the brittle BM to break and form angioid streaks.[2,17,18] Therefore, mechanical stress may induce growth of angioid streaks throughout life. Besides a slow growth with age, angioid streaks may also progress more rapidly, for example due to trauma causing pressure or acute retinopathy.[19,20] In this cross-sectional study, it is not possible to determine the underlying mechanism of the progression of angioid streaks. Acute retinopathy in PXE is rather rare with a presumed incidence of 5% and most patients are advised to minimize the risk of suffering from an ocular trauma (avoiding contact sports for example). Therefore, we assume that rapid progression of angioid streaks due to trauma or associated with acute retinopathy alone cannot explain the age-specific prevalence seen in our cohort.

Interestingly, the growth of the angioid streaks after the fifth decade appears to slow down (Figure 2A). It is plausible that the centrifugal spread of BM calcification stops around that age, which impedes angioid streaks to grow longer. Though, the calcified BM is still brittle and prone to break from mechanical stress, and theoretically this may lead to a growth of angioid streaks in the form of branching. However, longitudinal data is required to support this theory, and the clinical relevance of this is unclear. It is possible that the extent of angioid streaks distinguishes well in younger patients but that patients over 50 years require a different approach to visualize the severity of disease. In these patients, often the first signs of macular degeneration are already visible, which probably provide more information on the visual prognosis. Thus, in patients over 50 years, the combined information on presence of CNV, atrophy and pattern-dystrophy like changes should be taken into account when counseling patients.

We found that longer angioid streaks are associated with a higher risk of CNV. Angioid streaks are full-thickness defects of BM that allow the ingrowth of neovascular tissue, thus it is plausible that longer and wider angioid streaks increase the risk of CNV.[5,21] A previous study found that patients with longer angioid streaks had a higher prevalence of CNV.[22] However, this study did not correct for age, and not all patients had PXE. In our study, we only assessed the presence of CNV in the posterior pole, and not along the angioid streaks towards the retinal periphery. In theory, this might have led to an underestimation of the prevalence, but in clinical practice we only observe CNV in the posterior pole.

It is also plausible that longer angioid streaks, and thus a larger area of BM calcification, means that the BM calcification in the posterior pole is more dense and severe as well, and thereby increase the risk of CNV. More dense calcification in BM will impair oxygen diffusion from the choroid to the outer retina.[23] Together with the higher oxygen demand in the macular area, this leads to hypoxia and expression of vascular endothelial growth factors (VEGF) by the RPE.[24] The higher VEGF-level might initiate the growth of a CNV through an angioid streak. We found that longer angioid streaks increase the risk of CNV, which supports the hypothesis that the BM calcification is more dense. To further investigate if more dense BM calcification indeed increases the risk of CNV in PXE, an endpoint for the severity of BM calcification is required, in contrast to the measurement that was used in this study, which is based on angioid streaks and may thereby interfere with the risk of CNV.

We found that men with PXE are more at risk for CNV than women with PXE. This contradicts previous studies investigating the association of sex with CNV in other diseases. The majority of studies investigating late AMD did not find an effect of sex on CNV, but some studies mentioned a slightly higher prevalence of neovascular AMD in women.[25,26] If male PXE patients had more BM calcification, they would also be more at risk for macular atrophy, but we did not observe this. Possibly, other unknown factors, for example cardiovascular risk factors such as smoking, are confounders in the association between sex and CNV. However, it is also plausible that female PXE patients with a milder ophthalmological phenotype are overrepresented in the younger population, and thereby introduce a selection bias.

Visual impairment is common in PXE patients, and the visual acuity of the first eye often deteriorates around the fifth decade.[7,27–29] Because most, but not all PXE patients, develop CNV or macular atrophy, the visual prognosis varies and is difficult to predict for an individual.[7] For PXE patients, the foresight of losing vision impacts their quality of life, emotional wellbeing, and decisions in life planning.[30] Therefore, it is important to gain insight in determinants of macular degeneration for proper counseling of PXE patients.

Up to now, the presence of angioid streaks in the fovea or macula indicates whether a PXE patient is at risk for losing vision, because of the development of CNV. Predictors of macular atrophy have not yet been found in PXE patients, although increased fundus autofluorescence is associated with macular atrophy.[6] Our findings show that PXE patients with longer angioid streaks have a higher risk of macular degeneration, and implicate that the degree of BM calcification is an important determinant for the final visual prognosis. This is important for counseling PXE patients, especially younger patients under 40 years who have not yet developed CNV and do not show increased fundus autofluorescence. For example, we can assume that a PXE patient with angioid streaks longer than the posterior pole will have a higher risk of macular degeneration and a worse visual prognosis than a PXE patient with angioid streaks confined to the posterior pole. However, when counseling patients, it is important to realize that this study focuses on the loss of visual acuity. Other aspects of retinal function, such as impaired dark adaptation, contrast sensitivity and the extent and location of paracentral scotomata also affect the visual function of PXE patients.[31]

Not only are these findings relevant for counseling patients, they may also give insight in the pathogenesis of atrophy of the outer retina and RPE. Even though not all patients

develop RPE atrophy, our findings suggest that a higher degree of BM calcification increases the risk of RPE atrophy. This is supported by our findings that longer angioid streaks increase the risk of pattern dystrophy like changes. It is plausible that more BM calcification decreases the permeability of BM for diffusion of nutrients and waste products between the RPE and the choroid. Subsequently, this may lead to RPE dysfunction, which is visible as increased autofluorescence on FAF and often precedes RPE atrophy in PXE patients.[6] Recently, it was found that pattern dystrophy like changes are common in PXE patients over 50 years, which strengthens the hypothesis that BM calcification progresses throughout life.[32] For a better understanding of the role of BM calcification in RPE dysfunction, which may eventually progress to RPE atrophy, an *in vivo* biomarker for BM calcification is required. Recently, an OCT-based quantification for BM calcification in PXE patients was proposed.[33] However, further research and external validation is warranted before this is suitable as biomarker in normal subjects.

A strength of this study is the size of the study population, which is relatively large for a rare disease. We adjusted the effect of the extent of angioid streaks on macular degeneration for age and sex, leading to a better estimation of the true effect. Furthermore, the use of the left eye as a confirmation serves as an internal validation.

Some limitations have to be acknowledged. The extent of angioid streaks is a new surrogate marker for the extent of BM calcification and is not validated yet. Also, the classification of the extent of angioid streaks in zones instead of a continuous measure causes a loss of information, since there is a high variability of the extent of angioid streaks within the different zones. The extent of angioid streaks was not adjusted for the patients axial length, which might affect the precision of this measure. Furthermore, we did not account for the extent of branching of angioid streaks, which might be another indicator of the severity of angioid streaks. However, it is the first possible measure that can be used in nearly all PXE patients. Gliem et al quantified the eccentric border of peau d'orange, which likely matches with the extent of BM calcification.[34,35] This measurement can be performed best on 30° NIR imaging, which means that older patients with more eccentric peau d'orange are more difficult to measure. Also, in older patients, peau d'orange often is less visible, if the retina is not already affected by scarring or atrophy. Despite being a rough measure, the extent of angioid streaks can be measured in nearly all PXE patients and is thereby a useful surrogate marker, also in end stage disease. Lastly, the cross-sectional design of this study allows for descriptions on group level, but it limits detailed insight into an individuals' course of disease. A longitudinal design is required to describe the progression of BM calcification and the natural course of macular degeneration within

individuals. Since PXE progresses slowly, we estimate that such a longitudinal study would require a long follow-up time of roughly a decade, depending on the size and ages of the study sample.

Conclusion

In PXE patients, longer angioid streaks are associated with an increased risk of CNV and macular atrophy, even after adjustment for age. This information is relevant when counseling PXE patients on their visual prognosis. These findings attribute to a better understanding of the role of BM changes in the complex causal pathway of RPE atrophy.

References

1. Bergen AA, Plomp AS, Schuurman EJ, et al. Mutations in *ABCC6* cause pseudoxanthoma elasticum. *Nat Genet*. 2000;25(2):228-231.
2. Gliem M, De Zaeytijd J, Finger RP, Holz FG, Leroy BP, Issa PC. An update on the ocular phenotype in patients with pseudoxanthoma elasticum. *Front Genet*. 2013;4(APR):14.
3. Charbel Issa P, Finger RP, Gotting C, Hendig D, Holz FG, Scholl HPN. Centrifugal fundus abnormalities in pseudoxanthoma elasticum. *Ophthalmology*. 2010;117(7):1406-1414.
4. Naouri M, Boisseau C, Bonicel P, et al. Manifestations of pseudoxanthoma elasticum in childhood. *Br J Dermatol*. 2009;161(3):635-639.
5. Charbel Issa P, Finger RP, Holz FG, Scholl HPN. Multimodal imaging including spectral domain OCT and confocal near infrared reflectance for characterization of outer retinal pathology in pseudoxanthoma elasticum. *Invest Ophthalmol Vis Sci*. 2009;50(12):5913-5918.
6. Gliem M, Muller PL, Birtel J, Hendig D, Holz FG, Charbel Issa P. Frequency, Phenotypic Characteristics and Progression of Atrophy Associated With a Diseased Bruch's Membrane in Pseudoxanthoma Elasticum. *Invest Ophthalmol Vis Sci*. 2016;57(7):3323-3330.
7. Risseeuw S, Ossewaarde-van Norel J, Klaver CCW, Colijn JM, Imhof SM, van Leeuwen R. Visual Acuity in Pseudoxanthoma Elasticum. *Retina*. 2019;39(8):1580-1587.
8. Pfendner EG, Vanakker OM, Terry SF, et al. Mutation detection in the *ABCC6* gene and genotype-phenotype analysis in a large international case series affected by pseudoxanthoma elasticum. *J Med Genet*. 2007;44(10):621-628.
9. Plomp AS, Bergen AAB, Florijn RJ, et al. Pseudoxanthoma elasticum: Wide phenotypic variation in homozygotes and no signs in heterozygotes for the c.3775delT mutation in *ABCC6*. *Genet Med*. 2009;11(12):852-858.
10. Plomp AS, Toonstra J, Bergen AAB, van Dijk MR, de Jong PTVM. Proposal for updating the pseudoxanthoma elasticum classification system and a review of the clinical findings. *Am J Med Genet A*. 2010;152A(4):1049-1058.
11. World Health Organization. ICD-10 Definition.
12. ETDRS Research Group. No Title. In: *Early Treatment of Diabetic Retinopathy Study (ETDRS) Manual of Operations*. National Technical Information Service; 1985:1-74.
13. McHugh ML. Interrater reliability: the kappa statistic. *Biochem medica*. 2012;22(3):276-282.
14. Goodman LA, Kruskal WH. Measures of Association for Cross Classifications Author (s): Leo A . Goodman and William H . Kruskal Source : Journal of the American Statistical Association , Vol . 49 , No . 268 (Dec ., 1954), pp . 732- Published by : American Statistical Associati. *J Am Stat Assoc*. 1954;49(268):732-764.
15. Rea. LM, Parker RA. *Designing and Conducting Survey Research: A Comprehensive Guide*. 4th ed. Jossey-Bass Publishers.; 2014.
16. Mansour AM, Ansari NH, Shields JA, Annesley, Jr. WH, Cronin CM, Stock L. Evolution of Angioid Streaks. *Ophthalmologica*. 1993;207(2):57-61.
17. Hagedoorn A. Angioid streaks and traumatic ruptures of Bruch's membrane. *Br J Ophthalmol*. 1975;59(5):267.
18. Jampol LM, Acheson R, Eagle RC, Serjeant G, O'Grady R. Calcification of Bruch's Membrane in Angioid Streaks With Homozygous Sickle Cell Disease. *Arch Ophthalmol*. 1987;105(1):93-98.
19. Gliem M, Birtel J, Müller PL, et al. Acute Retinopathy in Pseudoxanthoma Elasticum. *JAMA Ophthalmol*. Published online August 8, 2019.
20. Jampol LM, Acheson R, Eagle RC, Serjeant G, O'Grady R. Calcification of Bruch's Membrane in Angioid Streaks With Homozygous Sickle Cell Disease. *Arch Ophthalmol*. 1987;105(1):93-98.

21. Jensen OA. Bruch's membrane in pseudoxanthoma elasticum. Histochemical, ultrastructural, and x-ray microanalytical study of the membrane and angioid streak areas. *Albrecht Von Graefes Arch Klin Exp Ophthalmol*. 1977;203(3-4):311-320.
22. Mansour AM, Shields JA, Annesley WH, El-Baba F, Tasman W, Tomer TL. Macular degeneration in angioid streaks. *Ophthalmologica*. 1988;197(1):36-41.
23. Booij JC, Baas DC, Beisekeeva J, Gorgels TGMF, Bergen AAB. The dynamic nature of Bruch's membrane. *Prog Retin Eye Res*. 2010;29(1):1-18.
24. Schlingemann RO. Role of growth factors and the wound healing response in age-related macular degeneration. *Graefe's Arch Clin Exp Ophthalmol*. 2004;242(1):91-101.
25. Colijn JM, Buitendijk GHS, Prokofyeva E, et al. Prevalence of Age-Related Macular Degeneration in Europe: The Past and the Future. *Ophthalmology*. 2017;124(12):1753-1763.
26. Rudnicka AR, Jarrar Z, Wormald R, Cook DG, Fletcher A, Owen CG. Age and Gender Variations in Age-related Macular Degeneration Prevalence in Populations of European Ancestry: A Meta-analysis. *Ophthalmology*. 2012;119(3):571-580.
27. Orssaud C, Roche O, Dufier J-L, Germain DP. Visual Impairment in Pseudoxanthoma Elasticum: A Survey of 40 Patients. *Ophthalmic Genet*. 2015;36(4):327-332.
28. Ebran J-M, Milea D, Trelohan A, et al. New insights into the visual prognosis of pseudoxanthoma elasticum. *Br J Ophthalmol*. 2014;98(1):142-143.
29. Hocaoglu M, Karacorlu M, Sayman Muslubas I, Arf S, Ozdemir H, Uysal O. Visual impairment in pseudoxanthoma elasticum: A survey of 53 patients from Turkey. *Eur J Ophthalmol*. 2016;26(5):449-453.
30. Finger RP, Fenwick E, Marella M, et al. The relative impact of vision impairment and cardiovascular disease on quality of life: the example of pseudoxanthoma elasticum. *Health Qual Life Outcomes*. 2011;9:113.
31. Hess K, Gliem M, Birtel J, et al. Impaired Dark Adaptation Associated With a Diseased Bruch Membrane in Pseudoxanthoma Elasticum. *Retina*. 2019;Publish Ah:1.
32. Murro V, Mucciolo DP, Giorgio D, et al. Pattern dystrophy-like changes and coquille d'oeuf atrophy in elderly patients affected by pseudoxanthoma elasticum. *Graefe's Arch Clin Exp Ophthalmol*. Published online 2020.
33. Risseeuw S, Bennink E, Poirot MG, et al. A reflectivity measure to quantify Bruch's membrane calcification in patients with pseudoxanthoma elasticum using optical coherence tomography. *Transl Vis Sci Technol*. Published online 2020.
34. Gliem M, Müller PL, Birtel J, et al. Quantitative fundus autofluorescence in pseudoxanthoma elasticum. *Investig Ophthalmol Vis Sci*. 2017;58(14):6159-6165.
35. Gliem M, Hendig D, Finger RP, Holz FG, Charbel Issa P. Reticular pseudodrusen associated with a diseased bruch membrane in pseudoxanthoma elasticum. *JAMA Ophthalmol*. 2015;133(5):581-588.

7

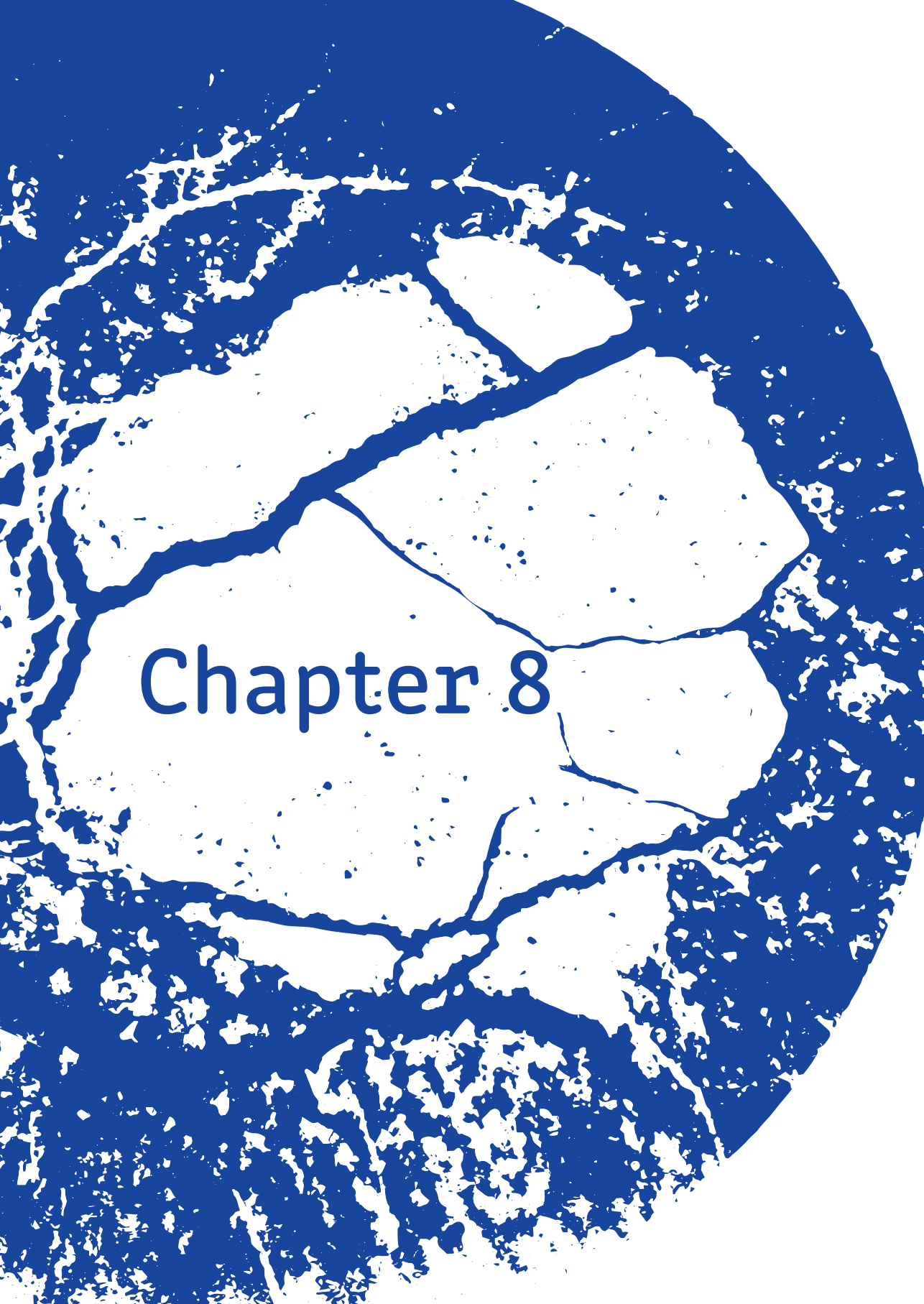
Chapter 8

The effect of etidronate on choroidal neovascular activity in patients with pseudoxanthoma elasticum

Sara Risseeuw
Redmer van Leeuwen
Saskia M. Imhof
Pim A. de Jong
Willem P.Th.M. Mali
Wilko Spiering
Jeannette Ossewaarde – van Norel

Accepted for publication in PLoS One

Abstract

Aim

To assess the effect of the bisphosphonate etidronate on choroidal neovascular (CNV) activity in patients with pseudoxanthoma elasticum (PXE).

Methods

This is an ancillary study in a single center, randomized, double-blind placebo-controlled trial (RCT) in which 74 patients with PXE were assigned to either one-year etidronate or placebo treatment. Spectral domain optical coherence tomography (SD-OCT) imaging and color fundus photography were performed every three months for one year and were systematically assessed on signs of CNV activity.

Results

In the etidronate group, 11 (30%) of the patients had CNV activity at baseline, compared to 25 (67%) of the patients in the placebo group ($P = 0.005$). The proportion of eyes with CNV activity during the study ranged from 18–33% in the etidronate group and 42-56% in the placebo group and no significant difference in improvement or worsening of CNV activity was found ($P = 0.168$). Using a generalized mixed model for repeated measures, there was a protective effect of etidronate in crude analysis (RR 0.86, 95% CI 0.75 – 0.98) that disappeared when adjusting for baseline CNV activity (RR 0.97, 95% CI 0.84 – 1.13).

Conclusion

In this post-hoc RCT analysis we did not observe a protecting or deteriorating effect of etidronate on CNV activity in patients with PXE after adjustment for baseline CNV.

Background

Choroidal neovascularization (CNV) is a common sight-threatening complication in chorioretinal diseases such as age-related macular degeneration (AMD), pathologic myopia and pseudoxanthoma elasticum (PXE).[1,2] Despite prompt treatment with anti-vascular endothelial growth factors (anti-VEGF), irreversible retinal damage and scarring often occurs.[3]

In PXE, bi-allelic mutations in the *ABCC6* gene cause ectopic mineralization in the skin, vasculature and in Bruch's membrane (BM) of the eye.[4] The latter results in BM breaks, so-called angioid streaks, which allow CNV to arise.[2] These cause visual impairment at a relatively young age.[5] Up to now, no causal treatment for PXE exists. Ectopic mineralization in PXE is likely caused by low levels of inorganic pyrophosphate (PP_i), an endogenic ectopic mineralization inhibitor.[6] Bisphosphonates, which are synthetic analogs of PP_i, might therefore have a beneficial effect on ectopic mineralization. To further study the effect of bisphoshonates on vascular calcification in patients with PXE, a randomized placebo-controlled double-blinded trial was conducted at the University Medical Center Utrecht ('Treatment of Ectopic Calcification in PXE' (TEMP) trial).[7]

At the start of the trial data on possible effects of bisphosphonates on CNV activity were conflicting.[8–11] Treatment of CNV due to AMD or myopia with alendronate was associated with better visual outcome in some studies.[8,9] However, a higher risk of CNV in AMD was found in users of oral bisphosphonates in a case-control study.[11] This might be explained by the pro-inflammatory properties of bisphosphonates.[12] These inconclusive findings gave reason to closely monitor the eye disease and CNV activity in participants of the TEMP trial. Earlier, we reported that users of etidronate had fewer subretinal neovascularization events. These were defined as indications to start or intensify anti-VEGF injections and considered to be serious adverse events (SAE). However, we did not directly and systematically measure the SAE on imaging.[7]

In this post-hoc analysis of the TEMP trial, we aim to assess the effect of the bisphosphonate etidronate on CNV activity as measured by optical coherence tomography (OCT) imaging in patients with PXE.

Methods

Study design and population

For this study, data was used from a single center, randomized, double-blind placebo-controlled trial to study the effect of etidronate on ectopic calcification in patients with PXE (Dutch Trial Register, number NTR5180).[7] This study was performed at the University Medical Center in Utrecht and the medical ethics committee approved the protocol (METC number 15/522). All participants provided written informed consent. In total, 74 patients were included who met the clinical criteria for PXE as proposed by Plomp et al[13] (patients should have at least two of the following features: characteristic skin lesions, eye involvement and/or genetic confirmation of PXE). An inclusion criterium was the presence of calcification in the femoral arteries, as this was the main outcome parameter of the trial. Retinal abnormalities were not taken into account as in- or exclusion criterion. Patients were randomized to either a daily dose of 20 mg/kg of etidronate during 2 weeks, followed by a 10-week period without treatment, or an identical regimen with placebo during 12 months. Further details on selection, randomization and treatment of patients can be found in a previous report on this trial.[7]

Assessment of outcome

All participants were seen at baseline and after 3, 6, 9 and 12 months follow-up. At each visit, imaging included color fundus photography (FF450 plus, Carl Zeiss Meditec AG, Jena, Germany) and spectral domain OCT imaging (SD-OCT) (Spectralis HRA-OCT, Heidelberg Engineering, Heidelberg, Germany). SD-OCT imaging consisted of 25 horizontal B-scans of 6 mm length and interscan distance of 250 µm, so that the major part of the macular area was included. Eye-tracking technology allowed the B-scans to be positioned at the exact same anatomical location at each follow-up visit. At baseline and 12 months follow-up, best-corrected visual acuity (BCVA) was measured using Early Treatment of Diabetic Retinopathy Study (ETDRS) letter charts.[14] Clinical monitoring of CNV and anti-VEGF treatment was performed by the referring ophthalmologist according to current guidelines, independent from study visits. In case of concerns regarding CNV activity at study visits, the ophthalmologists involved in the trial consulted the referring ophthalmologists promptly.

Information on anti-VEGF treatment in the 12 months before and during the trial was systematically collected. This information consisted of the date and type of injected drug per eye (bevacizumab, ranibizumab or aflibercept), in case the patient was treated.

For the purpose of this post-hoc study, assessment of imaging was performed blinded to study arm by three individual graders (SR, JOvN, RvL), by systematically grading all SD-OCT imaging and fundus color photographs of both eyes at each visit. Both the presence and a change in amount of intra- or subretinal fluid (compared to the previous investigation) were scored. Unfortunately, fluorescence angiography was not available to detect leakage of CNV. We believe that this should not be a problem, because angiography does not add information regarding CNV activity in PXE patients in most cases.[15] CNV activity was diagnosed if at least one of the following criteria was present: 1) hemorrhage in posterior pole on color fundus photography and/or 2) one or more intraretinal cysts of >50 µm diameter and/or subretinal fluid of >200 µm width, with signs of a CNV nearby, and/or 3) obvious growth of a subretinal neovascular complex. In this paper, for simplicity, this suspicion of neovascular activity is called 'neovascular activity (CNV activity)'. Change in the intra- or subretinal fluid, which we

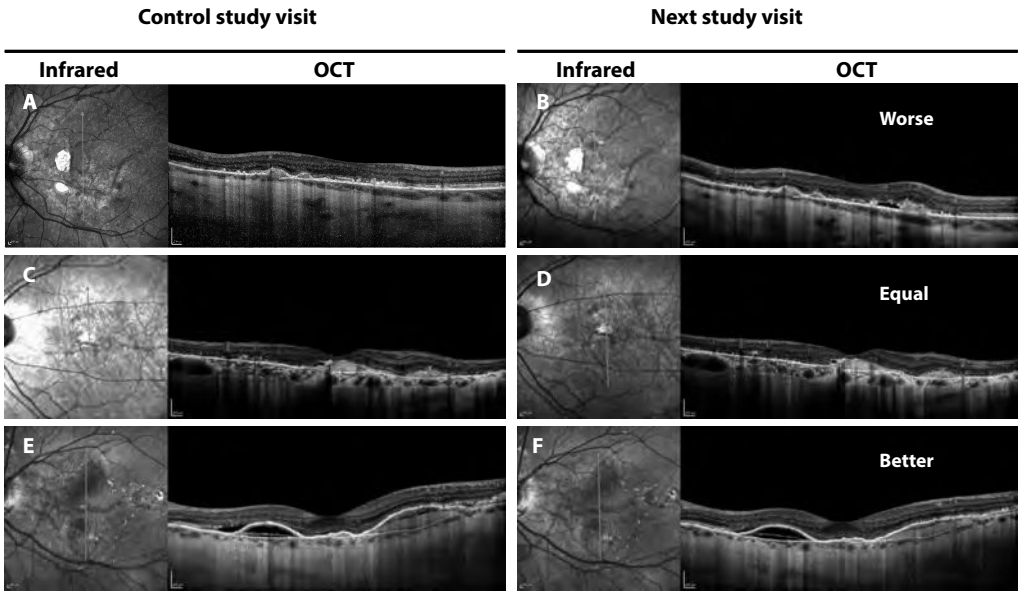

Figure 8.1 Changes in CNV activity. Optical coherence tomography (OCT) imaging of changes in CNV activity in patients with pseudoxanthoma elasticum with corresponding infrared image. The time interval between the study visit and the next visit is three months. The upper images (A and B) show an increase of subretinal fluid and outgrowth of the CNV complex and illustrates a worsening of CNV activity. In the middle (C and D), the CNV is inactive and stable. Below (E and F) a decrease of subretinal fluid is seen, illustrating an improvement of CNV activity.

defined to be signs of CNV activity, was graded as 'better', 'equal' or 'worse', based on an overall conclusion of all 25 B-scans as compared with the previous OCT-scan (as illustrated in Figure 8.1) In case of discrepancy, the major vote of the three graders was taken for both CNV activity and the change in CNV activity. Furthermore, the macular phenotype was assessed according to previously reported criteria and the eyes were categorized in four groups: atrophic, CNV lesions, mixed or no CNV or atrophy.[5]

Statistical analysis

BCVA was converted to the logarithm of the minimum angle of resolution (logMAR) for statistical purposed. Descriptive data are presented as numbers with percentage (%), mean with standard deviation or median with interquartile range, depending on the distribution of the values. At baseline, data are presented at patient level, to illustrate the differences between the etidronate group and the placebo group. For descriptive data regarding CNV activity, data are presented per eye. Differences between the groups were tested with the chi-square test for categorical variables, students' t-test for normal distributions or Mann-Whitney U test for non-parametric distributions. We considered a *P* value lower than 0.05 statistically significant.

Regression analysis was used to investigate associations between treatment and outcome. A mixed effects Poisson regression model for repeated measures was used to analyze the association between etidronate and the presence of CNV activity per eye.[16] In the crude analysis, treatment status and time of visit were included as fixed effects. The individual patient and the left or right eye (nested within the patient) were considered random effects. In the adjusted analysis, baseline CNV activity of the concerning eye was included as a fixed effect. For the effect of etidronate on change in BCVA, we used the difference in ETDRS letters between baseline and 12 months follow-up in a linear regression model.

Interobserver consistency was measured using the percentage of agreement for all three graders on a random subset of 74 eyes..[17]

Statistical analysis was performed with R version 3.4.1 (www.R-project.org). The packages 'irr' and 'lme4' (version 1.1-15) were used for agreement and mixed effects analysis, respectively.

Results

Baseline data

In total, 74 patients were included. One patient in the etidronate group discontinued treatment after six months due to hypersensitivity complaints but remained in the study. One patient in the placebo group discontinued participation in the trial after three months due to uveitis following an anti-VEGF injection.[7] In four eyes (all without SAE), comparison of OCT scans was impaired by low quality and the data from these scans were excluded from the presented results.

The mean age was 57 years and 51% was male. The macular phenotype and the BCVA were similar in the placebo and intervention group. However, there was a baseline imbalance regarding CNV activity (Table 8.1). In the placebo group, 25 patients (67.6%) had CNV activity in one or both eyes, compared to 11 (29.7%) in the etidronate group ($P = 0.005$). This baseline imbalance was not seen in the median number of anti-VEGF injections 3 months before the start of the trial (2.0 in the etidronate group vs 2.5 in the placebo, $P = 0.848$). Comparison of the median number of anti-VEGF injection 6 and 12 months before the trial yielded similar results.

Proportion of and change in CNV activity

The proportion of eyes with CNV activity in both the etidronate and the placebo group during the 12 months of the trial is presented in Figure 8.2. Of the two patients that discontinued treatment, only the available imaging during the treatment is presented. The proportion of eyes with CNV activity ranged from 13-24 (18–33%) in the etidronate group and 31-40 (42-56%) in the placebo group. Out of all these patients having CNV activity, only ten patients had clinically relevant CNV activity in the TEMP trial, requiring immediate start or intensifying of anti-VEGF treatment.

Of all patients, 52 (69%) had at least one neovascular active episode during the trial (22 patients in the etidronate and 30 patients in the placebo group). Of those patients, the change in CNV activity per eye is presented in Figure 8.3. CNV activity worsened in 1-9 (2-21%) of the eyes in the etidronate group and 5-9 (8-16%) in the placebo group, when compared to the previous study visit. CNV activity improved in 1-4 (2-9%) of the eyes in the etidronate group and 6-9 (10-16%) in the placebo group, when compared to the previous study visit. Overall, the change in CNV activity was similar between the etidronate group and the placebo group ($P = 0.168$ (chi-square test)). The percentage of agreement was 73% for presence of CNV activity and 69% for change in CNV activity.

Table 8.1 Baseline ocular characteristics of participants

	Etidronate	Placebo	*P* value
	n = 37	n = 37	
Age (mean ± SD)	56.9 ± 8.6	57.0 ± 8.0	0.956*
Male (%)	19 (51)	19 (51)	0.999
Ocular phenotype			
Macular phenotype: right eye (%)			0.156**
Atrophy	1 (3)	7 (19)	
CNV	11 (30)	10 (27)	
Mixed	15 (41)	13 (35)	
No CNV or atrophy	10 (27)	7 (19)	
Macular phenotype: left eye (%)			0.220**
Atrophy	0	2 (5)	
CNV	10 (27)	15 (41)	
Mixed	18 (49)	15 (41)	
No CNV or atrophy	9 (24)	5 (14)	
BCVA (in logMAR) of right eye (median [IQR])	0.32 [0.00 – 1.36]	0.34 [0.10 – 1.18]	0.935***
BCVA (in logMAR) left eye (median [IQR])	0.56 [0.04 – 1.52]	0.70 [0.07 – 1.32]	0.816***
Best BCVA (in logMAR)	0.14 [0.00 – 0.88]	0.26 [0.06 – 0.96]	0.681***
Worst BCVA (in logMAR)	1.18 [0.14 – 1.60]	1.18 [0.18 – 1.44]	0.762***
Neovascular activity at baseline			
Activity per patient (%)			0.005***
No CNV activity	26 (70)	12 (32)	
One eye	9 (24)	19 (51)	
Both eyes	2 (5)	6 (16)	
CNV activity in right eye (%)	7 (19)	14 (38)	0.122***
CNV activity in left eye (%)	6 (16)	17 (46)	0.012***

	Etidronate	Placebo	*P* value
	n = 37	n = 37	
Neovascular activity at baseline			
Activity per patient (%)			0.005***
No CNV activity	26 (70)	12 (32)	
One eye	9 (24)	19 (51)	
Both eyes	2 (5)	6 (16)	
CNV activity in right eye (%)	7 (19)	14 (38)	0.122***
CNV activity in left eye (%)	6 (16)	17 (46)	0.012***
Patient treated with anti-VEGF before the start of the trial?			
Three months before start of trial	14 (38)	14 (38)	0.999***
Number of injections (median [IQR])[a]	2.0 [2.0 - 3.0]	2.5 [2.0 - 3.0]	0.848**
Six months before start of trial	16 (43)	15 (41)	0.999**
Number of injections (median [IQR])[a]	4.0 [2.8 - 6.0]	4.0 [3.0 - 5.5]	0.826***
12 months before trial	17 (46)	17 (47)	0.999**
Number of injections (median [IQR])[a]	8.0 [5.0 - 11.0]	9.0 [5.0 - 12.0]	0.809***

Abbreviations: SD; standard deviation, BCVA; Best corrected visual acuity, logMAR; logarithm of the minimum angle of resolution, CNV; choroidal neovascularization, ETDRS; Early treatment of Diabetic Retinopathy Treatment Study group, IQR; interquartile range, VEGF; vascular endothelial growth factor.

a. The number of injections is presented only for the patients that received anti-VEGF treatment prior to the trial.

* Differences tested with students t-test

** Differences tested with chi-square test

*** Differences tested with Mann-Whitney U test

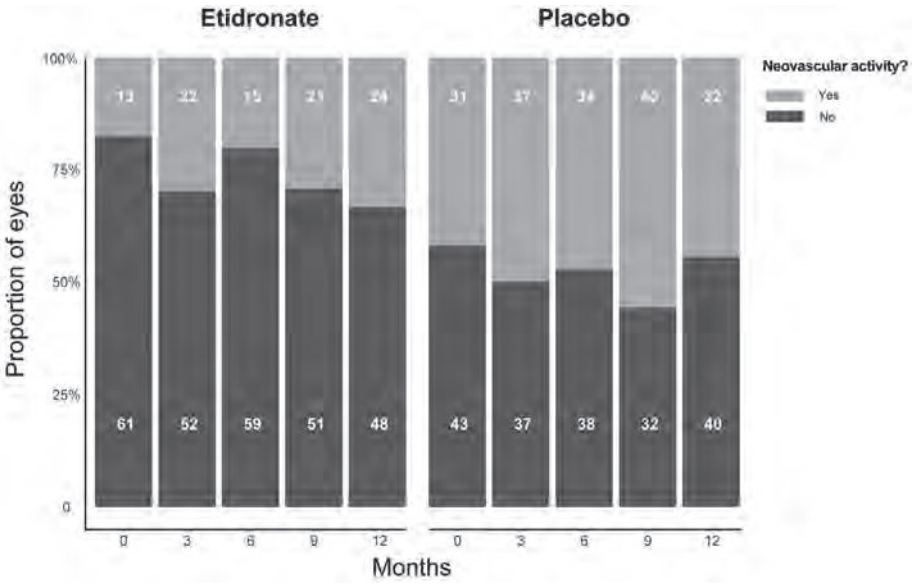

Figure 8.2 Proportion of eyes with CNV activity[a]. CNV; choroidal neovascularization. The white numbers represent the absolute number of eyes per group.
a. CNV activity was diagnosed if at least one of the following criteria was present: hemorrhage in the posterior pole on color fundus photography, and/or intra- or subretinal fluid with signs of CNV nearby, and/or growth of a CNV complex.

Effect of treatment

The median number of anti-VEGF injections administered during the TEMP trial to patients having at least one episode with CNV activity (n=52), was similar between the etidronate and placebo group (placebo group (n = 30) 3.5 (IQR 0 – 8) versus etidronate group (n = 22) 0 (IQR 0 – 6), *P* = 0.223, Mann-Whitney U test). Confining to patients who had at least one injection (n= 28), there was also no difference: median of 8 (IQR 6 – 9) injections in the placebo group (n = 18) compared to 6 (IQR 4 – 9) in the etidronate group (n = 10) (*P* = 0.485, Mann-Whitney U test).

Nearly all events occurred in the second half year of the trial, thereby possibly increasing the number of injections. Considering the number of injections in the first 6 months of the TEMP trial, no significant difference was found: the placebo group (n = 13) received a median of 4 injections (IQR 3 – 5) compared to 3 (IQR 2 – 4) in the etidronate group (n = 10) (*P* = 0.271, Mann-Whitney U test).

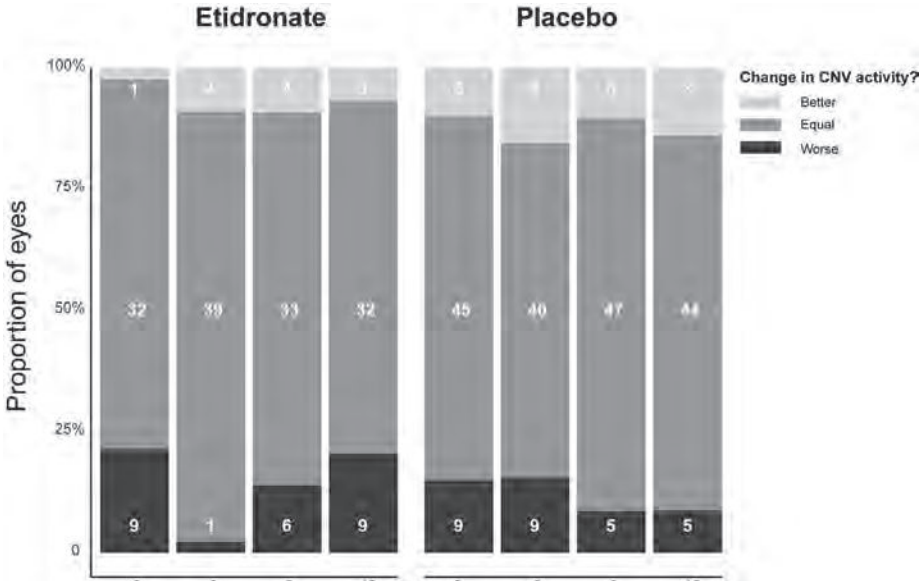

Figure 8.3 Change in CNV activity in patients (n=52) with at least one neovascular active period in one or both eyes during the trial.[a] CNV; choroidal neovascularization. The white numbers represent the absolute number of eyes per group.
a. Change in CNV activity was based on a subjective assessment of all B-scans compared to the previous examination.

The effect of etidronate on presence of CNV activity was analyzed using repeated measurements in a mixed effects Poisson regression model. Crude analysis showed a protective effect of etidronate (relative risk (RR) 0.86, 95% CI 0.75-0.98) on CNV activity. When correcting for baseline activity in multivariable analysis, this effect disappeared and was no longer statistically significant (RR 0.97, 95% CI 0.84-1.13). Baseline CNV activity was an indicator of CNV activity during follow-up (RR 1.60, 95% CI 1.38-1.85).

The median BCVA in logMAR at twelve months in the etidronate group was 0.36 (IQR 0.03 – 0.1.38) in the right eye and 0.67 (0.10 – 1.47) in the left eye. In both eyes, the BCVA was not significantly different from the placebo group (0.63 (IQR 0.11 – 1.20) in the right eye and 0.74 (IQR 0.13 – 1.28) in the left eye (P = 0.906 and P = 0.977, respectively (Mann-Whitney U test). In unadjusted linear regression analysis, etidronate was not associated with a change in BCVA (β -0.03 (95% CI -0.09 -0.03) in the right eye, β -0.01 (95% CI -0.04-0.05) in the left eye).

Discussion

We found no protecting or deteriorating effect of the bisphosphonate etidronate on the activity of CNV in patients with PXE after adjustment for baseline CNV activity in this randomized, placebo-controlled, double-blind trial.

This post-hoc study provides additional evidence regarding the effect of bisphosphonates on CNV in a monogenetic disorder. So far, study results regarding the effect of bisphosphonates on CNV were conflicting. In a large observational study, the use of the bisphosphonates alendronate, ibandronate and risedronate was associated with an increased risk of neovascular AMD.[11] However, due to the non-randomized design and the disproportionality analysis this study was not able to correct for confounding due to age-related comorbidities. Also, change in CNV activity was not assessed in relation to the registered drug use. Another prospective non-randomized trial in 40 eyes with CNV due to AMD or myopia found a beneficial effect of alendronate on the lesion size and visual acuity after six months.[8] However, this study was uncontrolled and prone to selection bias, since patients were recruited who declined anti-VEGF treatment and may have had less severe CNV. Another study retrospectively observed eyes with myopic CNV, among which 15 eyes included in the previous study.[8,9] Patients treated with alendronate maintained vision after two years in contrary to the untreated group, and this effect was comparable to the effect of photodynamic monotherapy. The small sample size and risk of selection bias made it difficult to draw a reliable conclusion. The authors suggested that bisphosphonates may have anti-angiogenic properties, next to pro-inflammatory properties.

CNV activity responds to intravitreal anti-VEGF therapy, not only in pathological myopia and AMD, but also in PXE.[18] Therefore, if the bisphosphonate etidronate would have anti-angiogenic properties, this might also be expected to observe in PXE patients. In an *in vitro* study in mice with CNV, alendronate inhibited VEGF gene expression.[10] In contrast, clodronate showed no difference in gene expression *in vitro*.[10] Another study in human RPE cells found that both etidronate and alendronate reduce expression of angiogenic factors, among which basic fibroblast growth factor.[12] In both studies, the observed effect was dose-dependent. Considering the limited evidence regarding anti-angiogenic factors, the potential opposing effect of pro-inflammatory properties, and the null effect in our post-hoc analysis in a randomized double-blind intervention trial, the role of bisphosphonates in retinal angiogenesis seems to be negligible.

In this cohort of PXE patients, the proportion of eyes with CNV activity during a one-year observation period ranged from 18 to 56%. Since this is the first study to report on the occurrence of CNV activity in PXE, it is difficult to compare these percentages to the natural course of the disease. However, we think that actual CNV activity is overestimated in this study. Firstly, participants of this trial were selected based on vascular calcification. Since PXE is a progressive disease, the study cohort represents older PXE patients who suffer more often from CNV than younger patients.[19] Secondly, according to the aforementioned criteria, all intraretinal cysts with signs of a nearby CNV were graded as CNV activity. Especially in end stage disease, intraretinal cysts may represent atrophy rather than active CNV. Since fluorescein angiography was not available at all examinations, this imaging tool was not included in the CNV criteria. We considered our clinical approach to be as objective as possible, since the macular pathology in PXE influenced imaging quality in such a way that volumetric measurements regarding fluid or CNV complex were not possible in a major part of the OCT-scans.

In the main paper of the TEMP trial, we reported a statistically significant lower incidence of subretinal neovascularisation events during the study in the etidronate group compared to the placebo group (1 event versus 9 events, respectively).[7] The difference with the results reported in the present study can be explained by a different outcome definition and method of analysis. In the main paper, the definition of a subretinal neovascular event was based on clinical relevance, necessitating immediate therapeutic intervention with anti-VEGF and all events were reported as SAE's to the Medical Ethics Committee and the Data Safety and Monitoring Board. To assess the subretinal neovascularization events, we used all available information from medical records regarding CNV activity, with the aim to establish safety since we did not know the possible effects of etidronate on CNV activity. Also, the results presented in the paper of the TEMP trial were based on differences between the etidronate group and the placebo group, unadjusted for baseline CNV activity. In contrast, in the present study, our aim was to investigate all changes in CNV activity blinded for treatment status, based on the SD-OCT imaging and fundus photography throughout the study, and also including subtler changes. We used a mixed model approach to incorporate the multiple study visits and to control for baseline CNV activity, instead of only testing differences between treatment groups. Univariable analysis showed that the use of etidronate was associated with a lower incidence of CNV activity. When correcting for baseline CNV activity in a mixed effects model for repeated measures, this association diminished and was no longer statistically significant. Therefore, we conclude that

baseline CNV activity is an important predictor of both change in CNV activity and of subretinal neovascular events, as defined in the previous report.

The dosage of etidronate used in this trial is different from standard care. Patients received a dose of etidronate which is at least four times higher than dosing for regular osteoporosis treatment. However, since the effect of etidronate appears to be dose-dependent,[12,20] we hypothesize that this high dose would only increase the effect size, if there was any. Thus, given that no effect was found on either worsening or improvement of CNV activity, we assume that a common dosage of bisphosphonates would not change these findings.

We do not know whether the type of bisphosphonates is relevant regarding anti-angiogenic effects. Etidronate belongs to the group of non-aminobisphosphonates, which is less potent in the inhibition of bone resorption and prevention of fractures than the newer aminobisphosphonates, such as alendronate. Etidronate acts predominantly on the mineralization process, while aminobisphosphonates inhibit activity of osteoclasts.[21,22] Another difference between these two groups is that aminobisphosphonates produce more pro-inflammatory cytokines.[23] Both types of bisphosphonates are associated with reduced angiogenesis, but the clinical relevance in ophthalmology is unclear.[9,24,25] Also, it is unclear whether the effect of varying cytokine levels, as influenced by different bisphosphonates, on the activity of CNV is clinically relevant. Therefore, generalization of these findings to aminobisphosphonates is difficult.

However, it is important to realize there is substantial evidence that etidronate can halt systemic calcification.[7,26,27] The inhibition of calcification might be another mechanism, independent of angiogenesis and inflammation, by which etidronate may be beneficial for ophthalmological disease in PXE. To determine the effect of etidronate on BM calcification, further investigation with methods that visualize the calcification process at Bruch's membrane are warranted and require a longer follow-up to show an effect on visual acuity, the area of retinal atrophy and number of anti-VEGF injections.

There are some limitations to be addressed. This study was a post-hoc analysis of a trial that was not powered on CNV activity as an outcome measure. Therefore, the sample size is relatively small and the imaging was not optimized to quantify CNV activity, which likely reduced statistical power. The criteria to grade CNV activity and change in CNV activity in PXE based on OCT have been developed by the authors,

since the macular pathology made it too difficult to apply quantitative measures on imaging. The interobserver consistency of grading the CNV activity and change in activity was not high, which stresses the difficulty of assessing CNV activity in PXE patients. Subtle CNV activity is sometimes difficult to distinguish from natural variation in the amount or size of residual intraretinal cysts or subretinal fluid. We anticipated that the agreement would not be perfect due to complicated assessment of the extensive pathology and we accounted for this by using the major vote. By using the major vote instead of one grader, we have decreased the risk of misclassification bias, which could reduce the power of the associations. Even though the CNV assessment has not been validated yet, the randomized, placebo-controlled design and blinded grading make these assessments comparable between both groups.

Furthermore, the schedule of the anti-VEGF injection treatment was determined by the referring ophthalmologist and was independent of the study visits, thus the time interval between study visits and injections was not standardized. However, the referring ophthalmologists were blinded for treatment status, therefore the time interval from anti-VEGF injection to study visit varies at random. Also, the analysis of the number of anti-VEGF injections during the TEMP-trial showed that the possibility of longer intervals since the visit with their referring ophthalmologist in the placebo group cannot explain the higher number of neovascular events in the placebo group in the TEMP trial.

A limitation of our analysis using repeated measures is that we did not use robust errors variance in our model, which can be considered as a modification of a Poisson regression for binomial data.[28] Therefore, we performed a sensitivity analysis using logistic regression. This showed similar crude and adjusted effects. However, this analysis yielded high odds ratios and was therefore difficult to interpret. Lastly, the generalizability of these findings to patients with CNV secondary to AMD or pathologic myopia is unknown. Perhaps bisphosphonates act through PXE specific pathologic processes, i.e. calcification of Bruch's membrane. This hypothesis has still to be proven. If bisphosphonates have a direct anti-angiogenic effect, it seems plausible that a similar association would be observed in the activity of CNV due to AMD and myopia.

In conclusion, in this randomized, placebo-controlled, double-blind trial, no protecting or deteriorating effect of the bisphosphonate etidronate on CNV activity in patients with PXE was found after adjustment for baseline CNV activity. Based on this high-dosing trial, it seems safe to prescribe bisphosphonates to PXE patients and further research on long-term effects and on Bruch's membrane calcification is warranted.

References

1. Wong TY, Ferreira A, Hughes R, Carter G, Mitchell P. Epidemiology and Disease Burden of Pathologic Myopia and Myopic Choroidal Neovascularization: An Evidence-Based Systematic Review. *Am J Ophthalmol*. 2014;157(1):9-25.e12.
2. Gliem M, De Zaeytijd J, Finger RP, Holz FG, Leroy BP, Issa PC. An update on the ocular phenotype in patients with pseudoxanthoma elasticum. *Front Genet*. 2013;4(APR):14.
3. Colijn JM, Buitendijk GHS, Prokofyeva E, et al. Prevalence of Age-Related Macular Degeneration in Europe: The Past and the Future. *Ophthalmology*. 2017;124(12):1753-1763.
4. Bergen AAB, Plomp AS, Schuurman EJ, et al. Mutations in *ABCC6* cause pseudoxanthoma elasticum. *Nat Genet*. 2000;25(2):228-231.
5. Risseeuw S, Ossewaarde-van Norel J, Klaver CCW, Colijn JM, Imhof SM, van Leeuwen R. Visual Acuity in Pseudoxanthoma Elasticum. *Retina*. 2019;39(8):1580-1587.
6. Jansen RS, Duijst S, Mahakena S, et al. *ABCC6*-mediated ATP secretion by the liver is the main source of the mineralization inhibitor inorganic pyrophosphate in the systemic circulation-brief report. *Arterioscler Thromb Vasc Biol*. 2014;34(9):1985-1989.
7. Kranenburg G, de Jong PA, Bartstra JW, et al. Etidronate for Prevention of Ectopic Mineralization in Patients With Pseudoxanthoma Elasticum. *J Am Coll Cardiol*. 2018;71(10):1117-1126.
8. Honda S, Nagai T, Kondo N, et al. Therapeutic effect of oral bisphosphonates on choroidal neovascularization in the human eye. *J Ophthalmol*. 2010.
9. Miki A, Honda S, Nagai T, Tsukahara Y, Negi A. Effects of oral bisphosphonates on myopic choroidal neovascularisation over 2 years of follow-up: comparison with anti-VEGF therapy and photodynamic therapy. A pilot study. *Br J Ophthalmol*. 2013;97(6):770-774.
10. Nagai T, Imai H, Honda S, Negi A. Antiangiogenic Effects of Bisphosphonates on Laser-Induced Choroidal Neovascularization in Mice. *Investig Opthalmology Vis Sci*. 2007;48(12):5716.
11. Mammo Z, Guo M, Maberley D, Matsubara J, Etminan M. Oral Bisphosphonates and Risk of Wet Age-Related Macular Degeneration. *Am J Ophthalmol*. 2016;168:62-67.
12. Or C, Cui J, Matsubara J, Forooghian F. Pro-inflammatory and anti-angiogenic effects of bisphosphonates on human cultured retinal pigment epithelial cells. *Br J Ophthalmol*. 2013;97(8):1074-1078.
13. Plomp AS, Toonstra J, Bergen AAB, van Dijk MR, de Jong PTVM. Proposal for updating the pseudoxanthoma elasticum classification system and a review of the clinical findings. *Am J Med Genet A*. 2010;152A(4):1049-1058.
14. ETDRS Research Group. No Title. In: *Early Treatment of Diabetic Retinopathy Study (ETDRS) Manual of Operations*. National Technical Information Service; 1985:1-74.
15. Birtel J, Lindner M, Mishra DK, et al. Retinal imaging including OCT angiography for detecting active choroidal neovascularization in pseudoxanthoma elasticum. *Clin Experiment Ophthalmol*. Published online August 31, 2018.
16. Ying G-S, Maguire MG, Glynn R, Rosner B. Tutorial on Biostatistics: Statistical Analysis for Correlated Binary Eye Data. *Ophthalmic Epidemiol*. 2018;25(1):1-12.
17. McHugh ML. Interrater reliability: the kappa statistic. *Biochem medica*. 2012;22(3):276-282.
18. Gliem M, Figuer RP, Fimmers R, Brinkmann CK, Holz FG, Charbel P. Treatment of choroidal neovascularization due to angioid streaks. A Comprehensive Review. *Retina*. 2013;33(7):1300-1314.
19. Gliem M, Muller PL, Birtel J, Hendig D, Holz FG, Charbel Issa P. Frequency, Phenotypic Characteristics and Progression of Atrophy Associated With a Diseased Bruch's Membrane in Pseudoxanthoma Elasticum. *Invest Ophthalmol Vis Sci*. 2016;57(7):3323-3330.
20. Li Q, Sundberg JP, Levine MA, Terry SF, Uitto J. The effects of bisphosphonates on ectopic soft tissue mineralization caused by mutations in the *ABCC6* gene. *Cell Cycle*. 2015;14(7):1082-1089.

21. Drake MT, Clarke BL, Khosla S. Bisphosphonates: mechanism of action and role in clinical practice. *Mayo Clin Proc*. 2008;83(9):1032-1045.
22. Uitto J, Li Q. Vascular Mineralization in Pseudoxanthoma Elasticum: Etidronate to the Rescue? *J Am Coll Cardiol*. 2018;71(10):1127-1129.
23. Thompson K, Roelofs AJ, Jauhiainen M, Mönkkönen H, Mönkkönen J, Rogers MJ. Activation of γδ T Cells by Bisphosphonates. In: *Advances in Experimental Medicine and Biology*. Vol 658. ; 2009:11-20.
24. Yamamoto K, Yoshino S, Shue G, Nagashima M. Inhibitory effect of bone resorption and inflammation with etidronate therapy in patients with rheumatoid arthritis for 3 years and in vitro assay in arthritis models. *Rheumatol Int*. 2006;26(7):627-632.
25. Ishtiaq S, Edwards S, Sankaralingam A, et al. The effect of nitrogen containing bisphosphonates, zoledronate and alendronate, on the production of pro-angiogenic factors by osteoblastic cells. *Cytokine*. 2015;71(2):154-160.
26. Kranenburg G, Bartstra JW, Weijmans M, et al. Bisphosphonates for cardiovascular risk reduction: A systematic review and meta-analysis. *Atherosclerosis*. 2016;252:106-115.
27. Bartstra JW, de Jong PA, Kranenburg G, et al. Etidronate halts systemic arterial calcification in pseudoxanthoma elasticum. *Atherosclerosis*. 2020;292(September 2019):37-41.
28. Zou G. A Modified Poisson Regression Approach to Prospective Studies with Binary Data. *Am J Epidemiol*. 2004;159(7):702-706.

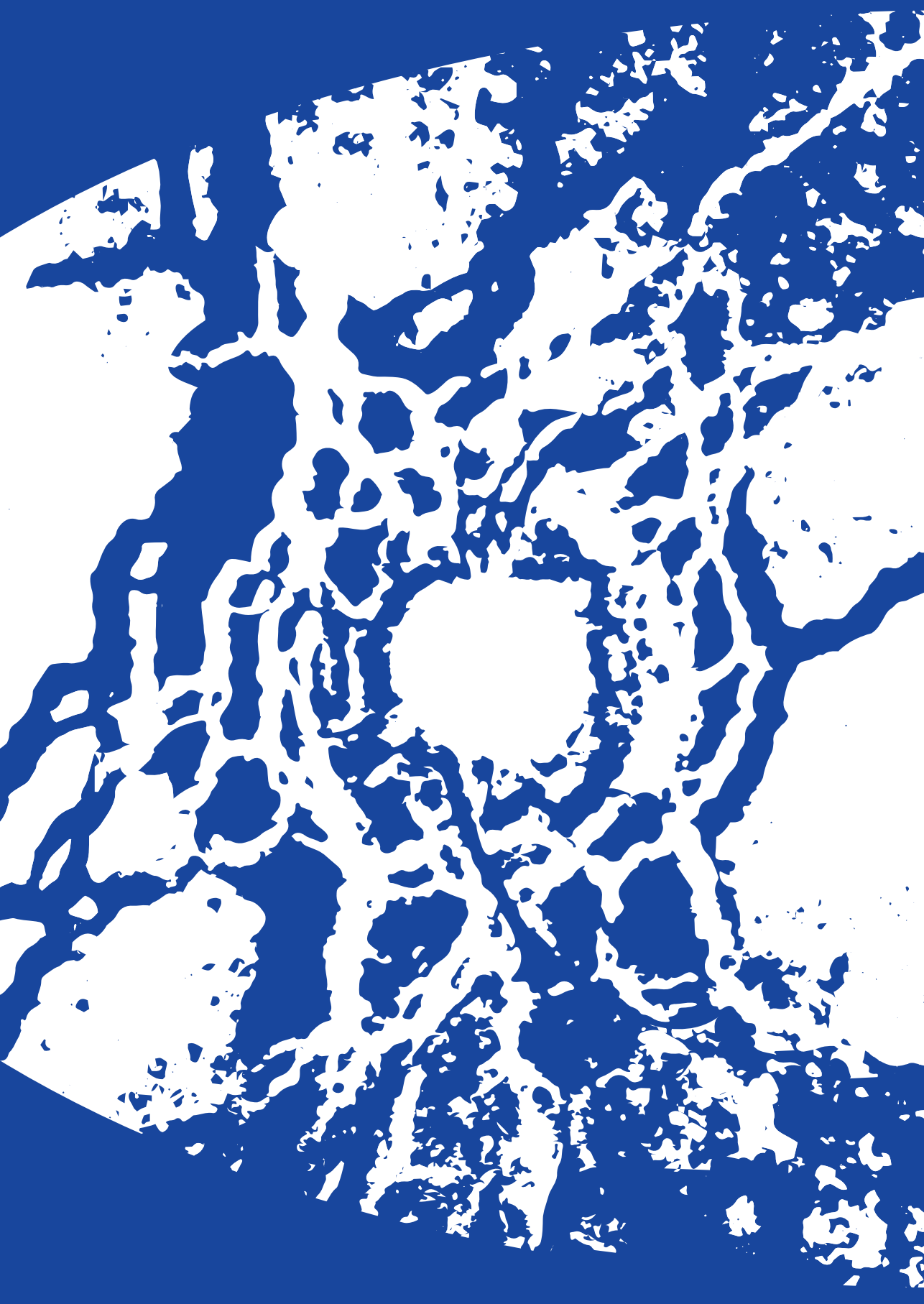


PART THREE

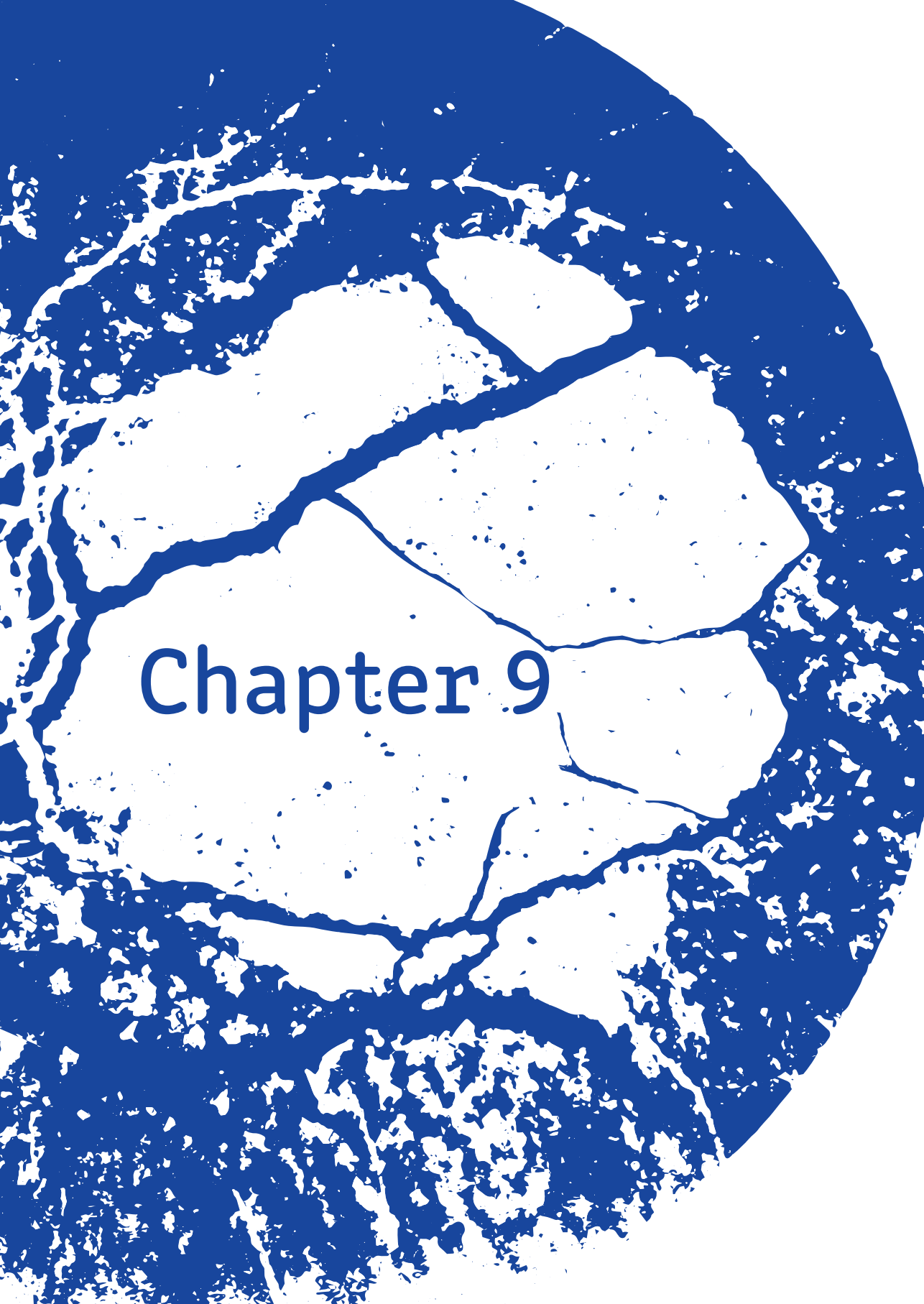
Chapter 9

A reflectivity measure to quantify Bruch's membrane calcification in patients with pseudoxanthoma elasticum using optical coherence tomography

Sara Risseeuw
Edwin Bennink
Maarten G. Poirot
Pim A. de Jong
Wilko Spiering
Saskia M. Imhof
Redmer van Leeuwen
Jeannette Ossewaarde – van Norel

Translational Vision Science & Technology, 2020;9(8):34.

Abstract

Purpose

Progressive calcification of Bruch's membrane (BM) causes considerable visual morbidity in patients with pseudoxanthoma elasticum (PXE). Since calcification is hyperreflective on optical coherence tomography (OCT), our aim was to measure BM calcification with OCT imaging.

Methods

Case-control study with 45 patients with PXE under 40 years (range 11-39) and 25 controls (range 14-39). Spectralis HRA-OCT imaging consisted of seven macular B-scans with 250µm spacing. Retinal segmentation was performed with the IOWA Reference Algorithms. MATLAB was used to extract and average z-axis reflectivity profiles. Layer reflectivities were normalized to the ganglion cell and inner plexiform layers. Both median and peak layer reflectivities were compared between patients with PXE and controls. The discriminative value of the retinal pigment epithelium (RPE)-BM peak reflectivity was analyzed using receiver operating characteristic analysis.

Results

The reflectivity profile of patients with PXE differed from controls in the outer retinal layers. The normalized median RPE-BM reflectivity was 41.1 (interquartile range [IQR] 26.3-51.9) in patients with PXE, compared with 22.5 (IQR, 19.3-29.5) in controls (P=2.09×10-3). The normalized RPE-BM peak reflectivity was higher in patients with PXE (67.5; IQR, 42.1-84.2) than in controls (32.7; IQR, 25.7-38.9; $P = 2.43\times10^{-5}$) and had a high discriminative value with an area under the curve of 0.85 (95% confidence interval, 0.76-0.95). In patients with PXE under 40 years, increasing age did not have a statistically significant effect on the RPE-BM peak reflectivity (patients under 20 years: 44.2

[IQR, 40.5–74.6], 20-30 years: 66.0 [IQR, 45.1–83.8], 30-40 years: 70.8 [IQR, 49.0-88.0], *P* = 0.47).

Conclusions

BM calcification can be measured as increased RPE-BM reflectivity in young patients with PXE and has a high discriminative value.

Translational relevance

In patients with PXE, the OCT reflectivity of Bruch's membrane may be the first biomarker for Bruch's membrane calcification and a valuable ophthalmological end-point in clinical trials.

Introduction

In patients with pseudoxanthoma elasticum (PXE), a rare disease with an estimated prevalence of at least 1:56000, biallelic mutations of the *ABCC6* gene lead to ectopic mineralization in the vasculature, skin and eyes.[1,2] Progressive calcification of Bruch's membrane (BM) initially presents as peau d'orange and typically causes formation of angioid streaks.[3] Eventually, this leads to significant visual morbidity at a relatively young age, due to choroidal neovascularization (CNV) and macular atrophy.[4] Similar to geographic atrophy in age-related macular degeneration (AMD), macular atrophy in PXE cannot be treated yet. A recent study has shown a beneficial effect of the bisphosphonate etidronate on vascular calcification.[5] In order to investigate the effect of etidronate and future potential treatments on retinal calcification, a reliable endpoint is warranted.

An increased reflectivity at the level of BM was observed on spectral domain optical coherence tomography (SD-OCT) in patients with PXE.[3,6,7] SD-OCT provides information on morphologic and reflective properties of tissues, which can be affected by increasing age or retinal disease.[8] The thickness of BM ranges from 2 to 5 μm,[9] which is comparable with the axial resolution of SD-OCT. Therefore, on SD-OCT, the BM cannot be distinguished from the above lying retinal pigment epithelium (RPE), and together these layers form the hyperreflective RPE-BM complex. It is plausible that the increased reflectivity of the RPE-BM complex on SD-OCT represents the calcification process in BM in patients with PXE. Therefore, the RPE-BM reflectivity may serve as a biomarker for the severity of PXE in the eye. However, commercial SD-OCT imaging is not developed to measure absolute reflectivity, and the measured reflectivity values are processed to create high-contrast images.[10] Also, patients with PXE frequently develop structural abnormalities such as CNV with increasing age, which may have different reflective properties than the cell layers of a healthy retina. Possibly, this causes attenuation of the OCT signal and thereby it might alter the reflectivity values of underlying retinal layers including the RPE-BM complex.[11]

We hypothesize that the reflectivity of BM may serve as a biomarker for retinal calcification in PXE. Our aim is to test this hypothesis by comparing the RPE-BM reflectivity on SD-OCT in young patients with PXE at an early disease stage with healthy controls.

Methods

Study design and population

This retrospective, observational case-control study was conducted at the University Medical Center Utrecht, The Netherlands, where the Dutch National Expertise Center for PXE is situated. The study adhered to the Declaration of Helsinki and its further amendments and the study protocol was approved by the Institutional Ethics Committee (METC 19/257). We included patients with PXE aged under 40 years at the time of OCT measurement and who had a definitive diagnosis of PXE according to the Plomp criteria.[12] In total, 52 patients with PXE (104 eyes) were included. Our aim was to quantify the increased reflectivity due to calcification at the level of BM. Since the absolute reflectivity may be affected by acquisition parameters, quantification of reflectivity values requires normalization to other retinal layers.[8] The other retinal layers need to be intact and unaffected to ensure that the measured effect solely derives from BM calcification and is not due to differences in the optical properties of the other retinal layers. Therefore, for the purpose of this study we first excluded all eyes with a best-corrected visual acuity below 0.9 decimals and subsequently all eyes with structural retinal pathology on SD-OCT to minimize a potential effect of a diseased retina on OCT reflectivity values.

Per eye, retinal imaging consisted of central and midperipheral color fundus photography (FF 450 plus; Carl Zeiss Meditec AG, Jena, Germany), 55° fundus autofluorescence, 55° near-infrared reflectance imaging (central and midperipheral) and macular SD-OCT (both Spectralis HRA-OCT; Heidelberg Engineering, Heidelberg, Germany). The images were systematically assessed by an experienced grader (SR) and graded as (1) only peau d'orange, (2) presence of angioid streaks, (3) CNV or fibrotic scarring, (4) macular atrophy, and (5) abnormalities on fundus autofluorescence or other abnormalities. Of these categories, eyes with only peau d'orange or presence of angioid streaks were included, since these abnormalities are inherent to BM calcification in patients with PXE and represent an early disease stage. The control group consisted of 25 age-matched controls (44 eyes) with no ophthalmic abnormalities or myopia of more than –6 diopter and did not have any systemic diseases. In six controls, imaging was performed in only one eye.

Image acquisition

SD-OCT imaging (Spectralis HRA-OCT; Heidelberg Engineering) consisted of two OCT volumes covering the central macular area. These volumes each covered an area of 20 × 5 degrees (approximately 6 × 1.5 mm) with a distance of ~250 µm between seven B-scans. The OCT image size was 1024 × 7 × 496 voxels and transverse and axial resolution was approximately 6 µm and 4 µm, respectively. The automatic real-time tracking was set to 25 frames per B-scan. The images were exported to DICOM format for analysis.

Image segmentation

Automated segmentation of 11 different retinal surfaces was performed using the Iowa Reference Algorithm (Retinal Image Analysis Lab, Iowa Institute for Biomedical Imaging, Iowa City, IA).[13–15] This resulted in 10 different retinal layer volumes. The following layer volumes were obtained: retinal nerve fiber layer (RNFL), ganglion cell layer (GCL), inner plexiform layer (IPL), inner nuclear layer (INL), outer plexiform layer, outer nuclear layer (ONL), inner photoreceptor segments (IS), outer photoreceptor segment (OS), photoreceptor outer segment (OPR) and the RPE combined with BM (see Supplementary Figure S9.1). All B-scans were visually inspected for both integrity of the outer retinal layer and BM, as well as for correct segmentation of all retinal layers. If a part of the B-scan did not match these criteria, corresponding A-scans were excluded from further analysis. This was done by using the 'Undefined Regions' tool of the Iowa Reference Algorithm (example in Supplementary Figure 1). To prevent observer bias, incorrect segmentation was left unadjusted and excluded. The remainder of the total of 1024 A-scans per B-scan was used for further analysis. Coordinates of the surfaces and data on the included A-scans were saved as .xml files.

Image processing

The OCT reflectivity and segmentation data were imported in MATLAB (version 9.1.0; the MathWorks, Inc., Natick, MA, USA) using in-house built software. The exported images had an 8-bit precision and the reflectivity values were transformed by the manufacturer to enhance visual contrast in areas with low reflectivity. This process was inversed to restore the original reflectivity values; the calibration curve is shown in Supplementary Figure S9.2. The retinal layer surface segmentations provide an estimate for the layer thickness in each A-scan. Linear interpolation was used to stretch the A-scan profiles, for each layer, to the same standardized length of twice the maximum layer thickness within the B-scan (see Supplementary Figure S9.1B). For each included A-scan, we computed z-axis reflectivity profiles as a vector of 650

x-values. To calculate the median intensity profile for each layer, we first extracted the layer-specific reflectivity profiles from the stretched A-scans. Then, we calculated the median reflectivity profile by taking the median of all pixels at the same depth weighed to the original thickness of that A-scan. This was done in order to correct for local differences in layer thicknesses that might introduce measurement errors, such as the local thinning of the GCL in the foveal area. The median B-scan specific reflectivity was stored per row, resulting in 650 values per B-scan.

Image analysis

We visualized the plotted reflectivity profiles using in-house built software. For this, the profiles were first averaged per OCT volume and then per patient. The reflectivity was normalized to the mean reflectivity of the GCL-IPL layer, unless otherwise stated. This layer is relatively far from the diseased outer retina and has a reasonable thickness. To enhance the contrast in areas with low reflectivity, the plots were rescaled to the fourth root of the normalized values.

We adhered to the nomenclature for outer retinal bands as proposed by Spaide and Curcio.[16] Therefore, we averaged the reflectivity of the IS and OS layers, which together form the ellipsoid zone (EZ) on the reflectivity profile. We used the layer-specific median and peak intensities for further analysis.

Subgroup analysis

We excluded the A-scans with visible segmentation errors, but it is plausible that small errors remained. We used a subset of four patients with PXE and four controls to test the effect of small remaining errors in the segmentation algorithm. Of each person, we manually adjusted the segmentation in all seven B-scans in both the horizontal and vertical OCT scans and compared the reflectivity values and layer thickness to the original, unadjusted segmentation.

We tested the reproducibility of the reflectivity measurements in a subset of eight patients with PXE (30 OCT volumes) and four controls (16 OCT volumes). Repeated OCT scans were performed within a maximum of 6 months. We do not assume a significant progression of BM calcification within this time span. Eye-tracking technology was used to ensure that the exact same location was used for the follow-up scan. We extracted acquisition parameters such as scan focus, sensitivity, and image quality from the Heidelberg Eye Explorer to investigate their influence on agreement between repeated measures, as well as a visual inspection of the OCT scans (on motion artefacts or possible other disturbing phenomena).

Furthermore, we hypothesized that retinal vessels with shadowing artifacts might bias the measured RPE-BM reflectivity. These artifacts are caused by the retinal blood vessels in the GCL-IPL layers attenuating the signal. In A-scans with retinal blood vessels, this leads to a higher reflectivity in the GCL-IPL layer and a lower reflectivity in the RPE-BM layer. This effect is enlarged when the reflectivity is normalized. To investigate the size of this possible effect, we used the before mentioned subset of eight patients with PXE and four controls in whom we repeated the image segmentation using the IOWA Reference Algorithm. Using the "Undefined Regions" tool, we excluded all A-scans with visible retinal vessels with shadowing artifacts, besides the before mentioned exclusion criteria.

Data analysis

All values are presented as numbers with percentage (%), mean with standard deviation (± SD), or as median with interquartile range (IQR). Distribution of values was tested with the Shapiro-Wilk test. Differences between groups were tested with Student's t-test, chi-square test, Mann-Whitney U test, or Kruskal-Wallis test when appropriate. Differences in the subgroup analyses were tested with paired t-test or Wilcoxon signed-rank test, when appropriate. To control for multiple testing, the *P* values of layer-specific analyses were adjusted according to Benjamini and Hochberg.[17]

Receiver operating characteristic (ROC) analysis was used to test discriminative performance of the RPE-BM reflectivity values, from which the area under the ROC curve (AUC) was calculated. The discriminative performances of the ROC curves were compared with the method as proposed by DeLong et al.[18] Spearman correlation analysis was used for correlation analysis. To investigate the correlation of reflectivity values between scans, we compared the left and right eyes for within-patient correlation and the horizontal and vertical OCT scan within the same eye for within-eye correlation. We visualized the agreement of the reflectivity between the repeated measurements in a plot proposed by Bland and Altman[19] and calculated the 95% limits of agreement.

Statistical analysis of the data was performed with R (version 3.4.1). The packages 'pROC' (version 1.13.0) and 'BlandAltmanLeh' (version 0.3.1) were used for ROC analysis and agreement analysis, respectively.[20]

Results

Of all 52 patients with PXE under 40 years (104 eyes), 11 eyes had retinal pathology, and an additional 18 eyes had a best-corrected visual acuity lower than 0.9 and were thus excluded from analysis. This resulted in OCT data of 75 eyes of 45 patients with PXE with a mean age of 27 years (range 11 – 39 years) and 44 eyes of 25 normal controls with a mean age of 27 years (range 14 – 39 years) (Table 9.1). The mean age was similar between the groups. Most patients with PXE were female (87%), compared with 56% females among controls (P = 0.01). The thickness of the reference layer was similar between patients with PXE and controls: the mean GCL-IPL thickness was 78 ± 4 µm in patients with PXE, compared with 77 ± 5 µm in controls (P = 0.14). In patients with PXE, the retina was 7 µm thinner than in controls, with statistically significant differences in the RNFL, INL, EZ and RPE-BM layers. Layer specific thicknesses are presented in Supplementary Table S9.1.

Reflectivity characteristics

The mean reflectivity profiles show differences in reflective bands of the retinal layers between PXE and controls (Figure 9.1). The RPE-BM peak appears to be higher in patients with PXE. When quantified, the RPE-BM peak reflectivity was twice as high in patients with PXE (67.5; IQR, 42.1 – 84.2) as in controls (32.7; IQR, 25.7 – 38.9, adjusted $P = 2.43 \times 10^{-5}$). Consequently, the median reflectivity of the RPE-BM layer was higher in patients with PXE than in controls: 41.1 (IQR, 26.3 – 51.9) compared with 22.5 (IQR, 19.3 – 29.5; adjusted $P = 2.09 \times 10^{-3}$). The RPE-BM peak reflectivity performed best in distinguishing patients with PXE and controls with an AUC of 0.85 (95% CI, 0.76 – 0.95), compared to the RPE-BM median reflectivity with an AUC of 0.77 (95% CI, 0.66 – 0.88) ($P = 8.16 \times 10^{-5}$). The ROC curves are visualized in Figure 9.2. Furthermore, the median reflectivity of the photoreceptors of patients with PXE is lower than that of controls with nominal statistical significance but not when adjusted for multiple testing (Table 9.1).

Effect of age

The RPE-BM peak reflectivity increased with age in patients with PXE but not in controls (Figure 9.3). The RPE-BM peak reflectivity was 44.2 (IQR, 40.5 – 74.6) in patients with PXE under 20 years (n=7), compared with 66.0 (IQR, 45.0 – 83.8) in patients aged 20 to 30 years (n= 22), and 70.8 (IQR, 49.0 – 88.0) in patients with PXE aged 30 to 40 years (n= 16). However, these differences were not statistically significant (P = 0.48). Median layer reflectivity also did not show statistically significant differences with increasing age. Detailed information can be found in supplementary Table S9.2.

Table 9.1 Patient characteristics and layer reflectivity

	PXE	Control	Nominal *P*	Adjusted *P**
	n = 45	n = 25		
Patient data				
Age (years)	27 ± 7	27 ± 6	0.96	
Gender (male)	6 (13%)	11 (44%)	0.01	
Proportion of A-scans	93% [92%, 96%]	95% [94%, 96%]	0.02	
Scan quality (dB)	35.2 ± 3.2	34.8 ± 2.6	0.64	
Median layer reflectivity				
Retinal nerve fiber layer	2.2 [2.0, 2.7]	2.3 [2.0, 2.6]	0.93	0.96
Ganglion cell layer	0.71 [0.67, 0.75]	0.69 [0.67, 0.73]	0.18	0.34
Inner plexiform layer	0.78 [0.73, 0.83]	0.79 [0.76, 0.82]	0.16	0.31
Inner nuclear layer	0.37 [0.32, 0.39]	0.36 [0.35, 0.40]	0.54	0.67
Outer plexiform layer	0.66 [0.56, 0.75]	0.69 [0.65, 0.78]	0.22	0.38
Outer nuclear layer	0.23 [0.19, 0.27]	0.24 [0.22, 0.28]	0.06	0.17
Ellipsoid zone	14.0 [8.3, 20.0]	17.2 [14.0, 27.0]	0.02	0.10
Outer photoreceptor segments	14.5 [9.1, 23.3]	21.7 [16.1, 29.7]	0.02	0.10
RPE and Bruch's membrane	41.1 [26.3, 51.9]	22.5 [19.3, 29.5]	1.90×10^{-4}	2.09×10^{-3}
Peak layer reflectivity				
Retinal nerve fiber layer	5.2 [4.3, 6.1]	4.7 [4.3, 6.5]	0.75	0.83
Ganglion cell layer	3.2 [2.9, 3.5]	3.1 [2.9, 3.4]	0.54	0.67
Inner plexiform layer	0.99 [0.92, 1.06]	0.99 [0.97, 1.05]	0.52	0.67
Inner nuclear layer	0.85 [0.76, 0.90]	0.82 [0.79, 0.92]	0.55	0.67
Outer plexiform layer	0.94 [0.78, 1.09]	0.97 [0.89, 1.08]	0.31	0.48
Outer nuclear layer	0.71 [0.61, 0.84]	0.77 [0.69, 0.96]	0.07	0.17
Ellipsoid zone	35.6 [24.4, 57.5]	40.6 [34.7, 59.4]	0.12	0.25
Outer photoreceptor segments	27.4 [17.5, 43.1]	38.2 [27.4, 56.3]	0.03	0.11
RPE and Bruch's membrane	67.5 [42.1, 84.2]	32.7 [25.7, 38.9]	1.10×10^{-6}	2.43×10^{-5}

Abbreviations: PXE; pseudoxanthoma elasticum, RPE; retinal pigment epithelium.
All reflectivity values are normalized to the GCL-IPL layer.
* *P*-values were adjusted according to the method as proposed by Benjamini and Hochmann.

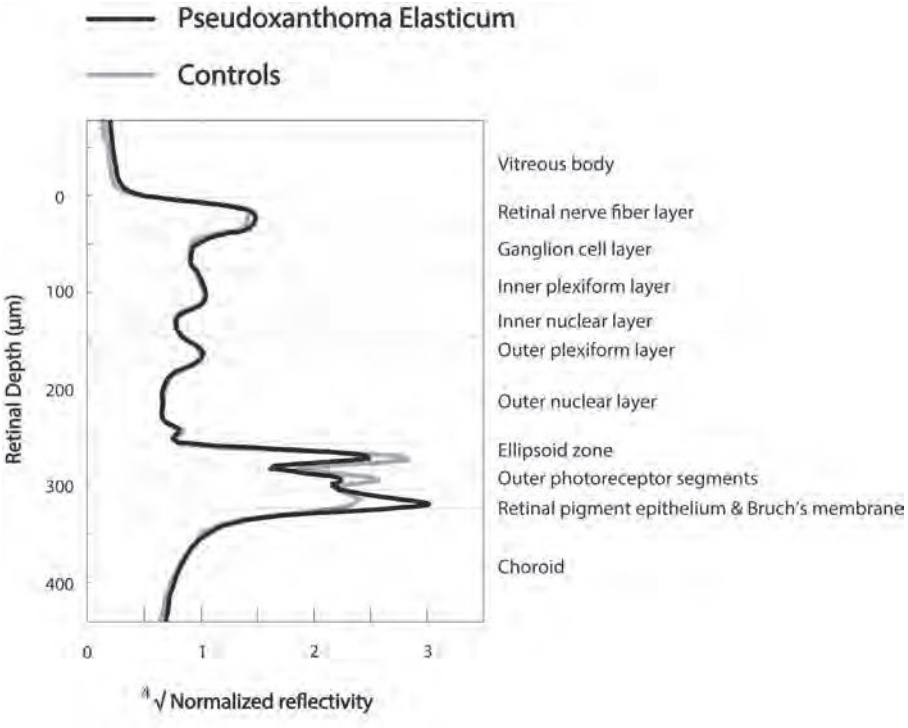

Figure 9.1 Averaged reflectivity profiles of patients with pseudoxanthoma elasticum (PXE) (n=45) and controls (n=25). The normalized reflectivity is plotted against the retinal depth. On the right side, the corresponding retinal layers are noted. The GCL-IPL layer was used as the reference layer for normalization. The fourth root of the normalized reflectivity was used for better visualization.

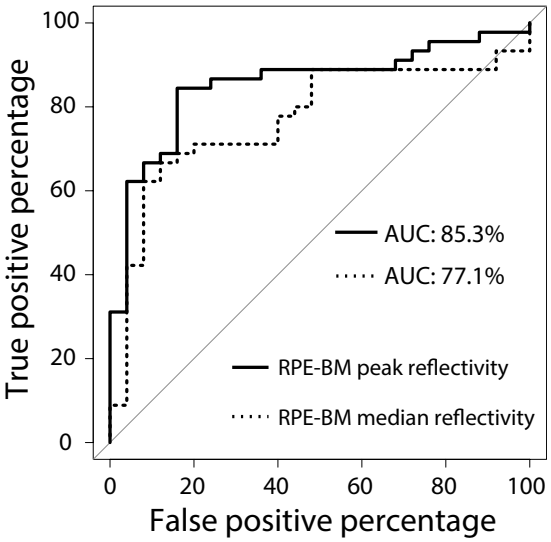

Figure 9.2 Reciever Operating Characteristic curve of the RPE-BM peak reflectivity and RPE-BM median reflectivity (normalized to the GCL-IPL layer). Reflectivity values were averaged per person.

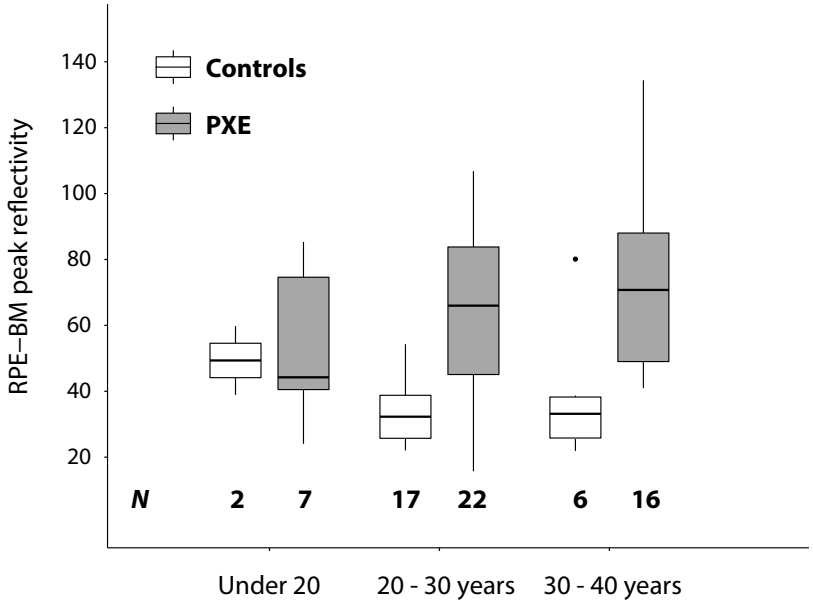

Figure 9.3 RPE-BM peak reflectivity of patients with pseudoxanthoma elasticum (PXE) and controls, plotted by their age category. The RPE-BM reflectivity is normalized to the GCL-IPL layer. The horizontal bars represent the median value, and the boxes represent the interquartile range. Per person, the reflectivity values were averaged. The number of patients per category are listed in the bottom of the figure.

Within-eye and within-patient correlation

In patients with PXE, the RPE-BM peak reflectivity had a strong correlation between horizontal and vertical B-scans within the same eye (P = 0.80; adjusted $P < 2.2\times10^{-16}$; Figure 9.4). For controls, this within-eye correlation was moderate (P = 0.56; adjusted $P = 1.03\times10^{-3}$). The within-patient correlation of the RPE-BM peak reflectivity between both eyes was moderate for patients with PXE and strong for controls (P = 0.42; adjusted P = 0.03 and ρ = 0.71; adjusted P = 0.01, respectively, Figure 9.4).

The within-eye correlation for the median RPE-BM reflectivity was strong for patients with PXE (Spearman's ρ = 0.77; adjusted $P < 2.2\times10^{-16}$) and for controls (ρ = 0.65; adjusted $P = 1.06\times10^{-5}$). The within-patient correlation for the median RPE-BM reflectivity was moderate for patients with PXE (P = 0.43; adjusted P = 0.03) and strong for controls (P = 0.68; adjusted P = 0.01). Further details on within-eye and within-patient correlations of median layer reflectivity can be found in Supplementary Table S9.3.

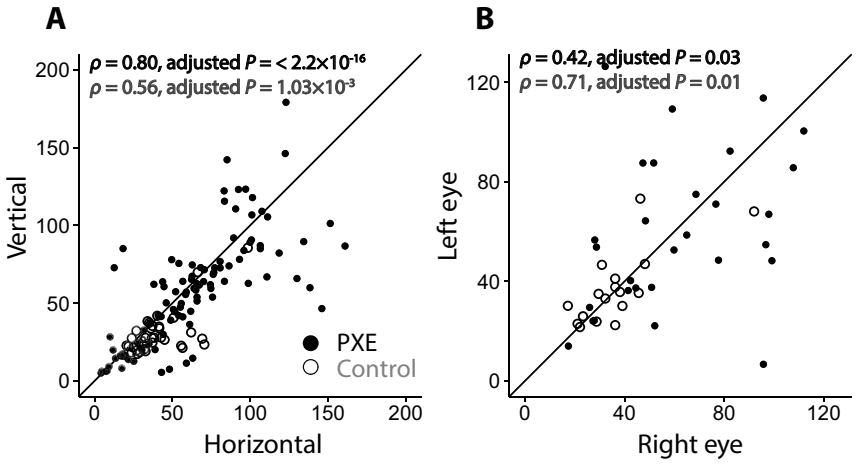

Figure 9.4 Within-eye (A) and within-subject (B) correlation of RPE-BM peak reflectivity of patients with pseudoxanthoma elasticum (PXE) and controls. Within-eye correlation is measured with horizontally- and vertically orientated OCT scans. For within-eye correlation, there were 101 comparisons for patients with PXE and 36 comparisons for controls. For within-subject correlation, there were 29 pairs of observation in patients with PXE and 19 pairs of observation in controls. The diagonal line represents the perfect correlation. In the top left corner the Spearman correlation coefficients (ρ) are shown for patients with PXE (black) and controls (grey).

Manual correction of segmentation

Manually adjusting all small segmentation errors in a subset of four patients with PXE (four eyes) and four controls (four eyes) did not result in statistically significant changes in the retinal layer thickness or in the GCL-IPL reflectivity (serving as the reference layer for normalization) or RPE-BM peak reflectivity (Supplementary Table S9.4). The correlation between RPE-BM peak reflectivity with and without adjusted segmentation for all OCT scans is visualized in Supplementary Figure S9.3. In this subset, the absolute difference of the RPE-BM peak reflectivity between PXE and controls becomes slightly larger: the absolute difference is 54 (95% CI, 22 – 80) for the unadjusted OCT scans, while this is 61 (95% CI, 27 – 84) for the adjusted OCT scans.

Reproducibility

We tested the reproducibility of the RPE-BM peak reflectivity in a subset of eight patients with PXE (15 eyes) and four controls (8 eyes). The agreement for the RPE-BM peak reflectivity, averaged per eye, is visualized in the Bland-Altman plot (Supplementary Figure S9.4). The mean absolute difference between the first and second measurements was 13.7 for patients with PXE and – 1.8 for controls. The 95% limits of agreement were – 53.0 and 79.5 for patients with PXE and – 34.2 and 30.5 for controls. In this subset, the acquisition parameters scan focus, sensitivity, and image quality were not associated with the GCL-IPL reflectivity, which was used for normalization, nor with the reproducibility.

Shadowing artifacts

Excluding all A-scans with retinal blood vessels and shadowing artefacts on the B-scan from analysis resulted in a statistically significant lower proportion of included A-scans: 83.3% ± 5.8% A-scans per B-scan while excluding retinal blood vessels, versus 93.7% ± 5.7% in normal segmentation ($P < 2.2\times10^{-16}$). The RPE-BM peak reflectivity was slightly higher if retinal blood vessels were excluded: the median difference in patients with PXE was 1.20 (95% CI, 0.8 – 1.6; $P = 1.65\times10^{-6}$) and 0.8 (95% CI, 0.6 – 1.2; $P = 4.21\times10^{-7}$) in controls. The absolute difference in RPE-BM peak reflectivity patients with PXE and controls remained the same: 48.0 (95% CI, 38.3 – 61.1) if A-scans with retinal blood vessels were excluded versus 47.5 (95% CI, 37.9 – 61.1) with normal segmentation.

Discussion

To our knowledge, this is the first study on the reflectivity characteristics of SD-OCT in patients with PXE. We found that the reflectivity profiles of relatively young patients with PXE are different from controls and that the RPE-BM peak reflectivity performs well in discriminating patients with PXE from controls.

Our findings confirm previous observations of OCT imaging in PXE, which describe increased reflectivity at the level of the RPE-BM complex.[3,6,21,22] This finding is also compatible with the histopathologic evidence of calcification in BM.[23] The increased reflective properties of the calcified BM cause the hyperreflectivity of the RPE-BM complex on SD-OCT, which appears to correlate with its bright reflex on near-infrared imaging.[7] Besides near-infrared imaging, late-phase indocyanine green angiography also visualizes the pattern of BM calcification.[24,25] However, quantification methods for these retinal imaging techniques are not available yet. The distance between the temporal border of the optic disc and the central border of peau d'orange has been used as a proxy for the extent of calcification.[26] The eccentricity of the border of the peau d'orange may provide relevant information regarding the progression of the extent of BM calcification, but it is unclear whether this parameter also represents severity of retinal calcification.[26] A recent study showed reduced quantitative autofluorescence in PXE, which suggests reduced lipofuscin levels within the RPE.[27] These levels were associated with the extent of calcification, implicating that BM calcification in PXE affects the vitality of the outer retina.

In this study, we investigated the use of SD-OCT reflectivity values, normalized to the GCL-IPL reference layer, as a quantifiable biomarker for PXE. Quantification of reflectivity values is hardly used, in contrast to quantification of layer thickness, because interpretation of reflectivity values is less straightforward. Since the reflectivity values are influenced by multiple factors such as media opacities and signal-to-noise ratio and SD-OCT imaging is not calibrated, absolute reflectivity values are not considered a reliable metric.[8] Approaches to obtain reliable reflectivity data include normalization to image quality or signal strength, to a reference layer, or by using an attenuation coefficient.[11,28] The RNFL or RPE has been suggested as the best reference layer, since these layers show the highest reflectivity values.[29] On the other hand, the ONL which shows the lowest reflectivity values in the retina, has been proposed because of the best correlation with image quality.[8] For the purpose of our study, both candidates are not ideal; the macular RNFL is rather thin, and normalizing the high RPE-BM

reflectivity to the low ONL reflectivity could result in a biomarker that is extremely sensitive to measurement errors in the reference layer having a low signal-to-noise ratio.[8] Moreover, the ONL represents the nuclear bodies of the photoreceptor cells, which theoretically will suffer first from a diseased RPE-BM complex in PXE. The GCL-IPL layer is, besides the RNFL, furthest away from the outer retina, and the thickness and reflectivity values of the GCL-IPL layer allow for easy segmentation. Only in the foveal area does the GCL-IPL layer almost diminish, which likely causes noise in the reference layer reflectivity. Therefore, we selected the GCL-IPL layer as a reference layer corrected for the foveal thinning by weighing the reflectivity profiles to the layer thickness, to normalize the reflectivity values.

We observed a large variability in normalized reflectivity values, both between patients and within patients. The high variability between patients might partly be explained by age and the severity of the disease. However, this does not explain the variability within patients and thus the low reproducibility. It is in line with a study that found that reflectivity values may vary up to 29% due to sensitivity fall-off (decreasing sensitivity with increasing retinal depth) and patient-induced motions, such as a heartbeat, that cause axial shift.[30] Also, a change in the angle of the infrared light beam attributes to the variability of measured reflectivity.[31] Therefore, it is complicated to obtain a reproducible measure of OCT reflectivity, which is often prone to substantial intrapatient variation.[32] Unfortunately, our dataset with repeated measures was rather small and lacked statistical power to investigate the reproducibility more in depth. Future research should therefore focus on gaining insight into and improving reproducibility. Progress in OCT technology, such as the introduction of the Spectralis OCT2, providing faster imaging with a higher signal-to-noise ratio, is expected to be beneficial for improving the reproducibility.[33] Also, another approach for normalizing the reflectivity may be worth investigating. The approach proposed by Vermeer et al.[34] could be valuable, since it does not rely on a reference layer but uses a pixel-specific attenuation coefficient to characterize the retinal tissue. Even though we cannot use the RPE-BM reflectivity as an individual biomarker yet, the RPE-BM reflectivity is a reliable parameter to compare groups with a random measurement error.

We could not demonstrate a statistically significant effect of age on the RPE-BM peak reflectivity. It is known that BM calcification in PXE increases with age and is hypothesized to spread centrifugally.[25] Gliem et al. [27] recently found that the extent of calcification increases with age but has a large between-patient variability. Interestingly, our data also suggest a possible trend of increasing RPE-BM peak reflectivity with increasing

age. However, we should take into account that we only measured patients aged under 40 years, and thus the reflectivity throughout life is still unknown. Moreover, it is plausible that the large variability between patients and the relatively small sample size impede reaching statistical significance. Also, it is likely that the excluded patients with PXE with CNV or macular atrophy had more severe BM calcification than patients with PXE of the same age without these complications. It would therefore be interesting to study the hypothesis that the RPE-BM peak reflectivity in PXE increases with age by including older and more severe patients with PXE or by increasing the study population. However, even though our findings provide convincing evidence that we can detect BM calcification in PXE already at a young age and may suggest that the BM calcification progresses with age, the characteristics of the RPE-BM peak reflectivity need to be validated in an external cohort of patients with PXE. Also, there was a substantial and at this moment unexplained variability between patients, which is known from other measures in patients with PXE.[27] Therefore, before the RPE-BM peak reflectivity is suitable as a longitudinal biomarker, the reproducibility needs to be improved.

Changes in BM also occur with normal aging, which means that BM calcification in PXE may represent a part of the normal aging process. Also, the RPE reflectivity increases with age, which is attributed to enlarged melanosomes in the RPE.[35] Since BM is very thin, it is hard to investigate the BM reflectivity separate from the RPE reflectivity. Both phenomena, however, cannot explain the observed difference in RPE-BM peak reflectivity between patients with PXE and controls.

Furthermore, changes in BM occur as part of the pathophysiology of AMD.[36,37] AMD may progress to a neovascular or atrophic stage due to changes in the anatomical complex consisting of the photoreceptors, RPE- BM, and the choriocapillaris.[36] Patients with AMD also have a different OCT reflectivity profile: the ellipsoid zone has a lower reflectivity than controls which correlates with retinal function.[38] Possibly, the OCT reflectivity profile also shows differences in the RPE-BM complex due to BM calcification or other changes in the complex consisting of choriocapillaris, RPE-BM, and the photoreceptors.[39] Therefore, OCT reflectivity profiles may be an interesting biomarker to monitor early changes in patients with AMD, or even as a screening tool for detection of early AMD.[40]

Interestingly, we also found an indication that patients with PXE have a lower photoreceptor reflectivity than controls, with nominal statistical significance (Table 9.1). The interpretation is yet uncertain. An altered optical Stiles Crawford effect may contribute to this difference between patients with PXE and controls. The optical Stiles-Crawford effect describes the phenomenon that OCT reflectivity depends on the directionality of the retinal tissue.[41] The directionality of the photoreceptors might be altered by retinal pathophysiology, which then leads to an altered absorption and reflection of light.[42] Possibly, BM calcification affects the directionality of the photoreceptors and thereby its reflectivity. However, it is also plausible that BM calcification affects the vitality of the photoreceptors by impeding the diffusion of nutrients and oxygen from the choriocapillaris. This may then cause photoreceptor dysfunction and degeneration. Despite the lack of large-scale studies providing convincing evidence, the existing literature indicates that patients with PXE have impaired retinal function. Three studies in 35, 15 and 4 patients with PXE found reduced retinal function or dark adaptation, which supports this hypothesis.[43–45] However, one study did not find retinal dysfunction in seven patients with PXE.[46] Future research should compare retinal function with OCT reflectivity to further investigate the mechanism of lower photoreceptor reflectivity in patients with PXE.

Moreover, we found differences in thickness of the total retina and in several retinal layers. Two previous studies reported on a lower retinal thickness in eyes with PXE, but these studies included later stages of PXE with CNV and/or atrophy, making it difficult to compare our findings.[47,48] Since there are no data on retinal layer thickness in PXE, it is difficult to interpret these findings. Perhaps BM calcification already affects the thickness of some retinal layers at an early disease stage. However, it is also very plausible that the segmentation algorithm attributed to the differences in layer thickness. The IOWA segmentation algorithms rely on signal strength, and the higher RPE-BM reflectivity in patients with PXE may slightly affect the algorithm.[49] Last, the method of thickness measurements differs from commonly used methods (e.g. measuring along the length of the standardized Early Treatment of Diabetic Retinopathy grid). Both the uncertainty regarding why the layers differ in thickness, as well as the method of measurement should be taken into account when interpreting or comparing the retinal layer thicknesses.

Some limitations need to be addressed. The IOWA reference algorithms that we used to segment the retinal layers are based on a three-dimensional approach, which models the surfaces of retinal layers, whereas our OCT volumes consist of seven B-scans. This

might result in small segmentation errors at the fovea. However, in this study all B-scans were visually inspected and in case there were clearly visible segmentation errors, the A-scans in that area were excluded. Also, manual adjustment of small segmentation errors did not affect the results; the small, nonsignificant changes are seen in both patients with PXE and controls, and they follow the same direction. They will thus not weaken the differences seen between PXE and controls. Therefore, we do not assume that this has affected the validity of our findings. Then, the RPE-BM peak reflectivity might have been slightly affected in patients with PXE due to the presence of angioid streaks that were not detectable on OCT. In most cases, however, angioid streaks are visible on OCT as breaks in BM[7] and we excluded those A-scans with our approach. This resulted in a lower proportion of included A-scans per B-scan in patients with PXE compared with controls. Hypothetically, undetected angioid streaks could lower RPE-BM peak reflectivity, but we assume that the proportion of A-scans with undetected streaks is so small that a large effect on reflectivity values is unlikely. At last, we found that the shadowing artifacts of retinal blood vessels affected the RPE-BM reflectivity, but this effect was relatively small and did not influence the large difference between reflectivity in patients with PXE and controls. However, it does indicate that the RPE-BM reflectivity might be slightly affected by above lying structures. To prevent this, an approach based on attenuation coefficients could be an option in future research.

In conclusion, we showed that patients with PXE have increased normalized RPE-BM reflectivity, presumably as a result of BM calcification. The normalized RPE-BM peak reflectivity has potential to be the first biomarker for the severity of BM calcification in patients with PXE. This finding is relevant to gain insight not only into PXE pathology but into normal aging and AMD as well. Further research is warranted to confirm our findings and to further improve the reproducibility of the RPE-BM peak reflectivity.

References

1. Bergen AA, Plomp AS, Schuurman EJ, et al. Mutations in *ABCC6* cause pseudoxanthoma elasticum. *Nat Genet*. 2000;25(2):228-231.
2. Kranenburg G, Baas AF, de Jong PA, Asselbergs FW, Visseren FLJ, Spiering W. The prevalence of pseudoxanthoma elasticum: Revised estimations based on genotyping in a high vascular risk cohort. *Eur J Med Genet*. 2019;*62*(2):90-92.
3. Gliem M, De Zaeytijd J, Finger RP, Holz FG, Leroy BP, Issa PC. An update on the ocular phenotype in patients with pseudoxanthoma elasticum. *Front Genet*. 2013;4(APR):14.
4. Risseeuw S, Ossewaarde-van Norel J, Klaver CCW, Colijn JM, Imhof SM, van Leeuwen R. Visual Acuity in Pseudoxanthoma Elasticum. *Retina*. 2019;39(8):1580-1587.
5. Kranenburg G, de Jong PA, Bartstra JW, et al. Etidronate for Prevention of Ectopic Mineralization in Patients With Pseudoxanthoma Elasticum. *J Am Coll Cardiol*. 2018;71(10):1117-1126.
6. Spaide RF. Peau d'orange and angioid streaks: manifestations of Bruch membrane pathology. *Retina*. 2015;35(3):392-397.
7. Charbel Issa P, Finger RP, Holz FG, Scholl HPN. Multimodal imaging including spectral domain OCT and confocal near infrared reflectance for characterization of outer retinal pathology in pseudoxanthoma elasticum. *Invest Ophthalmol Vis Sci*. 2009;50(12):5913-5918.
8. Chen X, Hou P, Jin C, et al. Quantitative analysis of retinal layer optical intensities on three-dimensional optical coherence tomography. *Invest Ophthalmol Vis Sci*. 2013;54(10):6846-6851.
9. Ramrattan RS, Van der Schaft TL, Mooy CM, De Bruijn WC, Mulder PGH, De Jong PTVM. Morphometric analysis of Bruch's membrane, the choriocapillaris, and the choroid in aging. *Investig Ophthalmol Vis Sci*. 1994;35(6):2857-2864.
10. Chen C-L, Ishikawa H, Wollstein G, et al. Individual A-Scan Signal Normalization Between Two Spectral Domain Optical Coherence Tomography Devices. *Investig Opthalmology Vis Sci*. 2013;54(5):3463.
11. Vermeer KA, van der Schoot J, Lemij HG, de Boer JF. RPE-Normalized RNFL Attenuation Coefficient Maps Derived from Volumetric OCT Imaging for Glaucoma Assessment. *Investig Opthalmology Vis Sci*. 2012;53(10):6102.
12. Plomp AS, Toonstra J, Bergen AAB, van Dijk MR, de Jong PTVM. Proposal for updating the pseudoxanthoma elasticum classification system and a review of the clinical findings. *Am J Med Genet A*. 2010;152A(4):1049-1058.
13. Garvin MK, Abràmoff MD, Wu X, Russell SR, Burns TL, Sonka M. Automated 3-D intraretinal layer segmentation of macular spectral-domain optical coherence tomography images. *IEEE Trans Med Imaging*. 2009;28(9):1436-1447.
14. Antony B, Abràmoff MD, Tang L, et al. Automated 3-D method for the correction of axial artifacts in spectral-domain optical coherence tomography images. *Biomed Opt Express*. 2011;2(8):2403-2416.
15. Li K, Wu X, Chen DZ, Sonka M. Optimal surface segmentation in volumetric images--a graph-theoretic approach. *IEEE Trans Pattern Anal Mach Intell*. 2006;28(1):119-134.
16. Spaide RF, Curcio CA. Anatomical correlates to the bands seen in the outer retina by optical coherence tomography: literature review and model. *Retina*. 2011;31(8):1609-1619.
17. Benjamini Y, Hochberg Y. Controlling the False Discovery Rate: A Practical and Powerful Approach to Multiple Testing. *J R Stat Soc Ser B*. 1995;57(1):289-300.
18. DeLong ER, DeLong DM, Clarke-Pearson DL. Comparing the areas under two or more correlated receiver operating characteristic curves: a nonparametric approach. *Biometrics*. 1988;44(3):837-845.
19. Bland JM, Altman DG. Statistical methods for assessing agreement between two meathods of clinical measurement. *Lancet (London, England)*. Published online 1986:307-310.
20. Robin X, Turck N, Hainard A, et al. pROC: an open-source package for R and S+ to analyze and compare ROC curves. *BMC Bioinformatics*. 2011;12(1):77.

21. Ari Yaylali S, Akcakaya AA, Erbil HH, Salar S, Karakurt Y. Optical coherence tomography findings in pseudoxanthoma elasticum. *Eur J Ophthalmol*. 2010;20(2):397-401.
22. Charbel Issa P, Finger RP, Holz FG, Scholl HPN. Multimodal Imaging Including Spectral Domain OCT and Confocal Near Infrared Reflectance for Characterization of Outer Retinal Pathology in Pseudoxanthoma Elasticum. *Investig Opthalmology Vis Sci*. 2009;50(12):5913.
23. Jensen OA. Bruch's membrane in pseudoxanthoma elasticum. Histochemical, ultrastructural, and x-ray microanalytical study of the membrane and angioid streak areas. *Albrecht Von Graefes Arch Klin Exp Ophthalmol*. 1977;203(3-4):311-320.
24. De Zaeytijd J, Vanakker OM, Coucke PJ, De Paepe A, De Laey J-J, Leroy BP. Added value of infrared, red-free and autofluorescence fundus imaging in pseudoxanthoma elasticum. *Br J Ophthalmol*. 2010;94(4):479-486.
25. Charbel Issa P, Finger RP, Gotting C, Hendig D, Holz FG, Scholl HPN. Centrifugal fundus abnormalities in pseudoxanthoma elasticum. *Ophthalmology*. 2010;117(7):1406-1414.
26. Gliem M, Hendig D, Finger RP, Holz FG, Charbel Issa P. Reticular pseudodrusen associated with a diseased bruch membrane in pseudoxanthoma elasticum. *JAMA Ophthalmol*. 2015;133(5):581-588.
27. Gliem M, Müller PL, Birtel J, et al. Quantitative fundus autofluorescence in pseudoxanthoma elasticum. *Investig Ophthalmol Vis Sci*. 2017;58(14):6159-6165.
28. Sun M, Zhang Z, Ma C, Chen S, Chen X. Quantitative analysis of retinal layers on three-dimensional spectral-domain optical coherence tomography for pituitary adenoma. Malik RA, ed. *PLoS One*. 2017;12(6):e0179532.
29. Neudorfer M, Weinberg A, Loewenstein A, Barak A. Differential optical density of subretinal spaces. *Invest Ophthalmol Vis Sci*. 2012;53(6):3104-3110.
30. Teussink MM, Cense B, van Grinsven MJJP, Klevering BJ, Hoyng CB, Theelen T. Impact of motion-associated noise on intrinsic optical signal imaging in humans with optical coherence tomography. *Biomed Opt Express*. 2015;6(5):1632-1647.
31. Huang X-R, Knighton RW, Feuer WJ, Qiao J. Retinal nerve fiber layer reflectometry must consider directional reflectance. *Biomed Opt Express*. 2016;7(1):22.
32. Mehta N, Lavinsky F, Gattoussi S, et al. Increased Inner Retinal Layer Reflectivity in Eyes With Acute CRVO Correlates With Worse Visual Outcomes at 12 Months. *Investig Opthalmology Vis Sci*. 2018;59(8):3503.
33. Bosche F, Andresen J, Li D, Holz F, Brinkmann C. Spectralis OCT1 versus OCT2: Time Efficiency and Image Quality of Retinal Nerve Fiber Layer Thickness and Bruch's Membrane Opening Analysis for Glaucoma Patients. *J Curr glaucoma Pract*. 2019;13(1):16-20.
34. Vermeer KA, Mo J, Weda JJA, Lemij HG, de Boer JF. Depth-resolved model-based reconstruction of attenuation coefficients in optical coherence tomography. *Biomed Opt Express*. 2013;5(1):322-337.
35. Chen B, Gao E, Chen H, et al. Profile and Determinants of Retinal Optical Intensity in Normal Eyes with Spectral Domain Optical Coherence Tomography. *PLoS One*. 2016;11(2):e0148183.
36. Bhutto I, Lutty G. Understanding age-related macular degeneration (AMD): Relationships between the photoreceptor/retinal pigment epithelium/Bruch's membrane/choriocapillaris complex. *Mol Aspects Med*. 2012;33(4):295-317.
37. Booij JC, Baas DC, Beisekeeva J, Gorgels TGMF, Bergen AAB. The dynamic nature of Bruch's membrane. *Prog Retin Eye Res*. 2010;29(1):1-18.
38. Wu Z, Ayton LN, Guymer RH, Luu CD. Relationship Between the Second Reflective Band on Optical Coherence Tomography and Multifocal Electroretinography in Age-Related Macular Degeneration. *Investig Opthalmology Vis Sci*. 2013;54(4):2800.
39. Reumueller A, Schmidt-Erfurth U, Salas M, et al. Three-Dimensional Adaptive Optics–Assisted Visualization of Photoreceptors in Healthy and Pathologically Aged Eyes. *Investig Opthalmology Vis Sci*. 2019;60(4):1144.

40. Garcia Garrido M, Beck SC, Mühlfriedel R, Julien S, Schraermeyer U, Seeliger MW. Towards a quantitative OCT image analysis. *PLoS One*. 2014;9(6):e100080.
41. Snyder AW, Pask C. The Stiles-Crawford effect-explanation and consequences. *Vision Res*. 1973;13(6):1115-1137.
42. DeLint PJ, Berendschot TTJM, Van Norren D. A comparison of the optical stiles-crawford effect and retinal densitometry in a clinical setting. *Investig Ophthalmol Vis Sci*. 1998;39(8):1519-1523.
43. Audo I, Vanakker OM, Smith A, et al. Pseudoxanthoma Elasticum with Generalized Retinal Dysfunction, a Common Finding? *Investig Opthalmology Vis Sci*. 2007;48(9):4250.
44. François J, Rouck A. Electrophysiological Studies in Groenblad-strandberg Syndrome. In: ; 1980:19-25.
45. Hess K, Gliem M, Birtel J, et al. Impaired Dark Adaptation Associated With a Diseased Bruch Membrane in Pseudoxanthoma Elasticum. *Retina*. 2019;Publish Ah:1.
46. Holz FG, Jubb C, Fitzke FW, Bird AC, Pope FM. Dark adaptation and scotopic perimetry over "peau d'orange" in pseudoxanthoma elasticum. *Br J Ophthalmol*. 1994;78(1):79-80.
47. Dolz-Marco R, Andreu-Fenoll M, Hernández-Martínez P, Pinazo-Durán MD, Gallego-Pinazo R. Automated macular choroidal thickness measurement by swept-source optical coherence tomography in pseudoxanthoma elasticum. *Int J Retin Vitr*. 2016;2:15.
48. Ellabban AA, Tsujikawa A, Matsumoto A, et al. Macular choroidal thickness and volume in eyes with angioid streaks measured by swept source optical coherence tomography. *Am J Ophthalmol*. 2012;153(6):1133-1143.
49. Darma S, Kok PHB, van den Berg TJTP, et al. Optical density filters modeling media opacities cause decreased SD-OCT retinal layer thickness measurements with inter- and intra-individual variation. *Acta Ophthalmol*. 2015;93(4):355-361.

Supplementary data

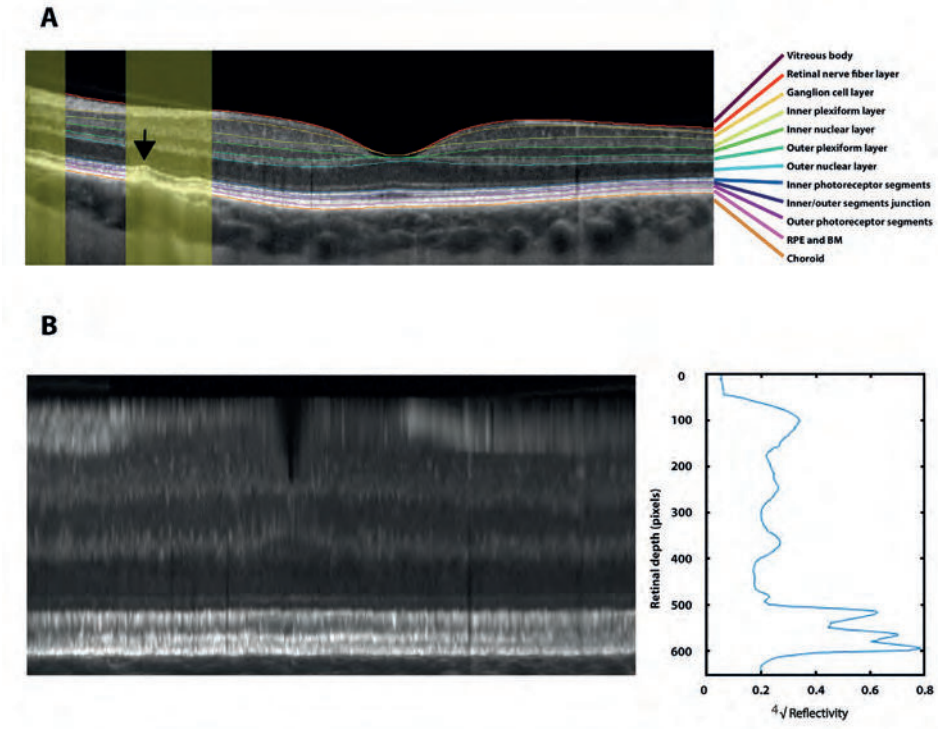

Figure S9.1 Processing of optical coherence tomography (OCT) imaging. A: Example of automated segmentation of a PXE OCT scan. The colored lines represent the 11 different surfaces and the corresponding retinal layers are presented at the right side. The vertical yellow lines represent A-scans that will be excluded from analysis. In this example, A-scans in which the outer retina was not completely intact were excluded. The black arrow indicates an angioid streak. B: For all selected A-scans, each layer was stretched using linear interpolation to the same standardized length of twice the maximum layer thickness within the B-scan. The reflectivity profile was created by taking the weighted median of all pixels at the same depth.

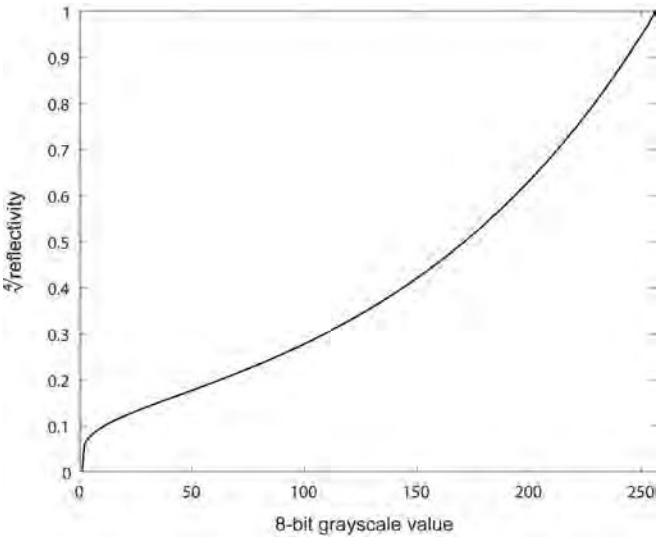

Figure S9.2 Calibration curve for converting 8-bit grayscale values to reflectivity values for further analysis. This curve was made by comparing the 8-bit grayscale values from DICOM scans with the corresponding reflectivity values from the raw data (OCT scans as VOL files).

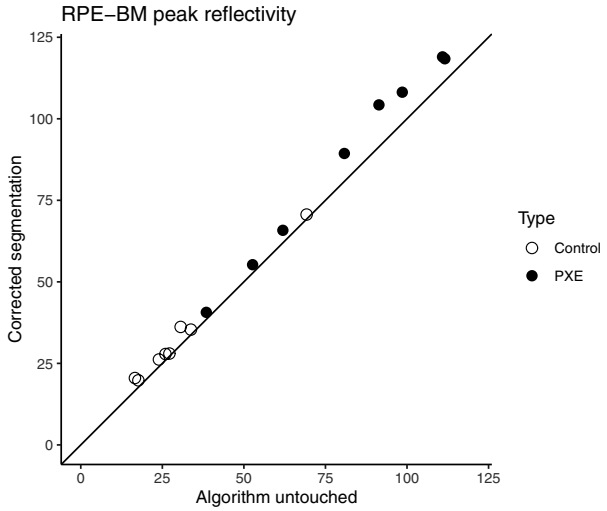

Figure S9.3 Correlation of the RPE-BM peak reflectivity for manual adjustment of small segmentation errors for 8 OCT scans of 4 patients with PXE and 8 OCT scans of 4 controls. Each OCT scan consisted of 7 B-scans. The diagonal line represents the perfect correlation.

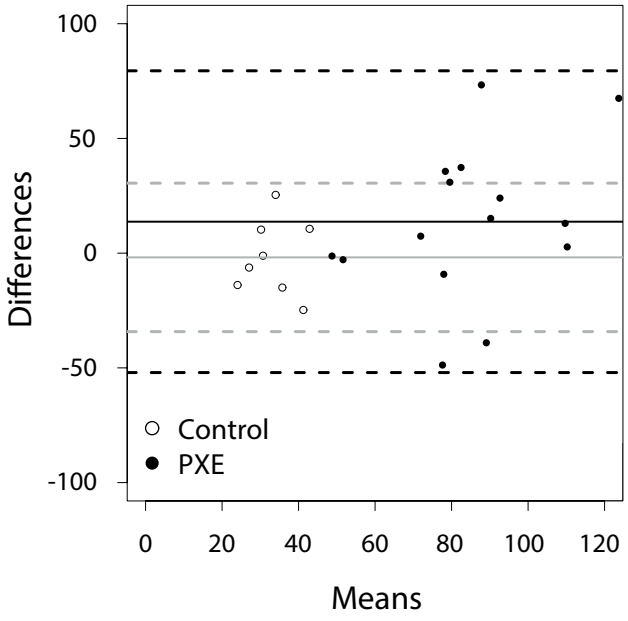

Figure S9.4
Bland-Altman plot of repeated RPE-BM peak reflectivity averaged per eye. In total, 8 PXE patients (15 eyes) and 4 controls (8 eyes) had repeated measures within 6 months.

Supplementary Table S9.1 Layer specific retinal thickness

	PXE	Control	Nominal P-value	Adjusted P-value*
	N=45	N=25		
Total retinal thickness in µm	321 ± 13	328 ± 11	0.025	0.051
Layer specific thickness in µm				
Retinal nerve fiber layer	34 ± 2	36 ± 3	0.005	0.015
Ganglion cell layer	39 ± 4	41 ± 4	0.069	0.098
Inner plexiform layer	38 ± 3	38 ± 2	0.862	0.862
Inner nuclear layer	33 ± 2	35 ± 2	0.006	0.015
Outer plexiform layer	28 ± 3	28 ± 2	0.465	0.517
Outer nuclear layer	82 ± 7	85 ± 6	0.081	0.101
Ellipsoid zone	27 ± 1	26 ± 1	0.001	0.005
Outer photoreceptor segments	20 ± 4	19 ± 2	0.062	0.098
RPE and Bruch's membrane	19 ± 2	21 ± 2	1.97×10^{-4}	0.002

Values are presented as mean ± standard deviation. *P*-values were based on the two-sample *t*-test.
* *P*-values were adjusted according to the method as proposed by Benjamini and Hochberg.

Supplementary Table S9.2 Age specific median and peak reflectivity of the retinal layers in patients with PXE

	Layer	Under 20 years	20 – 30 years	30 – 40 years	Nominal *P*	Adjusted *P**
		n = 7	n = 22	n = 16		
Median layer reflectivity	Retinal nerve fiber layer	2.74 [2.23, 2.98]	2.26 [2.05, 2.64]	2.06 [1.87, 2.33]	0.04	0.22
	Ganglion cell layer	0.69 [0.64, 0.74]	0.72 [0.67, 0.74]	0.73 [0.67, 0.76]	0.49	0.69
	Inner plexiform layer	0.74 [0.69, 0.76]	0.78 [0.74, 0.83]	0.78 [0.73, 0.82]	0.23	0.69
	Inner nuclear layer	0.31 [0.30, 0.36]	0.39 [0.34, 0.40]	0.37 [0.33, 0.39]	0.29	0.69
	Outer plexiform layer	0.61 [0.56, 0.69]	0.68 [0.57, 0.80]	0.65 [0.56, 0.68]	0.50	0.69
	Outer nuclear layer	0.19 [0.18, 0.21]	0.24 [0.17, 0.28]	0.23 [0.19, 0.25]	0.64	0.83
	Ellipsoid zone	13.51 [11.12, 22.54]	14.52 [9.94, 19.90]	13.04 [8.07, 19.40]	0.78	0.86
	Outer photoreceptor segments	11.23 [9.20, 17.71]	14.61 [11.50, 23.39]	15.12 [8.46, 24.03]	0.93	0.93
	RPE and Bruch's membrane	26.51 [24.11, 46.00]	43.20 [26.53, 51.31]	39.97 [30.40, 53.56]	0.45	0.69
Peak layer reflectivity	Retinal nerve fiber layer	6.63 [5.90, 8.45]	5.15 [4.18, 5.86]	4.48 [4.14, 5.24]	4.15×10^{-3}	0.06
	Ganglion cell layer	3.69 [3.46, 3.81]	3.31 [2.96, 3.59]	3.03 [2.82, 3.31]	0.01	0.06
	Inner plexiform layer	0.93 [0.85, 0.99]	1.02 [0.95, 1.06]	0.99 [0.94, 1.05]	0.25	0.69
	Inner nuclear layer	0.73 [0.69, 0.84]	0.88 [0.77, 0.91]	0.81 [0.77, 0.87]	0.28	0.69
	Outer plexiform layer	0.90 [0.78, 1.02]	0.97 [0.82, 1.14]	0.89 [0.78, 0.95]	0.39	0.69
	Outer nuclear layer	0.67 [0.62, 0.69]	0.77 [0.65, 0.88]	0.70 [0.58, 0.82]	0.46	0.69
	Ellipsoid zone	35.63 [27.83, 59.33]	40.63 [28.46, 55.96]	35.33 [22.35, 58.01]	0.81	0.86
	Outer photoreceptor segments	19.61 [16.85, 31.37]	28.40 [21.99, 43.17]	26.80 [18.90, 44.33]	0.76	0.86
	RPE and Bruch's membrane	44.24 [40.52, 74.62]	65.99 [45.09, 83.80]	70.76 [49.02, 88.02]	0.47	0.69

Abbreviations: PXE; pseudoxanthoma elasticum, RPE; retinal pigment epithelium.
All reflectivity values are normalized to the GCL-IPL layer.
* *P*-values were adjusted according to the method as proposed by Benjamini and Hochberg.

Supplementary Table S9.3 Layer specific within-eye and within-patient correlation of median reflectivity values

		PXE			Controls		
	Retinal layer	Spearman's ρ	*P*-value Nominal	*P*-value Adjusted*	Spearman's ρ	*P*-value Nominal	*P*-value Adjusted*
Within eye: Horizontal & vertical	Retinal nerve fiber layer	0.57	6.05×10^{-10}	7.77×10^{-10}	0.61	1.91×10^{-5}	3.44×10^{-5}
	Ganglion cell layer	0.37	1.44×10^{-4}	1.44×10^{-4}	0.04	0.90	0.80
	Inner plexiform layer	0.39	6.09×10^{-5}	6.85×10^{-5}	0.19	0.24	0.27
	Inner nuclear layer	0.59	7.13×10^{-11}	1.07×10^{-10}	0.39	0.01	0.01
	Outer plexiform layer	0.70	3.08×10^{-16}	6.93×10^{-16}	0.56	1.35×10^{-4}	2.03×10^{-4}
	Outer nuclear layer	0.69	9.42×10^{-16}	1.70×10^{-15}	0.64	7.33×10^{-6}	1.65×10^{-5}
	Ellipsoid zone	0.72	$<2.2\times10^{-16}$	$<2.2\times10^{-16}$	0.82	8.12×10^{-11}	7.31×10^{-10}
	Outer photoreceptor segments	0.72	$<2.2\times10^{-16}$	$<2.2\times10^{-16}$	0.76	1.05×10^{-8}	4.72×10^{-8}
	RPE and Bruch's membrane	0.77	$<2.2\times10^{-16}$	$<2.2\times10^{-16}$	0.65	3.53×10^{-6}	1.06×10^{-5}
Within patient: Left & right eye	Retinal nerve fiber layer	0.37	0.05	0.05	0.41	0.09	0.10
	Ganglion cell layer	-0.06	0.76	0.76	0.26	0.27	0.27
	Inner plexiform layer	0.57	1.23×10^{-3}	2.77×10^{-3}	0.67	1.83×10^{-3}	0.01
	Inner nuclear layer	0.57	1.13×10^{-3}	2.77×10^{-3}	0.46	0.04	0.06
	Outer plexiform layer	0.49	0.01	0.01	0.58	0.01	0.02
	Outer nuclear layer	0.51	4.45×10^{-3}	0.01	0.49	0.03	0.05
	Ellipsoid zone	0.68	5.73×10^{-5}	2.58×10^{-4}	0.55	0.01	0.02
	Outer photoreceptor segments	0.75	2.36×10^{-6}	2.12×10^{-5}	0.67	1.83×10^{-3}	0.01
	RPE and Bruch's membrane	0.43	0.02	0.03	0.69	1.05×10^{-3}	0.01

Abbreviations: PXE; pseudoxanthoma elasticum, RPE; retinal pigment epithelium
* *P*-values were adjusted according to the method as proposed by Benjamini and Hochberg.

Supplementary Table S9.4 The effect of manual adjustment of small segmentation errors on reflectivity and retinal layer thickness for patients with PXE and controls

	Adjusted segmentation	Unadjusted segmentation	*P*-value
Patients with PXE	N=8	N=8	
GCL-IPL reflectivity	0.0059 ± 0.002	0.0064 ± 0.002	0.666
RPE-BM peak reflectivity	87.6 ± 33.1	80.8 ± 27.3	0.643
Layer specific thickness in µm			
Retinal nerve fiber layer	32.8 ± 5.1	35.1 ± 5.4	0.398
Ganglion cell layer	40 ± 6.5	38.7 ± 6.6	0.699
Inner plexiform layer	37.4 ± 2.1	38.1 ± 2.1	0.515
Inner nuclear layer	33.8 ± 3.5	33.6 ± 3.3	0.884
Outer plexiform layer	28 ± 3.5	28.2 ± 3.4	0.917
Outer nuclear layer	83.5 ± 3.5	83.2 ± 3.5	0.869
Ellipsoid zone	26.2 ± 1.5	26.2 ± 1.5	0.964
Outer photoreceptor segments	19.5 ± 3.9	19.5 ± 3.9	0.995
RPE and Bruch's membrane	19.7 ± 1.9	19.7 ± 1.8	0.999
Controls	N=8	N=8	
GCL-IPL reflectivity	0.0111 ± 0.0035	0.0122 ± 0.0041	0.575
RPE-BM peak reflectivity	33.1 ± 16.3	30.6 ± 16.7	0.770
Layer specific thickness in µm			
Retinal nerve fiber layer	34.3 ± 6.2	36.4 ± 5.6	0.479
Ganglion cell layer	39.6 ± 4.4	38.8 ± 5.1	0.743
Inner plexiform layer	39.2 ± 3.1	39.6 ± 3	0.760
Inner nuclear layer	35.2 ± 2.4	35.4 ± 2.7	0.881
Outer plexiform layer	27.2 ± 1.9	27.2 ± 1.8	0.977
Outer nuclear layer	86.6 ± 3.3	86.4 ± 3	0.898
Ellipsoid zone	27.2 ± 1.7	27.2 ± 1.7	0.934
Outer photoreceptor segments	18.4 ± 2.9	18.4 ± 2.9	0.997
RPE and Bruch's membrane	20.6 ± 2.7	20.6 ± 2.7	0.997

Values are presented as mean ± standard deviation. *P*-values were based on the two-sample *t*-test. The number represents the amount of OCT-scans. Each OCT scan consisted of 7 B-scans. The segmentation was manually adjusted in one group and compared with the unadjusted segmentation.
Abbreviations: PXE; pseudoxanthoma elasticum, GCL; ganglion cell layer, IPL; inner plexiform layer, RPE; retinal pigment epithelium, BM; Bruch's membrane.

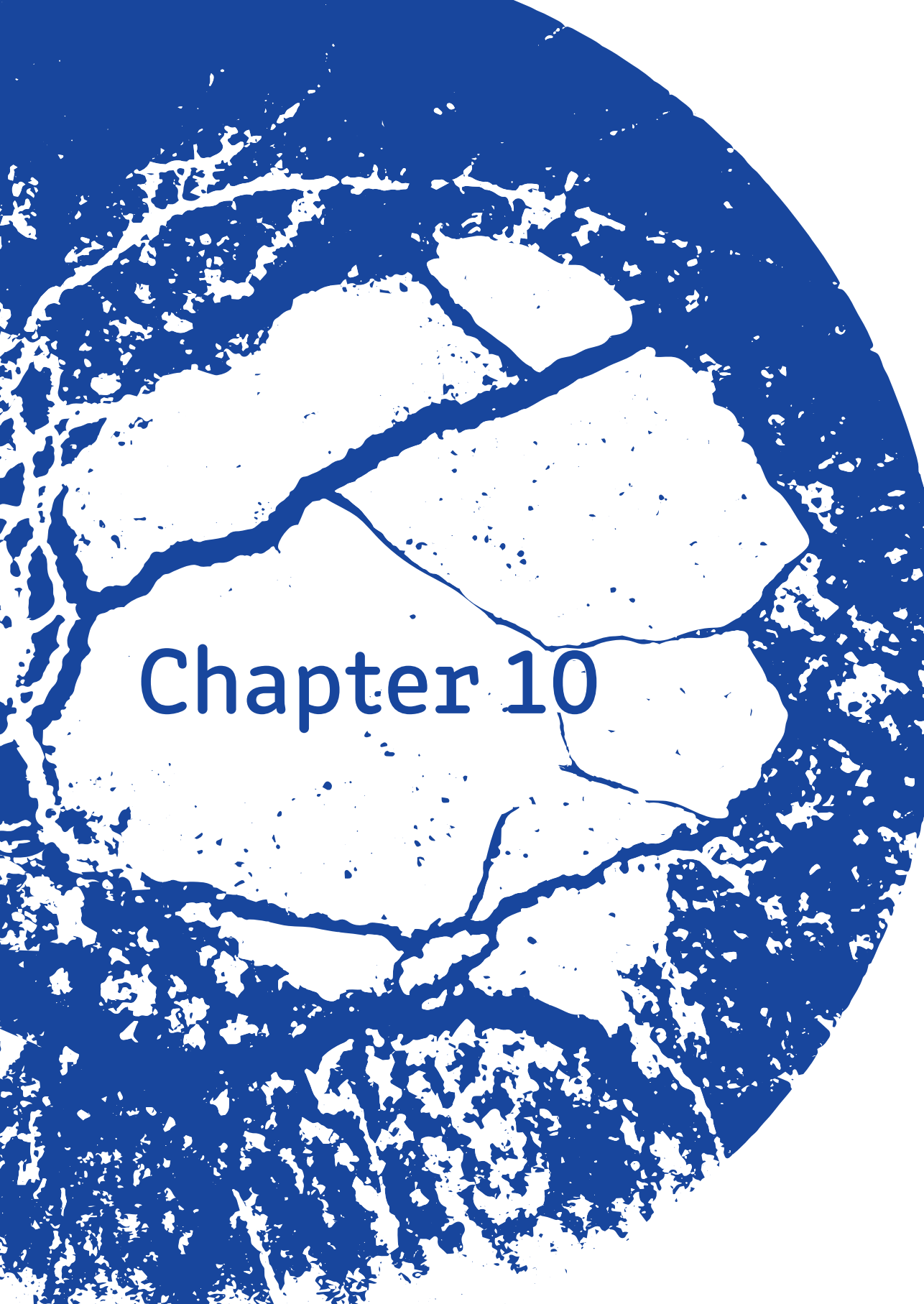
Chapter 10

General discussion

This thesis studies several aspects of BM calcification that will lead to more insight into the course of the disease, with the higher purpose to provide an individual prognosis and ultimately to improve visual outcome. The three major aims that we addressed in this thesis were:

I. To study the manifestations of PXE in the eye by investigating the natural history of BM calcification and describing its clinical consequences.
II. To gain insight into the determinants of the visual prognosis and to investigate whether treatment can modify disease complications.
III. To develop an imaging-based biomarker that will aid clinical monitoring of disease and may serve as an endpoint in research and upcoming trials.

This chapter discusses the main findings of this thesis, puts them in a broader perspective and addresses clinical implications and future research perspectives.

The natural history of Bruch's membrane calcification

BM calcification is hypothesized to spread centrifugal based on assessment of multimodal imaging including near-infrared reflectance imaging (NIR) and late-phase indocyanine green angiography (ICG-A) (Figure 1.8).[1] In **Chapter 2**, we confirmed this centrifugal spread in a cross-sectional analysis and detected longitudinal spread in individual patients. We also found that the peripheral border of the BM calcification appears to be rather constant during life, implicating that this is an area that is 'predetermined' for BM calcification in PXE patients. During life, this area confluences centrifugally (Figure 2.7).

The underlying mechanism of this predetermined area for BM calcification has yet to be unravelled. Probably, underlying structural changes in BM predispose calcification of fibres with certain properties. *ABCC6*$^{-/-}$ mice ("PXE mice") show mostly calcification of collagen fibres, as compared to mostly elastic fibres in PXE patients, which underpins the theory that tissue properties and species differences (partly) determine which fibres will calcify.[2,3] The elastic layer and its adjacent collagenous layers of BM are thicker in the periphery than the macula.[4,5] Possibly, the thickening is associated with changes in fibre properties and susceptibility for calcification.

Moreover, angioid streaks grow during life. Though not frequent, new angioid streaks develop also in patients over 30 years (Figure 2.2). The cross-sectional analysis showed an increasing prevalence of angioid streaks in the central 3000 μm of the macula with

increasing age (Table 2.1), which suggests a slow growth of angioid streaks throughout life. However, the growth appears to slow down after the fifth decade (Figure 7.2). Possibly, the centrifugal spread of BM calcification has reached its maximum area around the sixth decade, and angioid streaks cannot grow longer. However, branching of angioid streaks in the brittle BM is still possible, but longitudinal data in patients over 50 years is required to verify this hypothesis.

Physiological consequences of pathophysiological Bruch's membrane calcification

PXE patients have thinner choroids than controls, also in eyes without CNV or atrophy, which is probably caused by BM calcification. [6–8] Though, a damaging effect on the choroid of increased pulse pressure due to arterial stiffening in the intracranial internal carotid arteries cannot be ruled out. [9–11] We investigated the contribution of arterial stiffening to choroidal thinning in **Chapter 4** but did not find an independent association between arterial stiffening and choroidal thickness. We did find that choroidal thinning was most pronounced nasal from the macula, which is the presumed area with the most BM calcification, and in line with the other study that reported on eyes without CNV or atrophy.[6] This strengthens the theory that BM calcification reduces the permeability of BM.

Interestingly, a recent study reported a thicker choroid in PXE eyes without CNV or atrophy compared to controls (304 µm vs 267 µm, mean ages 38 and 46 years respectively).[12] This is almost 100 µm thicker than in the eyes in our study without CNV or atrophy (206 µm, mean age 49 years), and the age difference can only partly explain the large difference. The authors postulate that changes in BM at an early stage cause oxidative stress and a hyperpermeable choroid, and thereby a thicker choroid.[12] In later stages, this damage leads to secondary choroidal thinning.[12] Gliem et al found a reduced density of the vascular network of the choroid using en-face OCT in a PXE patient without CNV and atrophy, which could represent the before mentioned damage to the choroid.[6] Investigation of choroidal thickness in younger PXE patients might elucidate the process of choroidal thinning in PXE. Unfortunately, both our study and the study by Gliem et al had insufficient numbers of PXE patients under 40 years for subgroup analysis.[6]

PXE patients show a pattern of reduced fluorescence at late-phase ICG-A, which enlarges with age and appears associated with the degree of BM calcification (**Chapter 2**). Though numbers of patients with late-phase ICG-A are small, it is evident that peau

d'orange precedes the pattern of decreased fluorescence which develops around the fourth decade. Though ICG is a large molecule and mainly remains in the choroidal vessels, ICG dye was found in RPE cells of primates and in human RPE of a surgically removed membrane. Also, it was taken up by RPE cells *in vitro* and was visualized in RPE cells with adaptive optics.[13–16] This implies that ICG dye accumulates in the RPE and attributes to the late-phase ICG-A pattern of homogeneous fluorescence in normal eyes. Probably, the calcified BM inhibits the diffusion and uptake of the ICG dye by the RPE. This implicates that extent of the decreased fluorescence might be a marker for the degree of impaired diffusion of molecules through BM. Another theory is that the decreased fluorescence represents early RPE dysfunction. However, we did not see a clear correlation with increased fundus autofluorescence (FAF). Nevertheless, both explanations (impaired diffusion through BM and RPE dysfunction) suggest that the vitality of the RPE and photoreceptors is impaired.

Our findings in **Chapter 7** and **Chapter 9** indicate that PXE patients indeed have an impaired vitality of the RPE and photoreceptors. In **Chapter 7** we demonstrated that PXE patients often suffer from impaired RPE vitality. Longer angioid streaks as a proxy for the degree of BM calcification were associated with increased odds for pattern-dystrophy like changes, after adjustment for age and sex. Pattern-dystrophy like changes present as focally increased FAF patterns in PXE patients and are thought to represent RPE dysfunction since they often precede macular atrophy.[17–19] This implies that more BM calcification increases the risk of RPE dysfunction. Moreover, in **Chapter 9** we found that young PXE patients have a decreased reflectivity of the ellipsoid zone (EZ) of the photoreceptors on spectral-domain (SD) OCT. Decreased EZ reflectivity is associated with AMD and ageing, and correlates with a decreased cone density and cone function.[20–24] Recently it was reported that a PXE patient of 42 years without CNV or atrophy showed decreased cone density.[25] Thus, BM calcification might also lead to impaired vitality of the photoreceptors at an early disease stage.

Altogether, these findings emphasize the important role of BM in the relationship of the choroid-BM-RPE complex. Another rare disease with BM pathology, Sorsby fundus dystrophy, also shows choroidal thinning and decreased fluorescence on late-phase ICG-A.[26,27] The symbiotic relationship of the choroid-BM-RPE complex implicates that an alteration of one of the tissues may introduce a sequence of alterations in this complex.[28–30] Clinically, this implies that BM calcification leads to an impaired vitality of the outer retina. Since an impaired vitality of the outer retina is a precursor of macular atrophy, this should be considered as the natural endpoint of BM calcification.

Visual consequences and clinical implications of Bruch's membrane calcification

Of all PXE patients in our cohort, half has CNV and a quarter has macular atrophy (**Chapter 7**), leading to a high prevalence of visual impairment and legal blindness of 26% and 11%, respectively (**Chapter 3**). Visual impairment is age-dependent, and thus even more frequent in PXE patients over 50 years, of whom 37% is visually impaired and 15% legally blind. These proportions are comparable with late AMD but visual impairment present 20 years earlier in life when people are still working. The prospect of early visual deterioration and the fearing for it play a major role in emotional well-being, more than visual impairment itself.[31] This is similar to AMD patients, in which patients who are blind in one eye are more distressed than patients with two blind eyes.[32] The large impact of an uncertain poor visual prognosis, calls for better insight into the ophthalmological consequences of BM calcification in PXE for a better prediction of visual outcome.

The high prevalence of visual impairment is difficult to extrapolate directly to the younger generation of PXE patients. A large proportion of patients had already developed CNV before the introduction of VEGF inhibition as a treatment for CNV in 2006.[33] Therefore, a substantial sample of our cohort has been 'undertreated' according to the current standards of medical care. Though, recent studies found an increased risk for macular atrophy due to VEGF inhibition in AMD patients.[34,35] A major part of PXE patients requires VEGF inhibition early in life, often as early as the fourth or fifth decade which is undoubtedly necessary to halt CNV activity. Though, cumulative administration of VEGF inhibition might be detrimental for the already fragile balance of the choroid-BM-RPE complex in PXE. While awaiting conclusive evidence on the effect of VEGF inhibition on macular atrophy, this must be kept in mind when treating PXE patients, especially prophylactic regimes.

Despite macular atrophy has increasingly been described as a retinal phenotype in PXE, its effect on visual impairment in PXE was not known.[19,36] We found that at least 16% of the visually impaired eyes (a BCVA < 0.3) is due to macular atrophy. Probably, this is an underestimation of the true effect of macular atrophy because extensive scarring in end-stage disease limits the assessment of previously present macular atrophy.

Though CNV still is the major cause of visual deterioration in PXE, a considerable part of visual loss is caused by macular atrophy. This cannot be treated up to now, which

should be taken into account when counselling PXE patients for their visual prognosis. However, other aspects of visual function are relevant in PXE as well. Metamorphopsia due to CNV, visual field defects due to scotomas and impaired contrast sensitivity can have an impact on daily life apart from a reduced visual acuity. A recent study showed an impaired dark adaptation in PXE patients.[37] Furthermore, two out of three studies of electroretinogram (ERG) findings in PXE suggest a generalized dysfunction in PXE patients.[38–40] However, these studies were uncontrolled and raise suspicion of a publication bias.

Female PXE patients have long been advised not to undergo a normal vaginal delivery, or even not to get pregnant, fearing for retinal complications following the pushing during delivery.[41,42] In **Chapter 5**, we report that a normal vaginal delivery did not cause retinal changes in 11 female PXE patients with a vaginal delivery, which implicates that there is no indication for a caesarean section if only angioid streaks are present. Though CNV is not common at the child-bearing age, all pregnant PXE patients should be monitored for the presence of CNV. Theoretically, the increased central venous pressure during the pushing phase increases the risk of rupture of the fragile CNV vasculature and may cause retinal haemorrhage, though the literature on the bleeding risk lacks.

Moreover, there are concerns about the maternal and foetal safety of the use of VEGF inhibition to stabilize CNV activity during pregnancy.[43] The scattered available evidence points into the direction that VEGF inhibition could be administered in later stages of pregnancy, if absolutely necessary.[43,44] Of the available VEGF inhibitors, ranibizumab clears from the bloodstream the quickest with a systemic half-life of two hours and has the littlest effect on plasma VEGF levels.[45] If VEGF inhibition during pregnancy is required, ranibizumab may thus be the least harmful option. In clinical practice, the use of medical intervention during delivery or prophylactic VEGF inhibitors for a PXE patient with CNV should be considered individually and based on shared decision making. Though, the presence of angioid streaks alone, even in the foveal area, must not be a reason for assisted delivery or even a caesarean section.

Determinants of the visual prognosis in PXE

The type of variants in the *ABCC6* gene might have an effect on the residual amount of protein. Truncation variants likely lead to a complete loss of function and are probably more severe than non-truncating variants, which may still lead to some residual function.[46] In **Chapter 6** we investigated whether truncating variants are

associated with more ectopic calcification in PXE patients. Patients with two truncating *ABCC6* variants have more arterial calcification and longer angioid streaks with an earlier onset compared with patients with one or two non-truncating variants. Longer angioid streaks, as a proxy for the degree of BM calcification, increase the risk for CNV and more severe macular atrophy (**Chapter 7**). Therefore, a more severe genotype presumably leads to more BM calcification in the early disease stage which increases the risk of macular degeneration causing visual impairment. These findings can aid in counselling PXE patients, especially younger patients, about their visual prognosis.

These findings are in line with previous studies. One genotype-phenotype study showed that one or two truncating mutations are associated with a higher risk for retinal haemorrhage and scarring when compared to patients with two non-truncating variants.[47] Another study found that PXE patients with presumably more severe variants were younger at diagnosis and had more affected organs.[48] Probably, the remaining ATP efflux from the hepatocytes is part of the pathophysiological mechanism of PXE, which strengthens the theory that PXE patients suffer from ectopic calcification due to lower levels of inorganic pyrophosphate (PP_i).[49,50] However, other genotype-phenotype studies did not find correlations.[51–55] The rarity of PXE and the use of the Phenodex classification, which is a rough composite score of different clinical outcomes in PXE, probably impede sufficient power for analyses.[52] Nevertheless, the lack of a correlation between the genotype and clinical outcome such as the peripheral arterial disease, pseudoxanthomas and visual acuity emphasizes the role of other factors than *ABCC6* mutations.

Interestingly, a more severe genotype seems to predispose an earlier onset of ectopic calcification, but the measures for arterial and especially BM calcification appear to equalize for regarding the genotype after the sixth decade (Figure 6.2). Maybe, there is a limit for the maximum amount of ectopic calcification within an individual. Then, the lower the PP_i levels are, the more the process of ectopic calcification will be accelerated.

Moreover, one study that focused on the ophthalmological manifestations also found a higher prevalence of CNV in patients with longer angioid streaks, in line with our findings.[56] The increased prevalence of CNV with longer angioid streaks may not necessarily be the sole effect of more BM calcification, but may also be affected by the dimensions of BM defects, thus by the amount and size of angioid streaks. If there is a large extent of BM calcification with subsequent long angioid streaks, it is plausible

that the BM calcification is denser and more severely impedes oxygen diffusion. This might lead to relative hypoxia and expression of VEGF in the outer retina, which then initiates the growth of CNV through the 'available' BM defects.[57,58] Thus, theoretically, the increased risk of CNV in PXE can be explained by two pathophysiological pathways. A schematic visualization of the pathways to BM calcification and macular degeneration is presented in Figure 10.1.

Determinants of the variability in PXE

The large variability even within families, the presence of patients with a clear clinical PXE diagnosis but without genetic confirmation, and the presence of PXE-like fundus abnormalities in carriers of *ABCC6* mutations suggest that PXE might not strictly be a monogenetic disease.[51,59,60] Biallelic *ABCC6* mutations are the predominant cause of this but the presence of patients with a PXE phenotype without clear genetic confirmation and the large phenotypic heterogeneity indicate that other factors also play a role in ectopic calcification (Figure 10.1). Maybe, PXE should rather be considered as a typical phenotype of soft tissue calcification which is caused by a disbalance in calcification modulators – mainly lower levels of PP_i due to *ABCC6* mutations.[3,50,61]

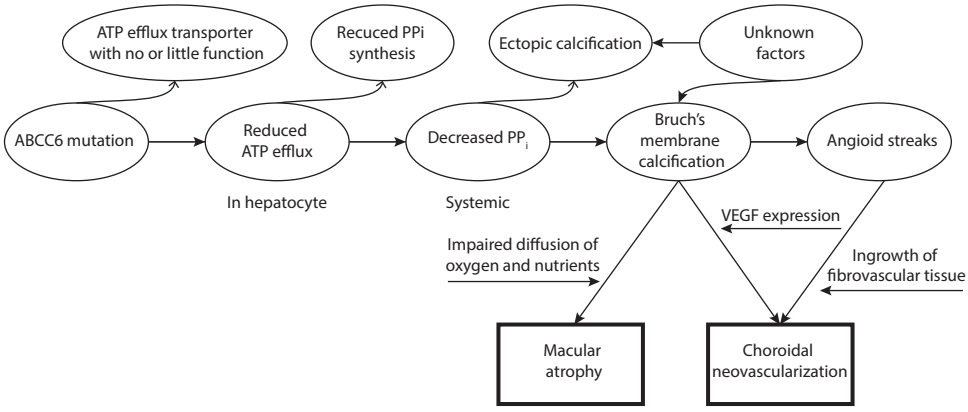

Figure 10.1 Presumed pathways leading to macular degeneration in patients with pseudoxanthoma elasticum. Besides the role of ABCC6 and inorganic pyrophosphate(PP_i) there are unknown factors that alter the course of disease.

Most likely, both genetic and environmental factors modify the severity of the phenotype.[62] Polymorphisms in the *VEGFA* gene are associated with worse visual outcome or need for VEGF inhibition and may predict CNV.[63,64] End-stage PXE and late AMD have shared phenotypes but may share genotypes as well, such as variants of the *CFH* gene.[65–67] Smoking may increase the risk for CNV, similar to AMD.[68] Furthermore, men have an increased risk for CNV and have longer angioid streaks (**Chapter 7**) which is in line with a recent study.[63] However, male patients do not have lower PP_i levels than female patients.[69] Possibly, female PXE patients with a milder phenotype are overrepresented in the first decades which introduces a selection bias.

Several eye-specific manifestations may also be associated with, or predict the visual outcome. Vision loss in PXE is most often caused by CNV and macular atrophy but recently it was found that acute retinopathy in PXE may also cause vision loss and alter the course of disease.[70] Acute retinopathy in PXE is most pronounced along angioid streaks, which suggests that BM defects may trigger an autoimmune reaction which then affects the outer retina with a varying degree of severity.[70] Acute retinopathy was observed in 5% of the PXE population but this might be an underestimation. The frequent end-stage disease and pre-existing visual impairment in PXE patients likely impede the diagnosis of acute retinopathy in PXE.[70]

Furthermore, some PXE patients have subretinal fluid which is not associated with CNV but rather with pattern-dystrophy like changes and does not respond to VEGF inhibitors.[71] Interestingly, the presence of subretinal fluid in AMD is associated with a reduced risk of geographic atrophy and better visual outcome in late AMD.[34,72] Possibly, the subretinal fluid in late AMD contains protective substances or protects the photoreceptors from the toxic CNV or diseased RPE.[73] Since the subretinal fluid in PXE is not always associated with CNV, its origin is unclear. Possibly, it represents a decreased RPE pump function since it is often associated with pattern-dystrophy like changes and thus RPE dysfunction.[74] However, the possible protective effect warrants further research.

Lastly, PXE patients have a relatively high prevalence of reticular pseudodrusen, which are associated with the degree of BM calcification and precede macular atrophy.[19,75] Reticular pseudodrusen predict progression to atrophy in AMD patients and are also prevalent in Sorsby fundus dystrophy which again illustrates the vital role of BM.[76–78] Probably, the presence of reticular pseudodrusen in PXE indicates an early stage of RPE dysfunction, similar to pattern-like dystrophy.

The effect of etidronate on CNV activity

In a post-hoc analysis of the TEMP trial we did not find a protecting, nor a deteriorating effect of etidronate on CNV activity in PXE patients (**Chapter 8**). The earlier findings could be explained by a baseline imbalance of CNV activity, even though the trial had a randomized design. This provides a lesson for future randomized trials to investigate a possible baseline imbalance in case of surprising findings, since not adjusting for baseline imbalance could bias the results and clinical implications.[79]

This study ensures that etidronate is safe regarding CNV activity but it is unclear whether etidronate can halt BM calcification, besides halting arterial calcification, since an imaging-based marker for BM calcification is lacking. Moreover, in PXE patients with macular degeneration, other measures than a quantifiable biomarker might be more appropriate clinical endpoints since end-stage retinal disease often reduces imaging quality. For example, pattern-dystrophy like changes on FAF and the progression of macular atrophy are clinically relevant since they precede or cause visual deterioration.[19,80]

Towards a measurement of BM calcification

We developed three surrogate markers for BM calcification: the extent of angioid streaks, the eccentricity of peau d'orange (both using NIR), and the RPE-BM reflectivity on SD-OCT. The extent of angioid streaks is a rough measure that classifies the length of the longest angioid streak in several zones and is applicable in nearly all disease stages but is not suitable for longitudinal measurements (**Chapter 7**). The eccentricity of peau d'orange is a subjective semi-quantitative measurement adapted from a method of Gliem et al and is probably most informative in earlier disease stages (**Chapter 2**).[75,81] It may detect progression in a few years but the measurement is subjective and depends on image contrast. Since BM calcification is hyperreflective on SD-OCT, we developed a method to quantify the SD-OCT reflectivity to obtain an objective marker for BM calcification (**Chapter 9**).[74,82,83] In this proof-of-concept study, we demonstrated that the reflectivity profile distinguishes PXE patients from controls and that the BM reflectivity is twice as high in PXE patients than in controls.

Quantification of OCT reflectivity

Measuring reflectivity is less straightforward than measuring thicknesses with SD-OCT. Reflectivity relies on image quality and the absolute values are affected by image processing.[84] The appearance and the peaks of reflectivity profiles are increasingly being used to measure retinal disease characteristics.[85,86] Our method is based on the

reflectivity profile but has several improvements that extend its application. First, all A-scans are aligned based on the segmentation coordinates, which allows measuring the total scanned area even though the reflectivity profiles in the fovea differ from more peripheral reflectivity.[21,87] Second, this approach allows normalization to a layer of choice, which is one of the options to correct for the image processing by the OCT device.[88,89] Third, all pixels are weighed to the retinal layer thickness to correct for local differences such as the thinning of the inner retina at the foveal dip.

Even though we demonstrated that the BM reflectivity differs between young PXE patients and controls, there is considerable variability both between and within patients. In PXE patients, different stages of BM calcification may attribute to the between-patient variability. Furthermore, the amount of melanin in the RPE slightly affects the RPE reflectivity and may also attribute to between-patient variability of the BM reflectivity, since the RPE cannot be visualized separately from the BM.[90] The large within-patient variability is likely caused by patient-induced motions and small changes in the direction of the laser beam which can have a large impact on the reflectivity values and notoriously affect the intra-patient variation of reflectivity measurements of OCT.[91–93] This effect may very well be enhanced in PXE patients because the OCT device normalizes all values depending on the peak signal. Because the peak signal is higher in PXE patients, the relative reflectivity difference between the signal and the constant noise floor will be larger, which might increase the variability of different measures within a patient.

The high within-patient variability limits the use of this measurement of BM reflectivity as a longitudinal biomarker at this moment. To improve the reproducibility, a larger sample with repeated measures is required to determine the determinants of variability. Possibly, normalization with the help of an attenuation coefficient improves the reproducibility.[89] Furthermore, the introduction of the Spectralis OCT2 module might improve the OCT quality since it has a scan rate twice as fast as the currently used module.[94] Moreover, this method needs to be validated in another cohort of PXE patients and needs to be correlated with other measures of BM calcification to investigate whether the BM reflectivity also represents the severity of BM calcification.

Interpretation and implications of the BM reflectivity measurement

The origin of the RPE-BM reflectivity is attributed to the mitochondria which are situated at the basal part of the RPE cells and are considered to be one of the most light-scattering organelles of a cell.[95–97] The contribution of BM to the RPE-BM

reflectivity is still unclear since the thickness of BM is below the axial resolution of an SD-OCT scan. A close look at the reflectivity profiles reveals that the RPE-BM peak reflectivity is located more posterior in PXE patients than in controls (Figure 9.1). This suggests that a higher reflective signal originates from BM in PXE patients and not from mitochondrial RPE alterations following BM pathology, which is in concordance with the histopathological localization of calcification in BM in PXE patients.[98]

Moreover, these findings suggest that BM attributes to the RPE reflectivity in normal subjects as well. In a previous study, increasing RPE reflectivity correlated with ageing and this effect was attributed to a hypothetical enlargement of melanosomes.[99] However, recent studies demonstrated that melanosomes probably are not the origin of RPE reflectivity.[90,96,100] Since BM shows increased calcification with ageing in normal subjects, it is plausible that the increased RPE reflectivity derives from the changes in BM.[99,101] This implicates that the reflectivity of the fourth reflective band not only derives from the RPE but the BM as well. BM calcification is not only involved in ageing but it partly drives AMD as well.[58] BM calcification likely is an early feature of AMD and the BM reflectivity might thus serve as an early marker for AMD.

Future perspectives and research opportunities

The research in the thesis attributes to a better knowledge of the ophthalmological consequences and visual prognosis of PXE. However, as always, this has raised more questions which warrant further research. For a better understanding of BM calcification in PXE, future research should focus on histopathological analysis of BM calcification, imaging-based biomarkers for BM calcification, investigating the early stage of BM calcification and a systems approach of PXE.

Histopathological analysis of BM calcification

The last histopathological study on PXE-related BM calcification in humans was published in 2003, and in mice in 2012.[2,3] These studies preceded the new insights in BM calcification that were found due to new and multimodal retinal imaging, such as the spread of peau d'orange and the finding of ICG-A hypofluorescence.[1,71] The insights from clinical imaging of previous studies and this thesis necessitate histopathological research to correlate the imaging findings with BM pathology. Histopathological analysis of PXE eyes might elucidate what BM changes underpin the different zones as seen in PXE eyes, what the differences are between different degrees of calcification and what properties of BM and/or type of fibres predetermine BM calcification.

Recently, we were able to investigate calcification (hydroxyapatite) in four postmortem PXE eyes. Using a hydroxyapatite specific fluorescence dye[102], we found a unique meshwork of hydroxyapatite deposition (Figure 10.2) that can be separated by "cracks" developing within the Bruch's membrane (Figure 10.2, B and C). Based on the green autofluorescence of the Bruch's membrane, these likely represent angioid streaks (Figure 10.2, C) observed on clinical imaging. Further analytical investigation of these eyes and a correlation between clinical retinal imaging of the same patient is the research focus in the upcoming months.

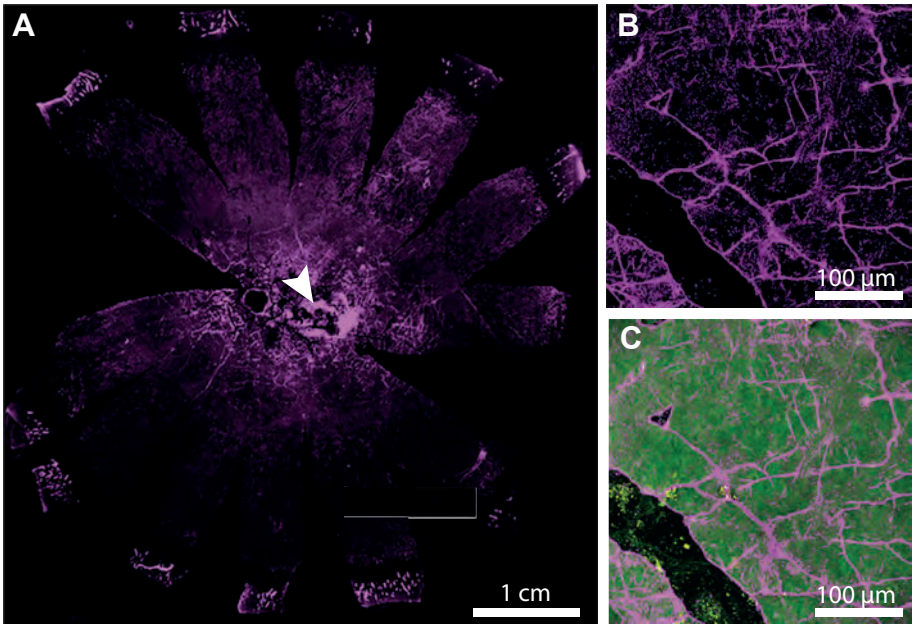

Figure 10.2 Presence and distribution of hydroxyapatite deposits (magenta/purple) in a PXE donor eye. After the removal of the neurosensory retina and the RPE, the whole mounted Bruch's membrane/choroid complex (A) shows the presence of hydroxyapatite in the entire posterior pole as 'streaks'. Image generated by a low resolution (21 µm by 21 µm) fluorescence scanner (LiCor Odyssey system). In the macula, a fibrotic scar is indicated with a white arrowhead. High resolution confocal microscopy (Leica SP8) images at the level of Bruch's membrane reveal that hydroxyapatite precipitates for a meshwork-like structure (B). The area where Bruch's membrane is separated, but the edges are labelled for hydroxyapatite is likely an angioid streak. Green is the natural autofluorescence of Bruch's membrane (C). This image is printed with permission from dr. I Lengyel, Queen's University Belfast.

This newly discovered meshwork of hydroxyapatite might also explain the origin and the different patterns of angioid streaks. It was assumed that the 'coquille d'oeuf' area represented a brittle BM which is prone to break and cause angioid streaks radiating from the optic nerve due to mechanical stress.[103] However, some young patients present with angioid streaks through peau d'orange, which is thought to be non-confluent BM calcification (Figure 2.2 B6). Since the edges of the presumed angioid streak stain for hydroxyapatite, it could be that the meshwork of hydroxyapatite deposition predisposes the 'cracks' in BM which will lead to clinical angioid streaks.

Assessment of BM calcification with new imaging techniques

New imaging techniques and adaptations of existing image techniques, such as fluorescence lifetime imaging ophthalmoscopy, adaptive optics and OCT elastography are emerging and might be promising to use in further PXE studies.

Fluorescence lifetime imaging ophthalmoscopy measures the fluorescence decay time, compared to the commonly used FAF which measures the fluorescence intensity.[104,105] Recently, the fluorophore tetracycline was used to stain hydroxyapatite in the human retina, which enables visualization of the hydroxyapatite depositions in the retina.[106] Though *in vivo* studies are awaited for, this approach might provide histopathological information on BM calcification during life.

Furthermore, adaptive optics allow for a near-microscopal view of retinal tissue of different imaging modalities by correcting for higher-order aberrations and allows *in vivo* visualization of the RPE mosaic.[16,107] Patients with AMD had an abnormal RPE morphology when visualized with adaptive optics enhanced ICG-A and FAF, also in areas with normal confocal FAF.[16,107] Adaptive optics enhanced ICG-A could provide detailed topographical information on the permeability of BM, and adaptive optics enhanced FAF could be an early marker for the RPE vitality in PXE patients.

Finally, BM calcification mainly affects the elastic fibres in BM which, presumably, subsequently affects the elasticity of BM.[108] OCT elastography quantifies the elasticity by detecting phase differences when applying pressure and provides information on the mechanical properties of tissue.[94,109] Though detailed information on the elasticity of the retina and the choroid-BM-RPE complex in humans are lacking, this approach seems promising to measure a plausibly impaired elasticity of BM due to BM in PXE calcification.[110]

A controlled study which combines these methods will be incredibly valuable for a better understanding of the effects of BM calcification in general. A correlation of *in vivo* hydroxyapatite staining with adaptive optics enhanced ICG-A might elucidate the effect of BM calcification on its permeability, while a correlation with adaptive optics enhanced FAF shows the early effects of BM calcification on early RPE damage. An *in vivo* hydroxyapatite staining of BM calcification correlated with OCT elastography might then provide information on the functional changes of BM during life.

A focus on the early stage of PXE

The ICG hypofluorescence in an early disease stage (**Chapter 2**) and the decreased EZ reflectivity in PXE patients younger than 40 years (**Chapter 9**) suggest that BM calcification impairs the vitality of the outer retina early in the disease. A cross-sectional study in PXE patients without macular degeneration with multimodal imaging (including SD-OCT, late-phase ICG-A and OCT angiography) and assessment of the retinal function with a multifocal ERG (mfERG) is warranted for further investigation.

Comparing the EZ reflectivity with the mfERG might elucidate whether the decreased reflectivity indeed represents decreased retinal function.[21] If so, the EZ reflectivity could serve as a marker for photoreceptor vitality in PXE patients. Next, comparing the extent of late-phase ICG-A hypofluorescence with mfERG will provide a topographical map of the retina which shows the effects of decreased BM permeability on the retinal function. Furthermore, structural SD-OCT and OCT angiography can then provide information on the vascular network and blood flow density of the choroid, to investigate the early effects of BM calcification on its adjacent tissues. Ideally, patients should be followed for at least 5 or 10 years to be able to detect considerable change in longitudinal data.

Furthermore, the effect of an early treatment with etidronate warrants investigation. Until now, etidronate has only been administered to patients in a later disease stage, but earlier treatment is probably required to prevent macular degeneration.[111–113] At the moment, a trial in the UMC Utrecht is being designed which will investigate whether early treatment with etidronate can halt or reverse ectopic calcification, and thereby may prevent macular degeneration.

A systems approach to PXE

Lastly, a systems approach including proteomics and metabolomics will provide a more complete overview of the systemic changes in PXE and might explain the different phenotypes. First, the characteristics of PXE patients should be compared to controls, to investigate which systemic changes are associated with PXE. Recent studies already indicated a different metabolite profile different expression of proteins which are associated with premature ageing ageing.[114,115] The presence of hydroxyapatite is associated with the release of IL-1β from monocytes, therefore PXE might also be associated with a different inflammosome.[116] Next, different phenotypes can be compared, e.g. patients with macular atrophy compared to patients without macular atrophy. Possibly, there are markers that can distinguish between different phenotypes which could provide a personalized prognosis.

References

1. Charbel Issa P, Finger RP, Gotting C, Hendig D, Holz FG, Scholl HPN. Centrifugal fundus abnormalities in pseudoxanthoma elasticum. *Ophthalmology*. 2010;117(7):1406-1414. doi:10.1016/j.ophtha.2009.11.008
2. Gorgels TGMF, Teeling P, Meeldijk JD, et al. Abcc6 deficiency in the mouse leads to calcification of collagen fibers in Bruch's membrane. *Exp Eye Res*. 2012;104:59-64. doi:10.1016/j.exer.2012.09.009
3. Gheduzzi D, Sammarco R, Quaglino D, et al. Extracutaneous ultrastructural alterations in pseudoxanthoma elasticum. *Ultrastruct Pathol*. 2003;27(6):375-384.
4. Chong NHV, Keonin J, Luthert PJ, et al. Decreased thickness and integrity of the macular elastic layer of Bruch's membrane correspond to the distribution of lesions associated with age-related macular degeneration. *Am J Pathol*. 2005;166(1):241-251. doi:10.1016/S0002-9440(10)62248-1
5. Newsome DA, Huh W, Green WR. Bruch's membrane age-related changes vary by region. *Curr Eye Res*. 1987;6(10):1211-1221. doi:10.3109/02713688709025231
6. Gliem M, Fimmers R, Muller PL, et al. Choroidal changes associated with Bruch membrane pathology in pseudoxanthoma elasticum. *Am J Ophthalmol*. 2014;158(3):644. doi:10.1016/j.ajo.2014.05.031
7. Dolz-Marco R, Andreu-Fenoll M, Hernández-Martínez P, Pinazo-Durán MD, Gallego-Pinazo R. Automated macular choroidal thickness measurement by swept-source optical coherence tomography in pseudoxanthoma elasticum. *Int J Retin Vitr*. 2016;2:15. doi:10.1186/s40942-016-0040-0
8. Ellabban AA, Tsujikawa A, Matsumoto A, et al. Macular choroidal thickness and volume in eyes with angioid streaks measured by swept source optical coherence tomography. *Am J Ophthalmol*. 2012;153(6):1133-1143. doi:10.1016/j.ajo.2011.12.013
9. Kranenburg G, de Jong PA, Mali WP, Attrach M, Visseren FLJ, Spiering W. Prevalence and severity of arterial calcifications in pseudoxanthoma elasticum (PXE) compared to hospital controls. Novel insights into the vascular phenotype of PXE. *Atherosclerosis*. 2017;256:7-14. doi:10.1016/J.ATHEROSCLEROSIS.2016.11.012
10. Kranenburg G, Visseren FLJ, de Borst GJ, de Jong PA, Spiering W. Arterial stiffening and thickening in patients with pseudoxanthoma elasticum. *Atherosclerosis*. 2018;270:160-165. doi:10.1016/J.ATHEROSCLEROSIS.2018.02.006
11. Kur J, Newman EA, Chan-Ling T. Cellular and physiological mechanisms underlying blood flow regulation in the retina and choroid in health and disease. *Prog Retin Eye Res*. 2012;31(5):377-406. doi:10.1016/j.preteyeres.2012.04.004
12. Hidalgo-Díaz T, Morillo-Sánchez MJ, Kamal-Salah R, Rius-Díaz F, García-Fernandez M, García-Campos JM. Macular choroidal thickness in patients with pseudoxanthoma elasticum measured by enhanced-depth imaging spectral-domain optical coherence tomography. *Int Ophthalmol*. 2020;40(7):1749-1758. doi:10.1007/s10792-020-01343-2
13. Chang AA, Morse LS, Handa JT, et al. Histologic localization of indocyanine green dye in aging primate and human ocular tissues with clinical angiographic correlation. *Ophthalmology*. 1998;105(6):1060-1068. doi:10.1016/S0161-6420(98)96008-0
14. Chang AA, Zhu M, Billson F. The Interaction of Indocyanine Green with Human Retinal Pigment Epithelium. *Investig Opthalmology Vis Sci*. 2005;46(4):1463. doi:10.1167/iovs.04-0825
15. Chang AA, Zhu M, Billson FA, Kumar NL, Beaumont. Indocyanine green localisation in surgically excised choroidal neovascular membrane in age related macular degeneration. *Br J Ophthalmol*. 2004;88(2):307-309. doi:10.1136/bjo.2003.024893

16. Tam J, Liu J, Dubra A, Fariss R. In vivo imaging of the human retinal pigment epithelial mosaic using adaptive optics enhanced indocyanine green ophthalmoscopy. *Investig Ophthalmol Vis Sci*. 2016;57(10):4376-4384. doi:10.1167/iovs.16-19503
17. Finger RP, Charbel Issa P, Ladewig M, Gotting C, Holz FG, Scholl HPN. Fundus autofluorescence in Pseudoxanthoma elasticum. *Retina*. 2009;29(10):1496-1505. doi:10.1097/IAE.0b013e3181aade47
18. Agarwal A, Patel P, Adkins T, Gass JDM. Spectrum of pattern dystrophy in pseudoxanthoma elasticum. *Arch Ophthalmol (Chicago, Ill 1960)*. 2005;123(7):923-928. doi:10.1001/archopht.123.7.923
19. Gliem M, Muller PL, Birtel J, Hendig D, Holz FG, Charbel Issa P. Frequency, Phenotypic Characteristics and Progression of Atrophy Associated With a Diseased Bruch's Membrane in Pseudoxanthoma Elasticum. *Invest Ophthalmol Vis Sci*. 2016;57(7):3323-3330. doi:10.1167/iovs.16-19388
20. Flores M, Debellemanière G, Bully A, et al. Reflectivity of the outer retina on spectral-domain optical coherence tomography as a predictor of photoreceptor cone density. *Am J Ophthalmol*. 2015;160(3):588-595.e2. doi:10.1016/j.ajo.2015.06.008
21. Wu Z, Ayton LN, Guymer RH, Luu CD. Relationship Between the Second Reflective Band on Optical Coherence Tomography and Multifocal Electroretinography in Age-Related Macular Degeneration. *Investig Opthalmology Vis Sci*. 2013;54(4):2800. doi:10.1167/iovs.13-11613
22. Gin TJ, Wu Z, Chew SKH, Guymer RH, Luu CD. Quantitative analysis of the ellipsoid zone intensity in phenotypic variations of intermediate age-related macular degeneration. *Investig Ophthalmol Vis Sci*. 2017;58(4):2079-2086. doi:10.1167/iovs.16-20105
23. Saleh M, Flores M, Gauthier AS, Elphege E, Delbosc B. Quantitative analysis of photoreceptor layer reflectivity on en-face optical coherence tomography as an estimator of cone density. *Graefe's Arch Clin Exp Ophthalmol*. 2017;255(11):2119-2126. doi:10.1007/s00417-017-3761-3
24. Hood DC, Zhang X, Ramachandran R, et al. The inner segment/outer segment border seen on optical coherence tomography is less intense in patients with diminished cone function. *Invest Ophthalmol Vis Sci*. 2011;52(13):9703-9709. doi:10.1167/iovs.11-8650
25. Sampson DM, Alonso-Caneiro D, Chew AL, et al. Enhanced Visualization of Subtle Outer Retinal Pathology by En Face Optical Coherence Tomography and Correlation with Multi-Modal Imaging. *PLoS One*. 2016;11(12):e0168275. doi:10.1371/journal.pone.0168275
26. Gliem M, Müller PL, Mangold E, et al. Sorsby fundus dystrophy: Novel mutations, novel phenotypic characteristics, and treatment outcomes. *Investig Ophthalmol Vis Sci*. 2015;56(4):2664-2676. doi:10.1167/iovs.14-15733
27. Soumplis V, Sergouniotis PI, Robson AG, et al. Phenotypic findings in C1QTNF5 retinopathy (late-onset retinal degeneration). *Acta Ophthalmol*. 2013;91(3):e191-e195. doi:10.1111/aos.12010
28. Saint-Geniez M, Kurihara T, Sekiyama E, Maldonado AE, D'Amore PA. An essential role for RPE-derived soluble VEGF in the maintenance of the choriocapillaris. *Proc Natl Acad Sci U S A*. 2009;106(44):18751-18756. doi:10.1073/pnas.0905010106
29. Mullins RF, Johnson MN, Faidley EA, Skeie JM, Huang J. Choriocapillaris Vascular Dropout Related to Density of Drusen in Human Eyes with Early Age-Related Macular Degeneration. *Investig Opthalmology Vis Sci*. 2011;52(3):1606. doi:10.1167/iovs.10-6476
30. Handa JT, Bowes Rickman C, Dick AD, et al. A systems biology approach towards understanding and treating non-neovascular age-related macular degeneration. *Nat Commun*. 2019;10(1):3347. doi:10.1038/s41467-019-11262-1
31. Finger RP, Fenwick E, Marella M, et al. The relative impact of vision impairment and cardiovascular disease on quality of life: the example of pseudoxanthoma elasticum. *Health Qual Life Outcomes*. 2011;9:113. doi:10.1186/1477-7525-9-113
32. Williams RA, Brody BL, Thomas RG, Kaplan RM, Brown SI. The psychosocial impact of macular degeneration. *Arch Ophthalmol*. 1998;116(4):514-520. doi:10.1001/archopht.116.4.514

33. Rosenfeld PJ, Brown DM, Heier JS, et al. Ranibizumab for Neovascular Age-Related Macular Degeneration. *N Engl J Med*. 2006;355(14):1419-1431. doi:10.1056/NEJMoa054481
34. Grunwald JE, Daniel E, Huang J, et al. Risk of geographic atrophy in the comparison of age-related macular degeneration treatments trials. *Ophthalmology*. 2014;121(1):150-161. doi:10.1016/j.ophtha.2013.08.015
35. Young M, Chui L, Fallah N, et al. Exacerbation of choroidal and retinal pigment epithelial atrophy after anti-vascular endothelial growth factor treatment in neovascular age-related macular degeneration. *Retina*. 2014;34(7):1308-1315. doi:10.1097/IAE.0000000000000081
36. Schoenberger SD, Agarwal A. Geographic chorioretinal atrophy in pseudoxanthoma elasticum. *Am J Ophthalmol*. 2013;156(4):715-723. doi:10.1016/j.ajo.2013.05.034
37. Hess K, Gliem M, Birtel J, et al. IMPAIRED DARK ADAPTATION ASSOCIATED WITH A DISEASED BRUCH MEMBRANE IN PSEUDOXANTHOMA ELASTICUM. *Retina*. Published online December 2019:1. doi:10.1097/IAE.0000000000002689
38. Audo I, Vanakker OM, Smith A, et al. Pseudoxanthoma elasticum with generalized retinal dysfunction, a common finding? *Invest Ophthalmol Vis Sci*. 2007;48(9):4250-4256. doi:10.1167/iovs.05-1604
39. Holz FG, Jubb C, Fitzke FW, Bird AC, Pope FM. Dark adaptation and scotopic perimetry over "peau d'orange" in pseudoxanthoma elasticum. *Br J Ophthalmol*. 1994;78(1):79-80.
40. François J, Rouck A. Electrophysiological Studies in Groenblad-strandberg Syndrome. In: ; 1980:19-25. doi:10.1007/978-94-009-9180-4_2
41. Farhi D, Descamps V, Picard C, Mahieu-Caputo D, Doan S, Crickx B. Is pseudoxanthoma elasticum with severe angioid streaks an indication for Caesarean section? *J Eur Acad Dermatology Venereol*. 2006;20(10):1361-1362. doi:10.1111/j.1468-3083.2006.01717.x
42. Camacho M, Rengel C, López-Herrero E, Carrillo JL, Eslava AJ, Valdivielso P. Approach to the management of pregnancy in patients with pseudoxanthoma elasticum: a review. *J Obstet Gynaecol (Lahore)*. 2016;36(8):1061-1066. doi:10.1080/01443615.2016.1196478
43. Peracha ZH, Rosenfeld PJ. Anti–Vascular Endothelial Growth Factor Therapy in Pregnancy. *Retina*. 2016;36(8):1413-1417. doi:10.1097/IAE.0000000000001200
44. Polizzi S, Mahajan VB. Intravitreal Anti-VEGF Injections in Pregnancy: Case Series and Review of Literature. *J Ocul Pharmacol Ther*. 2015;31(10):605-610. doi:10.1089/jop.2015.0056
45. Avery RL, Castellarin AA, Steinle NC, et al. Systemic pharmacokinetics following intravitreal injections of ranibizumab, bevacizumab or aflibercept in patients with neovascular amd. *Br J Ophthalmol*. 2014;98(12):1636-1641. doi:10.1136/bjophthalmol-2014-305252
46. Pomozi V, Brampton C, Fulop K, et al. Analysis of pseudoxanthoma elasticum-causing missense mutants of *ABCC6* in vivo; pharmacological correction of the mislocalized proteins. *J Invest Dermatol*. 2014;134(4):946-953. doi:10.1038/jid.2013.482
47. Legrand A, Cornez L, Samkari W, et al. Mutation spectrum in the ABCC6 gene and genotype–phenotype correlations in a French cohort with pseudoxanthoma elasticum. *Genet Med*. 2017;19(8):909-917. doi:10.1038/gim.2016.213
48. Schulz V, Hendig D, Szliska C, Gotting C, Kleesiek K. Novel mutations in the ABCC6 gene of German patients with pseudoxanthoma elasticum. *Hum Biol*. 2005;77(3):367-384.
49. Jansen RS, Duijst S, Mahakena S, et al. *ABCC6*-mediated ATP secretion by the liver is the main source of the mineralization inhibitor inorganic pyrophosphate in the systemic circulation-brief report. *Arterioscler Thromb Vasc Biol*. 2014;34(9):1985-1989. doi:10.1161/ATVBAHA.114.304017
50. Jansen RS, Kucukosmanoglu A, de Haas M, et al. *ABCC6* prevents ectopic mineralization seen in pseudoxanthoma elasticum by inducing cellular nucleotide release. *Proc Natl Acad Sci U S A*. 2013;110(50):20206-20211. doi:10.1073/pnas.1319582110
51. Plomp AS, Bergen AAB, Florijn RJ, et al. Pseudoxanthoma elasticum: Wide phenotypic variation in homozygotes and no signs in heterozygotes for the c.3775delT mutation in *ABCC6*. *Genet Med*. 2009;11(12):852-858. doi:10.1097/GIM.0b013e3181c00a96

52. Pfendner EG, Vanakker OM, Terry SF, et al. Mutation detection in the *ABCC6* gene and genotype phenotype analysis in a large international case series affected by pseudoxanthoma elasticum. *J Med Genet*. 2007;44(10):621-628. doi:10.1136/jmg.2007.051094
53. Iwanaga A, Okubo Y, Yozaki M, et al. Analysis of clinical symptoms and *ABCC6* mutations in 76 Japanese patients with pseudoxanthoma elasticum. *J Dermatol*. Published online February 2017. doi:10.1111/1346-8138.13727
54. Chassaing N, Martin L, Mazereeuw J, et al. Novel *ABCC6* mutations in pseudoxanthoma elasticum. *J Invest Dermatol*. 2004;122(3):608-613. doi:10.1111/j.0022-202X.2004.22312.x
55. Hendig D, Schulz V, Eichgrun J, Szliska C, Gotting C, Kleesiek K. New *ABCC6* gene mutations in German pseudoxanthoma elasticum patients. *J Mol Med (Berl)*. 2005;83(2):140-147. doi:10.1007/s00109-004-0588-2
56. Mansour AM, Shields JA, Annesley WH, El-Baba F, Tasman W, Tomer TL. Macular degeneration in angioid streaks. *Ophthalmologica*. 1988;197(1):36-41. doi:10.1159/000309915
57. Schlingemann RO. Role of growth factors and the wound healing response in age-related macular degeneration. *Graefe's Arch Clin Exp Ophthalmol*. 2004;242(1):91-101. doi:10.1007/s00417-003-0828-0
58. Spraul CW, Lang GE, Grossniklaus HE, Lang GK. Histologic and morphometric analysis of the choroid, Bruch's membrane, and retinal pigment epithelium in postmortem eyes with age-related macular degeneration and histologic examination of surgically excised choroidal neovascular membranes. *Surv Ophthalmol*. 1999;44(2 SUPPL. 1):10-32. doi:10.1016/S0039-6257(99)00086-7
59. Plomp AS, Toonstra J, Bergen AAB, van Dijk MR, de Jong PTVM. Proposal for updating the pseudoxanthoma elasticum classification system and a review of the clinical findings. *Am J Med Genet A*. 2010;152A(4):1049-1058. doi:10.1002/ajmg.a.33329
60. Gliem M, Wieg I, Birtel J, et al. Retinal findings in carriers of monoallelic *ABCC6* mutations. *Br J Ophthalmol*. Published online 2019:1-4. doi:10.1136/bjophthalmol-2018-313448
61. Nitschke Y, Baujat G, Botschen U, et al. Generalized arterial calcification of infancy and pseudoxanthoma elasticum can be caused by mutations in either ENPP1 or *ABCC6*. *Am J Hum Genet*. 2012;90(1):25-39. doi:10.1016/j.ajhg.2011.11.020
62. Hendig D, Knabbe C, Götting C. New insights into the pathogenesis of pseudoxanthoma elasticum and related soft tissue calcification disorders by identifying genetic interactions and modifiers. *Front Genet*. 2013;4:114. doi:10.3389/fgene.2013.00114
63. De Vilder EYG, Hosen MJ, Martin L, et al. VEGFA variants as prognostic markers for the retinopathy in Pseudoxanthoma elasticum. *Clin Genet*. Published online April 8, 2020. doi:10.1111/cge.13751
64. Zarbock R, Hendig D, Szliska C, Kleesiek K, Gotting C. Vascular endothelial growth factor gene polymorphisms as prognostic markers for ocular manifestations in pseudoxanthoma elasticum. *Hum Mol Genet*. 2009;18(17):3344-3351. doi:10.1093/hmg/ddp259
65. Edwards AO. Complement Factor H Polymorphism and Age-Related Macular Degeneration. *Science (80-)*. 2005;308(5720):421-424. doi:10.1126/science.1110189
66. Haines JL, Hauser MA, Schmidt S, et al. Complement factor H variant increases the risk of age-related macular degeneration. *Science (80-)*. 2005;308(5720):419-421. doi:10.1126/science.1110359
67. Klein RJ, Zeiss C, Chew EY, et al. Complement Factor H Polymorphism in Age-Related Macular Degeneration. *Science (80-)*. 2005;308(5720):385-389. doi:10.1126/science.1109557
68. Chakravarthy U, Augood C, Bentham GC, et al. Cigarette Smoking and Age-Related Macular Degeneration in the EUREYE Study. *Ophthalmology*. 2007;114(6):1157-1163. doi:10.1016/j.ophtha.2006.09.022
69. Sánchez-Tévar AM, García-Fernández M, Murcia-Casas B, et al. Plasma inorganic pyrophosphate and alkaline phosphatase in patients with pseudoxanthoma elasticum. *Ann Transl Med*. 2019;7(24):798. doi:10.21037/atm.2019.12.73

70. Gliem M, Birtel J, Müller PL, et al. Acute Retinopathy in Pseudoxanthoma Elasticum. *JAMA Ophthalmol*. Published online August 8, 2019. doi:10.1001/jamaophthalmol.2019.2910
71. Zweifel SA, Imamura Y, Freund KB, Spaide RF. Multimodal fundus imaging of pseudoxanthoma elasticum. *Retina*. 2011;31(3):482-491. doi:10.1097/IAE.0b013e3181f056ce
72. Waldstein SM, Wright J, Warburton J, Margaron P, Simader C, Schmidt-Erfurth U. Predictive Value of Retinal Morphology for Visual Acuity Outcomes of Different Ranibizumab Treatment Regimens for Neovascular AMD. In: *Ophthalmology*. Vol 123. Elsevier Inc.; 2016:60-69. doi:10.1016/j.ophtha.2015.09.013
73. Jaffe GJ, Ying GS, Toth CA, et al. Macular Morphology and Visual Acuity in Year Five of the Comparison of Age-related Macular Degeneration Treatments Trials. *Ophthalmology*. 2019;126(2):252-260. doi:10.1016/j.ophtha.2018.08.035
74. Gliem M, De Zaeytijd J, Finger RP, Holz FG, Leroy BP, Issa PC. An update on the ocular phenotype in patients with pseudoxanthoma elasticum. *Front Genet*. 2013;4(APR):14. doi:10.3389/fgene.2013.00014
75. Gliem M, Hendig D, Finger RP, Holz FG, Charbel Issa P. Reticular pseudodrusen associated with a diseased bruch membrane in pseudoxanthoma elasticum. *JAMA Ophthalmol*. 2015;133(5):581-588. doi:10.1001/jamaophthalmol.2015.117
76. Finger RP, Wu Z, Luu CD, et al. Reticular pseudodrusen: a risk factor for geographic atrophy in fellow eyes of individuals with unilateral choroidal neovascularization. *Ophthalmology*. 2014;121(6):1252-1256. doi:10.1016/j.ophtha.2013.12.034
77. Sadda SR, Abdelfattah NS, Lei J, et al. Spectral-Domain OCT Analysis of Risk Factors for Macular Atrophy Development in the HARBOR Study for Neovascular Age-Related Macular Degeneration. *Ophthalmology*. Published online 2020. doi:10.1016/j.ophtha.2020.03.031
78. Gliem M, Müller PL, Mangold E, et al. Reticular Pseudodrusen in Sorsby Fundus Dystrophy. *Ophthalmology*. 2015;122(8):1555-1562. doi:10.1016/j.ophtha.2015.04.035
79. Roberts C, Torgerson DJ. Understanding controlled trials. Baseline imbalance in randomised controlled trials. *Br Med J*. 1999;318(7203):185. doi:10.1136/bmj.319.7203.185
80. Murro V, Mucciolo DP, Giorgio D, et al. Pattern dystrophy-like changes and coquille d'oeuf atrophy in elderly patients affected by pseudoxanthoma elasticum. *Graefe's Arch Clin Exp Ophthalmol*. Published online 2020. doi:10.1007/s00417-020-04748-y
81. Gliem M, Müller PL, Birtel J, et al. Quantitative fundus autofluorescence in pseudoxanthoma elasticum. *Investig Ophthalmol Vis Sci*. 2017;58(14):6159-6165. doi:10.1167/iovs.17-22007
82. Charbel Issa P, Finger RP, Holz FG, Scholl HPN. Multimodal Imaging Including Spectral Domain OCT and Confocal Near Infrared Reflectance for Characterization of Outer Retinal Pathology in Pseudoxanthoma Elasticum. *Investig Opthalmology Vis Sci*. 2009;50(12):5913. doi:10.1167/iovs.09-3541
83. Spaide RF. Peau d'orange and angioid streaks: manifestations of Bruch membrane pathology. *Retina*. 2015;35(3):392-397. doi:10.1097/IAE.0000000000000420
84. Chen X, Hou P, Jin C, et al. Quantitative analysis of retinal layer optical intensities on three-dimensional optical coherence tomography. *Invest Ophthalmol Vis Sci*. 2013;54(10):6846-6851. doi:10.1167/iovs.13-12062
85. Garcia Garrido M, Beck SC, Mühlfriedel R, Julien S, Schraermeyer U, Seeliger MW. Towards a quantitative OCT image analysis. *PLoS One*. 2014;9(6):e100080. doi:10.1371/journal.pone.0100080
86. Khan KN, Borooah S, Lando L, et al. Quantifying the Separation Between the Retinal Pigment Epithelium and Bruch's Membrane using Optical Coherence Tomography in Patients with Inherited Macular Degeneration. *Transl Vis Sci Technol*. 2020;9(6):26. doi:10.1167/tvst.9.6.26
87. Spaide RF, Curcio CA. Anatomical correlates to the bands seen in the outer retina by optical coherence tomography: literature review and model. *Retina*. 2011;31(8):1609-1619. doi:10.1097/IAE.0b013e3182247535

88. Chen C-L, Ishikawa H, Wollstein G, et al. Individual A-Scan Signal Normalization Between Two Spectral Domain Optical Coherence Tomography Devices. *Investig Opthalmology Vis Sci*. 2013;54(5):3463. doi:10.1167/iovs.12-11484
89. Vermeer KA, Mo J, Weda JJA, Lemij HG, de Boer JF. Depth-resolved model-based reconstruction of attenuation coefficients in optical coherence tomography. *Biomed Opt Express*. 2013;5(1):322-337. doi:10.1364/BOE.5.000322
90. Wilk MA, Huckenpahler AL, Collery RF, Link BA, Carroll J. The Effect of Retinal Melanin on Optical Coherence Tomography Images. *Transl Vis Sci Technol*. 2017;6(2):8. doi:10.1167/tvst.6.2.8
91. Teussink MM, Cense B, van Grinsven MJJP, Klevering BJ, Hoyng CB, Theelen T. Impact of motion-associated noise on intrinsic optical signal imaging in humans with optical coherence tomography. *Biomed Opt Express*. 2015;6(5):1632-1647. doi:10.1364/BOE.6.001632
92. Huang X-R, Knighton RW, Feuer WJ, Qiao J. Retinal nerve fiber layer reflectometry must consider directional reflectance. *Biomed Opt Express*. 2016;7(1):22. doi:10.1364/BOE.7.000022
93. Mehta N, Lavinsky F, Gattoussi S, et al. Increased Inner Retinal Layer Reflectivity in Eyes With Acute CRVO Correlates With Worse Visual Outcomes at 12 Months. *Investig Opthalmology Vis Sci*. 2018;59(8):3503. doi:10.1167/iovs.18-24153
94. Aumann S, Donner S, Fischer J, Müller F. Optical Coherence Tomography (OCT): Principle and Technical Realization. In: *High Resolution Imaging in Microscopy and Ophthalmology*. Springer International Publishing; 2019:59-85. doi:10.1007/978-3-030-16638-0_3
95. Litts KM, Zhang Y, Bailey Freund K, Curcio CA. Optical coherence tomography and histology of age-related macular degeneration support mitochondria as reflectivity sources. *Retina*. 2018;38(3):445-461. doi:10.1097/IAE.0000000000001946
96. Cuenca N, Ortuño-Lizarán I, Pinilla I. Cellular Characterization of OCT and Outer Retinal Bands Using Specific Immunohistochemistry Markers and Clinical Implications. *Ophthalmology*. 2018;125(3):407-422. doi:10.1016/j.ophtha.2017.09.016
97. Wilson JD, Cottrell WJ, Foster TH. Index-of-refraction-dependent subcellular light scattering observed with organelle-specific dyes. *J Biomed Opt*. 2007;12(1):014010. doi:10.1117/1.2437765
98. Jensen OA. Bruch's membrane in pseudoxanthoma elasticum. Histochemical, ultrastructural, and x-ray microanalytical study of the membrane and angioid streak areas. *Albrecht Von Graefes Arch Klin Exp Ophthalmol*. 1977;203(3-4):311-320.
99. Chen B, Gao E, Chen H, et al. Profile and Determinants of Retinal Optical Intensity in Normal Eyes with Spectral Domain Optical Coherence Tomography. *PLoS One*. 2016;11(2):e0148183. doi:10.1371/journal.pone.0148183
100. Cuenca N, Ortuño-Lizarán I, Sánchez-Sáez X, et al. Interpretation of OCT and OCTA images from a histological approach: Clinical and experimental implications. *Prog Retin Eye Res*. 2020;(December 2019):100828. doi:10.1016/j.preteyeres.2019.100828
101. Curcio CA, Johnson M. Structure, Function, and Pathology of Bruch's Membrane. In: *Retina*. 5th ed. Elsevier; 2013:465-481. doi:10.1016/B978-1-4557-0737-9.00020-5
102. Thompson RB, Reffatto V, Bundy JG, et al. Identification of hydroxyapatite spherules provides new insight into subretinal pigment epithelial deposit formation in the aging eye. *Proc Natl Acad Sci U S A*. 2015;112(5):1565-1570. doi:10.1073/pnas.1413347112
103. Jampol LM, Acheson R, Eagle RC, Serjeant G, O'Grady R. Calcification of Bruch's Membrane in Angioid Streaks With Homozygous Sickle Cell Disease. *Arch Ophthalmol*. 1987;105(1):93-98. doi:10.1001/archopht.1987.01060010099039
104. Bernstein P, Dysli C, Fischer J, et al. Fluorescence Lifetime Imaging Ophthalmoscopy (FLIO). In: *High Resolution Imaging in Microscopy and Ophthalmology*. Springer International Publishing; 2019:213-235. doi:10.1007/978-3-030-16638-0_10
105. Schweitzer D, Hammer M, Schweitzer F, et al. In vivo measurement of time-resolved autofluorescence at the human fundus. *J Biomed Opt*. 2004;9(6):1214. doi:10.1117/1.1806833

106. Szmacinski H, Hegde K, Zeng H-H, et al. Imaging hydroxyapatite in sub-retinal pigment epithelial deposits by fluorescence lifetime imaging microscopy with tetracycline staining. *J Biomed Opt*. 2020;25(04):1. doi:10.1117/1.jbo.25.4.047001
107. Rossi EA, Rangel-Fonseca P, Parkins K, et al. In vivo imaging of retinal pigment epithelium cells in age related macular degeneration. *Biomed Opt Express*. 2013;4(11):2527. doi:10.1364/boe.4.002527
108. Ugarte M, Hussain AA, Marshall J. An experimental study of the elastic properties of the human Bruch's membrane-choroid complex: Relevance to ageing. *Br J Ophthalmol*. 2006;90(5):621-626. doi:10.1136/bjo.2005.086579
109. Kirby MA, Pelivanov I, Song S, et al. Optical coherence elastography in ophthalmology. *J Biomed Opt*. 2017;22(12):1. doi:10.1117/1.jbo.22.12.121720
110. Qu Y, He Y, Zhang Y, et al. Quantified elasticity mapping of retinal layers using synchronized acoustic radiation force optical coherence elastography. *Biomed Opt Express*. 2018;9(9):4054. doi:10.1364/boe.9.004054
111. Li Q, Kingman J, Sundberg JP, Levine MA, Uitto J. Etidronate prevents, but does not reverse, ectopic mineralization in a mouse model of pseudoxanthoma elasticum (*Abcc6-/-*). *Oncotarget*. 2018;9(56):30721-30730. doi:10.18632/oncotarget.10738
112. Kranenburg G, de Jong PA, Bartstra JW, et al. Etidronate for Prevention of Ectopic Mineralization in Patients With Pseudoxanthoma Elasticum. *J Am Coll Cardiol*. 2018;71(10):1117-1126. doi:10.1016/j.jacc.2017.12.062
113. Bartstra JW, de Jong PA, Kranenburg G, et al. Etidronate halts systemic arterial calcification in pseudoxanthoma elasticum. *Atherosclerosis*. 2020;292(September 2019):37-41. doi:10.1016/j.atherosclerosis.2019.10.004
114. Tiemann J, Wagner T, Vanakker OM, et al. Cellular and Molecular Biomarkers Indicate Premature Aging in Pseudoxanthoma Elasticum Patients. *Aging Dis*. 2020;11(3):536. doi:10.14336/ad.2019.0610
115. Kuzaj P, Kuhn J, Michalek RD, et al. Large-scaled metabolic profiling of human dermal fibroblasts derived from pseudoxanthoma elasticum patients and healthy controls. *PLoS One*. 2014;9(9):e108336. doi:10.1371/journal.pone.0108336
116. Pazár B, Ea H-K, Narayan S, et al. Basic Calcium Phosphate Crystals Induce Monocyte/Macrophage IL-1β Secretion through the NLRP3 Inflammasome In Vitro. *J Immunol*. 2011;186(4):2495-2502. doi:10.4049/jimmunol.1001284

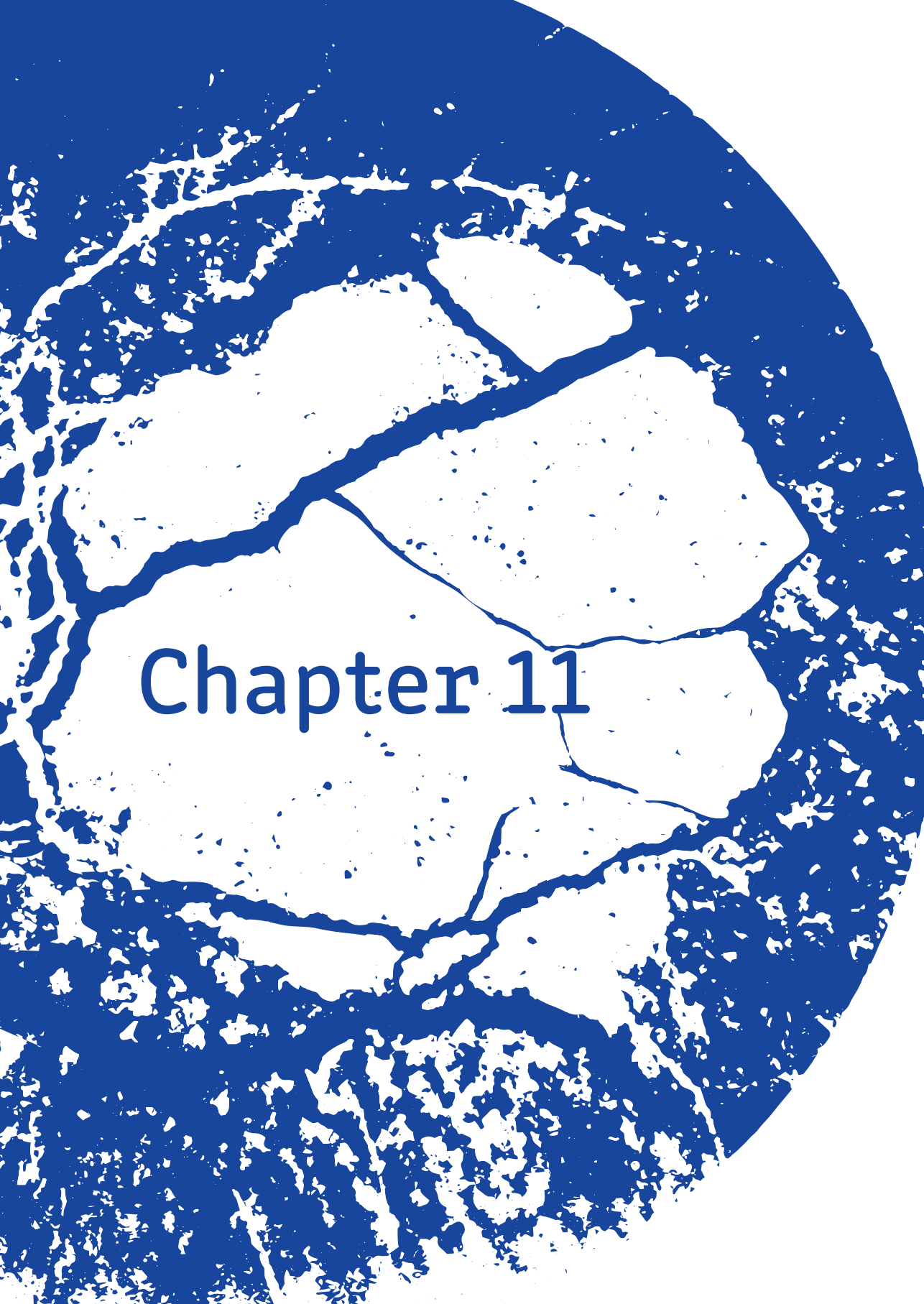
Chapter 11

A brief introduction of the retina (for laymen)

English summary

Nederlandse samenvatting

A brief introduction of the retina (for laymen)

The eye is the organ which lets us perceive light and allows us to see. The light around us enters the eye through the cornea and travels through the lens of the eye. The lens of the eye focuses the light beam on the central retina, which is the interior surface of the eyeball. The retina is actually brain tissue and is the only part of the central nervous system that can be seen without invasive techniques. It consists of multiple layers of neuronal tissue, amongst which the light-sensitive cells, the photoreceptors, commonly known as cones and the rods. One layer is not neuronal: this is the retinal pigment epithelium. The retinal pigment epithelium has multiple functions, amongst which providing nutrients to the retina. A healthy retinal pigment epithelium is important for the vitality of the photoreceptors.

The macula is the part of the retina which is essential for central vision. In this area, there is a high density of cones. The cones are the light-sensitive cells that are responsible for good color vision and good visual acuity, whereas the rods provide contrast in dim light and are important for peripheral vision. The center of the macula has a pit that is fully packed with cones, which is called the fovea. The fovea is therefore essential for detailed and accurate central vision, such as reading. In Figure 11.1A a color photograph of the inside of the eye is presented, which shows the location of the macula and fovea.

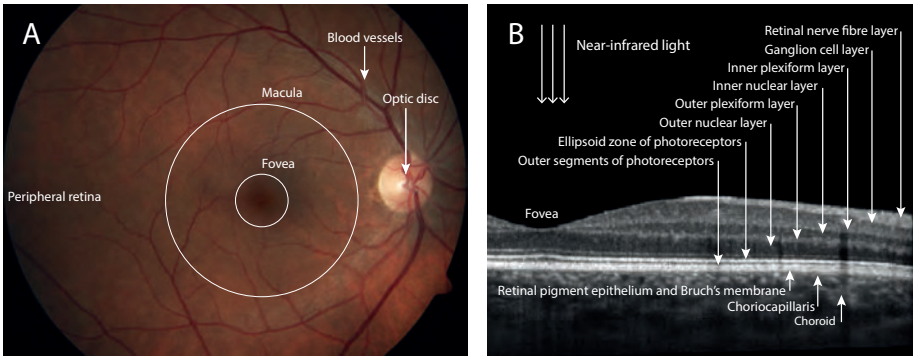

Figure 11.1 Illustration of a normal and healthy retina. On the left a color photograph of the inside of eye (**A**). The area of the fovea and the macula are indicated with circles. On the right an optical coherence tomography scan of a healthy macula (**B**) with indications of retinal layers that will be discussed in this thesis.

The cells in the outer retina get oxygen and nutrients from the choroid, which is a layer with vasculature that surrounds the retina. The choroid is supplied by the internal carotid artery, which is the artery in the neck that also supplies the brain. The blood in the choroid contains the oxygen and nutrients for the retinal layers which have to pass through the Bruch's membrane and retinal pigment epithelium to reach the retinal cells (the cones and rods, amongst others).

To visualize the layers in the retina, an optical coherence tomography (OCT) scan is often used. An OCT scan is made similar to an ultrasound image, but uses near-infrared light instead of sound waves and provides a cross-sectional image of the retina. An example of an OCT scan of a normal retina and its layers can be found in Figure 11.1B. This thesis focuses on Bruch's membrane, which is a very thin layer that separates the retina from the choroid. It is so thin that it cannot be visualized separately on an OCT scan and forms a reflective line together with the retinal pigment epithelium. Bruch's membrane calcifies in the rare disease pseudoxanthoma elasticum, which is studied in this thesis. Eventually, this calcification process often leads to visual-threatening complications in the retina, especially in the macula.

English summary of this thesis

Pseudoxanthoma elasticum (PXE) is a rare disease in which mutations in the *ABCC6* gene lead to ectopic calcification in the skin, vasculature and Bruch's membrane (BM). BM is a thin membrane between the choroid and the retina and facilitates the diffusion of oxygen and nutrients to the retina, and waste products and growth factors to the choroid. Alterations of BM could lead to an impaired diffusion and thereby impair the vitality of the tissues adjacent to BM.

Clinically, the ongoing BM calcification in PXE is visible in the fundus as a mottled and speckled aspect of the fundus, called 'peau d'orange'. This spreads centrifugally and as the calcified BM becomes brittle, this causes BM to break and form 'angioid streaks'. Eventually, PXE patients often develop macular degeneration similar to late age-related macular degeneration but PXE patient develop macular degeneration earlier in life. This leads to a high prevalence of visual impairment at a relatively young age, often due to choroidal neovascularization (CNV) but sometimes due to macular atrophy as well. CNV can be treated with intra-ocular injections but macular atrophy cannot be treated up to now. Unfortunately, a treatment which prevents BM calcification currently does not exist.

Often, PXE patients are aware of the vision loss of their relatives with PXE and have fear for eventual visual impairment. This uncertainty impacts their wellbeing and impedes the planning of major life decisions. Up to now, it is difficult to predict the individual visual prognosis due to various reasons, which are discussed in **Chapter 1**.

In the first part of this thesis, we describe the natural course of BM calcification and the clinical consequences.

In **Chapter 2** we studied age-specific changes of BM calcification by investigating the borders of peau d'orange, the extent of angioid streaks. We observed that there is an area in the fundus that is prone for BM calcification. Within this area, BM calcification slowly confluences and progresses during life.
Also, we studied the late-phase of indocyanine green angiograms. In PXE patients, this often reveals a typical pattern of reduced fluorescence in the central retina. We observed that this pattern appears in the fourth or fifth decade and that the extent of the pattern likely depends on the degree of BM calcification.

In **Chapter 3** the age-specific prevalence of visual impairment and the underlying cause are reported. The prevalence of visual impairment is similar to late age-related macular degeneration but the onset is 20 years earlier. Visual impairment is common in PXE patients, especially in patients over 50 years, of whom 37% is visually impaired and 15% is legally blind. At least 16% of the visual impairment can be attributed to macular atrophy, which currently cannot be treated.

The effects of BM calcification on the choroid are reported in **Chapter 4.** Our aim was to investigate whether arterial stiffness in the intracranial internal carotid artery attributes to choroidal thinning, because this artery supplies blood to the choroid and the choroidal autoregulation might not be sufficient to regulate the increased pulse pressures due to arterial stiffness. However, arterial stiffness was not independently associated with choroidal thinning. Therefore, we assume that choroidal thinning is solely caused by BM calcification.

In **Chapter 5**, we investigated whether a vaginal delivery is safe for the retina of pregnant PXE patients, since the fear for the pushing phase has been a reason for assisted deliveries or even caesarian sections. We showed that a vaginal delivery seems safe for pregnant PXE patients as long as they are monitored for CNV.

In the second part of this thesis we aim to gain insight in the determinants for the visual prognosis and to gain insight in the pathophysiological mechanisms which may help in optimizing a treatment for PXE.

In **Chapter 6** we analyzed whether PXE patients with more severe variants in the *ABCC6* gene have a higher risk of a more severe phenotype. We studied the amount of truncating variants. These truncating variants lead to a loss of function of the protein, non-truncating variants could still lead to a residual amount of function. A truncating variant could therefore be considered as more severe. PXE patients with two truncating variants have more severe arterial calcification, have an earlier onset of longer angioid streaks and have more often CNV than PXE patients with one or more non-truncating mutations. Presumably, PXE patients with a more severe genotype have more severe calcification of BM, but this has yet to be demonstrated.

In **Chapter 7** we studied the correlation between the length of angioid streaks, as a surrogate marker for the extent of BM calcification, and macular degeneration. We found that patients with longer angioid streaks have a higher risk of macular

degeneration, which is the major cause of vision loss in PXE. Therefore, this finding can aid in the clinical counseling of PXE patients for their visual prognosis at a relatively young age.

Lastly, the drug etidronate recently showed beneficial effects on halting arterial calcification but the effects on BM calcification and CNV activity are not conclusive. **Chapter 8** provides an analysis of the effect of etidronate on CNV activity and found that etidronate does not have a protecting, nor a deteriorating effect. This implies that etidronate is safe for the eyes, though the effect on BM calcification has yet to be established due to a lack of biomarkers for BM calcification.

We aimed to develop a biomarker for BM calcification in the third part of thesis. In **Chapter 9** we propose a method to measure BM reflectivity on optical coherence tomography (OCT) and performed a proof-of-concept study. After normalizing the reflectivity values, we found that young PXE patients have an increased reflectivity at the level of BM. This method is promising as a future biomarker for BM calcification.

Nederlandse samenvatting

Pseudoxanthoma elasticum (PXE) is een zeldzame en erfelijke ziekte waarbij er pathologische verkalking optreedt in de huid, bloedvaten en in het oog. In het oog verkalkt het membraan van Bruch, een dun membraan tussen het vaatvlies en het netvlies. Het membraan van Bruch is erg dun (2 – 4 µm), maar ook belangrijk omdat het membraan van Bruch de uitwisseling van stoffen als zuurstof, voedingsstoffen en groeifactoren tussen het vaatvlies en het netvlies faciliteert. Kleine veranderingen in het membraan van Bruch kunnen dus grote verstoringen in het vaatvlies of netvlies geven.

De verkalking van het membraan van Bruch in PXE patiënten is te zien in het oog. Het netvlies heeft een stippelig uiterlijk, de zogenaamde 'peau d'orange' (sinaasappelschil-aspect), wat naar de periferie lijkt uit te breiden. Het verkalkte membraan van Bruch wordt broos en kan breken, waardoor breuklijnen ontstaan, de zogenaamde 'angioide strepen'. De verkalking van het membraan van Bruch leidt tot de ontwikkeling van vaatnieuwvormingen onder het netvlies, die kunnen bloeden en lekken. Daarnaast verslechtert de kwaliteit van het netvlies, waardoor bij een gedeelte van de PXE patiënten het netvlies zal verdunnen.

Deze complicaties lijken op het late stadium van de veelvoorkomende ziekte 'leeftijdsgebonden maculadegeneratie', maar treden tientallen jaren eerder in het leven op. Uiteindelijk wordt een groot aantal patiënten slechtziend of zelfs maatschappelijk blind op een relatief jonge leeftijd. De vaatnieuwvormingen kunnen geremd worden met injecties in het oog, maar de verdunning van het netvlies kan nog niet voorkomen worden. Daarvoor moet uiteindelijk de verkalking van het membraan van Bruch geremd worden. Hiervoor wordt momenteel een medicijn (etidronaat) in het UMC Utrecht onderzocht.

Er is veel onzekerheid over de visuele prognose, ten eerste omdat er nog geen goede behandeling is, maar ook omdat PXE patiënten vaak doorhebben dat lotgenoten of familieleden slechter gaan zien. Helaas is het nog erg moeilijk om te voorspellen wie er slechtziend zal worden, en wie een redelijke visus zal houden. In **Hoofdstuk 1** bespreken we welke factoren belangrijk zijn voor de visuele prognose en waarom het nog zo moeilijk is om deze te voorspellen.

Het eerste deel van dit proefschrift beschrijft het beloop van de verkalking van het membraan van Bruch en wat de consequenties hiervan zijn voor PXE patiënten.

In **Hoofdstuk 2** is er gekeken naar het beloop en de verspreiding van de verkalking van het membraan van Bruch. We vonden dat een bepaald gedeelte van het netvlies aanleg lijkt te hebben om te verkalken, en dit is bovendien al op jonge leeftijd zichtbaar. In dit gedeelte breidt de verkalking zich langzaam uit gedurende het leven. Daarnaast hebben we gekeken naar de uitwasfase van een indocyanine groen angiogram, waarbij een fluorescerende groene kleurstof wordt gebruikt. Bij PXE patiënten zien we hier vaak een typisch patroon van sterk verminderde fluorescentie in het centrale deel van het netvlies. Dit patroon lijkt zich te ontwikkelen in het vierde of vijfde decennium van het leven en hangt vermoedelijk af van de mate van verkalking van het membraan van Bruch.

Om in kaart te brengen wat de impact van PXE is op het visueel functioneren hebben we gekeken hoeveel personen met PXE lijden aan slechtziendheid of blindheid in **Hoofdstuk 3**. De getallen zijn vergelijkbaar met de late vorm van leeftijdsgebonden maculadegeneratie, maar bij PXE treedt het visusverlies al zo'n 20 jaar eerder op. Van alle PXE patiënten ouder dan 50 jaar is 37% slechtziend en 15% maatschappelijk blind. Daarnaast blijkt dat verdunning van het netvlies, naast de vaatnieuwvormingen, minimaal 16% van de slechtziendheid verklaart.

Patiënten met PXE hebben door de verkalking van de bloedvaten vaak een verhoogde vaatstijfheid in de halsslagader. Ook hebben PXE patiënten een verdund vaatvlies. Mogelijk speelt de vaatstijfheid in de halsslagader hierbij een rol, omdat deze slagader het vaatvlies voorziet van bloed, en verhoogde vaatstijfheid leidt tot een hogere polsgolf van het bloed wat het vaatvlies misschien niet goed kan dempen. In **Hoofdstuk 4** hebben we gekeken of de vaatstijfheid effect heeft op de dikte van het vaatvlies, maar dit was niet het geval in zowel PXE patiënten als controles zonder PXE. Daarmee is het waarschijnlijk dat de verdunning van het vaatvlies in PXE enkel wordt veroorzaakt door een verkalkt membraan van Bruch.

In **Hoofdstuk 5** hebben we bij vrouwen met PXE onderzocht wat het effect is van een natuurlijke, vaginale bevalling op de ogen. Hier werd vroeger voor gewaarschuwd en tot op heden werden soms zelfs keizersnedes geadviseerd uit angst voor progressie van oogafwijkingen. Gelukkig zien we dat een natuurlijke bevalling geen kwaad kan, mits patiënten voorafgaand aan de bevalling geen vaatnieuwvormingen hebben ontwikkeld.

In het tweede deel van dit proefschrift onderzoeken we of we de visus kunnen voorspellen en welke factoren bijdragen aan visusverlies, om het effect van een behandeling beter te begrijpen.

In **Hoofdstuk 6** wordt onderzocht of PXE patiënten met een ernstigere mutatie ook ernstigere verschijnselen hebben. Hier hebben we gekeken naar het aantal truncerende mutaties. Deze mutaties leiden tot een verkort eiwit met verlies van functie. Niet-truncerende mutaties kunnen leiden tot zowel een verkeerd gevormd eiwit met enige resterende functie, of ook een verkort eiwit, waardoor de uiteindelijke resterende functie moeilijker te voorspellen is. Truncerende mutaties kunnen dus beschouwd worden als ernstigere mutaties. We hebben gevonden dat PXE patiënten met twee truncerende mutaties meer vaatverkalking hebben in het lichaam en al eerder langere breuklijnen en meer vaatnieuwvormingen in het oog hebben dan patiënten met een of twee niet-truncerende mutaties. Vermoedelijk komt dit doordat het membraan van Bruch ernstiger verkalkt is.

We vonden in **Hoofdstuk 7** dat langere breuklijnen, als een surrogaatmeting voor de uitgebreidheid van verkalking van het membraan van Bruch, een hoger risico geven op vaatnieuwvormingen of netvliesverdunning. Omdat vaatnieuwvormingen en netvliesverdunning doorgaans het visusverlies veroorzaken, zijn deze resultaten belangrijk voor het counselen van met name de jongere PXE patiënten, zodat zij gerustgesteld kunnen worden of juist een reëel beeld van hun visuele prognose kunnen krijgen.

In een uitgebreide studie naar het effect van het medicijn etidronaat in PXE patienten werd gevonden dat etidronaat de vaatverkalking kan verminderen, maar helaas hebben we dit (nog) niet voor de ogen aan kunnen tonen. Wel hebben we gekeken of etidronaat effect heeft op de activiteit van vaatnieuwvormingen in **Hoofdstuk 8**. Het blijkt dat etidronaat geen positief, maar ook geen negatief effect heeft, en dus 'veilig' voorgeschreven kan worden met betrekking tot de ogen.

Omdat er nog geen meting was voor de ernst van de verkalking, hebben wij deze geprobeerd zelf te ontwikkelen in **Hoofdstuk 9**. Op netviesscans is de verkalking te zien als een hyperreflectieve laag. Wij hebben een algoritme ontwikkeld waarmee we deze hyperreflectiviteit kunnen meten als een maat voor de ernst van de verkalking. Uit dit onderzoekt blijkt dat PXE patiënten een duidelijk hogere waarde van hyperreflectiviteit van het membraan van Bruch hadden vergeleken met controles. Op dit moment is de

meting nog niet precies genoeg en moet de meting verder doorontwikkeld worden, maar het is een veelbelovende maat om in de toekomst de ernst van de verkalking mee te kunnen meten voor zowel medisch-wetenschappelijk onderzoek als in de zorg.

Appendices

List of publications

S. Risseeuw, J. Ossewaarde – van Norel, C.C.W. Klaver, J.M. Colijn, S.M. Imhof, R. van Leeuwen. Visual acuity in pseudoxanthoma elasticum. *Retina.* 2019 Aug;39(8):1580-87.

S. Risseeuw, J. Ossewaarde – van Norel, C.C.W. Klaver, J.M. Colijn, S.M. Imhof, R. van Leeuwen. Reply to: Visual acuity in pseudoxanthoma elasticum. *Retina.* 2019 Jan;39(1):e8.

S. Risseeuw, H. Yildirim, W. Spiering, S.M. Imhof, R. van Leeuwen, J. Ossewaarde – van Norel. Is vaginal delivery harmful to patients with pseudoxanthoma elasticum? *Ret Cases Brief Rep*. 2020 Mar; online ahead of print.

S. Risseeuw, J.W. Bartstra, J. Ossewaarde – van Norel, L.J. Geurts, C.H.Z. Li, S.M. Imhof, W. Spiering, P.A. de Jong, R. van Leeuwen. Is arterial stiffness in the carotid artery associated with choroidal thinning in patients with pseudoxanthoma elasticum or controls? *Acta Ophthalmol*. 2020 Aug:98(5);492-499.

S. Risseeuw, H.E. Bennink, M.G. Poirot, P.A. de Jong, W. Spiering, S.M. Imhof, R. van Leeuwen, J. Ossewaarde – van Norel. A reflectivity measure to quantify Bruch's membrane calcification in patients with pseudoxanthoma elasticum using optical coherence tomography. *Trans Vis Sci Tech*. 2020;9(8):34.

S. Risseeuw, J. Ossewaarde – van Norel, C. van Buchem, W. Spiering, S.M. Imhof, R. van Leeuwen. The extent of angioid streaks correlates with macular degeneration in pseudoxanthoma elasticum. *Am J Ophthalmol. 2020;220:82-99.*

S. Risseeuw, R. van Leeuwen, S.M. Imhof, P.A. de Jong, W.P.Th.M. Mali, W. Spiering, J. Ossewaarde – van Norel. The effect of etidronate on choroidal neovascular activity in patients with pseudoxanthoma elasticum. Accepted for publication in *PLoS One*.

S. Risseeuw, J.H. de Boer, N.H. ten Dam – van Loon, R. van Leeuwen. Risk of rhegmatogenous retinal detachment in acute retinal necrosis with and without prophylactic intervention. *Am J Ophthalmol*. 2019 Oct;206:140-148.

G. Kranenburg, P.A. de Jong, J.W. Bartstra, S.J. Lagerweij, M.G. Lam, J. Ossewaarde – van Norel, **S. Risseeuw**, R. van Leeuwen, S.M. Imhof, H.J. Verhaar, J.J. de Vries, R.H.J.A. Slart, G. Luurtsema, A.M. den Harder, F.L.J. Visseren, W.P. Mali, W. Spiering. Etidronate for prevention of ectopic mineralization in patients with pseudoxanthoma elasticum. *J Am Coll Cardiol.* 2018 Mar;71(10):1117-1126.

Dankwoord

Onderzoek doen is bij uitstek zelfstandig werken en toch zal je het alleen nooit redden. Dit proefschrift is dan ook volledig tot stand gekomen dankzij de talloze bijdragen van anderen.

Ten eerste alle personen met PXE: helaas leven jullie (nog steeds) met een ziekte met (nog steeds) veel onzekerheid. Toch hebben jullie ontzettend veel veerkracht en bij alle persoonlijke contacten leer ik enorm veel van jullie over het omgaan met deze ziekte. Jullie belangeloze medewerking aan het medisch wetenschappelijk onderzoek is bewonderenswaardig en motiveert mij om relevant onderzoek voort te zetten.

Beste Redmer, mijn interesse in wetenschap, en daarmee mijn wetenschappelijke carrière, begon tijdens onze samenwerking in mijn laatste studiejaar. Dit vloeit voort uit hoe jij als onderzoeker bent: enorm integer en met passie voor de wetenschap. Zo heb jij ervoor gezorgd dat ik de master Epidemiologie kon doen, iets waar ik je enorm dankbaar voor ben. Ook nam je me ontzettend veel zorgen uit handen zodat ik me kon focussen op het uitvoeren van onderzoek. Ik kon (en kan) altijd bij je terecht en geen vraag is je teveel. Ik wil je bedanken dat je een 'onderzoeker in de dop' in mij hebt gezien en hoop op nog vele mooie samenwerkingen in de toekomst, zowel in het onderzoek als in de kliniek!

Beste Annette, waar andere mensen tegen een dichte deur aanlopen, zie jij altijd nog een kiertje. Jouw enorme betrokkenheid bij, en inzet voor patiënten is inspirerend. Ook voor het onderzoek zet jij altijd net dat stapje extra en je bent 'het geweten' van dit proefschrift. Je nauwkeurigheid en je affiniteit met beeldvorming heeft zonder meer het onderzoek in dit proefschrift naar een hoger niveau getild. Daarnaast kijk ik met veel plezier terug op onze overleggen - die soms een beetje uitliepen – waarin we filosofeerden over de pathofysiologische basis van de oogheelkundige veranderingen in PXE. Ik wil je enorm bedanken voor je betrokkenheid en onbegrensde motivatie voor dit onderzoek!

Beste Saskia, wat fijn dat jij ook in mijn promotieteam zit. Ik bewonder je vermogen tot overzicht houden – bijvoorbeeld wanneer mijn planning weer iets te optimistisch was. Ook je steun en begrip op momenten dat het nodig was heb ik als erg fijn ervaren. Ik kijk ernaar uit om in een andere functie onder jouw leiding te werken. Bedankt!

Members of the review committee, prof. dr. ir. M.J.C. Eijkemans, dr. P. Charbel Issa, prof. dr. M.M. van Genderen, prof. dr. R.O. Schlingemann and prof. dr. J.R. Vingerling, thank you for your time to review my thesis.

Beste Joke, ook jou wil ik bedanken voor je begeleiding en je interesse in mijn onderzoek. Ik waardeer het dat de deur altijd open stond om iets te bespreken, ook al deed ik geen onderzoek bij jou.

Iedereen die betrokken is bij het PXE onderzoek in het UMC Utrecht: dit proefschrift is echt een gezamenlijke prestatie. Dr. Spiering, beste Wilko, bedankt voor je vermogen tot doorpakken en je enorme drive tot het verbeteren van de zorg voor PXE patiënten. Je betrokkenheid bij PXE kan niet los worden gezien van het feit dat we nu de vruchten kunnen plukken van al het werk dat jij erin hebt gestopt. Prof. dr. de Jong, beste Pim, ik heb bewondering voor je overkoepelende blik over het PXE onderzoek en hoe je het beste in mensen naar boven kunt halen. Bedankt voor je snelle en doortastende correcties op mijn manuscripten en natuurlijk voor je hulp bij onze zoektocht naar metingen op OCT en late fase ICG angiogrammen. Prof. dr. Mali, beste Willem, bedankt voor je inspirerende gedachten over de mechanismen achter PXE. Beste Guido, wat was het leuk om in de eerste fase van mijn promotietraject met jou samen te werken! Je enthousiasme was aanstekelijk en jouw harde werk was een prachtige basis om verder op voort te bouwen. Bedankt! Beste Jonas, bedankt voor je nuchtere blik, onze koffiemomentjes en je pragmatische oplossingen, waar ik veel van heb geleerd. Veel succes met de laatste loodjes van jouw onderzoek! Beste Inge Klaassen en Corina Joosten, achter de schermen heb ik op logistiek gebied veel aan jullie gehad. Bedankt dat ik met vragen bij jullie terecht kon en voor jullie inzet voor het PXE onderzoek!

Beste Edwin, jij hebt een sleutelrol gehad in de OCT meting: met jouw ervaring op het gebied van beeldverwerking (en je geduldige reacties als ik weer eens vast zat in Matlab) hebben we gepionierd met een eindresultaat waar we trots op mogen zijn. Enorm bedankt voor het meedenken over het kwantificeren van verkalking op retinale imaging en je inzet hiervoor naast je eigen projecten.

Alle medewerkers van de afdeling oogheelkunde wil ik bedanken voor hun interesse en mij thuis te laten voelen op de afdeling. Een aantal personen wil ik in het bijzonder bedanken. Jos, Hilda, Irene, ik kijk met veel plezier terug op de woensdagochtenden die oogfotografisch vaak best uitdagend, maar ook ontzettend leerzaam waren. Toch

waren jullie altijd bereid om voor mij nog een extra en-face OCT scan van een paar minuten (met geluk) te maken. Bedankt voor jullie gedeelde enthousiasme voor oogheelkundige beeldvorming en natuurlijk voor de gezelligheid! Lisette Koene, bedankt voor je ondersteuning en het meewerken aan de TEMP en DECIPHER studie. Dagmar en Marjolein, ook jullie wil ik graag bedanken voor het verrichten van alle extra biometrie tussendoor voor de wetenschap. Alle baliemedewerkers wil ik bedanken voor hun begeleiding van de PXE patiënten door de vaak ingewikkelde looproute op onze afdeling, en Brigitte voor haar harde werk om de planning soepel te laten verlopen. Petra en Suzan, bedankt dat ik altijd bij jullie terecht kon met al mijn logistieke vragen, maar ook voor de gezellige praatjes! Joke en Saskia, bedankt voor jullie hulp bij de planning en een polikamer.

AIOS, bedankt voor jullie interesse in mijn onderzoek en de gezellige praatjes in de onderzoekshokken. Ik kijk ernaar uit om me bij jullie te voegen!

Beste Jonas Kuiper, bedankt voor je enthousiaste hulp bij al mijn methodologische, statistische en andere research-gerelateerde vragen.

Beste medewerkers van het researchbureau van de DHS, bedankt voor jullie hulp. Tamara en Els, bedankt voor het meedenken met, en meelezen van onderzoeksvoorstellen. Ferry en Ruud, bedankt voor het eindeloos helpen bij mijn ICT problemen, waardoor ik vaak toch weer gerust door kon werken.

Beste Rob Scholten, bedankt voor je fijne begeleiding en je betrokkenheid tijdens het laatste deel van de master Epidemiologie.

Alle mede-auteurs van de manuscripten in dit proefschrift wil ik bedanken voor het meedenken en hun waardevolle toevoegingen en opmerkingen.

I want to thank all persons who contributed to our current histopathological investigation of PXE donor eyes. Dear Imre Lengyel, although our combined efforts are not a part of this thesis, our collaboration has definitely motivated me. Your passion for fundamental research in retinal mineralization is contagious and working with you is a true joy. I also want to thank Connor, Lajos and Matt for their enthusiastic assistance. Beste prof. dr. A. Bergen, beste Arthur, bedankt voor het meedenken voor bij dit onderzoek, waarbij je kennis en ervaring zeer waardevol is, en dat je het mogelijk hebt gemaakt dat ik nog aan dit project kan werken. Beste Jaco, bedankt voor je fijne

logistieke hulp en pragmatische oplossingen! Beste Mary van Schooneveld, bedankt voor je ervaring, bijdrage en praktische hulp bij de explantatie van donorogen.

Beste studenten, beste Maarten, Rutger, Hilin, Colette, Catherina, Angelica, Sofie en Veerle, het was me een eer en een genoegen om jullie wetenschappelijke stages te mogen begeleiden. Ik heb ervan genoten om jullie te zien groeien in het onderzoek en hier enthousiast over te zien worden. Fantastisch om te zien dat een aantal van jullie door is gegaan in de wetenschap! Ik wens jullie veel succes en plezier in jullie loopbaan.

Lieve onderzoekers, bedankt voor jullie gezelschap, steun, slechte grappen en wijze raad. Nienke, Daniël, Anne-Mieke en Fleurieke, jullie stonden als ervaren onderzoekers voor me klaar met advies wanneer dit nodig was. Bedankt! Kamil, in het A-hok hebben we lief, leed en twijfelachtige muziek gedeeld en ik kijk met veel plezier terug op het sparren over onze onderzoeksprojecten. Anna, wij gingen van B naar Q naar A met nog een beetje R tussendoor. Bedankt voor het talloze meelezen van mijn schrijven en het tot in de letterlijke puntjes perfectioneren van mijn presentaties. Maar ook bedankt voor de zoetigheden die je speciaal voor mij in een overheerlijke veganistische variant hebt uitgebracht en voor de ABBA middagen die het werkplezier zeker ten goede kwamen. Ik kijk ernaar uit om straks weer met jullie samen te werken in de kliniek! Bas, jij kwam het A-hok versterken en wat was het fijn dat jij mijn Matlab frustraties snapte! Maar ook bedankt voor je geduldige hulp met Illustrator en natuurlijk onze gedeelde passie voor de Indiase keuken. Roos, dankzij jou kan ik überhaupt mijn proefschrift verdedigen, waarvoor natuurlijk mijn eeuwige dank. Verder heb ik genoten van onze (te korte) tijd samen in het A-hok, door jouw nuchtere opmerkingen en je - lichtjes opstokende - humor. Myrthe, Wouter, Brendan en Evianne, bedankt voor jullie meedenken, koffiepraatjes, speciaalbierborrels en leuke uitjes. Carlyn, Lude, Deniz, Janneau en Els, bedankt voor jullie gezelligheid en interesse in onze korte tijd van samenwerken! Antarctica blijft een gevoelig puntje, maar jullie gaan de volgende DOPS pubquiz vast winnen!

Succes is niets waard als je het niet kan delen. Ik ben mijn lieve vrienden en familie enorm dankbaar voor hun enthousiasme bij de mooie pieken en hun steun bij de onvermijdelijke dalen die bij het onderzoek horen.

Lieve Emma, ik bewonder hoe jij je eigen pad uitstippelt. Onze vriendschap heeft meerdere afstanden overwonnen en ik weet dat ik, ondanks een grote oceaan die

tussen ons ligt, altijd op je kan rekenen. Toch kijk ik ernaar uit om jou (en natuurlijk jullie toekomstige kleintje) in het echt weer te zien!

Lieve Lisanne, je helpt me herinneren dat het leven zoveel meer is dan werk! Bedankt voor de talloze leuke feestjes, maar ook voor je altijd luisterende oor en je interesse in mij.

Lieve Nadia, jij begrijpt als geen ander welke struggles bij het onderzoek kunnen horen. Bedankt voor je oprechte interesse in mijn onderzoek en in mij. Ik hoop dat we elkaar ook in het UMC nog vaak zullen tegenkomen!

Lieve Jori, zonder jouw peptalks was dit proefschrift een stuk dunner geweest! Jij kent mij beter dan ikzelf en als ik naar woorden zoek, weet jij ze voor mij te vinden. Ik ben je oneindig dankbaar voor je steun, de nodige flesjes bubbels en de ontelbare leuke herinneringen die wij samen hebben. Dankjewel voor wie je bent.

Lieve Arti's, bedankt voor de heerlijke afleiding op de dinsdagen en al onze uitjes en jullie interesse in wat ik doe (en het is echt niet erg als jullie 'pseudoxanthoma elasticum' niet onthouden hoor!). Het is ontzettend inspirerend om zulke ambitieuze en maatschappelijk betrokken vrouwen in mijn omgeving te hebben. Lieve Sietske, niet alleen in de grappenjury ben jij mijn 'spartner' in crime (+5?), ook als woordkunstenaar ben je onmisbaar, bedankt voor het meelezen! Lieve Tess, bedankt voor de talloze fijne gesprekken en dat je me altijd meesleept om leuke dingen te doen. Lieve Tessa, wat fantastisch dat jij altijd voor me klaarstaat om alle aspecten van het leven te delen. Niet alleen onze kleding- en (soms onconventionele) muzieksmaak maar ook de zaken die om meer reflectie vragen. Met jou twinnen is de hoofdprijs winnen!

Alle vrienden die niet specifiek genoemd zijn: bedankt voor jullie interesse, kopjes koffie en de vele borrels ter afleiding!

Lieve familie, lieve tantes, ooms, nichten en neven, ik vind het heel bijzonder hoe goed onze familieband is. Ik wil jullie allemaal enorm bedanken voor jullie interesse in mijn onderzoek. In het bijzonder wil ik mijn oma's bedanken. Lieve oma Lammie, helaas bent u er niet meer bij, maar ik ben u ontzettend dankbaar voor uw buitengewone interesse en betrokkenheid in mij en anderen, waarin u een voorbeeld voor mij bent. Lieve oma Sari, ik bewonder uw zelfstandigheid, nuchterheid en doorpakkend vermogen (en groene vingers). Ik vind het bijzonder en mooi dat wij naamgenoten zijn en ik ben trots toch een beetje Zeeuwse te zijn!

Lieve schoonfamilie, ik had me geen leukere familie dan jullie kunnen wensen. Tijs en Ana, Daan en Quiyrine, bedankt voor jullie interesse en voor alle gezellige uitjes en familietripjes! Lieve Astrid en Ulco, wat kwam ik bij jullie in een warm bad terecht. Dankjewel dat ik altijd bij jullie terecht kan!

Querida Kathy, que lindo que seas parte de la familia! Me gusta que ver Derek y tu estén felices juntos. Espero que tengamos muchos más buenos recuerdos en Utrecht!

Mijn paranimfen, Derek en pap, wat een eer dat jullie mij willen bijstaan. Ik twijfel er niet aan dat de 'leerdrang' in ons gezin heeft bijgedragen aan mijn keuze voor het onderzoek. Beiden zijn jullie dichtbij het academische wereldje gekomen, maar jullie hebben bewust gekozen voor een ander, beter passend pad. Toch weet ik zeker dat het met zulke knappe koppen aan mijn zijde straks niet mis kan gaan.

Lieve Derek, lief broertje, reismaatje en gymbuddy, jij bent er voor mij geweest in alle fasen van het leven. Ik bewonder je zachtmoedigheid en je intelligentie en ben er trots op dat jij altijd jezelf blijft. Dankjewel voor alles!

Lieve pap en mam, waar moet ik beginnen. Aan jullie heb ik alles te danken en jullie hebben mij onvoorwaardelijk gesteund in mijn eigen keuzes. Jullie betrokkenheid bij anderen en passie om door te blijven ontwikkelen is inspirerend en een voorbeeld voor mij. Ik kan altijd bij jullie terecht en geen moeite is jullie te veel. Bedankt, voor alles, en voor meer.

Lieve Rick, jij haalt het beste in mij naar boven en biedt mij het tegenwicht wat ik nodig heb. Als mijn grootste fan zorg je ervoor dat de kleine successen gevierd worden, ook al zie ik ze zelf niet, en klaag je niet als ik weer eens compleet verdwaald in mijn eigen gedachten ben. Bedankt voor de bruisende, lieve, attente en gekke persoon die je bent. Ik kijk uit naar al onze avonturen samen, wat ze ook zullen zijn en waar ze ook zullen plaatsvinden.

About the author

Sara Risseeuw was born on June 15th 1991 in Doorn, the Netherlands. She is the daughter of Adri and Brechtje and has a younger brother, Derek. During secondary school (Revius Lyceum in Doorn), Sara took an interest in biology and in elective subjects such as philosophy and arts. After graduating cum laude in 2009, she moved to Utrecht and started her medical training at Utrecht University.

Focus on Ophthalmology

Sara's internship at Saint Francis Hospital in Katete, Zambia, sparked her interest in Ophthalmology. In Zambia, she experienced the importance of Ophthalmology for global health and wellbeing. Sara decided to focus on Ophthalmology in her final year of studies. For her master thesis, she investigated strategies to prevent retinal detachment in acute retinal necrosis, under the supervision of Redmer van Leeuwen. This started her enthusiasm for clinical research and science.

Ophthalmological research

In 2016, Sara obtained her medical degree and started her PhD track at the Ophthalmology department of the University Medical Center in Utrecht. For her PhD, she investigated the ophthalmological manifestations of pseudoxanthoma elasticum. Sara was supervised by Annette Ossewaarde – van Norel, Redmer van Leeuwen and Saskia Imhof. Parallel to conducting clinical research, Sara graduated from the post-graduate master Epidemiology and its specialty tracks Clinical Epidemiology and Medical Statistics.

Currently, she is investigating the histopathological changes in eyes with pseudoxanthoma elasticum. For this study, Sara collaborates with Imre Lengyel (Queens University Belfast) and Arthur Bergen (Academic Medical Center, Amsterdam) and has received grants from the Stichting tot verbetering van het Lot der Blinden and the FC Donders Binkhorst Stichting.

Future plans

Together with Rick, Sara lives in Utrecht. They are converting a campervan, to embark on an unforgettable roadtrip. Afterwards, Sara will start her residency to become an ophthalmologist. She is passionate about hiking and camping, philosophy and animal welfare.